The University of Nottingham
UNITED KINGDOM · CHINA · MALAYSIA

Smith, Karon Lesley (2002) Remote sensing of leaf responses to leaking underground natural gas. PhD thesis, University of Nottingham.

Access from the University of Nottingham repository:
http://eprints.nottingham.ac.uk/12911/1/247133.pdf

Copyright and reuse:

The Nottingham ePrints service makes this work by researchers of the University of Nottingham available open access under the following conditions.

This article is made available under the University of Nottingham End User licence and may be reused according to the conditions of the licence. For more details see: http://eprints.nottingham.ac.uk/end_user_agreement.pdf

A note on versions:

The version presented here may differ from the published version or from the version of record. If you wish to cite this item you are advised to consult the publisher's version. Please see the repository url above for details on accessing the published version and note that access may require a subscription.

For more information, please contact eprints@nottingham.ac.uk

Remote Sensing of Leaf Responses to Leaking Underground Natural Gas

By Karon Lesley Smith, BSc

Thesis submitted to the University of Nottingham for the degree of Doctor of Philosophy, May 2002

Abstract

Detection of leaking gas pipelines is important for safety, economic and environmental reasons. Remote sensing of vegetation offers the potential to identify gas leakage.

The research aim was to determine the effects of elevated soil concentrations of natural gas on overlying vegetation. Pot-scale investigations were carried out to determine whether changes in spectral characteristics were specific to natural gas or were a generic response to soil-oxygen displacement. Natural gas, argon, nitrogen and waterlogging were used to displace soil-oxygen.

Leaf response to soil oxygen displacement was increased reflectance in the visible wavelengths and changes in the position and shape of the red-edge, which shifted towards longer wavelengths as the control plant matured, while the red-edge of the treated plant remained stationary indicating an inhibition of maturing. The shape of the red-edge differed in bean and barley with bean exhibiting a single peak in the first derivative that moved with plant maturity; barley exhibited a peak at 704 nm with a shoulder at 722 nm that shifted to shorter wavelengths during plant stress. Argon and waterlogging exhibited a greater response than natural gas, which had been administered non-continuously. These experiments suggest the response to natural gas was generic to soil-oxygen deficiency.

Field studies were conducted to determine whether spectral changes in leaves identified in pot trials were observable in crop canopies under field conditions. Reflectance of barley growing above a leaking gas pipeline was increased in the visible wavelengths and the red-edge was at a shorter wavelength. When the majority of the crop was fully developed, the barley above the gas leak was greener, suggesting that development was inhibited by soil-oxygen displacement.

It might be possible to detect leaking gas by remote sensing of vegetation in conjunction with pipeline maps, but limitations in the spatial resolution of current satellite sensors and the infrequency of cloud free skies in the UK suggest that further work is needed before an operational system could be available.

Acknowledgements

There are many people that I would like to thank for helping me during the course of this research.

First, I wish to acknowledge Advantica Ltd. for funding the research via a Postgraduate Research Scholarship as part of the BG Hub program. Acknowledgement also goes to Natural Environment Research Council (NERC) for the loan of the ASD Fieldspec Pro from the Equipment Pool for Field Spectroscopy (NERC-EPFS) at the University of Southampton.

To my supervisors Mike Steven and Jeremy Colls I would like to say thank-you for your encouragement and advice throughout the three years. I also wish to thank Johanna Laybourn-Parry and Helen West for encouraging me to undertake a PhD.

Next, I wish to thank those who have helped in the research. First, Russ Pride of Advantica for his general assistance and support and the members of Transco at Grimsby for help in locating the field site and at Leicester for lending an oxygas meter. I also wish to thank Bill Cooper of Haugham Slates farm and John Pearson at Wrisdale Farm at Louth for allowing me to traipse through their barley crops in search of gas stressed plants. I also wish to thank Margaret Lacy in the biochemistry department at Sutton Bonington for her assistance in chlorophyll determinations and also being available to switch on and off the gas supply when needed. Thanks also go to Gavin Lupton of the stores department for his assistance in transporting argon cylinders to the growth room.

On a more personal level I would like to thank my daughter Emily for being so understanding whilst she herself was taking

GCSE and A'levels and my parents for their support and encouragement.

Last but certainly not least, I wish to thank my husband John for his unfailing support throughout all my studies and his assistance in writing macros, producing diagrams and generally getting information for me. I could not have done it without his support.

Frontispiece: View along the gas pipeline at Haugham Slates Farm, Louth showing vegetation damage due to leaking gas. (Photograph courtesy of Bill Cooper)

Contents

List of Figures

List of Tables

1 Introduction

1.1 Background

The history of gas making can be traced back to 1792, when William Murdoch invented gasification of coal. He first used the newly harnessed energy to light his own home at Redruth in Cornwall, and within 30 years of Murdoch's successful experiment, gas manufacturing had become an established industry in Britain. At the turn of the 20th Century, some 700 gas companies were supplying 3.8 million customers through a 28 000 mile (45 000 km) network of gas mains and by the time of Nationalisation in 1949 the supply of gas had increased to 12 million customers and 77 600 miles (124 000 km) of gas mains (BG plc 1997).

In 1965, natural gas was discovered under the North Sea and a decision was made by the Gas Council in 1966 to change from man-made to natural gas. This required construction of a national high-pressure gas transmission system - an underground steel pipeline capable of supporting a range of pressures, flow and temperature variations of the transported gas[1].

1.2 Components of Natural Gas

Natural gas consists of a mixture of gases, the composition of which depends on the source, treatment and blending of the constituent gases. The major constituent is methane (CH_4), which comprises between 80-95% of the gas. Natural gas also contains nitrogen (N_2) - 1-12%, ethane (C_2H_6) - 3-7%, carbon dioxide (CO_2) - up to 2.5%, benzene, toluene and smaller amounts of other hydrocarbons of various chain

[1] The Origins and Progress of the Gas Industry over 200 Years. Http://www.igaseng.com/gashist.htm Accessed on 1/10/2001

lengths. When released in air the concentration of natural gas may be expressed either in % volume, parts per million (ppm) or as a percentage of the lower explosive limit of the air / gas mixture (%LEL) (Section 1.3.1).

Natural gas is odourless, so an odorant consisting of diethyl sulphide, ethyl mercaptan and tertiary butyl mercaptan (Watt Committee 1994) is added to the gas at the terminals where the gas comes ashore so that leaks can be more easily detected. The odorant is designed to have an immediate impact and be instantly recognisable as natural gas. The human nose can detect mercaptan at the level of just a few parts per million.

1.3 Description of gas pipeline network and need for study

Gas is delivered from gas producers operating rigs in about 100 fields beneath the sea around the British Isles to seven beach terminals (St. Fergus, Easington, Theddlethorpe, Bacton, Barrow, Teeside and Burton Point), where it is then transported through the gas transmission network. [2]

Transco, which is part of the Lattice group Plc, is responsible for the 278 000 km of gas transmission network that now crosses the UK. The network consists of three parts. The National Transmission System (NTS) forms the backbone of the gas distribution system, with 18 000 km of welded steel, high-pressure (between 7 and 84 bar) pipeline. There are also 10 000 km of high-pressure storage pipelines and 250 000 km of distribution pipelines at medium pressure (between 50 mbar and 7 bar). At several locations within a town the gas pressure will be reduced to 25 – 50 mbar for

[2] Delivering Gas Http://www.transco.uk.com . Accessed on 1/10/2001

distribution to houses for domestic consumption (Personal Communication, Advantica Technologies Ltd, 2001).

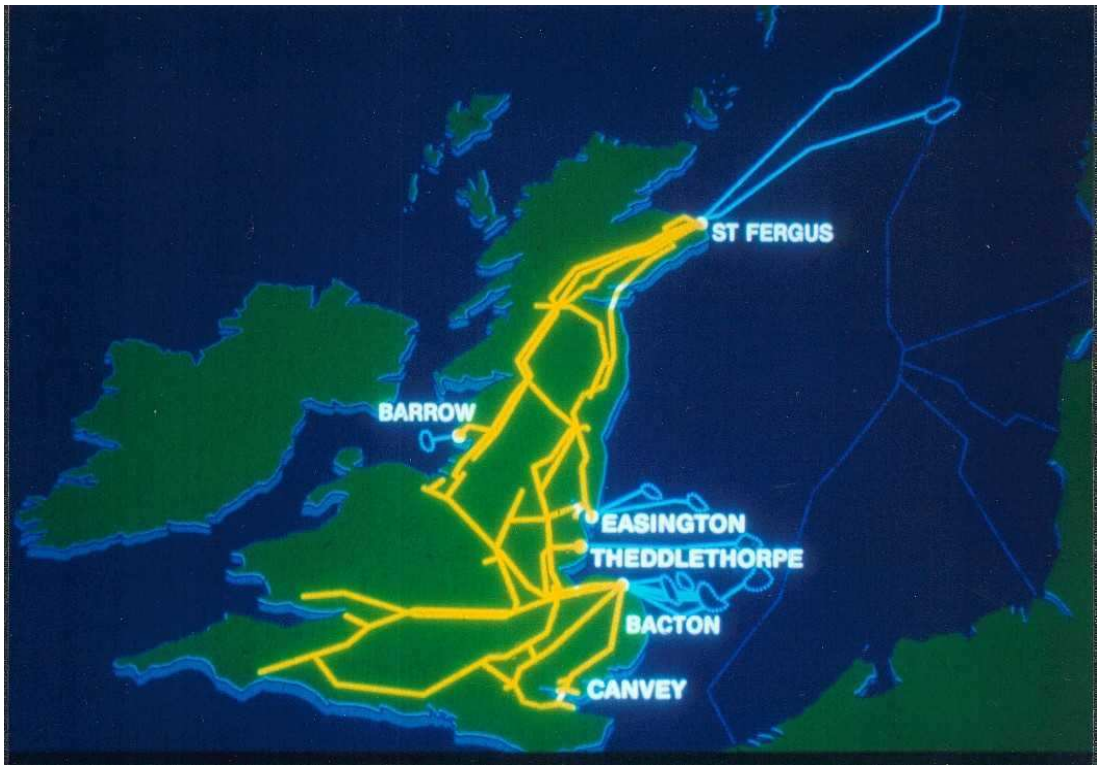

Figure 1.1 Map of the terminals and the National Transmission System (Photograph courtesy of Advantica Technologies Ltd.)

The high pressure National Transmission System is inspected on a fortnightly basis by flying helicopters along the full extent of the pipeline network looking for leaks, land subsidence or possible encroachment of the pipelines by third parties such as farmers and road contractors. Monitoring of the remainder of the medium - low pressure network is performed intermittently by pipeline walking by Transco service engineers (Personal Communication, Advantica PLC, 2000).

Helicopter pilots and pipeline engineers report observing vegetation change around the area of gas leaks. It has been suggested that leaking pipelines may be detected by the use of remote sensing of the surrounding vegetation to discover the early signs of plant

stress caused by gas leakage. Early detection of such gas leaks is important for safety, economic and environmental reasons.

1.3.1 Safety

Methane is explosive in concentrations between 5% (the lower explosive limit – LEL) and 15% (the upper explosive limit – UEL) volume in air. At concentrations above UEL or below LEL the gas will burn with a controlled flame. Any leakage of natural gas above LEL could pose an explosion risk.

The risk arising from gas leaks depends on the where in the network the leak occurs. In the high-pressure network the risk of damage is due to the high pressures involved. Any fracture of the high-pressure pipeline will lead to explosive craters forming around the pipeline as can be seen in Figure 1.2. In the medium to low pressure networks the risk arises due to the explosive nature of natural gas.

Continual monitoring of the high-pressure network by helicopter reduces the risk of damage to the pipeline by third parties. Monitoring the network by pipeline walking and using survey vans fitted with flame ionisation detectors, (Section 2.2.3), reduces the risks arising from leakage of gas from the medium to low-pressure network and reports from the public detecting the smell of gas also prompt rapid responses to detect and repair leaks.

Figure 1.2 Photograph showing a weld failure in a high pressure gas pipe (Photograph courtesy of Advantica PLC.)

1.3.2 Economics

Leakage leads to a loss of resources for Lattice Group. Lattice Group's annual report for the year ending 2000[3] stated that Transco transported 1101 TWh of natural gas

[3] Lattice group annual report 2000 http://annuals.lattice-group.com/ Accessed on 16/10/01

through its pipelines. This is equivalent to 1 x 10^{13} m^3 of gas per year. Transco turnover amounted to £2975 million and so leakage of just 1% of throughput (Watt Committee 1994) could lead to a significant £30 million loss of revenue for Transco.

Helicopter surveillance of the network every fortnight costs Transco 1.5 m euro per year and there is the additional costs in man-hours of the walk-the-line that occurs approximately four times a year (PRESENSE 2001). Monitoring of the network by helicopter is not only expensive but has inherent risks associated with low-level helicopter flight and relies on the accuracy of the pilot. Remote detection of leaks by satellite could reduce the risks of inspecting the network. Remotely sensed data could be handled by computer, thus increasing consistency, accuracy and reliability compared to a pilot's judgement.

1.3.3 Environment

Methane is a radiatively active gas at thermal infrared wavelengths. It is approximately 30 times more active per molecule than carbon dioxide and as such is a major contributor to the greenhouse effect (IPCC 1992). In 1994 UK atmospheric emissions of methane amounted to 3875 kt of which 365 kt was due to gas leakage[4]. Between 1990 and 1995 the total UK emissions of methane decreased from 4464 kt to 3817 kt. However, the amount contributed by fugitive emissions of oil and gas fuels (the leakage from equipment on a continuous basis that can be corrected through inspection and maintenance) has remained constant at about 480 kt yr^{-1} [4].

[4] National atmospheric emissions inventory (UK methane emissions) http://www.aeat.co.uk/netcen/airqual/emissions/report94.html Accessed on 16/10/01

Currently leakage of natural gas from European transmission systems amount to 343 000 tonnes CO_2 equivalent per year and it is estimated that CO_2 emissions could be reduced by 20% through improved leak detection. In addition 4 million litres of fuel are used annually across Europe for helicopter surveillance, equivalent to 13 000 tonnes of CO_2, and the use of satellite remote sensing would therefore reduce these emissions (PRESENSE 2001).

In terms of global warming potential leakage of methane from natural gas systems reduces the benefits gained from the reduction of carbon dioxide emissions and therefore escapes of natural gas should be reduced.

1.4 Extent of Leaks

In 1991 the total amount of natural gas emitted to the atmosphere from the UK amounted to 446 kt yr^{-1}, which represents about 408 kt of methane per annum (Watt Committee, 1994). This included losses from transmission operations, storage facilities, maintenance and venting of control equipment. Table 1.1 illustrates the breakdown of methane emissions from the gas industry in 1992.

Table 1.1 Breakdown of methane emissions from the gas industry. Adapted from Watt Committee report no 28 (1994)

	Methane losses t yr^{-1}
Transmission	
Terminals	690
Storage and LNG sites	296
Transmission operations	14 928
Distribution	
LP mains and service leakage	359 161
MP Mains leakage	16 814

Governors and Holders	2 359
Broken / purged mains etc	8 234
Commercial and Industrial	
Isolated releases	23
Continuous long term releases	5 969
Total	**408 474**

The majority of the emissions arose from leakage from the low-pressure mains. Pipeline leaks are caused by third party interference, corrosion, material defects and joint and fitting defects or failures, with most leaks occurring at the joints. Transco uses the loss of pressure in isolated lengths of pipeline as a measure of the rate of gas loss. Leakage varies in different parts of the distribution system because of the differences in age, construction materials, pipe-jointing techniques and operating pressures. The intermediate pressure system that operates at between 2 and 7 bar is mostly composed of welded steel pipelines with cathodic protection to prevent corrosion and so leakage from this system is very small. The low-pressure distribution main has a significant proportion of Victorian cast iron pipelines and this has the greatest leakage of natural gas. Natural gas is drier than the coal gas that was previously transported in these pipelines and this causes the jointing materials to dry out resulting in leaks. Based on figures calculated in the 1980s the average rate of leakage from cast iron pipes is 0.01-0.02 m^3 km^{-1} hr^{-1} $mbar^{-1}$. The overall leakage figure for the whole of the low-pressure distribution system was calculated using the rate of pressure drop in isolated pipelines and in 1992 was found to be 392 kt of natural gas per annum. In 1991 the throughput of natural gas through the transmission system was approximately 43 Mt and the total amount of natural gas emitted to the atmosphere was approximately 446 kt yr^{-1} (Watt Committee 1994), which amounts to

1.04% of the total gas throughput. As old cast iron pipes are replaced the amount of leakage is expected to decrease. In 1999 there was 4200 km of medium pressure ductile iron distribution mains and it is intended that 2360 km of this should have been replaced by the end of 2002 (Lattice Group 2000).

Other methods of estimating the leak rate from pipelines involve physically isolating sections of pipeline, pressurising the section and measuring the gas flow rate needed to maintain the pressure at standard operating conditions. The measured flow rate is taken to be equal to the leak rate from the pipe. However, although these methods provide accurate measurements of the natural gas leakage rate from the pipeline, they do not account for the effects of soil oxidation of the methane and do not reliably predict the emission rate of the natural gas from the soil surface (Lamb *et al.* 1996). They give an estimate of the economic loss of gas but not necessarily the environmental effect on the atmosphere. The amount of soil oxidation of methane will depend upon the depth of the pipeline in the soil, the moisture content and the extent of the leak. Populations of methanotrophs, bacteria capable of utilising methane as an energy source, will contribute to the oxidation of methane in the soil and thus reduce the impact of the natural gas leakage on the environment (Hoeks 1972, Czepiel *et al.* 1995).

1.5 Outline of the research

The aim of the research was to determine the effects of elevated soil concentrations of natural gas on the overlying vegetation. A primary objective was to identify spectral regions that may be used to remotely detect gas leaks so that leaks can be detected more rapidly, before an explosive risk develops.

The research program was conducted in two main areas. First, pot-scale investigations were carried out using several plant species and methods of displacing oxygen from the soil, with the aim of identifying whether changes in spectral characteristics were due to specific effects of the leaking natural gas or were a generic response to oxygen displacement in the soil. Natural gas, argon and nitrogen were used as gaseous methods of displacing oxygen from the soil and waterlogging was used as a non-gaseous method. It was expected that reduced oxygen surrounding the root with subsequent reduced uptake of water and nutrients from the soil would lead to decreased chlorophyll levels, leading to an increase in reflectance and a shift in the red-edge to shorter wavelengths.

Secondly, field-based studies were conducted on a field crop growing above a leaking gas pipeline. The objective of this study was to determine whether spectral changes in leaves identified during pot trials were observable in crop canopies under natural field conditions.

2 Literature review

2.1 Measurement of Soil-gas

Various methods have been used to measure the concentration of methane in soil. Many of these have been developed to detect levels of natural methane emitted from the soil by the action of methanogenic microorganisms or due to flooding of the soil in bogs or paddy fields. Alberto *et al.* (1996) used a 25 cm Plexiglass tube fitted with a gasbag to sample gas and soil in paddy fields. The head-space gases in the bag were analysed using gas chromatography with flame ionisation detection. Clymo and Pearce (1995) sampled methane and carbon dioxide gas using a 4 cm diameter cylinder with a 1 mm spiral groove on the surface, which was pushed into the soil to the required depth. Gas diffused from the water-saturated peat into the gas space in the groove and was transported to a quadrupole mass spectrometer for analysis. These methods both require the removal of large samples of gas and the availability of expensive pieces of field equipment.

Flux chambers have also been used to assess gas emissions from soil surfaces. Denmead (1979) used a cylindrical pipe fitted with a Plexiglass cover, which was driven into the soil. Air was drawn from the chamber and passed through an infrared gas analyser. This method was found to be unreliable when used to detect the flux from unsaturated soils because sucking gas out of the chamber results in a small decrease in pressure in the chamber that varies with flow rate. The reduced pressure results in an apparent higher leakage flux. Erno and Schmitz (1996) used an open flux chamber placed over a tray of soil, and compared the flow of gas in at the bottom of the tray with that drawn out of the chamber into the analyser. Methane concentration

in the gas outlet was found to reach a constant value within 5 minutes. However, this system is only suitable for determining the flux of gas out of the soil and not the concentration of methane within the soil-air and around plant roots.

Hoeks (1972b) used a Johnson-Williams combustible gas detector based on the combustion of methane to measure methane concentrations in the soil. Copper tubing was installed into the soil as permanent sampling points and samples of soil air were then sucked from these tubes and analysed for methane.

Similarly Godwin *et al.* (1990) used a Gastec model 1314 gas analyser to map methane concentrations in the soil around gas wells. However, the analyser only measured concentrations of methane up to 5% by volume in air and so was not adequate for high concentrations of methane. Soil-gas samples were taken by burying 15 cm diameter PVC drainage pipe capped at one end and with holes cut in the pipe. The holes were covered with nylon window screen to prevent filling with soil. Sample air was extracted to the analyser through a length of plastic tubing in the cap of the drainage pipe in order to measure methane concentrations. Later experiments used a thermal conductivity gas analyser (Nova 306S) to give concentrations for methane up to 100% by volume in air.

The method of sampling the soil-air may have an effect on the results. Most methods involve removing a sample of the soil-air, which may have the result of diluting the sample with air from the surface or disturbing the equilibrium of air within the soil. The effect of removing the sample is that oxygen diffuses into the soil as the methane is removed, and the new oxygen may be used by methanotrophs to consume even more methane. An ideal system would measure the gas concentration in-situ, or would re-circulate the sampled air back into the soil. If a soil-air sample must be removed then

it should be removed at a slow rate to reduce the sudden influx of air from the surface and allow time for the soil-air system to equilibrate.

2.2 Gas monitoring instruments.

Various types of portable gas monitoring equipment have been developed using a variety of techniques for analysis. This section will review the techniques available for gas detection and discuss their suitability for use in this research.

2.2.1 Catalytic oxidation

Pellisters consist of two coils of fine platinum wire, each of which is embedded in a bead of alumina; one of the beads is impregnated with a catalyst that promotes oxidation and the other is treated to inhibit oxidation. A current is passed through both the coils to raise them to a temperature of about 500°C. At this temperature the catalysed bead will combust the gas at a faster rate than the uncatalysed bead, thereby generating a temperature differential between the two beads. The electrical resistance of the beads is dependant upon temperature and so there is now a difference in resistance of the two beads. The current flowing in each of the beads is the same and hence the voltage drop across each of the beads is different and can be measured as an electrical output.

Pellisters detect the presence of any flammable gas but cannot distinguish between different gases. They also require an oxygen concentration of 12-15% in order to oxidise the gas and thus cannot detect gas concentrations if the oxygen level is low. This may lead to errors in the case of large gas leaks from underground pipes when the soil oxygen concentration may be very low. Errors in measurement may also occur for gas concentrations above the upper explosive limit (UEL) due to the reduced oxygen

concentration in the natural gas / oxygen mixture. Catalytic sensors are also "poisoned" in the presence of H_2S, which is often present in anaerobic soil. For this reason the use of pellisters alone was unsuitable for this project.

2.2.2 Thermal conductivity

Thermal conductivity is a measure of how well a material conducts heat and is a property that can be used to differentiate between different gases. Measurements are made of the difference in thermal conductivity of the sample stream relative to air. The advantage of this type of sensor is that it can be used to detect concentrations up to 100% by volume of gas present in the reference gas, usually air. However, it cannot distinguish between gases that have the same thermal conductivity. The thermal conductivity [5] of air is 0.0241 W m^{-1} K^{-1}, whereas that of methane is 0.0302 W m^{-1} K^{-1}. Thus differences in the thermal conductivity can be used to measure the methane concentration. However, the thermal conductivity of carbon dioxide also differs greatly from air (0.0145 W m^{-1} K^{-1}) and so high concentrations of carbon dioxide in the sample will affect the determination of methane concentration. Only when the methane concentration is high, as is the case close to a gas leak, will thermal conductivity give good results, as the concentration of carbon dioxide will then be low.

2.2.3 Flame ionisation

Flame ionisation sensors are based on recording the increase in ions produced when a combustible material passes through a hydrogen/air flame. This method is very sensitive but there must be sufficient oxygen to allow efficient combustion of the

---

[5] Data for thermal conductivities of gases http://www.physicsofmatter.com/Book/Chapters/Chapter5/5.html Accessed on 18/10/01

material. The device also produces erroneous readings in the presence of high levels of CO_2. This method of methane detection would not be suitable for this project due to the high concentrations of methane expected and elevated CO_2 levels caused by oxidation of methane in the soil by methanotrophs. The sensor is also a potential ignition source and thus is not intrinsically safe and could pose a potential explosion risk in methane rich areas.

2.2.4 Infrared absorption

Infrared absorption is based on the measurement of the absorption of radiation in the infrared region of the electromagnetic spectrum. Infrared analysers are used for a wide range of gases and are very sensitive and selective. The advantage of this system is that it does not consume the sample, and does not require an oxygen supply. However, the infrared spectra of some gases, especially hydrocarbons, often overlap and this can create difficulties in selecting a measuring wavelength unique to the gas of interest. The presence of water in the gas sample will also affect the readings as this has a broad band of absorption in the infrared, and so this method is unsuitable for detection of gas in soil samples.

2.2.5 Photoacoustic spectroscopy

Photoacoustic spectroscopy is based on the photoacoustic effect, in which the absorption of modulated light by a gaseous compound results in the generation of sound waves. It has been identified as an ultrasensitive technique for the monitoring and analysing of trace gases (Liang *et al.* 2000). Solid-state light sources such as optical parametric oscillators are used to excite the sample gases in the infrared region and photoacoustic detectors used to measure absorption at 3.34 μm. However, the complex tuning required limits the potential use of this device in field applications.

Diode lasers, which have been used for photoacoustic measurements of methane absorption in the near-infrared (NIR) spectral region at 1660 nm, have the advantage that they work at room temperature, but they have low absorption coefficients in the NIR. Sensitivities of 10 ppmV have been obtained which may be satisfactory for industrial applications but not for methane detection in the atmosphere where a sensitivity of at least 100 ppbV is needed (Liang *et al.* 2000).

2.2.6 Instrument selection

The instrument selected for this research was a Gasurveyor Mk II, (GMI instruments, Renfrewshire). This instrument uses a combination of sensors to measure the concentration of methane in air, in the ranges 0-1000 ppm, 0-100% LEL and 0-100% volume. It uses pellister-type technology to detect low levels of gas up to 100% LEL (5% volume) and then automatically switches to a sensor that measures the thermal conductivity of the gas when concentrations of gas between 5 and 100% volume are detected (Personal communication, GMI instruments).

2.3 Effect of natural gas on soil

Methane is produced naturally in soils exposed to reducing conditions such as flooding (for example rice fields) or oxygen deprivation, (for example in landfill sites). As soils become progressively more reduced then anaerobic decomposition of soil organic matter will produce methane and carbon dioxide. Table 2.1 illustrates the changes that occur as the redox potential of the soil changes. Natural gas released into the soil from leaking pipelines may have many secondary effects on both the microbial constituents and the chemistry of the soil.

Table 2.1 Reactions occurring in reducing soils. (Adapted from Marschner 1995)

Stage	Redox range (mV)	Active redox reaction
1	(+550)-(+450)	$NO_3^- \rightarrow N_2O, NO, N_2$
2	(+450)-(+350)	$MnO_2 \rightarrow Mn^{2+}$
3	330	Absence of free O_2
4	200	Absence of NO_3^-
5	(+150) –(-100)	$Fe(OH)_3 \rightarrow Fe^{2+}$
6	<(-50)	$SO_4^{2-} \rightarrow S^{2-}, H_2S$
7	<(-200)	$CO_2 \rightarrow CH_4$

The structure and appearance of soil can be affected by the leakage of natural gas. Schollenberger (1930) and Hoeks (1972) found that the gassed soil was darker than ungassed soil, and the normal structure of the soil was lost, affecting drainage so that the soil constantly puddled. Godwin *et al.* (1990) also found that the soil drainage was decreased in the vicinity of gas wells and that puddles formed at the surface.

Effects on nitrate concentration in gassed soils have also been observed (stage 1 of Table 2.1). Arif and Verstraete (1995) placed 5 kg samples of soils and 2 L of methane in sealed containers and incubated them at 22°C. They found that during soil methane incubation there was a large loss of nitrate (56 –90%), possibly due to denitrification as a result of loss of oxygen in the soil. This might lead to nitrate deficiency in the soil with subsequent plant growth reduction. However, Schollenberger (1930), Davis *et al.* (1964) and Coty (1967) reported increased total nitrogen concentration in soil near gas leaks due to the presence of some methane

oxidising bacteria capable of fixing atmospheric nitrogen. Harper (1939) suggested that increased nitrate in gassed soils might have been due to nitrogen fixation by *Clostridium spp* under anaerobic conditions and that the hydrocarbons in the gas were supplying the necessary energy for the growth of these microorganisms. Godwin *et al.* (1990) found a marked increase in ammonium-nitrogen close to gas wells, caused by ammonium release by decomposition of organic matter that had not been converted to nitrate due to the lack of oxygen. Further from the gas wells where more oxygen was available they found more nitrate.

Increases in organic matter have also been reported in soils affected by leaking methane. Hoeks (1972) found that the amount of soil organic matter in a gassed zone rose from 3.5 to 4.1%, and Godwin *et al.* (1990) also found a build up of organic matter in soil closest to a gas well. This is due to the increased bacterial activity and production of bacterial biomass, which can result in a build-up of waxy organic matter referred to as "paraffin dirt" (Schollenberger 1930).

Changes in soil chemistry can occur quickly, with almost all of the oxygen disappearing from the soil within a day of oxygen displacement. Nitrate disappears within 2-3 days and reduction of Fe^{3+} and Mn^{4+} occurs 1-3 and 2-4 weeks after displacement respectively (Ponnamperuma 1972). The soils become highly reduced due to the displacement of oxygen by the leaking methane. Methanotrophic activity can also increase the use of soil oxygen, causing further soil reduction. The availability of soil minerals is increased. Available manganese (Mn^{2+}) concentrations (up to 64 ppm) and iron (Fe^{2+}) were found by Schollenberger (1930) and Adams and Ellis (1960), and increased levels of manganese, iron, zinc and copper were found by Godwin *et al.* (1990). The alteration of the soil chemistry due to decreasing redox

potential caused by lack of oxygen at the root area may be one of the main causes of reduced plant growth in gas-affected areas. Both manganese and iron are essential minerals for plant growth. Manganese deficiency can reduce plant growth, but toxic levels of manganese, possibly as low as 4 ppm, can interfere with iron use by the plant and thus cause stress symptoms.

2.3.1 Methane oxidation in soil

Methane released into soil can be oxidised by methanotrophs present in the soil. Several species of methane-oxidising bacteria (e.g. *Methanomonas methanooxidans*) exist in the soil and are most abundant where methane and oxygen are present. The bacteria are highly active in an atmosphere of 10 – 40% O_2, up to 70% CH_4 and 5-20% CO_2 (Williams 1989). The soil microbial community adapts rapidly to elevated methane concentration and can effectively reduce methane levels. Bogner *et al.* (1997) found that it took about 2 weeks for the development of a methanotrophic bacterial population around a new gas leak. Hoeks (1972) found that in normal soil with no methane leakage the population of methanotrophs was small and oxidation of methane was low, but in a soil affected by gas leaks there was a strong increase in oxygen consumption after 4-5 weeks as the bacterial population increased and oxidised the methane. Arif and Verstraete (1995) incubated mineral-enriched soil with methane (10% v/v), and found that on the first addition of methane to the soil the methane was completely oxidised within 5 days. On subsequent methane additions, oxidation was accelerated and occurred within one day. They found a large increase in the soil microbial biomass utilising the methane as a source of energy.

Induction of methane oxidation by methanotrophs is influenced by soil properties such as soil type, structure, moisture and temperature. Hoeks (1972) reported oxidation

rates of 0.3 ml min^{-1} kg^{-1} of soil for methane leakage from natural gas pipes and found that methane oxidation is influenced by oxygen availability, carbon dioxide production, methane concentration and soil temperature. As induction of oxidation is oxygen dependant, it may present a strain on the oxygen supply in the soil. The optimum soil pH required for induction of oxidation is around neutrality and the optimum temperature is 25-35°C (Bender and Conrad 1995, Whalen *et al.* 1990). Soils will rarely reach this temperature in the UK and thus the conditions for oxidation will rarely be optimal. At low temperatures microbial activity decreases and the effect on the soil by the bacteria is reduced (Bender and Conrad 1995, Hoeks 1972). Bogner *et al.* (1997) found that soil moisture was a crucial factor affecting methane concentration in the soil because it influences both the movement of gases through the soil and the microbial activity.

Czepial *et al.* (1995) showed that methane oxidation rates were dependent upon soil depth, moisture and organic matter content. They found that the region of maximum oxidation potential was concentrated in a zone at 3–6 cm depth. Optimal soil moisture of 33% was needed as a balance between sufficient moisture to support the microbial community and the restricted diffusion of methane to the microbes at higher moisture levels due to the decreased diffusivity of methane in water. Organic matter of 14 % was also indicated for maximum oxidation of methane as high organic matter content affects soil texture by increasing pore volume, lowering bulk density and decreasing volumetric water content.

Lamb *et al.* (1996) studied oxidation of methane from simulated pipeline leaks in Washington, USA, and found that in the summer months when soil temperatures were at about 30°C methane oxidation was 90-95%. When temperatures were lower

(6-8°C) the oxidation rate fell to 10-30%. At high leak rates (250 cm^3 min^{-1}) the oxidation rate decreased due to the decreased residence time of the methane in the soil but with low to medium leak rates a high proportion (50-72%) of the methane is oxidised in the soil. They also found that oxidation of methane increased linearly with distance from the source.

Bacterial activity can thus be seen to lead to a reduction in the amount of methane present in the soil but in the process oxygen is consumed and so may exacerbate any vegetation stress effects due to lack of oxygen at the roots.

2.4 Effect of natural gas on vegetation

Natural gas may affect vegetation in many ways. The gas may be taken into the plant via the root system where it may be metabolised or passed through the plant in the transpiration stream. Alternatively natural gas may alter the soil environment so that plant stress is a secondary effect of the leaking gas.

Methane has not been shown to be toxic to plants. Aerial contact of plants with natural gas has not been shown to have any harmful effects. Various plants including tomato, sunflower, cyclamen and marigold showed no signs of altered growth or epinasty (a change in the angle between the petiole and the stem) when exposed to concentrations of 2% methane in air for up to 21 days (Gustafson 1944).

The main damaging effect on plant growth of natural gas leaking from pipelines into the soil is thought to be due to the displacement of soil oxygen. Arthur *et al.* (1985), when exposing tomato plants (*Solarnum lycopersicum*) to various root concentrations of methane, oxygen and carbon dioxide, found that methane concentrations of up to 45%, while not seen to be toxic during the first 8 days of exposure, were associated

with severe reductions in soil oxygen (to 2%), that were believed to be the cause of plant decline during the second week of exposure. When studying the growth of green ash (*Fraxinus lanceolata*) and hybrid poplar (*Populus spp.*) trees on a reclaimed landfill site, Gilman *et al.* (1982) found that saplings were better able to adapt to the conditions than more mature trees. This was due to the shallower rooting of the younger trees enabling adaptation to the landfill soil. Older trees had deeper roots and the high soil-gas environment of the landfill site (13.1% CO_2, 7.3% CH_4, 12.3% O_2) caused root death before the roots were able to grow towards the surface where oxygen was present.

Schollenberger (1930) observed that oats (A*vena L.*) germinated well on a methane-saturated soil but soon ceased to grow and died shortly after germination. This was associated with a marked increase in exchangeable manganese produced in reducing soils. Black (1957) suggested that as little as 4 ppm of exchangeable manganese could depress the yields of crops such as soybean, barley and corn, whilst 1 to 10 ppm damaged legume stands.

Natural gas effects on the soil and vegetation could also be due to the production of toxins by other microbial populations. Adamse *et al.* (1972) isolated methane-oxidising fungi from gassed soils. One of these, a green fungus, (possibly *Penicillium janthinellum*) produced ethylene in concentrations of up to 446 ppm in the soil air space. Ethylene in concentrations of 0.1-1.0 ppm in the soil atmosphere is harmful to plants causing inhibition of seminal roots and epinasty of the leaves.

The effects of contamination by natural gas leakage that have been observed on plants include restricted growth and reproduction, and decreased numbers of individuals (Adams and Ellis 1960, Arthur *et al.* 1985, Pysek and Pysek 1989, Godwin *et al.*

1990), or a change in the green colour of the leaves (Schollenberger 1930, Arthur *et al.* 1985, Pysek and Pysek 1989). Pysek and Pysek (1989) also found a shift in development stage in potato, sunflower and corn, deformation of underground organs, increased stomatal numbers and changes in the reflectance curves of the leaves showing a decrease in the near infrared reflectance.

Plants under stress may also be more likely to be attacked by rhizovores (Van Noordwijk *et al.* 1998). Some pathogenic fungi develop in conditions of oxygen deficiency or excessive carbon dioxide. Plant diseases occurring in conditions of oxygen deficiency may be due either to a decrease of the plant's resistance to infestation or to an increase in the population of pathogens in the soil. In soybean an oxygen shortage decreases the tissue content of phytoalexine, the compound that increases the resistance of the plant to disease (Glinski and Stepniewski 1985).

2.5 Effect of oxygen displacement from soil on vegetation

The gaseous composition of a well-aerated soil is similar to that of the external air because oxygen is rapidly replaced by diffusion and CO_2 is readily vented to the outside. However, in a poorly vented soil the air composition is much more variable and will depend on the time of year, temperature, soil moisture, depth, root growth, microbial activity, pH and the exchange of gases. Carbon dioxide concentration in the atmosphere is approximately 0.036% but in the soil may reach levels of 0.36% due to the oxidation of organic matter. An increase in CO_2 will be associated with a decrease in the concentration of O_2 (Hillel 1998). About 2.5 days supply of oxygen for respiration of plants and soil organisms is stored in the ground unless it is replaced by diffusion (Hillel 1998), and thus displacement of O_2 by mass flow of methane from

leaking pipelines and oxidation of the methane by bacteria can lead to severely decreased concentrations of O_2 and increased concentrations of CO_2 in the soil.

Plant roots have many functions. They are responsible for anchoring the plant in the soil, for the absorption of nutrients and water from the soil (for the growth of shoots), for the synthesis of plant hormones and plant growth regulators and in some plants they also act as food storage organs. In order to function correctly, roots need oxygen and this is generally obtained from the soil. Oxygen is required for aerobic respiration and the supply of metabolic energy, which is used for the production of new root cells for growth and for the uptake of nutrients from the soil (de Wit 1978).

It has been suggested that for the proper functioning of a healthy root system, a minimum oxygen content of the soil atmosphere of some 12-14% is needed (Adamse *et al.* 1972). Normal soil oxygen concentration is about 20% - similar to the external atmosphere. However, there are disagreements in the literature about the amount of oxygen needed in the soil, to prevent impairment of the root system. Drew (1983) suggested a wide range of partial pressure of O_2 at which root functions begin to be restricted. Some workers show that root extension rates are unaffected at O_2 concentrations as low as 0.02 atm (0.4 % O_2) whilst other workers show that root extension was slowed at concentrations of 0.1 atm (2 %). Greenwood (1968) suggested that aerobic respiration of the roots was unlikely to be impeded unless the O_2 concentration in the root approached zero but in 1971 Greenwood and Goodman showed that root elongation in mustard seedlings (*Brassica cretica*) stopped when the partial pressure of O_2 in solution was 0.005 atm (0.1%). Sojka *et al.* (1975) stated that plants are affected both indirectly by decreased O_2 concentration that influences nutrient availability and the ionic species present in the soil, and directly by affecting

the metabolic rates and pathways within the plant. They found that at 7% soil-O_2 the maximum respiration rate for wheat was reduced by 50% and that visible effects of retarded growth and chlorosis could be related to loss of nitrogen availability due to denitrification. Trought and Drew (1980a) found that in wheat (*Triticum L.*), the earliest effect of waterlogging was the failure to guttate, which was observed after only 6 hours when the O_2 concentration in the soil was still at about 10%. After 2 days of waterlogging, chlorophyll degradation in the leaf had begun and by 15 days of waterlogging the first 3 leaves had turned yellow. Drew and Sisworo (1979) found similar results in waterlogged barley, thus suggesting that even mild oxygen depletion from the soil can have significant effects on the normal functioning of plants.

Observed effects on plants of oxygen depletion in the soil include yellowing, wilting or epinasty of the leaves (an unequal cell expansion in the petioles leading to a downward bending of the leaves resulting from excessive growth to the upper surface) and inhibition of root and shoot growth (de Wit 1978, Drew and Lynch 1980, Anderson and Perry 1996). Absorption of minerals such as potassium, nitrate and phosphate may be inhibited immediately on the onset of O_2 depletion from the soil (Trought and Drew 1980b) but water absorption may only be inhibited after long periods of anaerobis.

Accumulation of CO_2 in the soil may affect the water permeability of roots more directly than O_2 deficiency and a build up of inhibitory concentrations of ethylene in anaerobic soils may affect plant growth (de Wit 1978, Trought and Drew 1980). Leaf chlorosis has been correlated with increased internal concentrations of ethylene in aerial tissues of bean and tomato growing in waterlogged soil. Ethylene also promotes epinasty in tomatoes (Drew and Lynch 1980).

Trought and Drew (1980a) suggested that O_2 depletion might cause disruption of the root metabolism that affects hormone balance of the shoot.

Oxygen-stressed roots exude greater amounts of soluble metabolites and ethanol and these may stimulate chemotactic movement of zoospores leading to susceptibility to disease. Biosynthesis of phytoalexins is sensitive to the partial pressure of oxygen and increased susceptibility to attack may arise indirectly from the poor nutrient status of the plant (Drew and Lynch 1980).

The inhibition of root growth due to inadequate oxygen in the soil may mean that the root system becomes inadequate to meet the requirements of the shoot and the smaller root system will no longer be a sufficient sink for assimilates produced in the leaves and may thus feed-back inhibition of photosynthesis in the leaves leading to reduced productivity in the plant.

In general, oxygen displacement from the soil, whether by waterlogging, by natural gas leakage from pipelines or other causes has a deleterious effect on vegetation growing in the soil leading to decreased growth, chlorosis and disease.

2.6 Remote sensing

The broad definition of remote sensing is the gathering of information about an object from a distance, without physical contact. Remote sensing can be carried out by satellites or aircraft. Laboratory based spectroradiometers are used to establish and test basic relationships between spectral signals and biophysical variables. The advantage of satellite remote sensing over aerial photography is that satellites operate at a greater height and can thus observe a larger area, with less distortion than aircraft. As satellites orbit the earth they automatically repeat coverage of a given area of land on a

regular basis and thus monitoring of changes in landscape processes can be carried out. The disadvantage of satellite remote monitoring is that atmospheric attenuation and scattering distort the biological signal, which then requires correction.

Problems arise when using satellite remote sensing to monitor vegetation, due to the presence of cloud. In the visible and infrared regions clear images cannot be obtained through cloud cover. Thus, if relying on an orbiting satellite for data, changes in vegetation images may only be available infrequently, particularly in the UK where the probability of clear skies coinciding with the passage of the satellite is low. Using data from a feasibility study from 1990 it was found that the number of days with less than 2 oktas cloud cover between June and September sampled by the SPOT (orbiting 11 times every 26 days) and Landsat (orbiting once every 16 days), systems were between 2 and 9 days (Steven *et al.* 1997). This would be insufficient for monitoring vegetation growing above pipelines that are at present monitored on a fortnightly basis.

The resolution of features by satellite can also be a problem. Spatial resolution is the minimum detectable feature size on the ground that can be seen using a satellite sensor system, and is a measure of the ability to distinguish small features on the land surface. When observing land vegetation, features smaller than the spatial resolution may not be seen, and thus individual fields may be identified but the detail of the vegetation within the field may not be differentiated. A resolution of 10 m would not be sufficient for monitoring pipelines, as finer detail will need to be resolved within fields to identify any areas of stress caused by leaks. However, a resolution of 1 m would enable vegetation damage caused by leaking pipelines to be monitored.

The Landsat 7 [6] Thematic Mapper has a spatial resolution of 15 m, and SPOT 4 HRV (High Resolution Visible Imaging System)[6] has a resolution of 10-20 m (SPOT 5 due to be launched in 2002 will have a higher ground resolution of 2.5 and 5 m in the panchromatic range and of 10 m in multispectral mode). These satellites are still insufficient for monitoring pipelines. However, in 1999 IKONOS [6,7] was launched, giving the highest spatial resolution currently available from a satellite. IKONOS is able to revisit every 3 days, providing 1 m resolution in the panchromatic range (450 - 900 nm) and 4 m resolution in the multispectral range and this would probably be suitable for monitoring pipelines if weather conditions allowed images to be collected.

Spectral resolution describes the detail with which the spectral characteristics of the Earth can be measured. Satellites often only measure in a few bands of the electromagnetic spectrum, for example the Landsat Thematic Mapper measures 7 bands between 450 and 2350 nm and SPOT HRV measures 3 between 500 and 900 nm [6,7]. Hence they cannot measure the full spectral signature of the surface to be viewed. However, the more prominent features can be detected, for example the difference between the red and near-infrared reflectance from vegetation. A laboratory-based spectroradiometer may measure the spectral reflectance in several hundred narrow bands and thus has very high spectral resolution. Orbview-4 [6,7], launched in 2001, was due to be the first truly hyperspectral satellite in orbit, with a 200 channel hyperspectral sensor (400 –2500 nm) with an 8 m resolution. However, it failed to reach orbit.

---

[6] NERC Earth observation data centre http://www.neodc.rl.ac.uk Accessed on 8/1/02

[7] Remote sensing instruments database http://www.es.ucsc.edu Accessed on 14/1/02

The Hyperion instrument onboard the EO-1 satellite provides a high resolution hyperspectral imager capable of resolving 220 spectral bands (from 400 to 2500 nm) with a 30 m resolution. Although spectral resolution is improved on this sensor the spatial resolution is inadequate for monitoring pipelines[8]. The Quickbird sensor, which was launched in October 2001 is able to offer panchromatic images (450 - 900 nm) at 61 cm resolution and 4 multi-spectral wavebands (450-900 nm) at 2.5 m resolution[9]. It is possible that images obtained by Quickbird will have the resolution capable of detecting leaks from gas pipelines.

Airborne systems have the advantages over satellites that they are simple, reliable and inexpensive means of acquiring remotely sensed images (Campbell 1996). They can fly on demand, they are not limited by cloud cover as they can fly beneath it, and they are not constrained by an orbit and so can cover an area as often as is necessary.

[8] http://eo1.gsfc.nasa.gov/Technology/Hyperion.html Accessed on 30/5/02

[9] http://www.digitalglobe.com/?goto=products/qb_standard Accessed on 30/5/02

The remote sensing equipment carried may be able to give greater spectral resolution, for example the HyMap sensor, which covers the range 440 to 2500 nm with 128 wavebands. However, it is not always possible for the pilot of an aircraft to maintain a straight course, which may leave gaps in the data (Barrett and Curtis 1976). Poor weather, for example high winds, may stop flying even if conditions would not stop the collection of data.

Changes in vegetation above a pipeline are generally in the range of about 2 m diameter (See Chapter 6), so in order to monitor vegetation change due to leaking gas pipes, satellite images with a spatial resolution of about 1 m would be required. A regular repeat visit by the satellite is also required to ensure that sufficient images were collected to comply with the present monitoring policy to monitor pipeline security. A repeat visit every 3 days would probably provide sufficient images during the summer months, but during the winter months the cloud cover in the UK would not enable scans to be taken frequently enough. Vegetation change due to gas leakage is likely to be slow in developing and so approximately four images per year would probably be sufficient to detect vegetation change due to leakage. Table 2.2 summarises features of some of the remote sensing instruments currently available or due to be launched on satellites.

Table 2.2 Features of remote sensing instruments (adapted from NERC Earth Observation data centre[6] and Remote Sensing Instrument Database[7])

Instrument	Spatial resolution (m)	Spectral resolution (nm)	No of bands	Return visit (days)	Launch date
HyMap	2-10	440-2500	128	On demand	Attached to aircraft
Hyperion	30	400-2500	220	3	Dec 2000
IKONOS 2	4	450 – 900 (Vis and NIR)	4	3	1999
IKONOS 2	1	450 – 900 (Panchromatic)	1	3	1999
Landsat 7	30	450-2350	7	16	1999
Orbview-4	4	VIS-NIR	4	2-3	2001 –did not achieve orbit
Orbview-4	8	400-2500	200	2-3	2001 –did not achieve orbit
Quickbird	0.61	450-900 (Panchromatic)	1	3	Oct 2000
Quickbird	2.5	450-900 (Vis and NIR)	4	3	
SPOT 4	20	500 –890 (Vis and NIR)	3	2-3	1998
SPOT 4	10	510 –730 (Panchromatic)	1	2-3	1998
SPOT 5	10	500 –890 (Vis and NIR)	3	2-3	2002
SPOT 5	2.5 -5	510 -730 (Panchromatic)	1	2-3	2002

2.6.1 Spectral signatures

The distinct pattern of reflectivity of an object is termed its spectral signature and can be used to identify surface objects. Vegetation has a characteristic spectral signature in the solar radiation wavebands (Figure 2.1). It has low reflectance (typically about 5%) in the visible wavebands (400-700 nm) and a very steep rise at about 700 nm to about 50% reflectance in the near infrared. This spectral signature can be explained by the structure and chemical composition of the leaf. Leaves contain chlorophyll and other pigments such as carotenes, xanthophylls, anthocyanin and amaranthin that absorb light strongly in the visible wavelengths and therefore have low reflectance. The exception is the small amount of green light that is reflected by chlorophyll. Chlorophyll, the major absorber of light in leaves, is contained mainly in the palisade tissue layer and comprises two forms. Chlorophyll *a* is found in all, and chlorophyll *b* in most, photosynthesising plants. Most pigments absorb in the blue region in the vicinity of 445 nm but only chlorophyll absorbs in the red at 645 nm (Gates *et al.* 1965). Near infrared light is not significantly absorbed or transmitted by pigments in the leaf and thus the reflectance is greater beyond 700 nm. At longer wavelengths (beyond 1350 nm) there is a decrease in reflectance as more radiation is absorbed by water within the leaf. The structure of the leaf, with many air-water interfaces, makes a very strong scattering medium that causes high reflectance and transmittance in any region where absorbance is low (Wooley 1971). Table 2.3 shows some of the features observed in vegetation spectra.

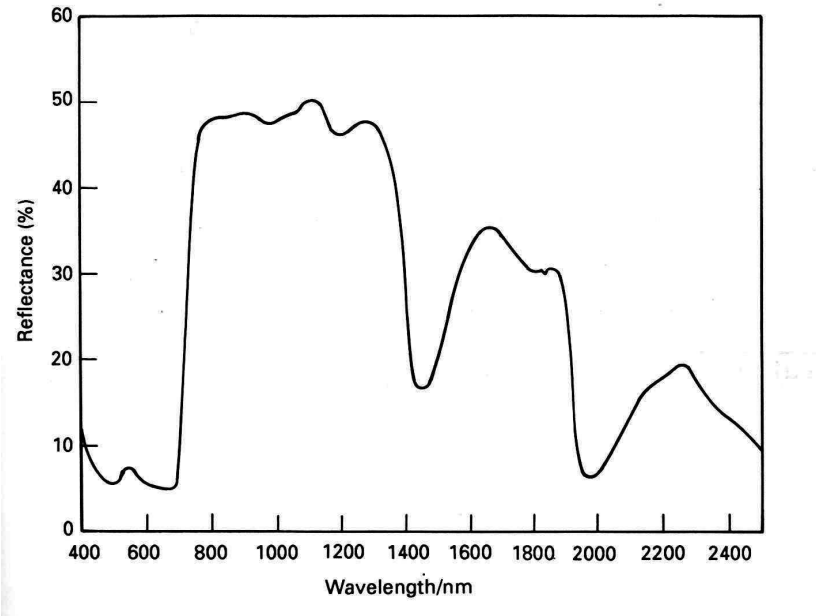

Figure 2.1 Spectral signature of a sycamore leaf, relative to a barium sulphate panel (Steven *et al.* 1990).

Table 2.3 Spectral features observed in vegetation spectra. (adapted from Zwiggelaar (1998)

Wavelength (nm)	Spectral feature	Contributing factor
380	Weak absorption	Atmosphere
435	Strong absorption	Chlorophyll a
480	Strong absorption	Chlorophyll b
420-480	Strong absorption	Carotene
400-550	Absorption	Anthocyanin
550	Strong reflectance	Chlorophyll
670-680	Strong absorption	Chlorophyll a, b
760	Strong absorption	Water, Oxygen
970	Weak absorption	Water

1450	Strong absorption	Water, CO_2

The sharp change in reflectance between wavelengths at 690 and 740 nm is termed the "red-edge" and characterises the boundary between the strong absorption of red light by chlorophyll and the increased multiple scattering of radiation in the leaf mesophyll and the absence of absorption by pigments in the near-infrared wavelengths (Wooley 1971, Gausman 1985, Curran *et al.* 1991). Information on the red-edge position provides a useful indicator of chlorophyll concentration, which can then be used as an indicator of vegetation productivity or stress.

2.6.2 Vegetation stress.

Larcher (1987) described vegetation stress as:

> *"..a state in which increasing demands made upon a plant lead to an initial destabilisation of functions…if the limits of tolerance are exceeded and the adaptive capacity is overworked, the result may be permanent damage or even death".*

Lichtenthaler (1988) suggested that a mild stress may activate cell metabolism and increase the physiological activity of the plant, without causing any damaging effects even at long duration. However, high stress will cause damage to the plant and induce early senescence and finally death if the stressor is not removed.

Plant stress can be induced by a variety of natural and anthropogenic stress factors. Stress effects in plants may manifest themselves by showing decreased or increased growth (hyperplasia) or decreased levels of chlorophyll leading to chlorosis of the leaves and thus decreased photosynthesis. These changes could be detected using remote sensing, but many stress effects are difficult to detect because they vary rapidly

or occur on fine spatial scales that are not detectable on the satellite imagery that is currently available. Chlorosis, yellowing of the vegetation, occurs in response to mineral deficiencies and diseases and so should be detectable by remote sensing as an increase in reflectance in the yellow wavelengths (around 580 nm) but although stress of the plants can be identified, it is difficult to determine the cause of the response, because chlorosis is a general plant response to many stresses (Carter 1993). Drought can produce canopy and temperature changes that should be detectable in the infrared wavelengths but which are difficult to differentiate from other stress and temperature-related effects, as plants tend to have a limited number of responses to a range of stresses. For example drought and fungal infection both produce similar effects in the infrared (Carter 1993). So, it should be possible to show that vegetation is stressed but it is difficult to identify exactly what is causing the stress.

Reflectance measurements via airborne or ground based spectroradiometers have been used to detect stress in plants in the field and laboratory.

2.6.2.1 Remote sensing of chlorophyll content

Many studies have been carried out to correlate spectral variations with chlorophyll content and thus enable detection of stress by measuring decreased chlorophyll content and chlorosis. The aim of this research has been to estimate photosynthetic pigments non-destructively using hyperspectral remote sensing.

The point of maximum slope of the "red-edge" has been positively correlated with chlorophyll concentration (Miller *et al.* 1990), and increases in chlorophyll concentration during seasonal development of the leaves produce a deepening and broadening of the chlorophyll absorption feature, which in turn move the boundary of

the red-edge to longer wavelengths. Conversly Horler *et al.* (1983) found that chlorotic leaves had higher reflectance in the visible wavelengths, with the greatest effect being found at 540 nm and that the red-edge was shifted towards shorter wavelengths. The chlorophyll content of a leaf was closely correlated with the red-edge shift. Close correlation between chlorophyll content and reflectance at 550 and 700 nm was also found by Gitelson and Merzylak (1997), who found that reflectance near 700 nm and in the range 530-630 nm were the only features to be sensitive to chlorophyll content over a wide range of chlorophyll variation. Curran *et al.* (1991), however, found that leaves with a high concentration of amaranthin (a red, non-chlorophyll pigment) showed no correlation between chlorophyll content and the red-edge. Thus, if plant stress leads to an increase in red pigmentation, such as occurs with phosphorus deficiency, then the use of red-edge measurements to detect decreased chlorophyll content as a result of stress may be ineffective.

Chappelle *et al.* (1992) found that the concentration of chlorophyll *a* had a strong linear relationship with the reflectance ratio R_{675}/R_{700}, (where R_{675} is the reflectance at 675 nm and R_{700} is the reflectance at 700 nm), whereas the concentration of chlorophyll *b* was related best to $R_{675}/(R_{675}xR_{700})$. Although this may work well at the leaf level it is not so consistent for canopies due to the effect of variations in background properties, and the effect of leaf layering and canopy structure (Chappelle *et al.* 1992, Carter 1998).

A pigment-specific simple ratio, $PSSR=R_{800}/R_{680}$ was found by Blackburn (1998) to have the strongest linear relationship with chlorophyll concentration in canopies. The optimum individual waveband for pigment estimation was 680 nm for chlorophyll *a*, 635 nm for chlorophyll *b* and 470 nm for carotenoids. A further reflectance index has

been proposed by Datt (1998), who used the index $(R_{850}-R_{710})/(R_{850}-R_{680})$ to determine the chlorophyll content of Eucalyptus leaves and found that it was insensitive to the effects of leaf scattering on reflectance and related strongly to the variation in reflectance caused by chlorophyll absorption.

2.6.2.2 Remote sensing of drought stress

Drought or water deficiency is thought to cause an increase in the red and infrared reflectance of canopies, due to chlorophyll breakdown and collapse of internal cell walls resulting in fewer internal reflective surfaces. The greatest increase in reflectance due to water loss is in the 1300-2500 nm range. As water is lost from the leaf, the number of boundaries between wet cell walls and intercellular air increases, thereby increasing the intensity of multiple reflections within the leaf (Carter 1991). Reflectance also increases in the 400-1300 nm range due to the secondary effects of the influence of water on the absorption of pigments and on wavelength-independent processes such as multiple reflections in the leaf (Carter 1991). Carter (1993) found that dehydration caused a peak in the yellow spectrum at 584 nm and Wooley (1971) found that reflectance at 580 nm increased as a leaf became less turgid but that the amount of change varied with leaf type. As the relative water content of a leaf decreased from 97 to 77%, reflectance from maize leaves increased, that from soybean leaves showed little change and that from cotton leaves decreased. Horler *et al.* (1983) found that small weight losses due to dehydration of the leaves caused small shifts of the red-edge to longer wavelengths, whereas larger weight loss of up to 35% caused a shift to shorter wavelengths due to a rise in reflectance at 675 nm caused by chlorophyll breakdown. Curran and Milton (1983) found that a cress canopy growing on a background of light grey cotton wool and subjected to drought stress did not

suffer from chlorophyll degradation and that the increase in red and infrared reflectance was due to a decrease in leaf area and an increase in the visible area of background.

2.6.2.3 Remote sensing of stress caused by waterlogging

Similarly to drought stress, Anderson and Perry (1996) found that flooded trees in wetland areas also showed elevated reflectance at 550 nm and in the near infrared at 770 nm when compared to non-flooded trees. Pickering and Malthus (1998) were able to locate a small leak from an aqueduct in Cheshire. The leak showed severe waterlogging of the soil and vegetation within the area was stunted, yellow and sparse. The centre of the leak had a higher visible reflectance and lower near-infrared reflectance compared to the surrounding unstressed vegetation.

2.6.2.4 Remote sensing of nutrient stress

Stress due to increased levels of toxic minerals and decreased levels of essential nutrients and micronutrients can cause changes in reflectance. Plants growing in soil containing high concentrations of metals show increased reflectance between 550 and 650 nm and a shift to shorter wavelengths of the red-edge. This was observed with greenhouse-grown hosta and soybean plants growing in soil contaminated with arsenic, cobalt, copper, nickel and zinc (Milton *et al.* 1989). Heavy metal damage to beech trees caused a gradual increase in reflectance from 13% to 22% in the green (525 nm) to yellow (575 nm) spectral range, and a shift of the red-edge to shorter wavelengths with increasing tree damage (Hoque and Hutzler 1992).

Phosphorus is essential at all phases of growth, and its deficiency is found to produce similar spectral changes to those found from soil contaminated with toxic metallic

elements. This is because phosphorus interacts in the soil with micronutrients such as copper, zinc, and molybdenum and binds with the potentially toxic elements aluminium, iron, and manganese, making them unavailable to plants. When phosphorus is deficient these elements are mobilised in the soil and are taken up by plants thus causing toxic effects (Milton *et al.* 1991).

In a study of mineral deficiencies, Masoni *et al.* (1996) found that all growth minerals caused modifications to the leaf absorption, reflection and transmission with the greatest variations at 555 and 700 nm, but it was difficult to determine the cause of the change in reflectance, i.e. between slight iron deficiency and severe magnesium deficiency. Variations in reflectance did not occur in the infrared between mineral deficient and normal plants. Thus in order to identify the stress causing spectral changes it is necessary to know both the plant species and the mineral involved.

Filella and Penuelas (1994) found that nitrogen-limited pepper (*Capsicum annuum*) plants showed higher reflectance in the visible and lower reflectance in the infrared, a shift towards shorter wavelengths and a decrease in the red-edge amplitude. These effects were not found with bean plants as nitrogen fixation compensated for low nitrogen fertilisation levels.

Iron deficiency decreases the amount of green pigment in plants, thus reducing photosynthetic rate and productivity. Mariotti *et al.* (1996) studied the effect of iron deficiency on both maize (*Zea mays* L.) and sunflower (*Helianthus annuus* L.) plants and found increased reflectance when iron was deficient. They also found that the red-edge shifted to shorter wavelengths although maize responded at a lower iron deficiency than sunflower.

2.6.2.5 Stress detection using remote sensing

Remote sensing has been used to detect stress in plants before visible symptoms have been observed. Carter (1993) used various stresses and plant species to detect changes in reflectance. He found that visible reflectance, particularly in the region near 550 nm and 710 nm, increased consistently in response to stress regardless of the stress agent or the species. The greatest changes occurred near 710 nm. Reflectance did not change in the infrared region with the exception of stress caused by fungal infection and dehydration, which gave differences at 1400, 1900, 2000 and 2400 nm. Changes due to fungal infection are due to the loss of reflective surfaces in the cells as the leaf spaces are invaded by fungal hyphae, further reducing reflection in the infrared. Carter and Miller (1994) found that reflectance within the 690-700 nm range is particularly sensitive to early stress-induced decreases in leaf chlorophyll content. When plots of soybean (*Glycine max* L.) were subjected to herbicide or drought stress, the reflectance sensitivity to stress-induced chlorosis was high in the 690-700 nm region, and remote sensing of vegetation in this band together with the 760 nm region (R_{694}/R_{760}) provided a means of early stress detection.

Carter *et al.* (1996) also tried to compare plant stress detection by narrow band reflectance with thermal infrared images. They found that herbicide-induced stress was detected by the increase in R_{694}/R_{760}, 16 days prior to the first visible signs of stress, whereas canopy temperature as indicated by imagery in the 8-12μm band never differed significantly between stressed and unstressed plots.

Airborne measurement of foliage stress on spruce trees at highly damaged sites due to air pollution detected a shift in the red-edge towards the blue of approximately 5 nm. This shift, which was due to a decline in chlorophyll in the pine needles, was detected

before visual symptoms became apparent and thus airborne monitoring may serve as an early indicator of forest damage (Rock *et al.* 1988).

Jago (1998) studied soil contamination at a former oil refinery site on the Isle of Grain, Kent. She used ground-based measurements with a field spectroradiometer to measure canopy biochemical concentration, and airborne imaging spectrometry to generate red-edge position images, and thus create maps of the red-edge position and canopy chlorophyll concentration. The uptake of oil by plants affects seed germination, reduces metabolite transport, respiration and photosynthetic rates. She used the correlation between the red-edge position map and canopy chlorophyll levels to estimate the levels of land contamination.

2.7 Remote sensing of hydrocarbons

Remote sensing has been used previously to detect hydrocarbon seepages although this has mainly been performed to aid in hydrocarbon exploration and is generally related to surface geochemistry. Detection of hydrocarbon seepages could indicate the presence of underground hydrocarbon wells. Macroseepage of hydrocarbons from underground oil reservoirs is shown by the visible presence of oil on the surface, whereas the invisible presence of hydrocarbons on the surface is termed microseepage. Detection of microseepage normally involves detecting the type of disturbance that would be produced by the hydrocarbon seep. Such seeps can only be detected in the visible and infrared regions if they cause some disturbance on the surface such as effects on the soil or vegetation.

Some remote sensing studies of vegetation change around hydrocarbon seepage have been carried out. De Oliveira (1996) studied hydrocarbon seepage in the Sao

Francisco basin, Brazil using digital image enhancement and found spectrally anomalous areas. They found that eucalyptus specimens in the anomalous areas were poorly developed and showed signs of nutritional deficiency. Airborne imagery of the eucalyptus stands using a Spectron spectroradiometer allowed the collection of reflectance spectra for the eucalyptus plantation. The data were averaged to obtain reflectance values simulating the spectral resolution of the Landsat TM. Higher reflectance values were observed for band 3 (chlorophyll absorption) for the sites under hydrocarbon influence. There was also a change in the internal structure of the canopy. De Oliveira *et al.* (1997) also studied the effect of hydrocarbon leakage on eucalyptus and grass leaves in a greenhouse simulation and found an overall increase in the reflectance of the plants affected by hydrocarbon leakage. A shift in the vegetation red-edge towards shorter wavelengths was observed, as was a decrease in soil reflectance.

Bammel and Birnie (1994) studied the spectral response of sagebrush (*Artemesia tridentata*) to determine its usefulness as a possible tool in commercial hydrocarbon exploration. They found that a consistent and significant blue shift of the green peak (560 nm) and red trough (670 nm) were the most reliable indicators of hydrocarbon-induced stress. In contrast, Yang *et al.* (1999) found a 7 nm shift of the red-edge towards longer wavelengths when studying the spectra of wheat affected by hydrocarbon microseepage. It was suggested that the hydrocarbons were serving as nutrients during the short growing season of the wheat.

Seepage of hydrocarbons from underground wells is likely to cover a larger area than that expected due to a leaking gas pipe, and hydrocarbon seepage from underground wells is likely to be in the unrefined state with a greater range of contaminants present.

Pipeline gas will have been refined to remove sulphur dioxide and other pollutants and odorants will have been added. Gas leaking from a pipeline will be more localised and thus the area of spectral change due to vegetation damage is likely to be smaller.

2.8 Conclusion

Very little work has been performed on the effects of leaking natural gas on the spectral characteristics of vegetation and of the latter's use as a method of early detection of leaking pipelines. The literature suggests that the main effect of the leaking gas is to displace the oxygen from the soil and it is the resulting anaerobism that leads to the plant stress. Many chemical changes in the soil have been identified as a result of leaking gas and these are generally due to the oxidation of the gas by methanotrophs (Schollenberger 1930, Davis *et al.* 1964, Coty 1967, Hoeks 1972, Godwin 1990). Some of these chemical changes can also have toxic effects on the plants, for example increased levels of ethylene in the soil or elevated levels of manganese in the soil solution (Schollenberger 1930, Adams and Ellis 1960, Hoeks 1972, Godwin 1990).

Symptoms of stress include low rates of shoot growth, wilting, leaf epinasty, senescence and chlorosis. Chlorosis of leaves is a symptom of nutrient deficiency as the production of chlorophyll is impaired. Changes in the level of chlorophyll or other pigments in the leaf can be detected as changes in the spectral characteristics of the leaf particularly in the visible wavelengths. Cell structure changes resulting from water stress can also be detected by changes in the spectral characteristics of the leaf. Remote sensing has been used by several researchers as a means of identifying stress with some results identifying stress effects up to 16 days before visible symptoms of stress occurred (Carter *et al.* 1996).

Natural gas leaking into the soil may lead to changes in the soil chemistry and soil air composition that may lead to the plant becoming deficient in water and some minerals necessary for optimum growth. Other changes may lead to the build up of toxic levels of some micronutrients in the soil solution that may also lead to stress in the plant.

In this study vegetation was subjected to leakage of natural gas and other methods of displacing the oxygen from the soil, to determine whether any spectral changes are a specific response to leaking natural gas or a generic response to lack of soil oxygen. High spectral resolution techniques were used to investigate changes in the reflectance spectra of the leaves with the objective of identifying specific wavelengths that could be used as a means of early leak detection.

3 Instrumentation and methods for pot trials

This chapter describes the instrumentation and methods used in the laboratory trials to determine the responses of various plant species to displacing oxygen from the soil. Other methods of oxygen displacement used were displacement by argon and nitrogen gases and waterlogging of the soil.

3.1 Design of pot experiments.

The research hypothesis is that displacement of soil oxygen by natural gas stresses the plants and leads to chlorosis and decreased growth. With this in mind, experiments were carried out to determine the best method of delivering natural gas to the soil in which plants were to be grown. The following sections describe the apparatus used for the experiments with some background to the trials undertaken to arrive at the final methodology.

3.1.1 Pot size

The plants were grown in plastic pots (23 cm diameter) that were large enough to contain at least 4 plants. The use of larger pots or troughs was investigated but either the diffusion of gas throughout the soil medium was insufficient, leading to non-homogenous distribution of the gas, or the approach required excessively large quantities of natural gas to be used, raising issues of both cost and safety. To reduce the loss of gas through the bottom of the pot and to prevent diffusion of oxygen into the pot from the bottom, the pots chosen did not contain drainage holes.

3.1.2 Delivery of gas

For safety reasons all natural gas experiments were carried out in a fume cupboard during working hours only. Gas was delivered to the plant pot via a ring of PVC tubing connected via a flowmeter to a laboratory gas supply (Figure 3.1). Various combinations of tube diameter, hole size and distribution were tested to determine the appropriate pressure drop across the tubing holes. The greatest dispersion of gas was found using tubing having an internal diameter of 6 mm, with 0.5 mm holes drilled every 2.5 cm along one side. The ring of tubing had a circumference of 35 cm, so that, with equal volumes of soil inside and outside the ring, distribution of gas was even throughout the soil. The tubing was placed in the pots with the holes pointing downwards to force dispersion of the gas throughout the compost and to prevent blockage of the holes by soil particles. The tubing left the pot through a small hole drilled 2.5 cm above the base so that the ring was held clear of any water in the bottom of the pot. The perforated ring of tubing was connected via a further length of PVC tubing to a flowmeter and a laboratory gas supply.

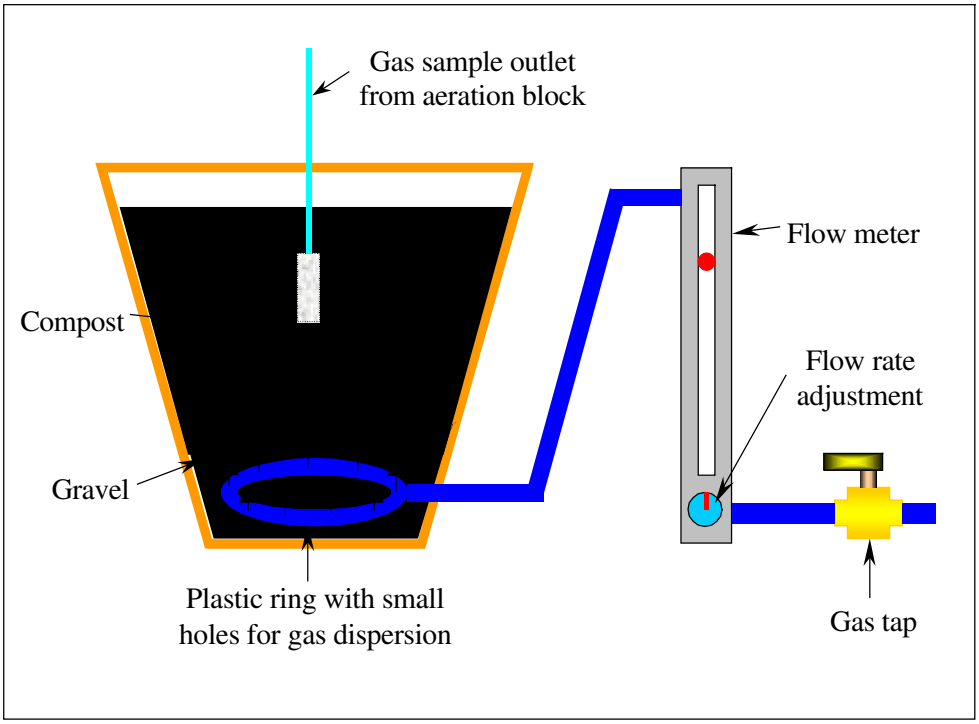

Figure 3.1 Diagram illustrating gas delivery to pots

3.1.3 Soil medium

The pots were filled with 2.5 cm depth of pea gravel, which increased dispersion of the gas throughout the compost and assisted drainage, as there were no drainage holes in the pot. The pot was then filled to within 5 cm of the top with John Innes Potting compost (No 2). John Innes compost [10] is a blend of loam, sphagnum moss peat, coarse sand or grit (in the ratio 7:3:2) and fertilisers, designed to achieve the optimum air and water-holding capacity and nutrient content. Compost No. 2 is suitable for general potting of most plants into medium sized pots. Nutrients include nitrates, phosphates, potash and trace elements sufficient for 1-2 months of plant growth.

[10] History of John Innes compost Http://rareplants.co.uk/johninne.htm Accessed on 1/10/01

A fresh bag of potting compost was used for each trial to ensure that the compost in each pot was of uniform moisture and nutrient content at the start of the trial.

3.2 Measurement of soil / natural gas concentration

3.2.1 Soil-gas extraction

In order to collect a sample of soil air from the compost in which the plants were growing, aeration blocks (Hagen Ltd, Montreal), (2.5 cm (length) x 1.5 cm (diam)) were buried in the soil at a depth of 5 cm. It was expected that natural gas introduced into the soil would diffuse into the aeration block, which is of a coarse-grained porous composition, so that the concentration of natural gas in the block would be in equilibrium with the natural gas concentration in the soil. The aeration block was connected via tubing to a methane detector (Gasurveyor Mk II, GMI Ltd, Renfrew, Scotland).

3.2.2 Measurement of natural gas concentration

The Gasurveyor methane detector was used to measure the concentration of natural gas present in the soil air. This instrument uses a combination of sensors to measure methane concentration in the ranges of 0-1000 ppm, 0-100% LEL and 0-100% volume. It uses pellister-type technology to detect low levels of gas up to 100% LEL (5% volume) and then automatically switches to a sensor that measures the thermal conductivity of the gas when concentrations of gas above 5% volume are detected. An internal pump with a volume flow rate of 30 l hr^{-1} extracts the sample of gas.

The instrument used was calibrated for measurement of methane, although in our trials standard domestic natural gas was used. The Gasurveyor instrument thus underestimates the proportion of natural gas because it is not pure methane. It can be

corrected by multiplying the readings obtained by a factor of 1.16 (personal communication, Advantica plc).

Early trials indicated that extraction of soil-gas samples using the Gasurveyor internal pump disturbed the soil air equilibrium. Large samples of gas, up to 250 cm^3 per sample, were extracted during sampling and this led to rapid diffusion of air into the soil, decreasing the concentration of natural gas in the soil air. To overcome this problem a low-flow sampler pump (SKC Inc, Eighty Four, PA.) was used to draw the soil-gas sample into the Gasurveyor, at a rate of 80 cm^3 min^{-1}. With a typical sampling time of 15 seconds a soil air sample of only 15-20 cm^3 was extracted at each measurement.

3.2.3 Gas distribution throughout the soil

Pot trials involving addition of natural gas into pots of compost showed that methane concentrations of between 50 and 80% could be obtained in the soil air. Samples taken at the edge and centre of the pot showed that the natural gas was being evenly distributed throughout the compost (<5% difference), and that soil-gas concentrations of up to 80% gas were obtained within 30 minutes of switching on the gas supply.

Gas concentration within the soil was affected by the frequency of soil-gas sampling and so measurement of soil methane concentration was restricted to one sample at the end of the day prior to switching off the gas. When the gas supply was disconnected, the concentration of methane in the compost decayed rapidly such that within 2 hours of switching off the supply the soil methane concentration decreased to almost zero. Figure 3.2 illustrates the effect of sampling rate on the decay of gas concentration in the soil following disconnection of the gas supply.

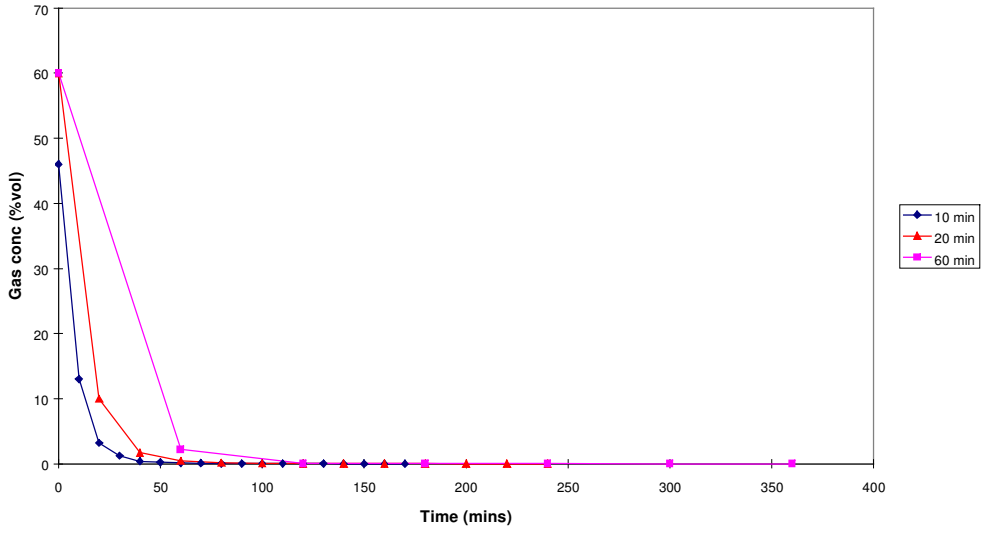

Figure 3.2 The effect of different sampling intervals on the decay of gas concentration in the soil following disconnection of the gas supply.

3.2.4 Measurement of soil oxygen

The short-term loan of an Oxygas meter (GMI Ltd, Renfrew, Scotland) in February and March 2001 allowed soil oxygen concentrations to be measured during some of the argon exposure trials (Section 3.4.2). This instrument is similar in design to the Gasurveyor and measures methane in the range 0-100% LEL and 0-100% volume gas, but is also able to measure oxygen concentration in the range 0-25% using an electrochemical cell. A soil-air sample was extracted with the low flow sampler in the same manner as for natural gas.

3.3 Plant trials

3.3.1 Description of plant species used

Three species of plant were used in the oxygen displacement investigations.

Dwarf bean (*Phaseolus vulgaris* L. cv Tendergreen), Barley (*Hordeum vulgare* L. cv Optic) and Radish (*Raphanus sativus* L. cv Early Scarlet Globe) were used in the investigations. Dwarf bean are dicotyledonous plants that have large leaves suitable for placement in the integrating sphere of the spectroradiometer (see Section 3.5); they were used in investigations with natural gas, waterlogging, argon and nitrogen. Barley, which is a monocotyledon, was used to determine whether spectral changes were different between mono- and dicotyledons and also because barley represents a more likely type of vegetation to be growing above leaking gas pipes in farmers' fields. Barley was used in investigations using argon and waterlogging. Radish, which is also a dicotyledon with large leaves, was used as a fast growing alternative to Dwarf bean in waterlogging trials.

3.4 Exposures

Several treatments and methods of displacing oxygen from the soil were investigated. Laboratory natural gas was used as the primary means of emulating the effects of a leaking gas pipe. However, due to constraints of cost and safety, which prevented continuous gassing of plants in the laboratory, alternative methods of stressing the plants were also investigated. As it was thought that the main effect of leaking gas is to displace air (and hence oxygen) from the soil surrounding plant roots, rather than direct toxicity, other methods of displacing gas were used. Nitrogen and argon were used as gaseous methods of oxygen displacement, and waterlogging as a non-gaseous method.

3.4.1 Natural gas

Natural gas was used in 3 trials to displace oxygen from Dwarf bean (*Phaseolus vulgaris* L. cv Tendergreen).

Seeds were germinated in a growth room at 18°C with a 16-hour light / 8-hour dark cycle. Four bean plants were transplanted into two experimental pots fitted with a ring of perforated PVC tubing to deliver the gas and an aeration block buried in the centre of the pot to measure the soil air methane concentration. Two control pots without gas delivery tubes were also set up. The plants were then moved to a laboratory fume cupboard. Space limitations within the fume cupboard meant that only four pots could be used. It was difficult to maintain adequate light levels for healthy plant growth in the fume cupboard but fluorescent tube lighting was used to reduce shading in the cupboard. Figure 3.3 shows the experimental set up for natural gas exposure in the preliminary trials.

Laboratory natural gas with a methane concentration of 85% (measured with the Gasurveyor) was delivered via a flow meter at a flow rate of 13 l hr^{-1} per pot to two pots for 8 hours per day. Treatment with natural gas was started approximately two weeks after germination when the first trifoliate leaves had emerged. Safety considerations meant that continuous gas flow could not be utilised and the gas supply was disconnected overnight and at the weekends. The gas concentration in the soil air was measured daily using the Gasurveyor attached to a low flow sampler to draw the soil air sample into the unit. The flow rate of gas used led to concentrations of gas in the soil of between 50 and 70% by volume with lower concentrations being attained after the weekend when no gas had been delivered and the soil had dried. Due to the

cramped conditions and inability to carry out continuous gassing, the natural gas exposure was only carried out three times.

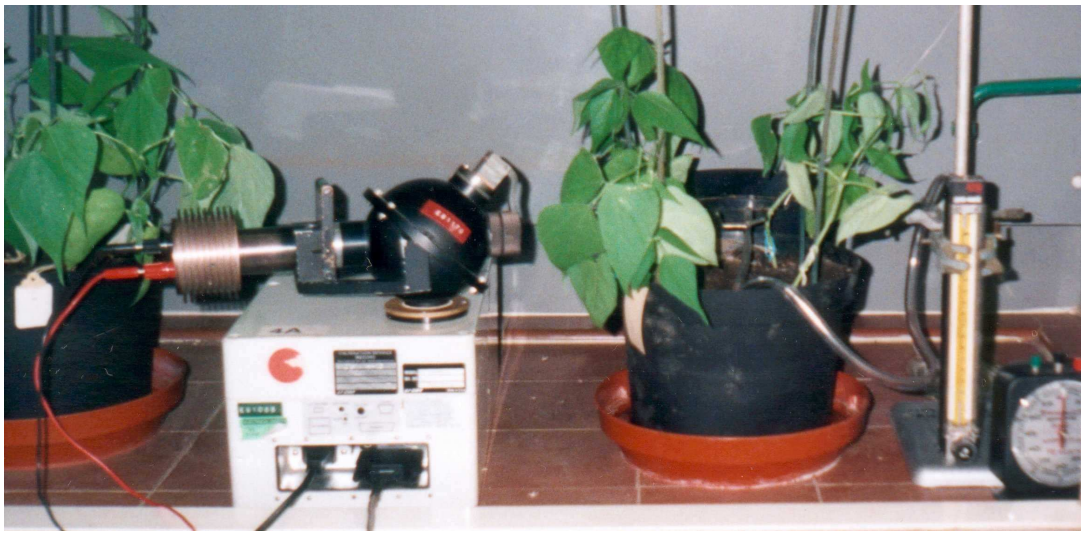

Figure 3.3 Natural gas exposure of bean plants in a fume cupboard showing the LI-1800 spectroradiometer fitted with integrating sphere, gas delivery system and flowmeter.

3.4.2 Argon

In order to test whether the action of methane on plant stress is a particular effect of methane or a generic effect of oxygen displacement from the soil, argon was used in place of natural gas. Argon is colourless, odourless and tasteless; it is an inert gas and is chemically very stable. Its composition in the atmosphere is 0.94% by volume.

Plants used in these trials were bean and barley. The experimental apparatus used was as previously described for the natural gas trials (Section 3.4.1.) but experiments were performed in a growth room at 18°C with a 16-hour light / 8-hour dark cycle. Lighting was provided by two banks of fluorescent tubes.

Bean plants were germinated and transplanted as previously described. Argon, from a pressurised gas cylinder, was delivered to the pots through a flow meter for 24 hours per day. The density of argon gas is higher than that of methane and so adjustments were made to ensure that the flow-rate of argon was comparable to that used in the natural gas trials. The flow rate of argon was at least 11 l hr^{-1} per pot. No method was available to measure the concentration of argon in the soil air but since a similar flow rate was used as for natural gas the assumption was made that a similar concentration of argon would be attained in the soil, and hence a similar decrease in the oxygen content of the soil would be achieved. During two of the trials an Oxygas meter was used to measure the oxygen concentration in the soil and showed average oxygen concentrations of 10.9% (SE 0.58) in the argon-flooded pots and 20.7% (SE 0.01) in the control pots. The method used to extract a soil-gas sample was as described for measuring methane concentration in the soil (Section 3.2.2). A total of four trials of argon on bean were performed.

Barley was sown and germinated directly in the experimental pots to avoid the need for transplanting the seedlings. Twenty seeds were planted and when the seedlings were approximately 10 cm tall, (after approximately 12 days growth) they were thinned to 16 plants and the argon treatment was started.

Three treatment pots and three control pots containing either four bean plants or sixteen barley plants were used. A total of four trials of argon on barley were performed.

3.4.3 Waterlogging

Waterlogging was used as a non-gas method of displacing oxygen from the soil and was carried out on bean, radish and barley. Four bean plants were transplanted into each of six pots as described above, but without the gas delivery system. After a few days for the plants to acclimatise, three pots were flooded with water to a depth of 2.5 cm above the soil surface and three other pots were watered normally to act as controls. The experiments were carried out in the growth room with the same light and temperature regime as before. Four trials of waterlogging on bean were performed.

Twelve radish plants were also transplanted into each of six pots and these were waterlogged as above, with three pots of radishes treated as controls. Three trials of waterlogging on radish were performed. Similarly six pots of barley seeds were planted, and when the seedlings were approximately 10 cm tall they were thinned to sixteen plants. Waterlogging was applied to three of the pots as before. Four trials of waterlogging on barley were performed.

3.4.4 Nitrogen

Nitrogen makes up 78% of the atmosphere. It is a colourless, odourless and mostly inert gas. However, although nitrogen is mostly inert, certain bacteria in the soil are able to fix atmospheric nitrogen into a form usable for plant use.

The effects of using nitrogen gas to displace oxygen from the soil were studied using bean. Four bean plants were transplanted into each of four pots as described for the argon study. Nitrogen gas was delivered from a cylinder at a flow-rate of 13 l hr^{-1} and was used to displace the oxygen from the soil in two pots. Gassing was maintained for 24 hours per day. Two pots were not gassed and were treated as controls. The

experiments were conducted in the growth room. Meters were not available to measure nitrogen or oxygen during these trials and so flow rates equal to those of the natural gas trials were used. Only one trial of nitrogen on bean was performed.

3.4.5 Soil moisture

Plants were checked daily and soil moisture content was monitored using a Rapitest moisture meter (Tenax Ltd, Wrexham, UK) that indicates soil moisture levels in a range of 0 to 10 with 0 being dry soil and 10 being wet. All pots except those subjected to waterlogging were watered to maintain a meter value of 5.

3.4.6 Trial length

Exposures were continued for four to five weeks, unless the plants became so stressed that the leaves were no longer usable. Repetition of the exposure trial was then carried out. A summary of the treatments carried out and the instruments used can be seen in Table 3.1.

Table 3.1 Treatment summary

Treatment	Crop	No. of trials	Location	Dates	No of treatment days	Spectroradiometer	Chlorophyll and Equivalent Water Thickness analysis
Methane	Bean	3	Fume cupboard	14/06/00-17/07/00	33	LI-1800 + ASD	No
				31/07/00-01/09/00	32	LI-1800 + ASD	No
				13/09/00-28/09/00	15	LI-1800	No
Argon	Bean	4	Growth room	30/08/00-25/09/00	26	LI-1800	No
				15/05/01-25/06/01	41	LI-1800	No
				23/07/01-17/08/01	25	LI-1800	No
				03/10/01-09/11/01	37	LI-1800	Yes
Argon	Barley	4	Growth room	03/10/00-02/11/00	30	LI-1800	Yes
				05/12/00-22/12/00	17	LI-1800	Yes
				15/01/01-16/02/01	32	LI-1800	Yes
				22/02/01-30/03/01	36	LI-1800	No
Waterlog	Bean	4	Growth room	13/06/00-22/06/00	9	LI-1800 + ASD	No
				07/07/00-10/08/00	34	LI-1800 + ASD	No
				02/05/01-22/06/01	51	LI-1800	Yes
				08/07/01-10/08/01	33	LI-1800	No
Waterlog	Barley	4	Growth room	03/10/00-02/11/00	30	LI-1800	Yes
				05/12/00-22/12/00	17	LI-1800	Yes
				22/02/01-30/03/01	36	LI-1800	No
				21/05/01-22/06/01	32	LI-1800	Yes
Waterlog	Radish	3	Growth room	10/05/00-23/05/00	13	LI-1800 + ASD	No
				13/06/00-06/07/00	23	LI-1800 + ASD	No
				07/07/00-10/08/00	34	LI-1800 + ASD	No

Nitrogen	Bean	1	Growth room	05/07/00-10/08/00	38	LI-1800 + ASD	No

3.5 Spectral measurements

Detection of stress effects due to displacement of oxygen from the soil was carried out by measuring spectral changes in the reflectance from the plant leaves. Two instruments were used. The main instrument in all studies was a LI-1800 portable spectroradiometer (LI-COR ltd, Nebraska, USA) fitted with an integrating sphere (Macam Photometrics Ltd, Livingston, Scotland). On some occasions an Analytical Spectral Devices (ASD) Fieldspec Pro (ASD Inc, Boulder, Co. USA) instrument was borrowed from the NERC Equipment Pool for Field Spectroscopy (EPFS) (University of Southampton). When this instrument was available spectral scans were carried out using both instruments.

3.5.1 Description of instruments

3.5.1.1 LI-1800 spectroradiometer

The LI-1800 spectroradiometer scans at 2 nm intervals, in the wavelength range 300 - 1100 nm and thus measures both visible and near infra-red wavebands. It measures the spectral distribution of light by filtering the radiation, then dispersing the radiation with a diffraction grating monochromator, and measuring the resulting spectrum with a silicon detector. Light enters the instrument via the integrating sphere or a fibre optic probe and is passed through one of seven filters on a filter wheel, which reduces stray light by filtering out light that is not in the same spectral region as that being measured. Each filter in the wheel corresponds to a particular wavelength range.

The filtered radiation then enters the monochromator, which disperses the radiation into its spectral components and selects the narrow bandwidth to be measured. The width of the exit slit on the monochromator determines the spectral width of the

waveband that reaches the detector. The 0.5 mm exit slit in the LI-1800 gives a waveband at half-power of 4 nm, and total bandwidth of 8 nm. Therefore, when the monochromator is selecting 500 nm, it effectively sees all of the radiation at 500 nm, half the radiation at 498 and 502 nm and no radiation below 496 or above 504 nm (LI-COR 1983). Having been passed through the monochromator the light strikes the silicon detector and generates a current.

The LI-1800 internal computer handles all data collection, storage and communications operations. Interaction with the LI-1800 is via a laptop computer using the Microsoft Hyperterminal program.

3.5.1.2 Integrating sphere

The integrating sphere is a device for collecting radiation that has been reflected from or transmitted through a sample material. The integrating sphere used in this study consists of a 10 cm diameter hollow sphere that is coated on the inside with a highly reflecting layer of barium sulphate. There are two ports. Light from the lamp enters by one and shines directly on the reflectance measurement port where there is a device for holding the sample. Light is scattered throughout the sphere and collected at the third port for measurement. Transmittance measurements may also be made by mounting the sample between the lamp and the sphere. (Figure 3.3).

For reflectance measurements the sample is held in the reflectance port so that it makes up part of the sphere wall. Light from a 20W tungsten-filament halogen bulb is focussed onto the reflectance port that is occupied by the leaf sample. Light is then reflected from the sample back into the integrating sphere where it is reflected around

the interior by the barium sulphate lining. Diffuse light leaves the sphere via the exit port and enters the LI-1800.

A measurement of reflectance involves comparing the sphere internal wall illumination caused by a focused beam of radiation reflected from the sample material to that reflected from a reference material. The reference material used was a disc of barium sulphate.

3.5.1.3 ASD Fieldspec Pro

The ASD Fieldspec Pro is a high performance single beam spectroradiometer measuring over the visible to short-wave infrared wavelength range (350 – 2500 nm). The ASD covers the ranges 350 – 1000 nm at a sampling interval of 1.4 nm, and 1000 - 1700 nm and 1700 - 2500 nm at a sampling interval of 2 nm. The full-width-half-maximum spectral resolution of the instrument is 3 nm for the region 350 - 1000 nm and 10 nm for the region 1000 – 2500 nm. The instrument contains 3 spectrometers in the same unit. The VNIR (Visible and Near InfraRed) spectrometer uses a fixed concave holographic reflective grating that disperses the light onto a fixed photodiode array that has 512 individual detection elements. The SWIR1 spectrometer (Short Wave InfraRed) operating from 1000 – 1700 nm, uses a concave holographic reflective grating that rotates up and down on its axis, scanning the dispersed light across a single InGaAs graded detector. The SWIR2 spectrometer (1700 – 2500 nm) operates in the same way as the SWIR1 spectrometer except that the grating and detector are manufactured for the longer SWIR2 wavelength region (ASD 1999). Radiation is collected and transferred to all three spectrometers via an optic cable fitted with an 8° field of view. The VNIR spectrometer measures all channels simultaneously, while the two SWIR spectrometers measure successive wavelengths of

light sequentially. Each spectrometer detector converts the photons into electrons and accumulates a signal. The signal is then converted into a voltage and digitised by an analogue to digital converter (Rollin *et al.* 1996). The instrument measures the signal continuously and saves the spectra to a portable computer that contains the operating software.

3.5.2 Method of taking reflectance measurements from leaves

3.5.2.1 LI-1800

The LI-1800 spectroradiometer fitted with the Macam integrating sphere was used to obtain the reflectance spectra of each plant. The integrating sphere lamp was switched on 20 minutes prior to scanning to eliminate spectral changes in the lamp as it warmed. After instrument warming but before taking any reflectance scans the lamp was switched off and a measurement of the dark current was taken. Four scans were taken between 450 and 900 nm with the reference disc in position and were averaged in the LI-1800 internal computer. The bulb was then switched on and a reference scan of a barium sulphate disc was taken prior to scanning the leaves. The LI-1800 can scan in the range 300 – 1100 nm but it was found that excessive noise was obtained below 400 nm. This was probably due to the sensitivity of the silicon detector, which declines at short wavelengths. Between 800 and 1100 nm little additional information was obtained and scans were therefore taken between 450 and 900 nm to save memory space on the LI-1800 internal memory.

The first trifoliate leaf of each bean plant was scanned without removing the leaf from the plant. The leaf was placed in the reflectance port of the integrating sphere, ensuring that the central midrib of the leaf was avoided and that the adaxial (upper)

surface was facing the light source. Four scans were taken of one leaf from each plant, in the wavelength range 450-900 nm, once per week. The same leaf was used each week to measure spectral changes consistently, avoiding interleaf variability. When this was not possible, because of senescence and detachment of the leaf, the next oldest leaf was used.

With radish, four leaves were selected from each pot, removed and scanned in the integrating sphere. The time between detachment of the leaf and spectral measurement was less than one minute and so changes in the leaf before scanning would have been minimal. Barley leaves were not large enough to be placed directly into the integrating sphere and so two leaves were placed side-by-side and taped top and bottom with Sellotape to enable easy positioning of the leaves in the port. Care was taken to ensure that the leaves were butted together but were not overlapping. The time between detachment of the leaves and scanning was slightly longer than for radish leaves but was still unlikely to have resulted in changes in the leaves. The leaves were then placed in the port of the integrating sphere ensuring that the taped areas were not in the line of the light beam.

3.5.2.2 ASD Fieldspec Pro

A leaf sample was detached from the plant and positioned so that the leaf completely filled the field of view of the fibre optic probe. The sample was illuminated with a 1000 W halogen lamp angled at 45° to the vertical and approximately 1 m away from the target. The lamp and ASD were both switched on and left to warm for 20 minutes prior to use to allow the sensors to warm up. Optimisation of the instrument, which measures a dark current spectrum and sets the integration, gain and offsets of the detectors, was carried out prior to any scanning and at approximately 20-minute

intervals during data collection. A spectral scan was taken of a Spectralon reference panel. The panel was then removed and a leaf positioned beneath the fibre optic probe. A spectral scan takes milliseconds to record and 25 scans were taken and averaged. The instrument was operated in white reference mode, which automatically converts the signal into a reflectance relative to the Spectralon panel. The reflectance was instantly visible on the computer screen and thus the leaf could be repositioned if it was not completely in the field of view of the fibre optic probe. Figure 3.4 shows the ASD Fieldspec Pro in use.

Figure 3.4 ASD Fieldspec Pro showing computer interface and fibre optic probe.

3.5.3 Errors involved in LI-1800

Several sources of error were identified during the use of the spectroradiometer and integrating sphere and precautions were taken to minimise them.

3.5.3.1 Temperature changes

The silicon detector in the spectroradiometer is mechanically rugged and has good long term and temperature stability. The laboratory area allocated for scanning was unheated and so temperature fluctuated with the seasons, but was generally stable during each period of scanning. The lamp was switched on and left to warm for 20 minutes, before any scans were carried out, to allow the lamp to reach thermal stability with the surroundings and reduce lamp output irradiance variation.

3.5.3.2 Barium sulphate reflectance

Barium sulphate has a reflectance of approximately 95% across the spectrum. Reflectance from the sample is calculated by comparing the radiation reflected from the sample material to that reflected from the barium sulphate reference disc. A correction factor obtained from a standardised barium sulphate sample (Personal communication- E Rollin, EPFS, University of Southampton) was applied to the signal obtained from the LI-1800 to give true reflectance from the sample (Equation 3.1).

$$\rho = \left(\frac{R_{sample} - R_{dark}}{R_{ref} - R_{dark}} \right) \times \rho_{ref}$$

Equation 3.1 Correction factor applied to the reflectance, where R_{sample} is the signal from the sample, R_{ref} is the signal from the barium sulphate disc, R_{dark} is the dark current and ρ_{ref} is the standard reflectance of the $BaSO_4$ disc.

Comparison of scans taken with the LI-1800 of the barium sulphate reference disc over two years showed a drift in the reflectance observed from the disc. Figure 3.5 shows the drift observed which appeared to be due to external temperature change and deterioration of the surface of the reference disc. Reference reflectance measurements

were taken at the beginning of each set of reflectance scans. The drift was about 8% in 23 months, representing a negligible rate over the few hours of scanning time and errors in reflectance from this source can be disregarded.

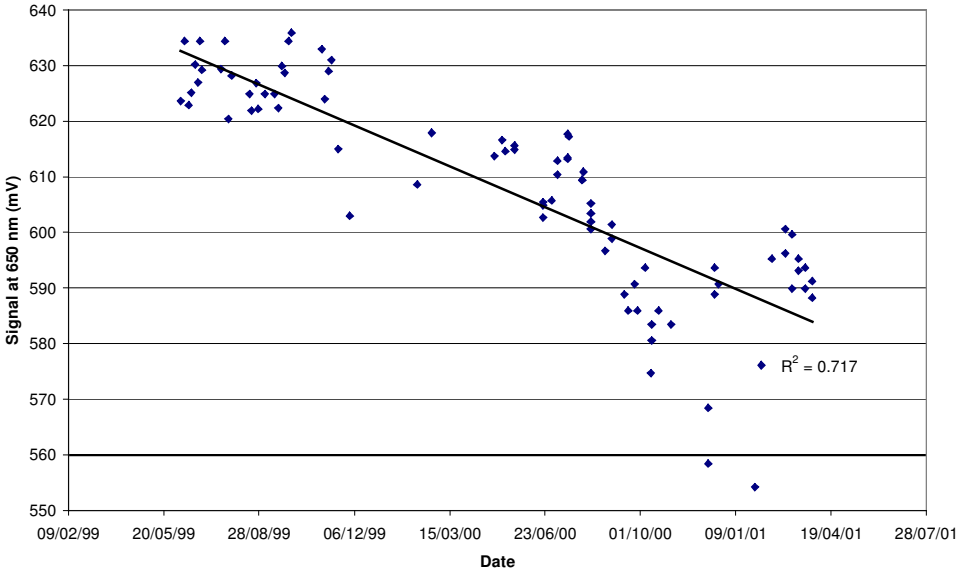

Figure 3.5 Comparison of reflectance signal at 650 nm of barium sulphate disc over 23 months

3.5.3.3 Dark current shift

The dark current is one type of noise that occurs in light-sensitive detectors. Such detectors emit a small signal even in the absence of light, mostly due to thermal activity in the photocathode and the dynodes. Hence operation at low temperature can alleviate the effect. Low level noise can also arise due to the operation of the instrument, particularly when operating in mains mode. When the LI-1800 was mains powered the dark current was higher than when operating in battery mode; however, most scans were carried out under battery power with dark current scans being taken at the beginning and end of the set of scans. Figure 3.6 illustrates the dark current when

the LI-1800 was being operated under mains or battery power. The mean dark current was calculated and deducted from both the reference and sample signal before processing the data.

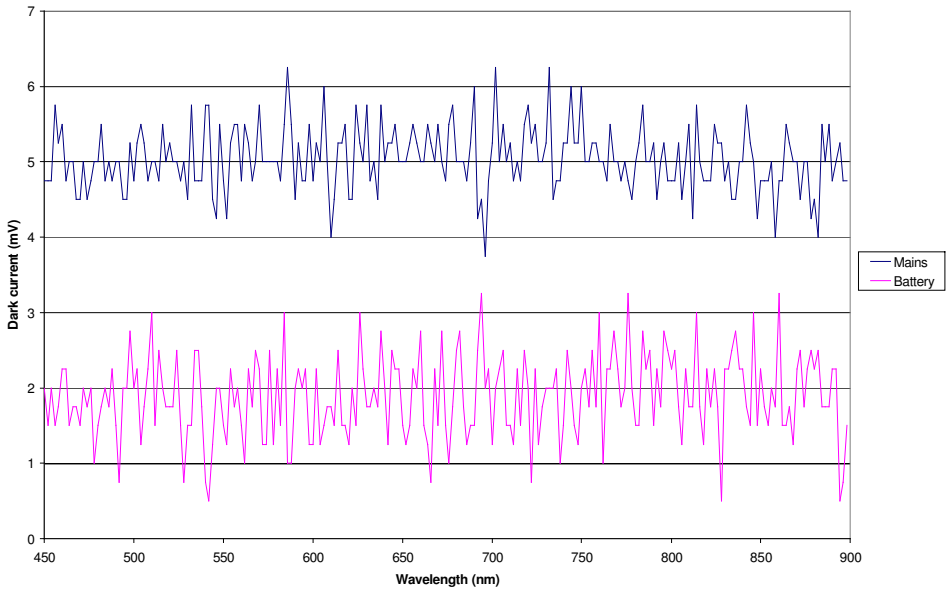

Figure 3.6 Dark current signal observed from the LI-1800 (11/12/00).

3.5.3.4 Stray light.

Stray light entering the instrument via gaps in ports or from lamplight that does not fall directly on the sample could affect the measurement of reflectance from samples. Investigations were carried out to determine the level of stray light entering the integrating sphere from the room lighting, by measuring the reflectance of a leaf without illumination from the integrating sphere bulb. This was then divided by the reflectance from the reference disc. The level of stray light was found to be less than 1% of that measured for a standard reflectance signal over the wavelength range 450 to 900 nm. Figure 3.7 shows the stray light entering the integrating sphere and Figure 3.8

compares the stray light and dark current to the normal reflectance signal from a leaf placed in the integrating sphere.

The average dark current signal was 1.79 mV and the average stray light signal was 2.05mV. The leaf reflectance signal varied between 5 mV and 237 mV and the signal from the barium sulphate disc varied from 46 to 564 mV. The effect of the dark current and stray light was noticed most at the wavelengths below 500 nm and so corrections were made by measuring the dark current at the beginning and end of each set of measurements and deducting the interpolated value from the signal.

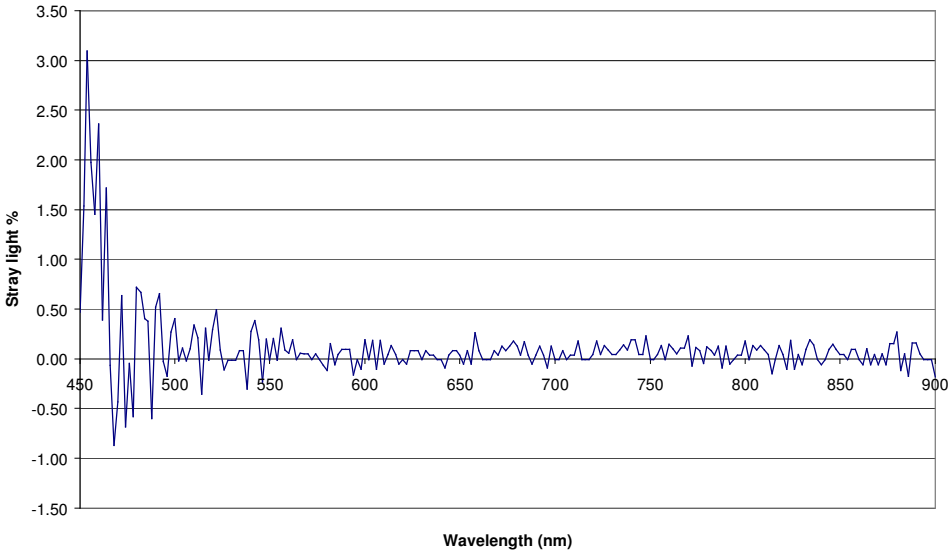

Figure 3.7 Stray light entering integrating sphere

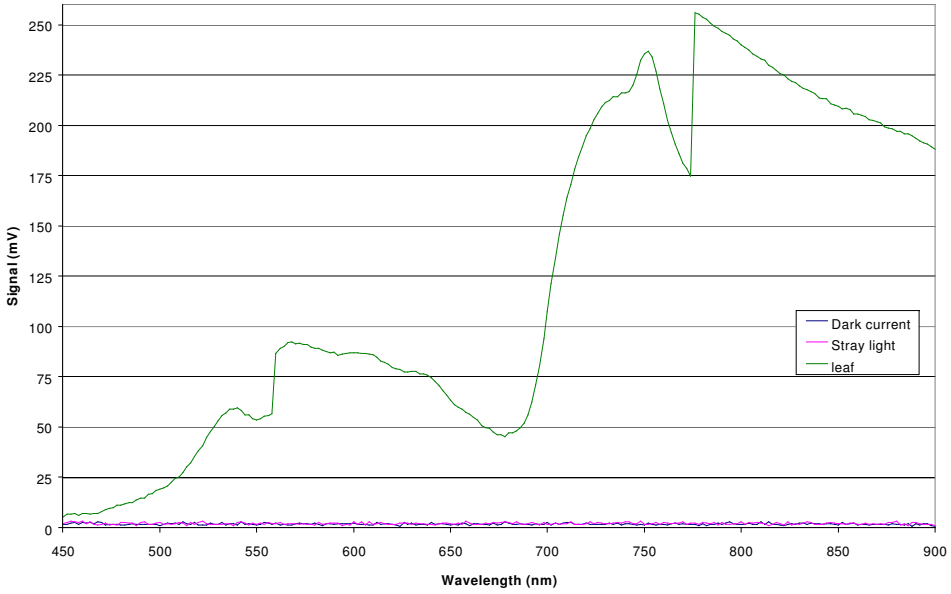

Figure 3.8 Dark current and stray light signal compared with normal reflectance signal from a leaf (20/9/01).

3.5.4 Errors involved in the ASD Fieldspec Pro

3.5.4.1 Leaf effects

Both bean and radish plants were investigated with this instrument. The leaves, particularly those of radish, were small and thus it was difficult to position the leaves to completely fill the field of view of the fibre optic probe. It was also difficult to scan areas of leaves so that leaf veins or midribs were not being viewed.

A 1000 W halogen lamp was used to illuminate the sample; the latter became very hot so that leaf samples had to be scanned rapidly to prevent wilting.

3.5.5 Temperature

The ASD Fieldspec Pro is known to produce spectral steps in data, but the exact reasons for this are unknown. Steps occur particularly at around 995 nm at the point of changeover between the two sensors. The EPFS have investigated the time and

temperature dependence of the ASD Fieldspec Pro and it was found that the measured signal from the ASD varied with time from power on. Variation in detector sensitivity was greatest during the first 30 minutes of operation and the total warm up period for the ASD was up to 2 hours (Andersen 2000). This suggests that the 20 - minute warm-up that was used in this research was too short and thus large steps (an error of approximately 5%), in the data are often observed.

3.6 Chlorophyll analysis

At the end of some exposure trials using barley or bean, chlorophyll analysis was carried out by removing, using a cork borer, four 1 cm diameter discs from the leaf of each plant that had been used for spectral scanning. Leaf discs were stored in polythene bags at 4°C in the dark to prevent chlorophyll breakdown, until chlorophyll extraction could be carried out. Chlorophyll extraction and analysis was usually done 24 – 48 hours after the sampling.

Chlorophyll extraction and analysis were carried out using the method of Bruinsma (1963). Chlorophyll samples were extracted by grinding the discs in a mortar with a pestle in 80% v/v propanone:water mixture. A small amount of calcium carbonate was added to neutralise plant acids that lead to chlorophyll breakdown. The samples were then centrifuged for 5 minutes at 2000 rpm, and the resulting supernatant made up to 10 cm^3 with 80% propanone. The absorbance of the chlorophyll solution was measured in a UV / visible UltraspecPlus (4054) spectrophotometer (LKB Biochrom, Cambridge, UK) at wavelengths 663 and 645 nm, using the 80% propanone solution as a standard.

Chlorophyll concentration of chlorophyll *a* and *b* in mg l^{-1} was calculated as:

$$\text{Chlorophyll } a \text{ (mg } l^{-1}) = 12.7\ A_{663} - 2.7\ A_{645}$$

$$\text{Chlorophyll } b \text{ (mg } l^{-1}) = 22.9\ A_{645} - 4.7\ A_{663}$$

where A_{643} and A_{645} are the absorbance at 645 and 663 nm respectively.

The concentration of chlorophyll in the leaf, expressed on an area basis, is found from:

$$\text{Chlorophyll (mg } cm^{-2}) = (V/A) \times \text{Chl}_x \text{ (mg } l^{-1})$$

Where V = volume of 80% propanone used in dilution, A = total area of the leaf discs and Chl_x = Chlorophyl *a* or *b* concentration of the solution in mg l^{-1}

3.7 Leaf dry matter analysis

In order to determine the dry weight and equivalent water thickness of the bean and barley leaves the leaf area, fresh weight and dry weight of the leaves were determined. The equivalent water thickness of leaves is the thickness of pure water that corresponds to the leaf moisture content (Downing *et al.* 1993).

3.7.1 Bean

After spectral scanning and the removal of one bean leaf for chlorophyll analysis all remaining bean leaves were removed from the stem. Leaves were stored in paper bags (one bag for each bean plant) until leaf area could be determined, which was usually within 2 hours. Leaf area was calculated for all leaves using a LI-3000A leaf area meter (LI-COR Ltd, Nebraska, USA) and then the fresh weight of the leaves from each plant was determined. Leaves were dried in an oven at 105°C for 48 hours before determining the dry mass of the leaves.

The dry weight per unit area (g cm^{-2}) was calculated as:

$$\text{Dry weight (g)} / \text{Leaf area (cm}^2\text{)}$$

The equivalent water thickness (cm) of the leaf was calculated as:

$$\frac{\text{Fresh Weight (g)} - \text{Dry Weight (g)}}{\text{Leaf area (cm}^2\text{)}}$$

3.7.2 Barley

For barley plants three sets of four leaves were removed at random from each pot, placed in paper bags and leaf area and dry matter analysis carried out in the same manner as for bean leaves.

3.8 Spectral data analysis

Reflectance data was stored in the internal computer of the LI-1800. Four scans were taken of each leaf and the data averaged internally in the LI-1800 processor. Data was then downloaded into a personal computer, and processed using a Microsoft Excel 97 macro (Appendix B).

3.8.1 Relative reflectance

Control, treatment, reference and dark current scans were downloaded for each exposure. The LI-1800 data was in the form of the reflectance signal from the reference or the sample in mV. The reference and sample data were first corrected for the effects of the dark current. The dark current measurements (taken at the beginning and the end of the session) were averaged and deducted from both sets of data. The relative reflectance was then obtained by dividing the signal for the sample by the

signal for the reference. A correction factor based on a standardised barium sulphate reflectance file (Personal communication, E. Rollin, EPFS, Southampton) was then applied to the resulting relative reflectance to compensate for the fact that barium sulphate is not 100% reflective (Equation 3.1, page 65).

The relative reflectances for control and treatment plants were averaged and plotted to show any changes in reflectance. To enable quantification of changes in reflectance between control and treatment measurements the maximum change in reflectance at six wavelengths was measured. The wavelengths selected represent particular leaf spectral characteristics and are illustrated in Table 3.2

Table 3.2 Wavelengths of the main leaf spectral characteristics selected to illustrate reflectance changes in vegetation (After Gemmel 1988).

Wavelength (nm)	Leaf spectral characteristic
550	Region of chlorophyll reflectance maximum
600	Region of minor reflectance peak
650	Region of second minor reflectance peak
680	Approximate wavelength of maximum chlorophyll absorbance.
700	Close to start of rapid transition to high reflectance in near infrared region
800	Located in region of high NIR reflectance due to leaf cellular structure

3.8.2 Spectral smoothing

Spectral smoothing involves removing the effects of random errors such as background noise produced by the instrument. Previous authors have applied various methods to smooth data. Savitzky and Golay (1964) used a least-squares-fitting procedure that simultaneously smoothed and differentiated data. A Fourier transform can also be used to smooth data. This separates the signal into high and low frequency components and then deletes the high frequency noise before recovering the signal (Berrenger 2000). A further method of smoothing is to use a mean filter algorithm that uses the mean value of samples within a smoothing window as the new value of the middle sampling point in the smoothing window. The primary factor controlling the extent of smoothing is the size of the filter window used for averaging. In general, the greater the size of the filter window, the smoother the result (Tsai and Philpot 1998). However, the risk arises of filtering out detail within the spectrum and so a compromise is needed between the amount of smoothing and the retention of data features. A further refinement of mean filter averaging is to use a weighted mean filter in which data points either side of the middle sampling point are given different weightings than that given to the middle point. The weighted sum of the values must be divided by the sum of the weights. For example, with a 5 point weighted filter:

$$n_1 = \left\{ \frac{m_{-2}}{4} + \frac{m_{-1}}{2} + \frac{m}{1} + \frac{m_{+1}}{2} + \frac{m_{+2}}{4} \right\} \Big/ 2.5$$

Where n is equal to the mean filtered mid point and m is equal to the unsmoothed points. This filter gives more weight to the central point and correspondingly less to the more distant points.

In this research a simple weighted mean moving average was used. The effect of different bandwidths of smoothing was examined and it was found that a 5 point weighted average gave sufficient smoothing without loss of fine spectral detail.

3.8.3 Calculation of first derivative spectra

Derivative spectroscopy concerns the rate of change of reflectance with wavelength. This technique was used primarily to locate the position of the red-edge, which is the position of maximum slope of the reflectance spectrum between 670 nm and 800 nm. A simple operation of dividing the difference between successive spectral values by the wavelength interval separating them was carried out.

Concern arose that with a difference on data smoothed using a simple moving average, that data within the smoothing window was being lost. For example with a 5 point moving average:

$$n_1 = \frac{m_{-2} + m_{-1} + m + m_{+1} + m_{+2}}{5} \quad \text{and} \quad n_2 = \frac{m_{-1} + m + m_{+1} + m_{+2} + m_{+3}}{5}$$

To calculate the derivative

$$n_2 - n_1 = \frac{m_{+3} - m_{-2}}{\lambda_2 - \lambda_1}$$

Thus with a simple moving average, the contributions of the data points m_{-1}, m, m_{+1} and m_{+2} are cancelled out and the resulting derivative spectrum has lost any smoothing effect. In order to prevent this loss of data a smoothing via a weighted moving average was carried out prior to calculation of the derivative. In this case each data point

contributes towards the calculation of the smoothed point with a greater proportion being contributed by the data points closest to the mid point. Derivatives calculated by difference thus have contributions from all points.

For example:

$$n_1 = \frac{\frac{m_{-2}}{4} + \frac{m_{-1}}{2} + \frac{m}{1} + \frac{m_{+1}}{2} + \frac{m_{+2}}{4}}{2.5} \qquad n_2 = \frac{\frac{m_{-1}}{4} + \frac{m}{2} + \frac{m_{+1}}{1} + \frac{m_{+2}}{2} + \frac{m_{+3}}{4}}{2.5}$$

n_2-n_1 now becomes

$$n_2 - n_1 = \left(\frac{\frac{m_{-1}}{4} + \frac{m}{2} + \frac{m_{+1}}{1} + \frac{m_{+2}}{2} + \frac{m_{+3}}{4}}{2.5} \right) - \left(\frac{\frac{m_{-2}}{4} + \frac{m_{-1}}{2} + \frac{m}{1} + \frac{m_{+1}}{2} + \frac{m_{+2}}{4}}{2.5} \right)$$

$$n_2 - n_1 = -\frac{m_{-2}}{10} - \frac{m_{-1}}{10} - \frac{m}{5} + \frac{m_{+1}}{5} + \frac{m_{+2}}{10} + \frac{m_{+3}}{10}$$

3.8.4 Introduction of an error into the data

The effect of introducing an error into the data (a doubling of the reflectance at 680 nm) when calculating derivatives was studied to identify the best smoothing method to use.

Figure 3.9 shows the effect of different levels of smoothing and Figure 3.10 illustrates the effect of introducing an error into the original data on the calculation of the first derivative. Although the 7-point moving average (ma) showed the greatest amount of smoothing, detail in the spectra was lost. In the region between 700 and 750 nm, the peak that represents the red-edge is narrower than in the original data and in the other smoothing techniques. Small peaks at 732 and 746 that may represent important details are lost.

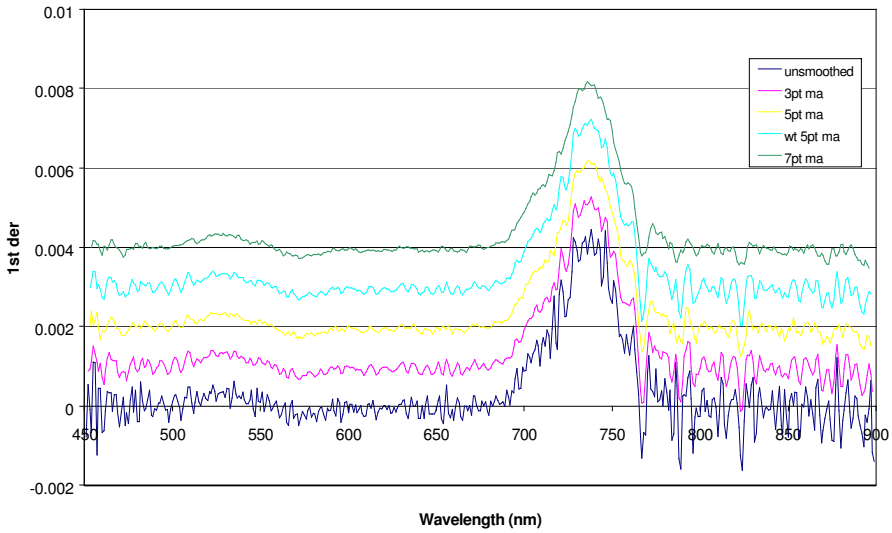

Figure 3.9 Effect of different levels of smoothing on calculation of the 1st derivative. An offset of 0.001 was added to each successive set of data to enable differences to be seen.

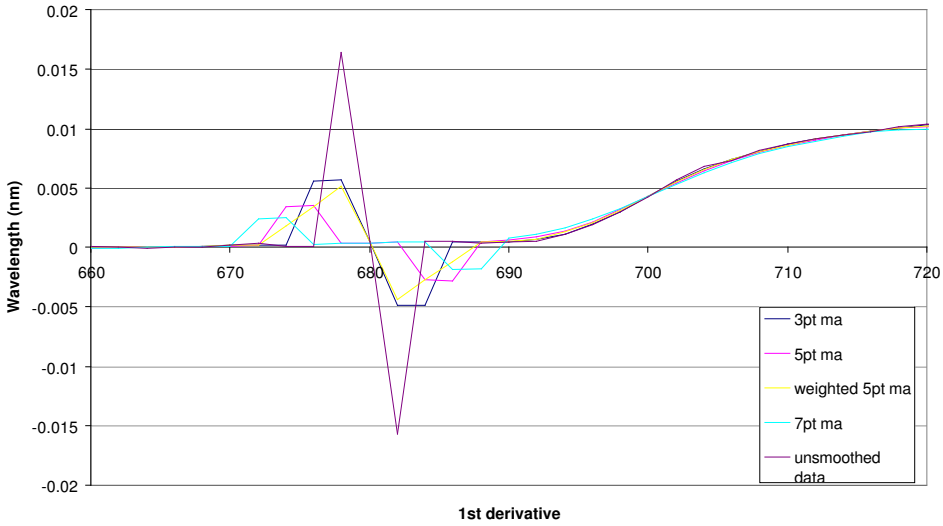

Figure 3.10 Effect of an error introduced into the original data at 680 nm.

The 5-point moving average and the weighted 5-point moving average both remove some noise but do not lose spectral detail. Addition of an error to the unsmoothed data shows that the weighted 5-point average smooths out the error but does not oscillate the error through the data in the same way that the unweighted moving average does.

The effect of unweighted smoothing is to shift the error to the extremes of the smoothing band. Thus, with a 7-point moving average, the error at 680 nm appears as a positive anomaly at 672 – 674 nm and a negative anomaly at 686-688 nm. The weighted average filter retains the error in its proper place.

The first derivative of reflectance was analysed to show the change in position and magnitude of the point of maximum inflection relating to the red-edge. The change in magnitude of inflection of other peaks was also investigated. The wavelengths selected for study are shown in Table 3.3. A representative graph showing the peaks and troughs selected is shown in Figure 3.11.

Table 3.3 Approximate wavelengths selected to show changes in inflection point in the first derivative of reflectance curve.

Wavelength (nm)	Leaf spectral characteristic
524	First major peak in reflectance derivative curve due to rising edge of the green reflectance peak.
574	Position of first major trough in derivative curve due to falling edge of the green reflectance peak.
600	Second major peak in derivative curve
616	Second major trough in derivative curve
634	Third major peak in derivative curve
644	Third major trough in derivative curve due to absorbance by chlorophyll
710	Fourth major peak, position of red-edge-due to rising edge of near-infrared reflectance peak

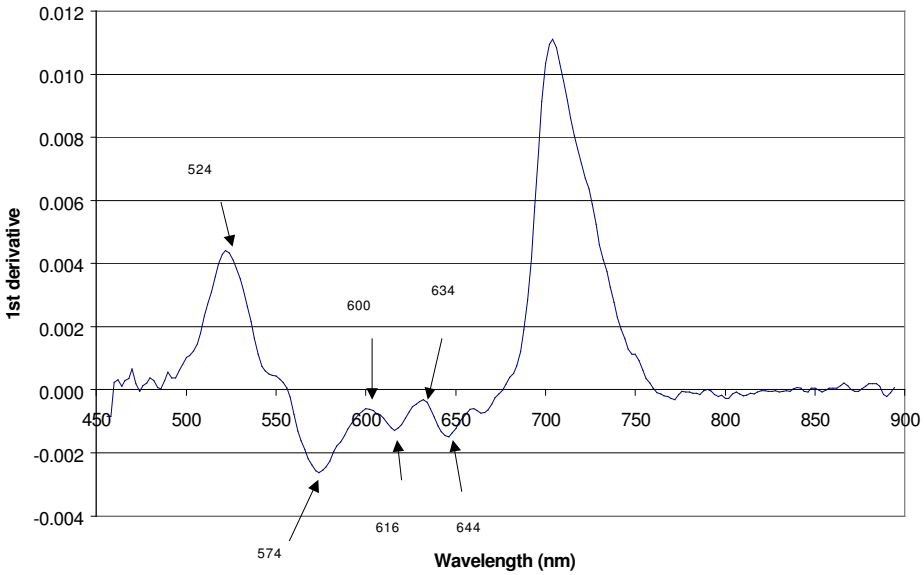

Figure 3.11 Representative first derivative plot showing position of peaks and troughs.

4 Spectral reflectance changes in plants treated with soil oxygen displacement by a variety of methods in the laboratory

Two plant types were exposed to different methods of oxygen displacement. Barley (*Hordeum vulgare* L. cv Optic), a monocotyledonous species was exposed to argon and waterlogging treatments. Monocotyledons are flowering plants with one cotyledon (seed leaf). The leaves of these plants have parallel veins. Two dicotyledonous species, which have networks of leaf veins, were also exposed to treatments. Bean (*Phaseolus vulgaris* L. cv Tendergreen) was exposed to natural gas, argon, waterlogging and nitrogen gas treatments, whilst radish (*Raphanus sativus* L. cv Early Scarlet Globe) was exposed to waterlogging.

This section will describe the effect on each plant type of soil oxygen displacement produced by the various methods.

4.1 Bean

4.1.1 Natural gas

Three repeat experiments were carried out on the effects of leaking natural gas on the growth of bean. Methane concentrations in the soil were measured daily throughout the trial and were maintained at between 60-70% vol. methane whilst the gas was flowing. However, within one hour of switching off the gas overnight (for safety reasons), the soil concentration fell to 0% thus allowing re-oxygenation of the soil.

Each trial was carried out for several weeks (Table 3.1) and the change in reflectance varied with time. The plants were grown in pots in a fume cupboard, at room temperature and under fluorescent lighting.

Maximum changes in reflectance and red-edge shift were observed after two to three weeks of exposure. Graphs of relative reflectance show that compared to controls, reflectance for bean plants treated with methane was higher in the visible wavelengths, but there was little change in the infrared regions (Figure 4.1). The greatest normalised percentage increases in reflectance occurred at 550, 600 and 650 nm. In trial 1 (Table 3.1) the increase was respectively 19, 26 and 24% and in trial 2 it was 13, 17 and 10%. In trial 3 the increases were smaller at 5, 7 and 7%.

T-test statistical analysis showed the wavelength ranges for which significant differences occurred between the treatment and control plants. Figure 4.2 shows a plot of the p value against wavelength. All wavelengths between 500 and 728 nm show significant differences between the control and treatment plants ($p = 1.8 \times 10^{-3}$ to 0.05, n=8).

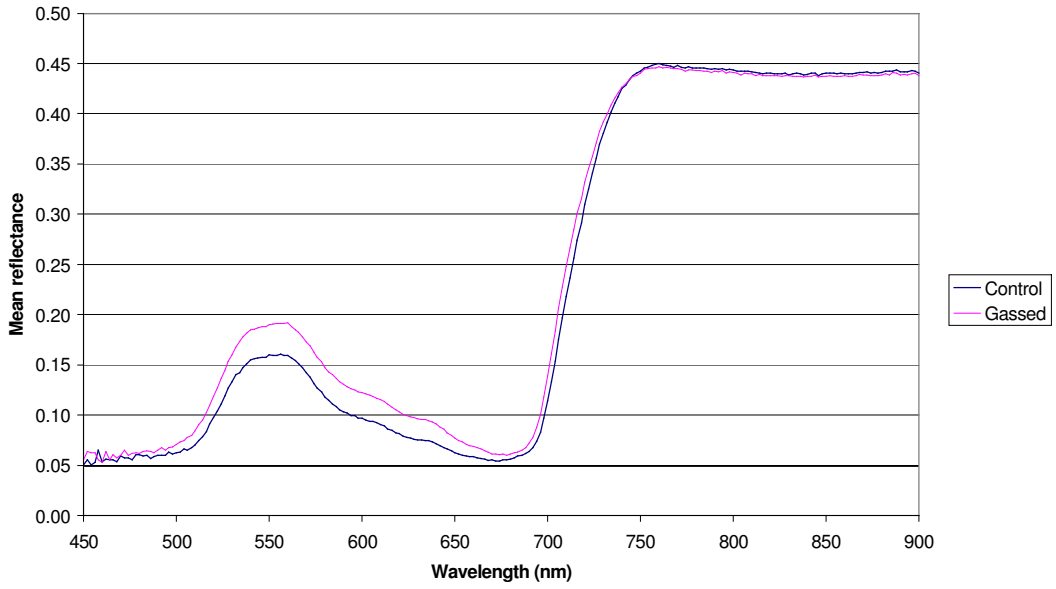

Figure 4.1 Mean reflectance of control and natural gassed bean (relative to a barium sulphate disc) on 30/6/00 after 16 days of treatment.

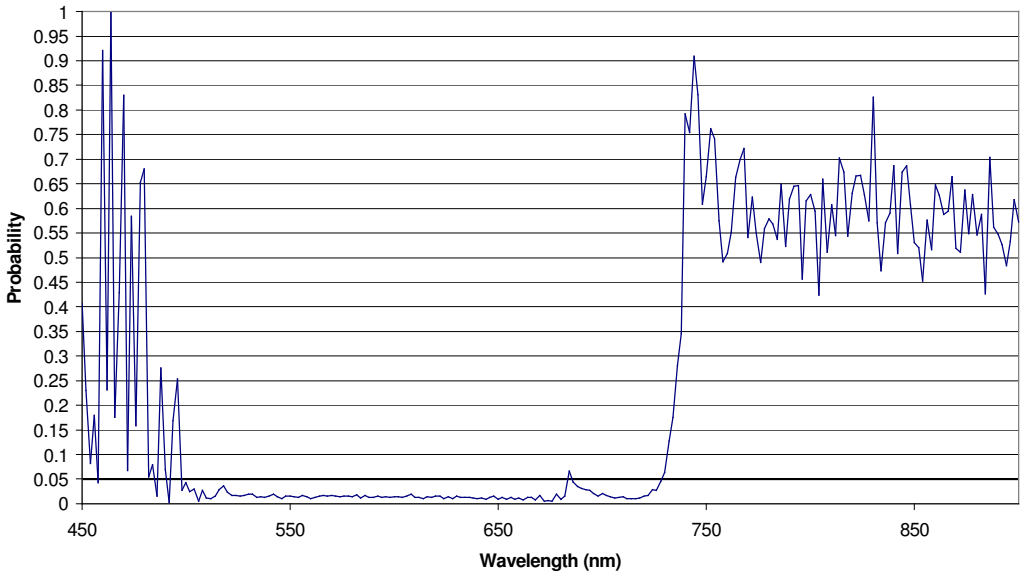

Figure 4.2 T-test analysis showing probability of control and gassed treatments showing no difference 30/6/00, n=8, (16 days after start of treatment).

The first derivative of reflectance was analysed to show the change in wavelength and amplitude of the point of maximum inflection that relates to the red-edge (Figure 4.3). The change in amplitude of other inflection peaks was also investigated and show differences between gassed and control plants in the region of 524, 616, 634 and 644 nm. In bean the first derivative of reflectance showed the red-edge as a single peak at around 706 nm. The position of the red-edge varied by up to 4 nm, which is within the resolution of the spectroradiometer.

Each trial was carried out for a similar amount of time and under the same conditions. The changes in reflectance observed in each trial were of a similar order and so the data from the three trials were combined, which allowed general shifts in the red-edge and changes at the other wavelengths to be followed based on the number of days that the trial had been running (Figure 4.4). After an initial shift in the red-edge of 3 nm,

towards the blue, by day 28 the red-edge for the control plants had returned to its original position. The red-edge of the methane stressed plants showed the same pattern of movement although there was a greater initial shift of 6 nm towards the blue, after which the red-edge position remained stationary and then shifted towards the red by 3 nm. The red-edge of the treatment plants remained at shorter wavelengths than the control plants throughout the trial.

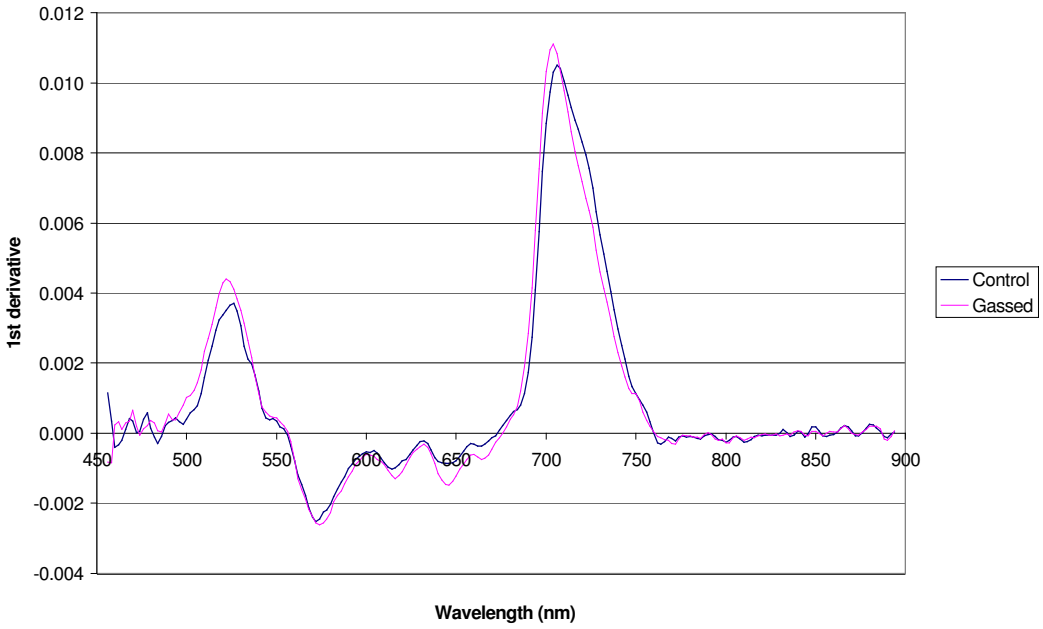

Figure 4.3 First derivative of reflectance for control and natural gassed bean on 30/6/00 after 16 days of treatment

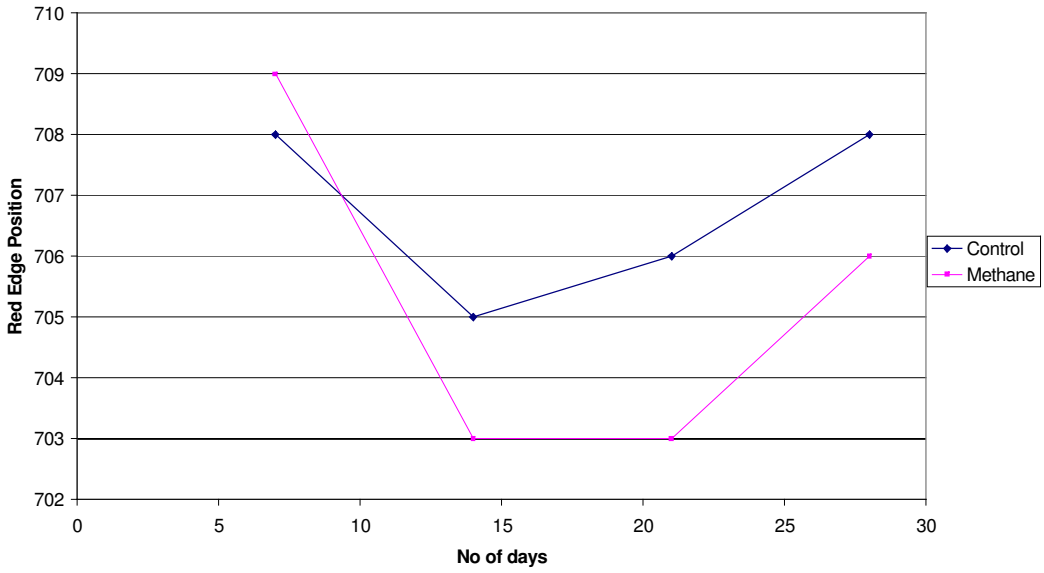

Figure 4.4 Change in red-edge position with time for methane gassed bean – 3 data sets combined.

Examination of the first derivative at other wavelengths showed that at 524 nm, after an initial decrease in the first derivative of reflectance there was an increase in the magnitude, and thus in the size of the peak, of the first derivative of the gassed bean after 3 weeks of treatment (Figure 4.5).

At 574 nm there was an initial increase followed by a decrease in the amplitude of the first derivative, showing as a deepening of the trough. The magnitude of the first derivative of reflectance was slightly smaller for the control bean throughout the trial. A similar pattern in the first derivative of reflectance between the control and gassed bean were also observed at 600, 616, and 634 nm. An initial increase in the magnitude of the first derivative was followed by a decrease and levelling out of the change in magnitude of the first derivative. At 644 nm the magnitude of the first derivative increases for both the control and gassed plants up until the third week when the

magnitude of the derivative declines with the derivative of the reflectance from the gassed plants declining at the greatest rate. At 600 and 634 nm, which are both relative peaks in the first derivative, the magnitude for the gassed plants is smaller than that for the control plants, whereas at 616 and 644 nm the gassed plants show the deepest troughs. At most wavelengths there is little difference in the first derivative after 35 days as the control plants were becoming stressed due to the stress of growing in pots. The biggest differences in the first derivative of reflectance occurred in the fourth week of the treatment (after 21 days of treatment) and was particularly marked at 644 nm, which showed a relative decrease of 52% in the fourth week of the trial.

.

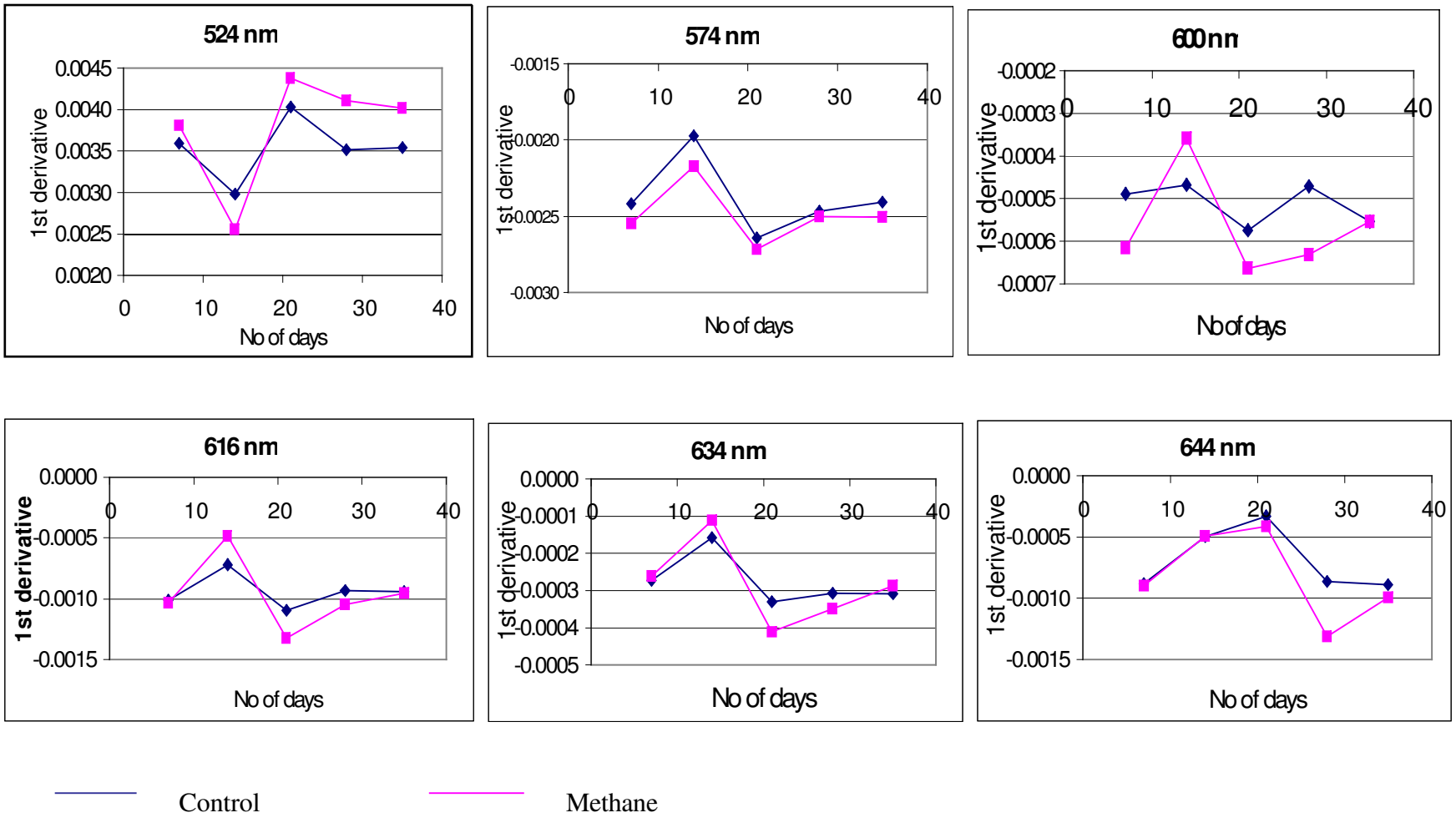
524 nm
1st derivative
0.0045
0.0040
0.0035
0.0030
0.0025
0.0020
0
10
20
30
40
No of days
574 nm
1st derivative
-0.0015
-0.0020
-0.0025
-0.0030
0
10
20
30
40
No of days
600 nm
1st derivative
-0.0002
-0.0003
-0.0004
-0.0005
-0.0006
-0.0007
0
10
20
30
40
No of days
616 nm
1st derivative
0.0000
-0.0005
-0.0010
-0.0015
0
10
20
30
40
No of days
634 nm
1st derivative
0.0000
-0.0001
-0.0002
-0.0003
-0.0004
-0.0005
0
10
20
30
40
No of days
644 nm
1st derivative
0.0000
-0.0005
-0.0010
-0.0015
0
10
20
30
40
No of days
Control
Methane

Figure 4.5 Changes in first derivative of reflectance for methane gassed bean over 5 weeks of treatment, data for three trials combined.

4.1.2 Argon

Argon was used as a method of displacing oxygen from the soil to determine if leaf responses to natural gas were specific to natural gas or generic to oxygen displacement from the soil. Four repeat experiments were carried out on bean plants growing in argon-flooded soil. Although there was no way of measuring the concentration of argon within the soil, the same flow rate was used as in the natural gas trials and it was assumed that the concentration of argon in the soil would be similar to that attained with natural gas. A GMI Oxygas meter was obtained so that it was possible to measure the oxygen concentration within the soil for some of the trials. Oxygen levels within the control pots were constant at 20.7% (SE 0.01) but were variable in the treatment pots. Oxygen concentration ranged between 1% and 17% with a mean value of 10.9% (SE 0.58).

Bean in the argon-flooded pots showed increased reflectance throughout the visible region, but slightly decreased reflectance in the infrared (Figure 4.6). T-test analysis showed that at all wavelengths between 494 and 728 nm, the reflectance of control plants was significantly different to that of treatment plants ($p = 7x10^{-7}$ to 0.05, n=12).

The position of the maximum of the first derivative of the red-edge moved 14 nm towards the blue, from 722 nm to 708 nm, with the maximum red-edge shift occurring after about 21 days of treatment. The first derivative for the argon-flooded bean also showed a rounding of the peak for the red-edge position when compared to that of the control plants (Figure 4.7). The first derivative of the reflectance showed that changes in gradient occurred at wavelengths of 524, 600, 616, 634 and 644 nm.

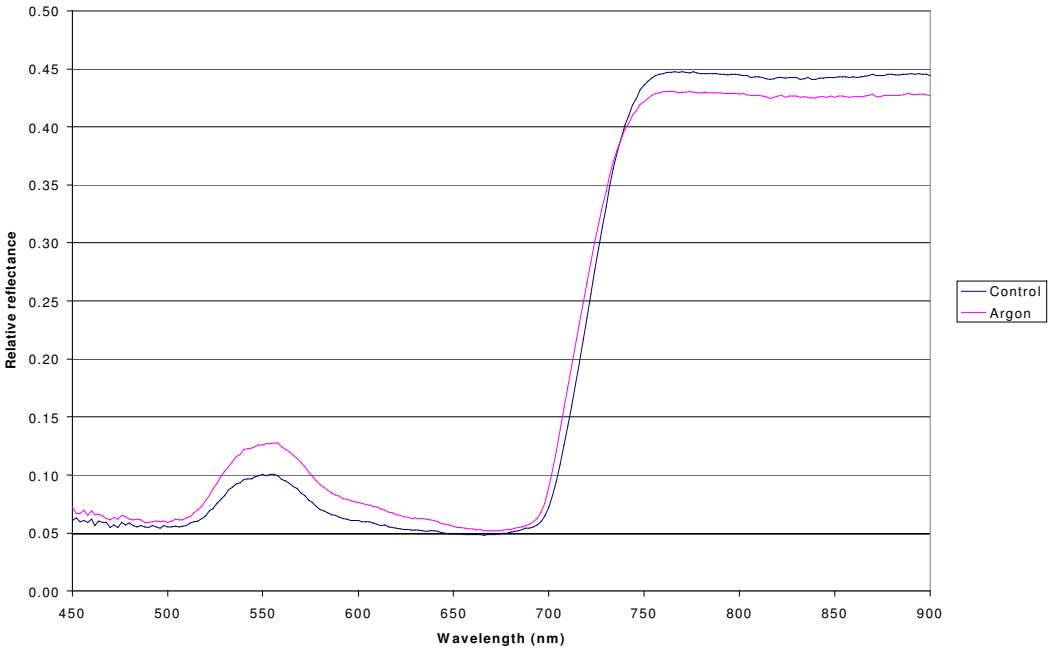

Figure 4.6 Mean reflectance for control and argon-flooded bean (relative to a barium sulphate disc) on 8/6/00 after 25 days of treatment.

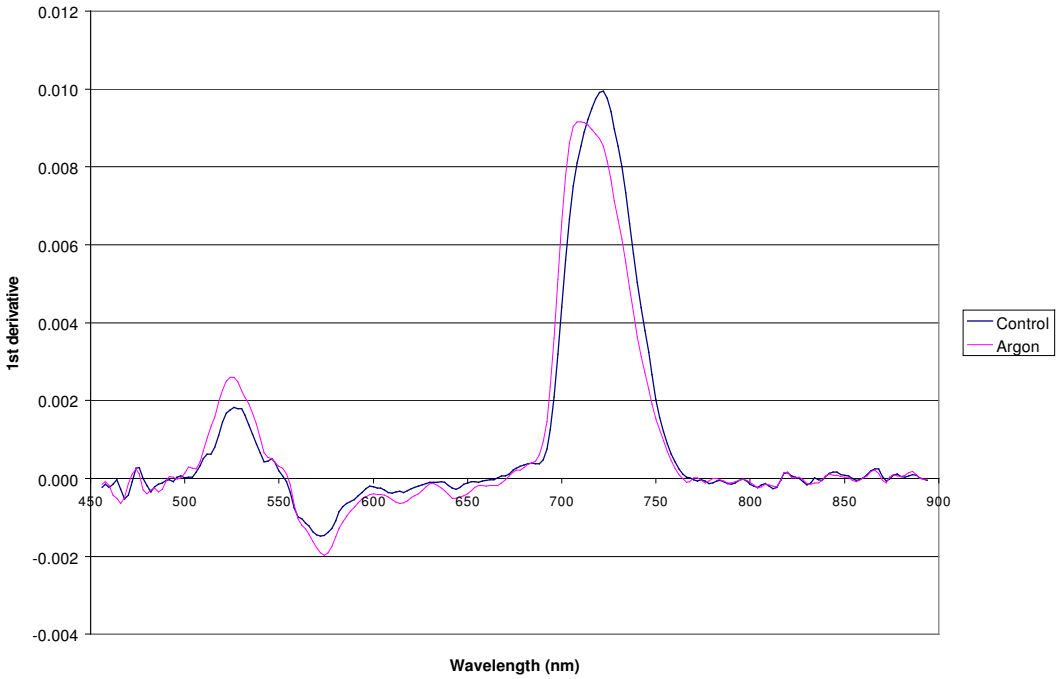

Figure 4.7 First derivative of reflectance for control and argon-flooded bean on 8/6/00 after 25 days of treatment.

Combining the four data sets showed a shift in the position of the red-edge towards longer wavelengths (from 708 to 722 nm) as the control plants matured whereas, the treated plants showed little change in the red-edge position. At the end of the trial both control and treatment plants showed a shift towards the blue, possibly in response to the stress of growing in pots. Figure 4.8 shows the change in red–edge in argon-flooded bean. The error bars show the standard error across the four trials where more than two sets of data occurred within each time period.

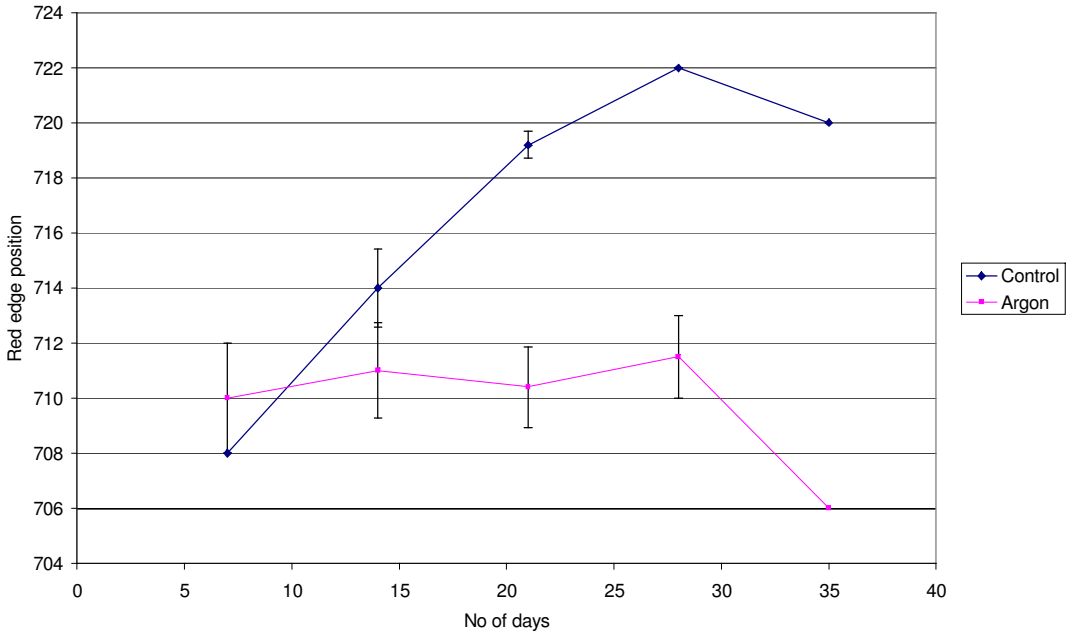

Figure 4.8 Change in the position of the red-edge in argon-flooded bean. The error bars denote the standard error across the four trials

Figure 4.9 shows the changes in the magnitude of the first derivative at other wavelengths from the four combined trials. At 524 nm the magnitude of the first

derivative showed an initial decrease and then remained constant for the control. The argon-flooded bean showed similar changes in first derivative but the magnitude increased by 30% relative to the control from the second week of treatment. At 574 nm the first derivative showed an initial increase in both the control and the argon-flooded bean and then levelled off with the argon-flooded bean showing a slightly decreased magnitude of first derivative (22% lower) after the third week of treatment. This pattern was also seen at 600, 616, 634 and 644 nm. Changes in magnitude in the first derivative of around 39% were seen at 600 nm, 49% at 616 nm, 81% at 634 and 114% at 644 nm after 21 days of treatment.

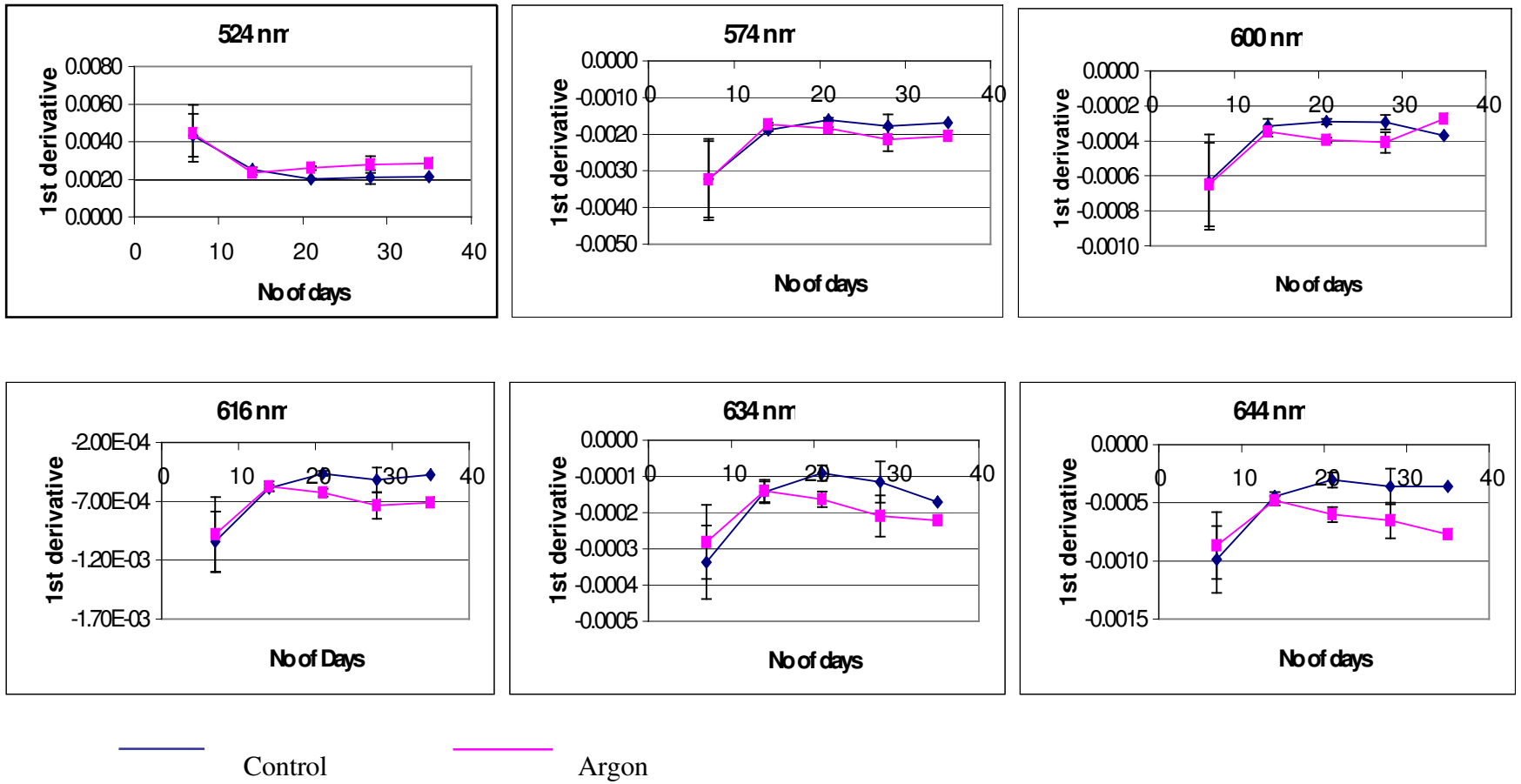

Figure 4.9 Changes in magnitude of first derivative of reflectance for argon-flooded bean over five weeks of treatment, data for four trials combined

4.1.3 Waterlogging

Waterlogging was used as an alternative method of displacing oxygen from the soil to determine if the response of leaves to natural gas was specific or generic to oxygen deficiency. Four waterlogging trials were carried out with bean and all showed increased reflectance in the visible region and little change in the infrared (Figure 4.10). T-test analysis showed that significant differences occurred in the wavelength ranges 508 to 654 nm and from 692 to 742 nm ($p = 2.7x10^{-3}$ to 0.05, n=12).

When the first derivative of reflectance was calculated for the four bean waterlogging trials, several changes could be identified. The point of inflection, which is used to identify the position of the red-edge, could be seen to move between 8 and 22 nm towards the blue. Figure 4.11 shows the first derivative of reflectance for waterlogged bean in trial 1 after 25 days of treatment.

Combination of the four data sets showed that over the time periods of the trials the red-edge of the control bean shifted 12 nm towards the infrared whereas that of the waterlogged bean moved 4 nm towards the blue (Figure 4.12).

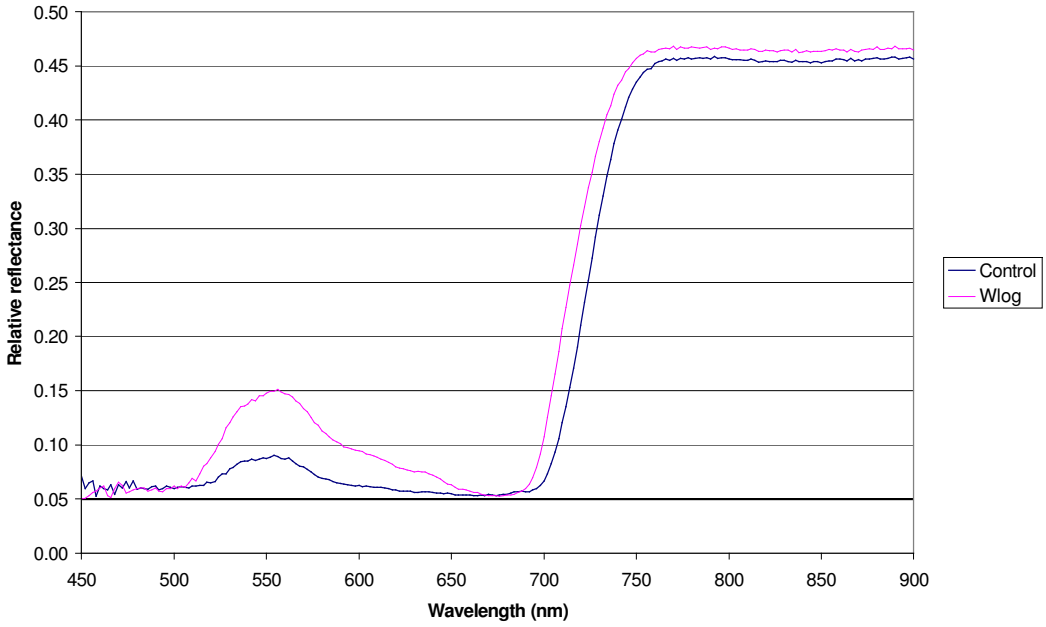

Figure 4.10 Mean reflectance of control and waterlogged bean on 1/8/00 after 25 days treatment

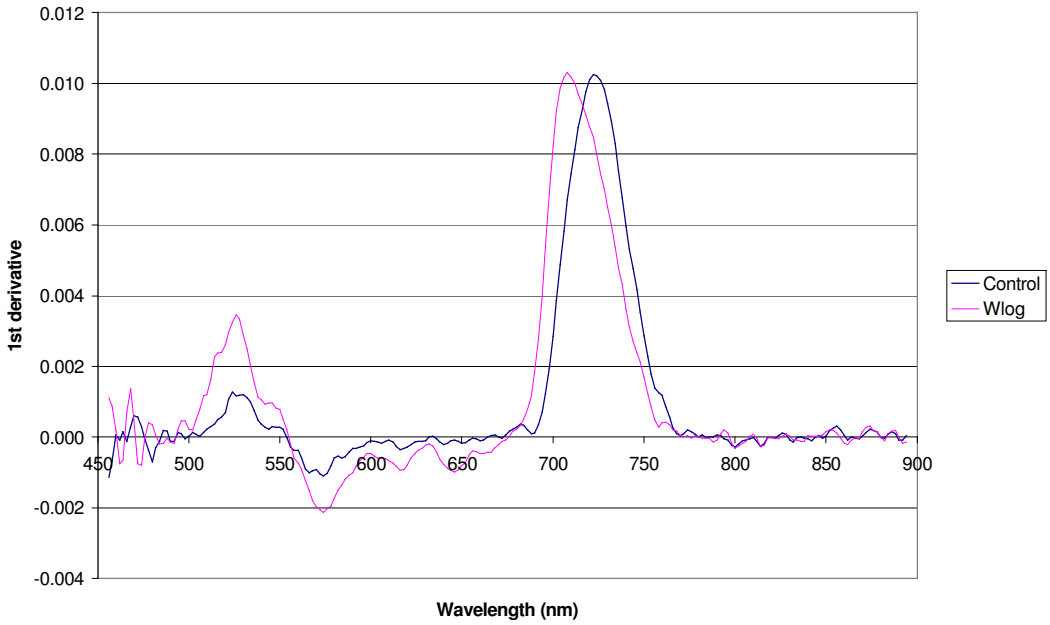

Figure 4.11 First derivative of reflectance for control and waterlogged bean on 1/8/00 after 25 days treatment (trial 1)

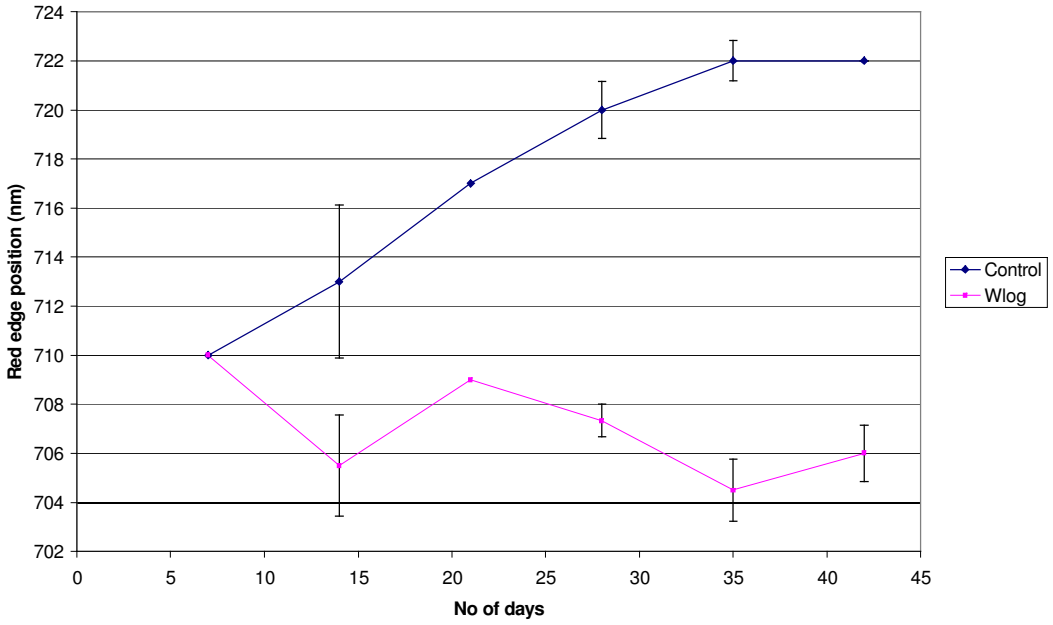

Figure 4.12 Change in the position of the red-edge in waterlogged bean (average of four trials). The error bars represent the standard error of the red edge across the four trials.

Figure 4.13 illustrates the combined changes observed in the first derivatives of reflectance at the six selected wavelengths over the four separate trials. All trials showed a large increase in the magnitude of the first derivative of reflectance at 524 nm. The control bean showed a slight decrease in magnitude of the first derivative at 524 nm as the trial progressed. However, after a slight increase the magnitude of the first derivative for the waterlogged bean remained constant such that there was a large difference between the control and waterlogged plants. The increase relative to the control was up to 113%. Similar changes were also identified at 574, 616, 644 and 664 nm where increases in the magnitude of the control plants first derivatives were contrasted to either little change or decreases in those of the waterlogged bean. At 574 nm there was a relative 65% decrease in magnitude of the first derivative for the

waterlogged plants leading to a deepening of the trough. At 600 nm the decrease was 107% for the waterlogged bean leading to a decrease in the amplitude of the peak. At 616 nm a decrease of 126% led to a deepening of the trough for the waterlogged bean. The biggest differences were at 634 nm and 644 nm, where at 634 nm the waterlogged plants showed a decrease of 212% in the magnitude of the peak and at 644 nm there was a 306% relative decrease in the magnitude of the first derivative giving a deepening of the trough for the waterlogged bean. Changes in all the wavelengths were observed by the third week of the trial (after 14 days of treatment).

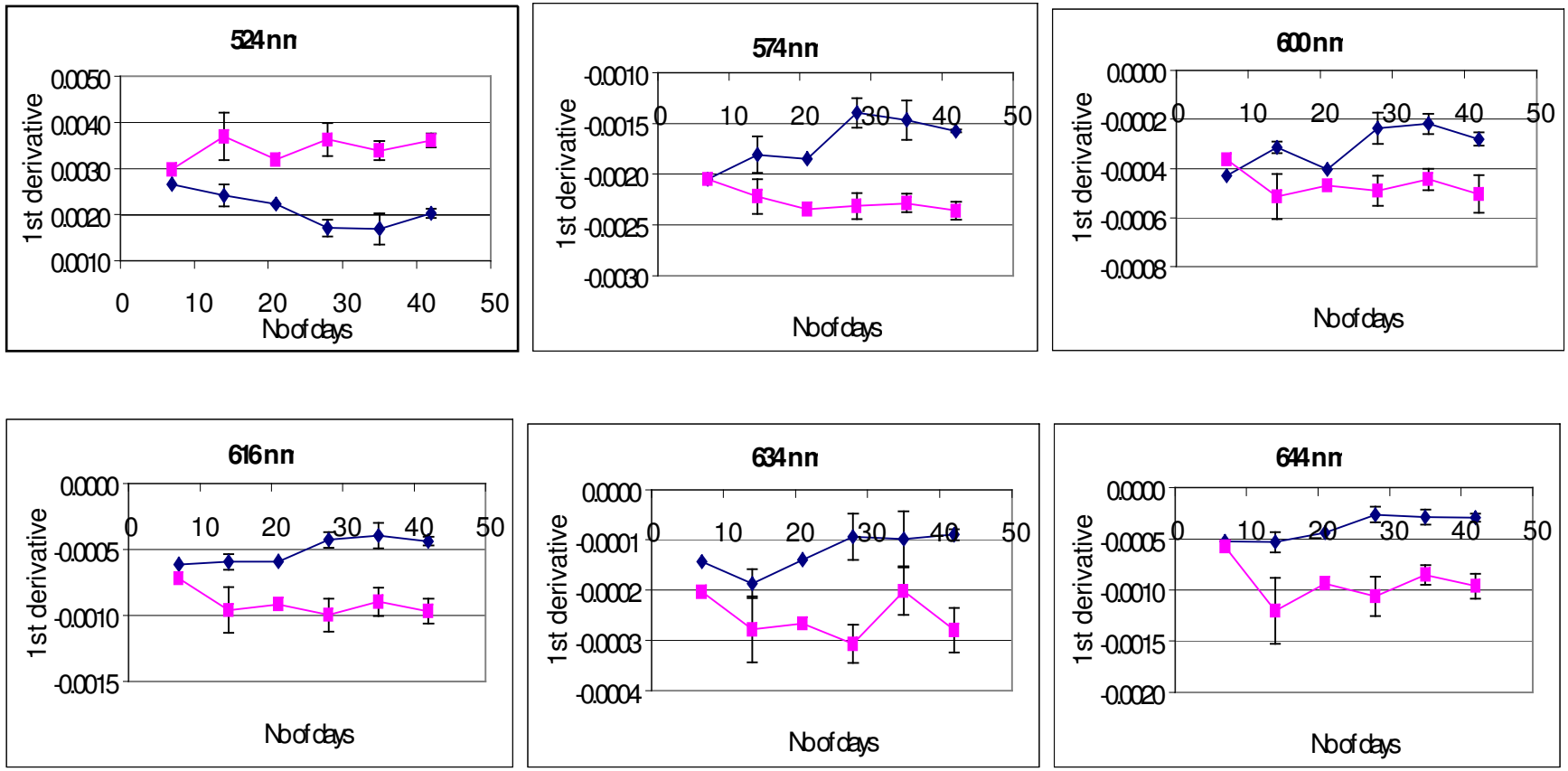
524nm
574nm
600nm
616nm
634nm
644nm
1st derivative
No of days
Control
Waterlogged

Figure 4.13 Changes in magnitude of first derivative of reflectance for waterlogged bean over five weeks of treatment (data from four trials was combined).

4.1.4 Nitrogen

A single experiment was carried out in which nitrogen gas was used to displace oxygen from the soil in which bean were growing. Changes in the relative reflectance and the first derivative of reflectance between the control and nitrogen flooded bean were small and there was no shift in the red-edge over the period of the trial (Figure 4.14, Figure 4.15).

Nitrogen is present in high concentrations in the atmosphere and in the soil air and is also a biologically active gas. Beans are able to fix atmospheric nitrogen to nitrate and thus increased levels of nitrogen in the soil may have the effect of increasing nitrate utilisation in the soil. It was noted that the roots of the bean flooded with nitrogen gas contained more root nodules than were present on the control bean. It was therefore decided that nitrogen gas was not a suitable method of displacing oxygen from the soil, and no further work on this gas was undertaken.

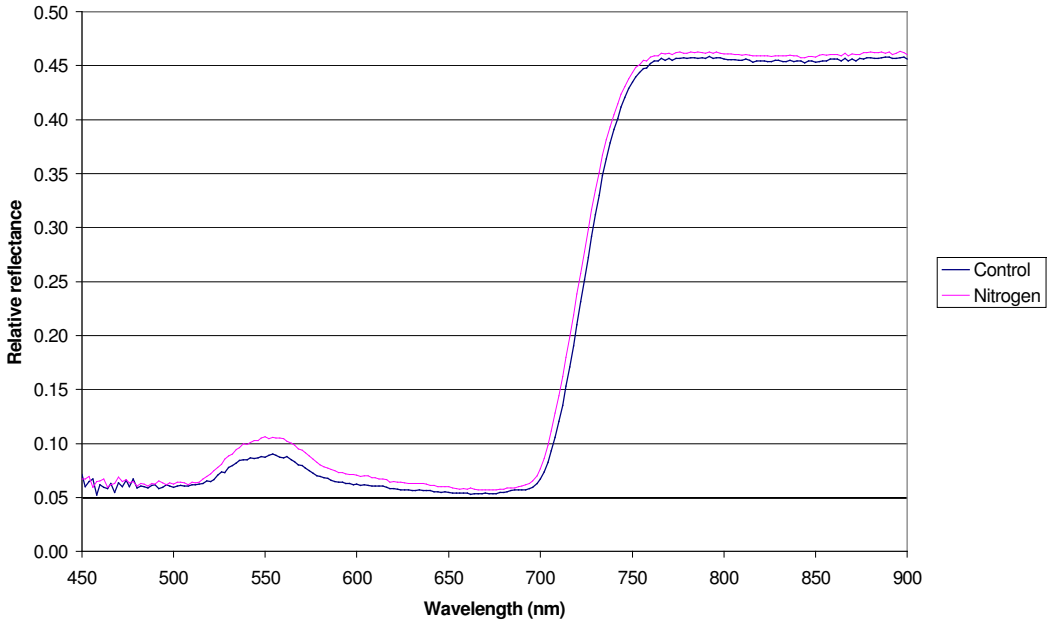

Figure 4.14 Mean reflectance of control and nitrogen flooded bean on 1/8/00 after 25 days treatment

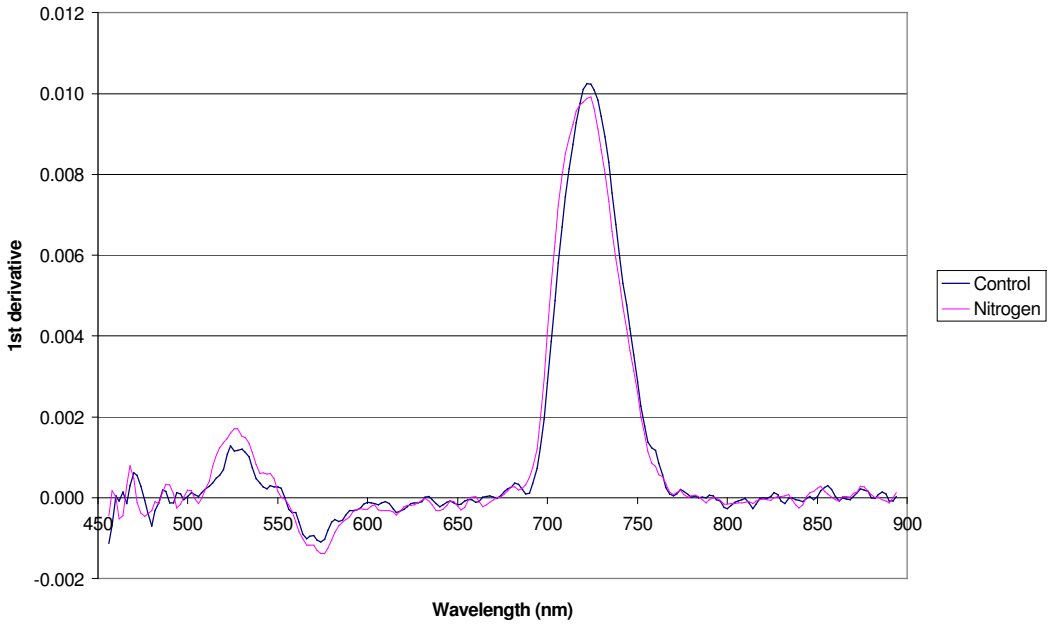

Figure 4.15 First derivative of reflectance for control and nitrogen-flooded bean on 1/8/00 after 25 days treatment

4.2 Radish

4.2.1 Waterlogging

Three waterlogging trials were carried out using radish as an alternative dicotyledonous plant to bean. As with bean, radish also showed increased reflectance in the visible wavelengths, and small changes in the infrared wavelengths (Figure 4.16). T-test analysis showed significant differences in reflectance across the wavelength ranges 476-726 nm ($p=5.5x10^{-4} – 0.05$, $n=12$). Shifts in the position of the red-edge of up to 10 nm towards the blue were observed for the waterlogged radish when compared to the control radish (Figure 4.18). In both the control and the waterlogged radish the red-edge position shifted to longer wavelengths as the plants matured but the red-edge position of the waterlogged plants remained at shorter wavelengths than the control plants.

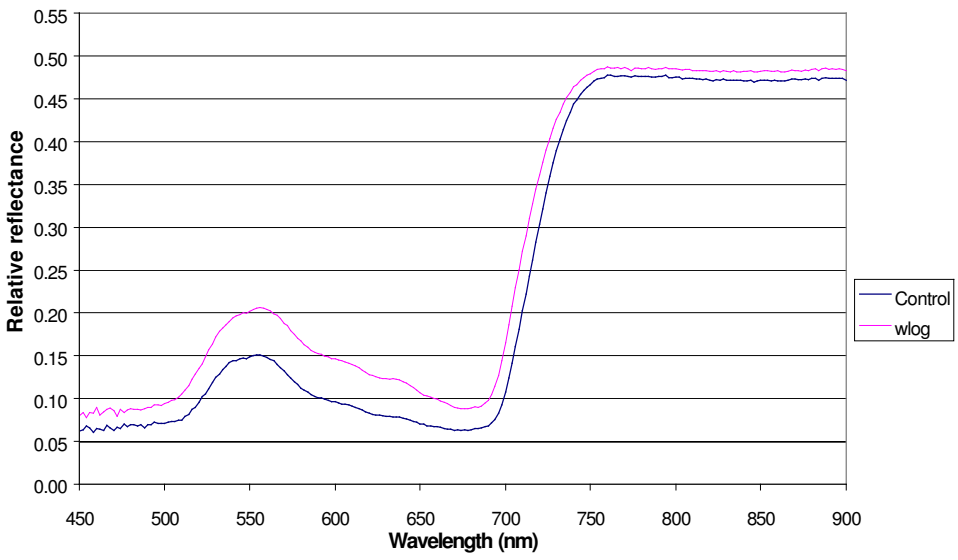

Figure 4.16 Mean reflectance of control and waterlogged radish on 30/6/00 after 17 days treatment

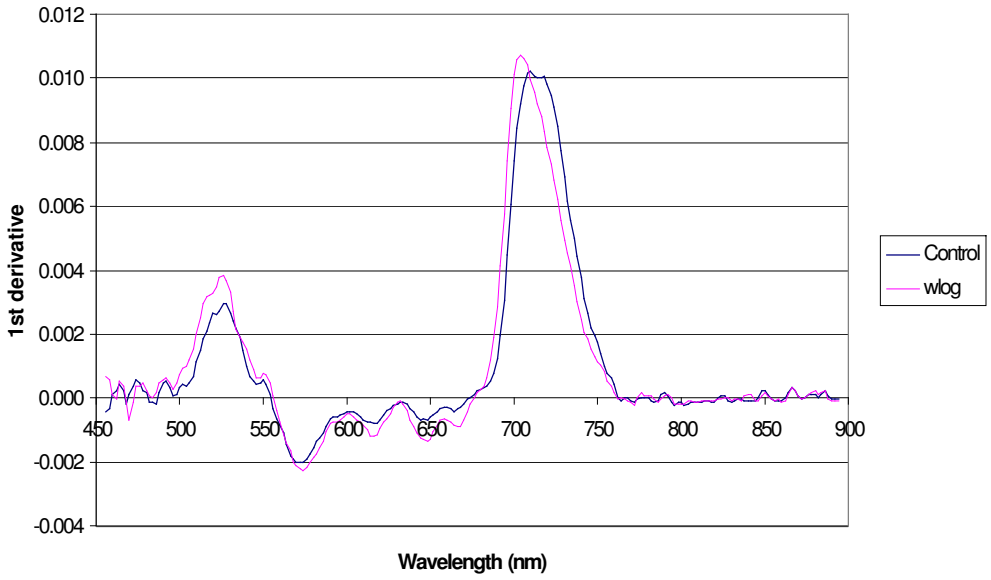

Figure 4.17 First derivative of reflectance of control and waterlogged radish on 30/6/00 after 17 days treatment

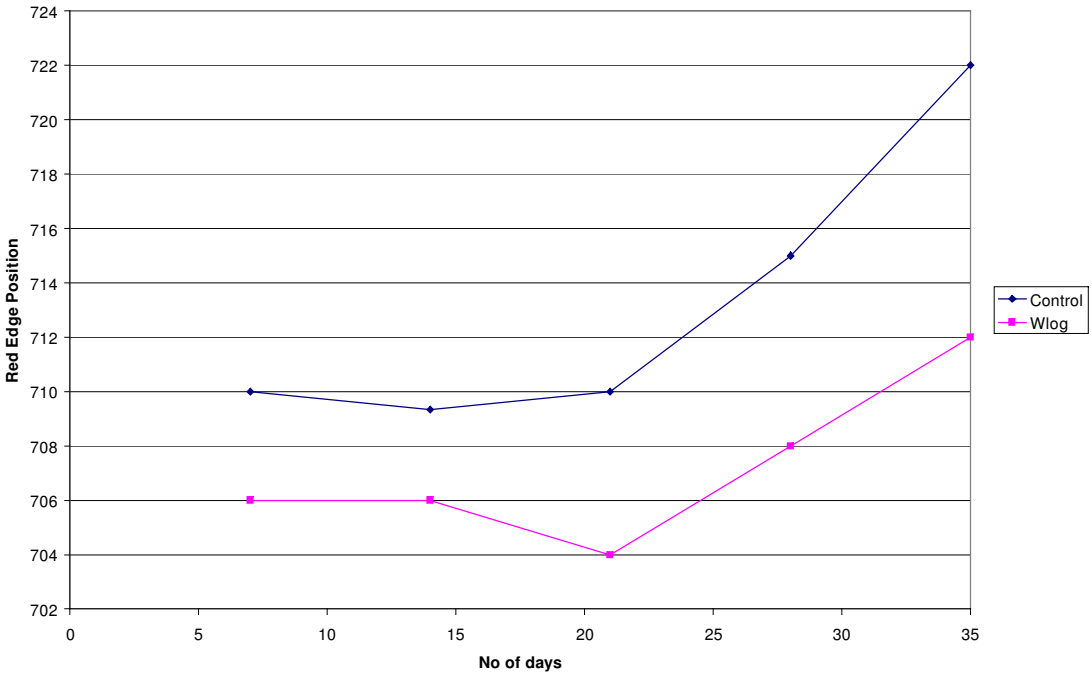

Figure 4.18 Change in the position of the red-edge for waterlogged radish.

Changes in magnitude of the first derivative were seen at all the selected wavelengths with the greatest relative change being observed at 616, 634 and 644 nm (Figure 4.17, Figure 4.19). At 524 nm the magnitude of the first derivative decreased as the trial progressed for both the control and the waterlogged radish but the waterlogged radish decreased less rapidly so that the difference between the first derivatives at the end of the trial was greater at 48%. At the other wavelengths the magnitude of the first derivative increased but the waterlogged radish had a lower magnitude of first derivative than the control plants. At 574 nm the relative difference between the control and waterlogged plants was 28% and at 600 nm the difference was 14%. The greatest difference relative to the control was seen at 616 nm (66%), 634 nm (65%) and 644 nm (110%).

The dicotyledons studied (bean and radish) both show increases in reflectance in the visible wavelengths and little change in the infrared when treated with different methods of displacing oxygen from the soil. Displacing the oxygen from the soil with water, natural gas and argon led to changes in the first derivative of reflectance of selected wavelengths that led to large relative percent differences in the control and treated plants. The position of the red-edge is seen to move to longer wavelengths in the control plants whereas there is little movement in the treated plants. Effects were smaller when oxygen was displaced from the soil with natural gas because it was not possible to carry out the treatment continuously.

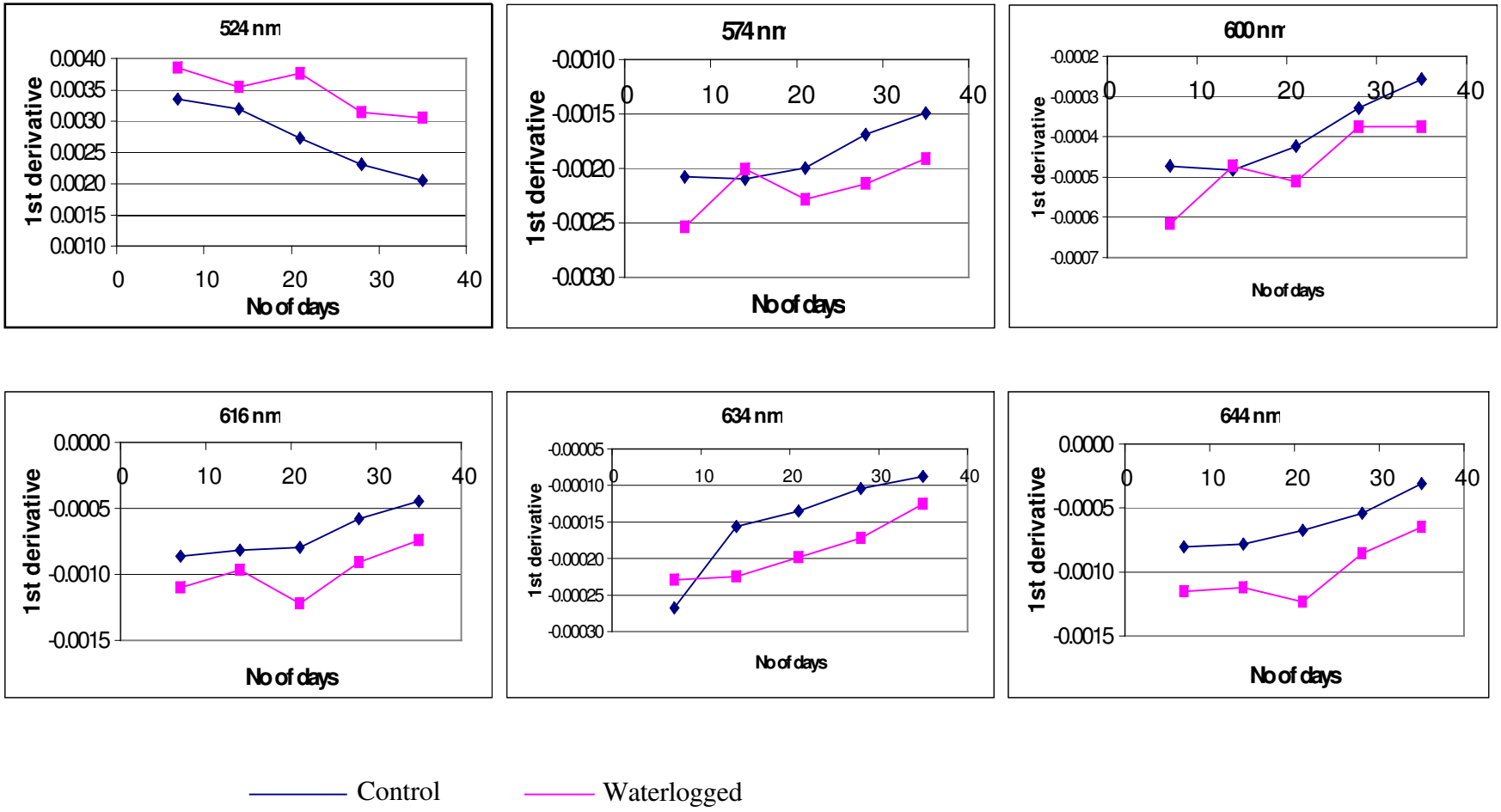

Figure 4.19 Changes in magnitude of first derivative of reflectance for waterlogged radish over five weeks of treatment

4.3 Barley

Barley was studied as an example of a monocotyledon. As barley is a cereal crop it is also an example of the type of vegetation often to be found growing on farm land traversed by gas pipelines. Experiments were carried out to investigate the effects of displacing the soil oxygen with water or argon gas on the spectral characteristics of barley leaves. Each exposure trial was repeated four times.

4.3.1 Waterlogging

As was seen for bean, waterlogging caused increased reflectance in the visible wavelength regions and only small changes in the infrared regions (Figure 4.20). Significant differences in reflectance were seen across the wavelength range 496 to 744 nm ($p=1x10^{-4}$ to 0.05, n=12). The main difference between bean and barley was seen in the first derivative of reflectance (Figure 4.21). Increases in the first derivative were observed at 524, 616 and 644 nm but these were not as marked as the changes observed in bean. At 524 nm there was an increase in the magnitude of the first derivative, in both control and waterlogged barley, as the trial progressed. The relative increase in waterlogged barley when compared to control barley is 18%. There was very little change at 574 and 616 nm with the difference being 6 and 11% respectively. At 616, 634 and 644 nm the change was more marked with the first derivative being respectively 21, 22 and 28 % lower than for the control plants. The shape of the peak that represents the red-edge position was also markedly different to that observed in bean. Bean shows a single peak in the region 702 to 724 nm and the change in position of this peak describes the change in position of the red-edge. In barley, however, the point of maximum inflection is followed by a second peak, giving a double peak with a second lower peak or shoulder to the right of the first peak at 722

nm. The first peak is consistently positioned at 704 to 706 nm, and does not move either as the plant develops or as the plant becomes stressed. However, when stressed the shape of the second peak or shoulder changes. As the barley becomes stressed the magnitude of the shoulder decreases and shifts towards the blue such that the double peak trends towards a single peak. In order to illustrate the change in shape of the double peak the data from the four repeats were combined and the magnitude of the first derivative at 722 nm was plotted (Figure 4.22). The graph shows that the magnitude of the first derivative of reflectance for the control barley does not change as the barley matures, whereas the magnitude for the waterlogged barley is lower throughout the trial and the difference increases as the trial progresses.

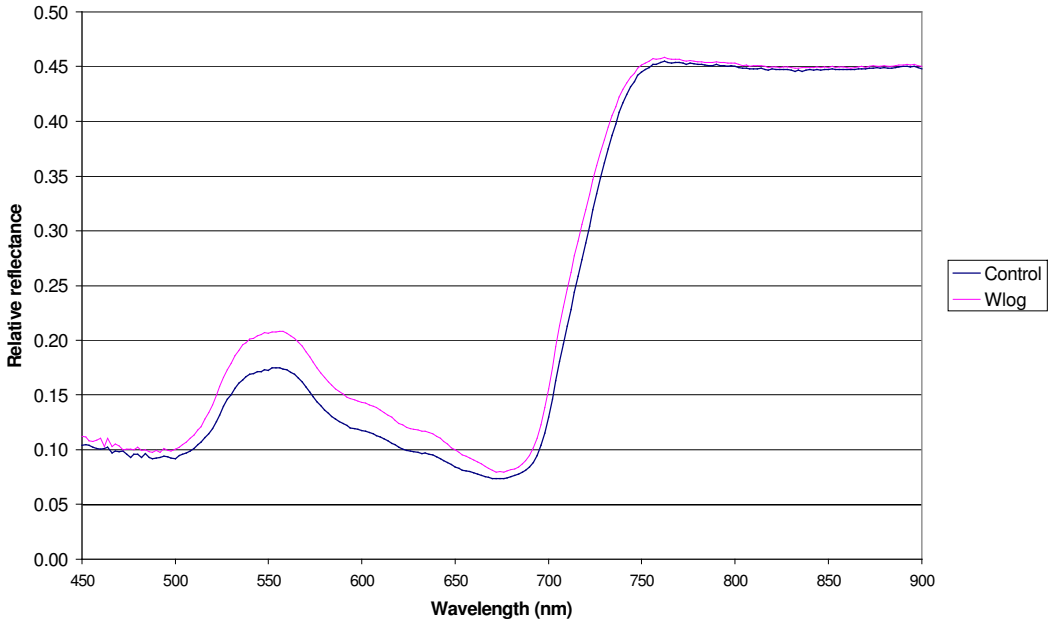

Figure 4.20 Mean reflectance of control and waterlogged barley on 23/3/01 after 29 days treatment

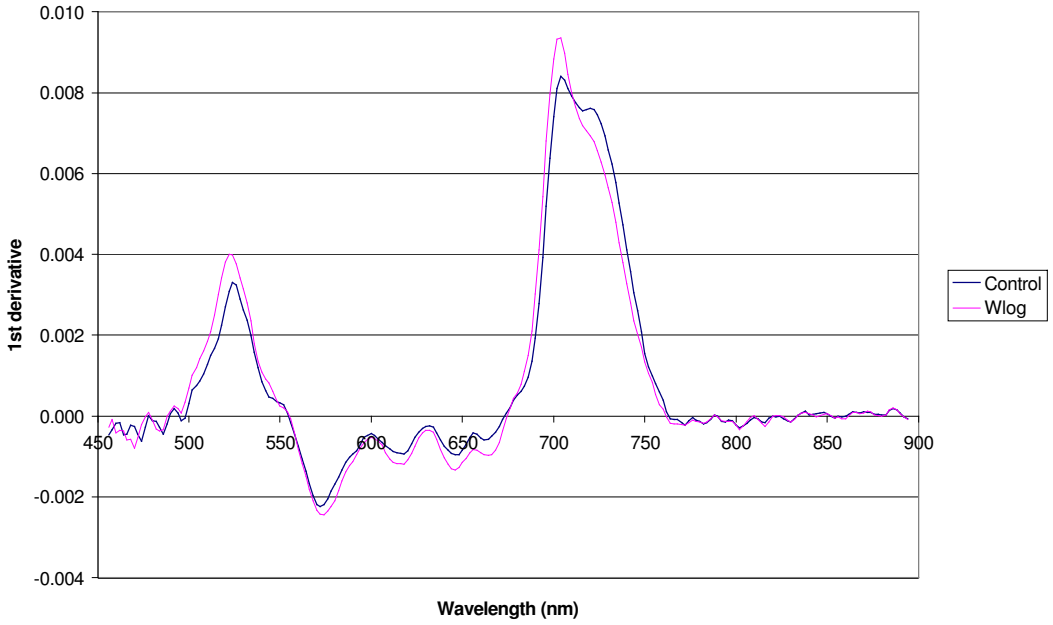

Figure 4.21 First derivative of reflectance of control and waterlogged barley on 23/3/01 after 29 days treatment

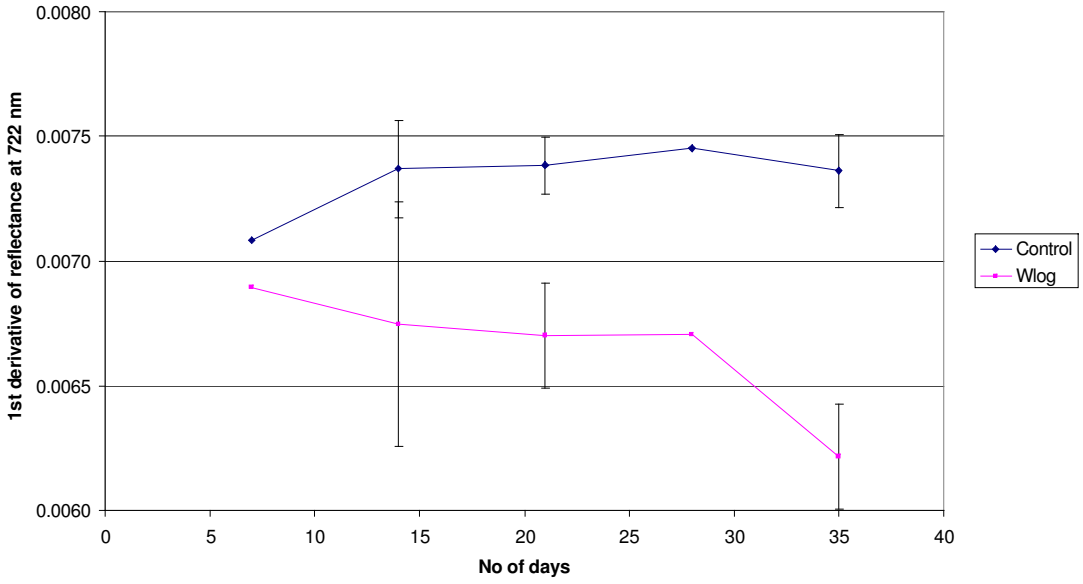

Figure 4.22 Change in the magnitude of the first derivative of reflectance at 722 nm in waterlogged barley (average of four trials combined).

Figure 4.23 shows the change in the magnitude of the first derivative at selected wavelengths. At 524 nm the slope of the reflectance from the waterlogged barley increased as the trial progressed and thus led to an increase in the amplitude of the peak for the waterlogged barley. At the other selected wavelengths there was a decrease in the magnitude of the first derivative in the waterlogged barley and the difference becomes more pronounced as the trial progressed, although effects at 600 nm are not as obvious as at the other selected wavelengths. Changes in the first derivative of reflectance between the control and waterlogged plants become apparent after the third week of the trial (after day 14).

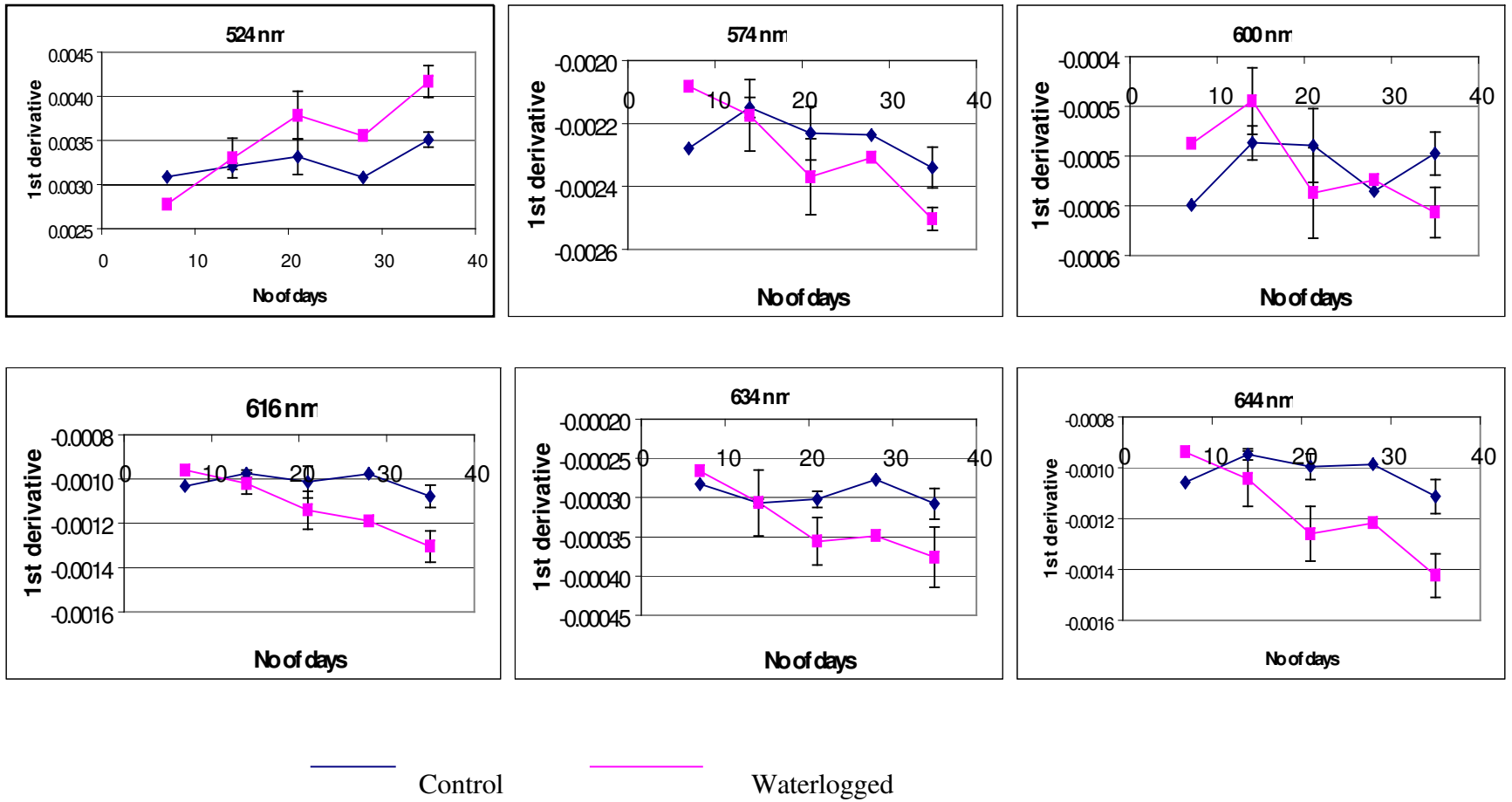

Figure 4.23 Changes in magnitude of first derivative of reflectance for waterlogged barley over five weeks of treatment (average of four trials).

4.3.2 Argon

Displacement of the soil oxygen with argon showed similar results with barley as were seen with bean. Increases in reflectance in the visible wavelengths, between 474 and 722 nm ($p = 1x10^{-3}$ to 0.05, n=12) and changes in the magnitude of the first derivative of reflectance at 524 nm and 644 nm were seen (Figure 4.24). There were also small changes observed at 600, 616 and 634 nm.

As with the waterlogging trial, the position of the red-edge was marked not with a single peak but with a double peak, with a plateau to the right of the first peak (Figure 4.25). The position of maximum inflection in the first derivative was located between 706 and 702 nm and did not change as the barley matured or as it became more stressed due to the oxygen decrease in the soil. Studies of the first derivative of reflectance at 722 nm show that the magnitude for the first derivative for the control plants tends to rise as the barley matures but that the argon-flooded plants show a decrease in the magnitude of the first derivative as the peak shifts towards the blue to give rise to a single peak (Figure 4.26).

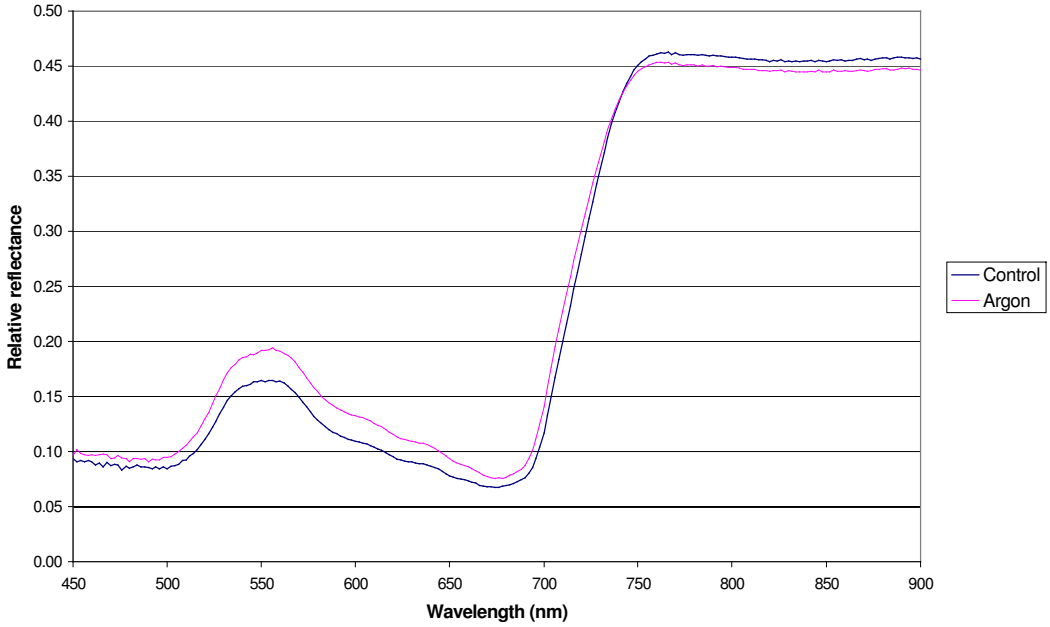

Figure 4.24 Mean reflectance of control and argon-flooded barley on 23/3/01 after 29 days treatment

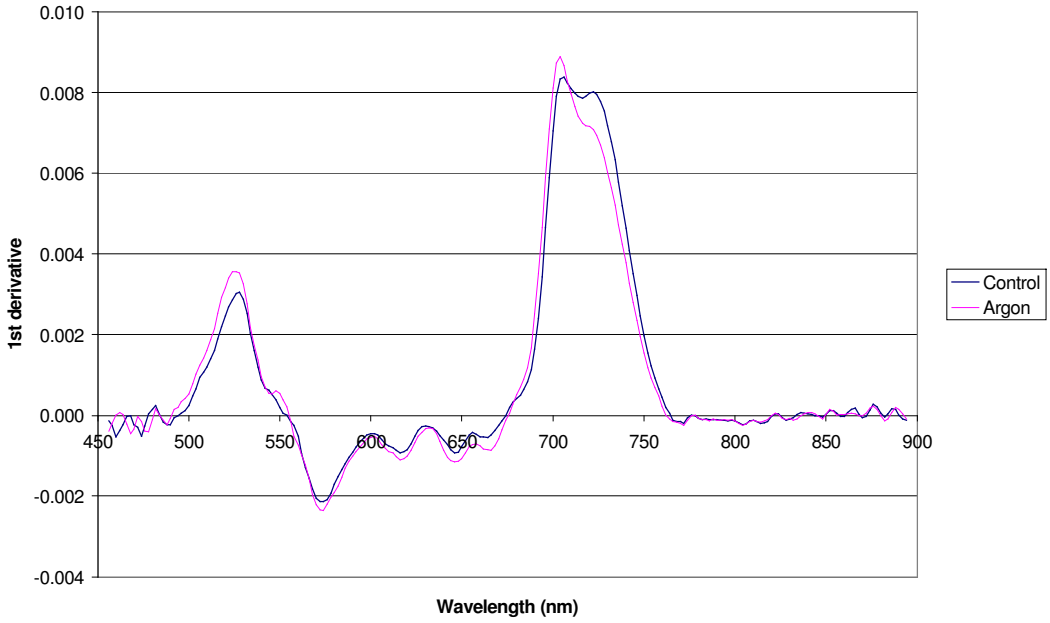

Figure 4.25 First derivative of reflectance of control and argon-flooded barley on 23/3/01 after 29 days treatment

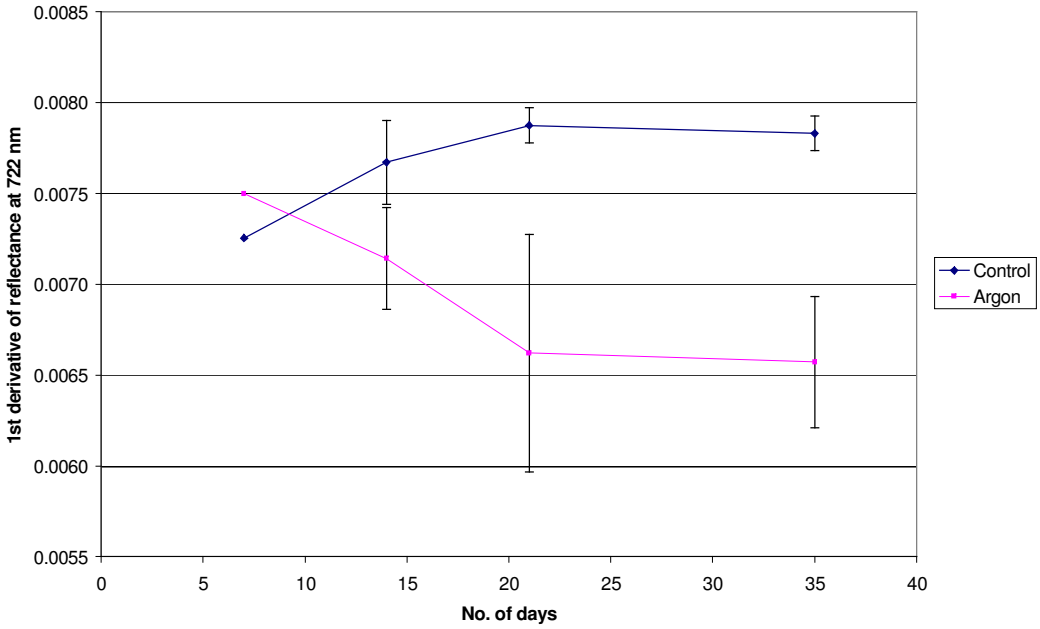

Figure 4.26 Change in the magnitude of the first derivative of reflectance at 722 nm in argon-flooded barley

Figure 4.27 illustrates the changes observed in the first derivative of reflectance at selected wavelengths for argon-flooded barley over the five weeks of the trial. There were differences between the control and the argon-flooded barley but these were not as pronounced as were observed in argon-flooded bean. At 524 nm the magnitude of the first derivative for the argon-flooded barley was greater than for the control barley (24%). At 574 nm there was an initial increase in the magnitude of the first derivative but this levelled out after the second week. Differences between the control and argon-flooded plants were small (13%). At 600 nm there was a gradual increase in the magnitude of the first derivative with time and this was greater in the control barley than in the argon-flooded barley such that by the end of the trial the difference in first derivative between control and treatment plants was 23%. A similar pattern was seen at 616, 634 and 644 nm with a slight increase in the first derivative with time. The

differences between the control and argon-flooded barley plants were greater than for the other wavelengths but not as large as for the bean plants. Differences were 23, 30 and 36% respectively.

Displacement of oxygen from the soil by argon or water is seen in most respects to have a similar effect on monocotyledons as is seen for dicotyledons. There is an increase in the reflectance in the visible wavelengths and little difference in the infrared. However, the pattern of the red-edge changes in a different way to dicotyledons. The red-edge appears to stay at a constant wavelength of around 704 nm, but the shape of the derivative curve changes as the plants become stressed, such that the red-edge feature changes from a broad double peak to a narrower single peak.

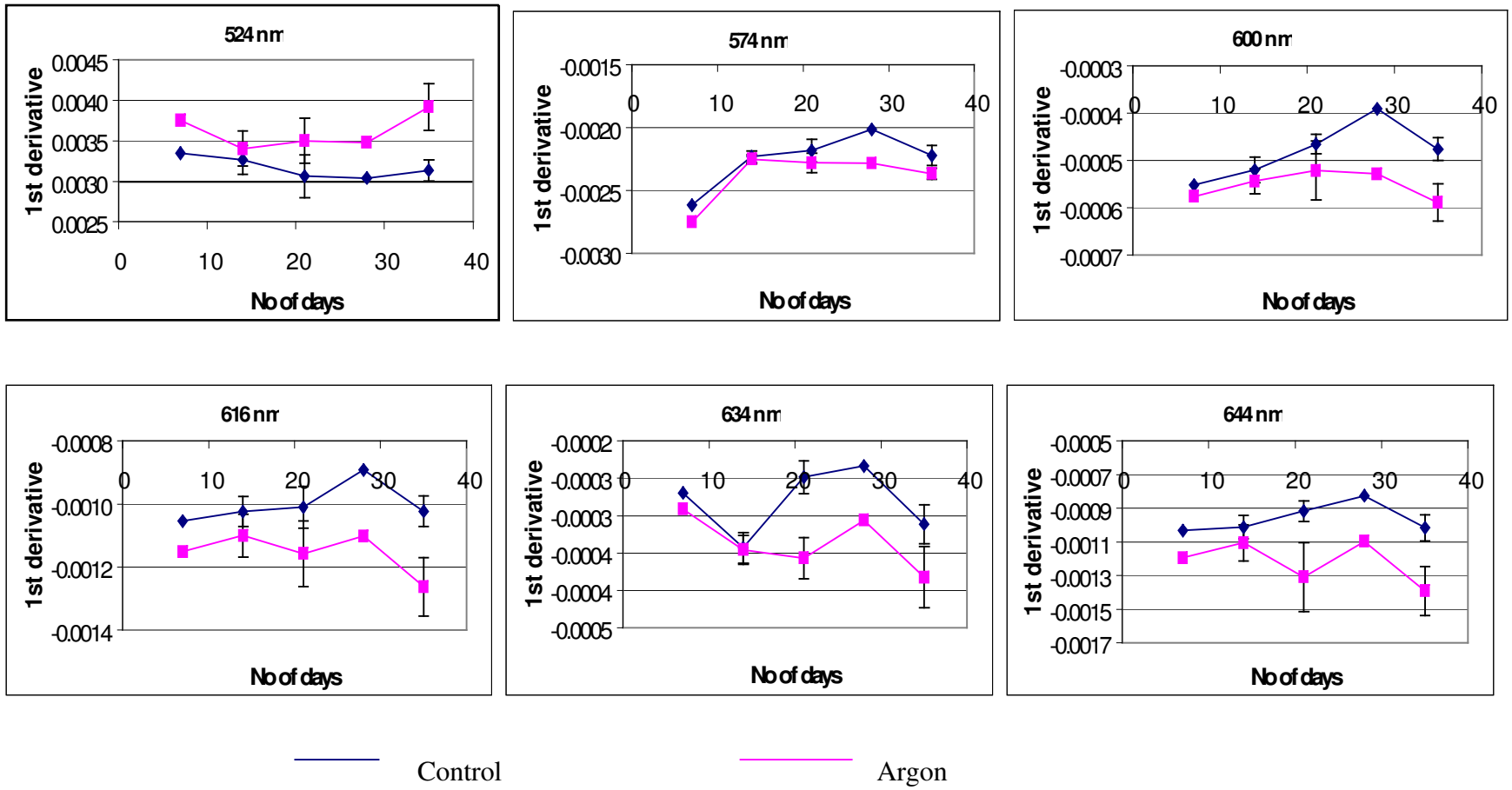

Figure 4.27 Changes in the magnitude of first derivative of reflectance for argon-flooded barley over five weeks of treatment (average of four trials).

4.4 Spectral reflectance measurements obtained using the ASD spectroradiometer.

The ASD Fieldspec Pro spectroradiometer was available on short-term loan from the Equipment Pool for Field Spectroscopy (NERC-EPFS) (University of Southampton), and was used during some of the trials to measure the reflectance of leaves from the trial plants. This instrument has a narrower bandwidth and measures over a wider spectral range than the LI-1800.

When this instrument was available measurements were obtained using both the ASD Fieldspec Pro and the LI-1800. Reflectance was measured using the LI-1800 over the wavelength range 450-900 nm in steps of 2 nm, whereas the ASD covered the range 350-2500 nm at 1 nm intervals. Time and space constraints meant that it was not possible to do both sets of measurements on the same day but the second set of readings was carried out as soon as possible afterwards. Table 4.1 shows the dates when the ASD Fieldspec Pro spectroradiometer and the LI–1800 were used and the shifts in the red-edge observed using both instruments.

Table 4.1 Dates when measurements were taken using the ASD Fieldspec Pro spectroradiometer

Date	Species	Treatment	ASD No. of days since treatment started	Red-edge shift	Licor No. of days since treatment started	Red-edge shift
22/6/00	Bean	Natural gas	8	704-704	7	708-708
22/6/00	Bean	Waterlogging	9	703-699	8	722-706
22/6/00	Radish	Waterlogging	9	704-700	8	708-704
12/7/00	Bean	Nitrogen	7	712-715	13	722-722
12/7/00	Bean	Natural gas	28	703-701	33	710-708
12/7/00	Bean	Waterlogging	5	713-705	10	722-712
12/7/00	Radish	Waterlogging	5	707-705	10	712-708
8/8/00	Radish	Waterlogging	32	714-708	34	724-712
8/8/00	Bean	Nitrogen	36	722-722	38	728-728
8/8/00	Bean	Natural gas	9	709-709	11	710-714
8/8/00	Bean	Waterlogging	31	722-704	33	726-708

Results obtained using the ASD Fieldspec Pro were different to those obtained using the LI-1800 spectroradiometer. A broad view of the results showed that both instruments gave increased reflectance in the visible regions of the spectra and shifts in the position of the red-edge towards the blue when the plants were stressed. However, the magnitudes of the increases in reflectance and red-edge shift were different. In most cases (9 out of 11) the LI-1800 showed a higher absolute magnitude of reflectance than the ASD, and in all cases the ASD showed the position of the red-edge between 5 and 10 nm closer to the blue end of the spectrum. An example of spectra obtained from the ASD spectroradiometer is shown in Figure 4.28. Increases in reflectance with waterlogging can be seen throughout the visible wavelength range and also throughout the infra-red wavelengths. Figure 4.29 and Figure 4.30 show the differences that occur when leaves are measured using the LI-1800 and the ASD spectroradiometers in the wavelength range 450 –900 nm. Possible reasons for these differences are discussed in Section 7.5.

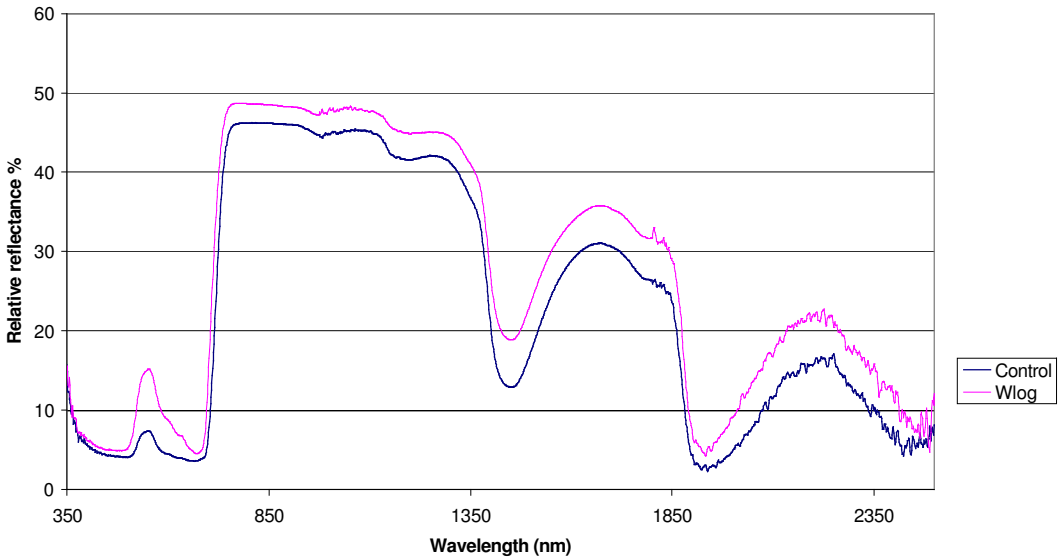

Figure 4.28 Mean reflectance for control and waterlogged bean 8/8/00 measured using the ASD Fieldspec Pro spectroradiometer.

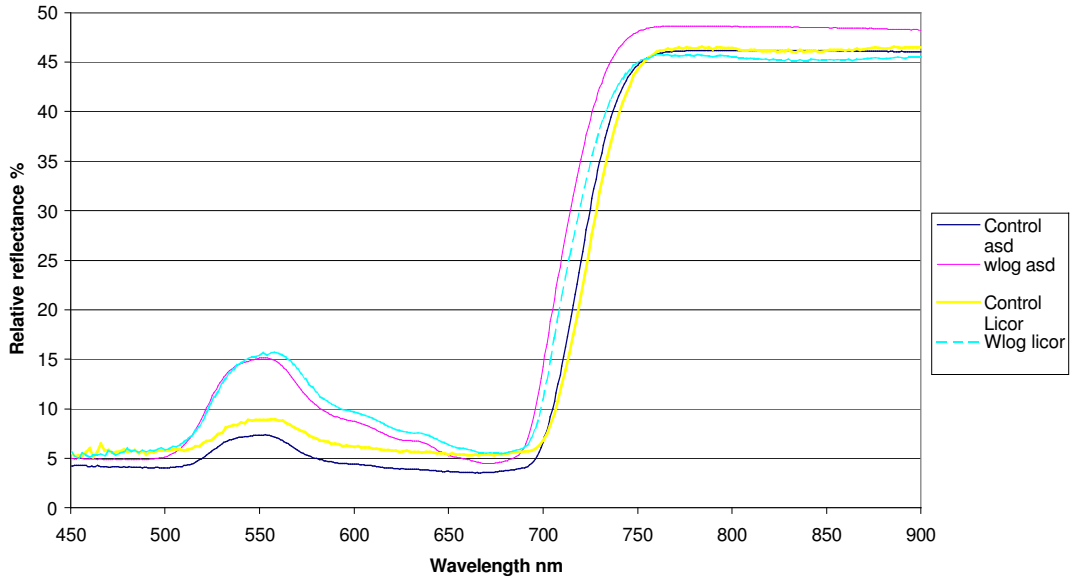

Figure 4.29 Graph comparing the ASD and LI-1800 reflectance from waterlogged bean leaves 8/8/00

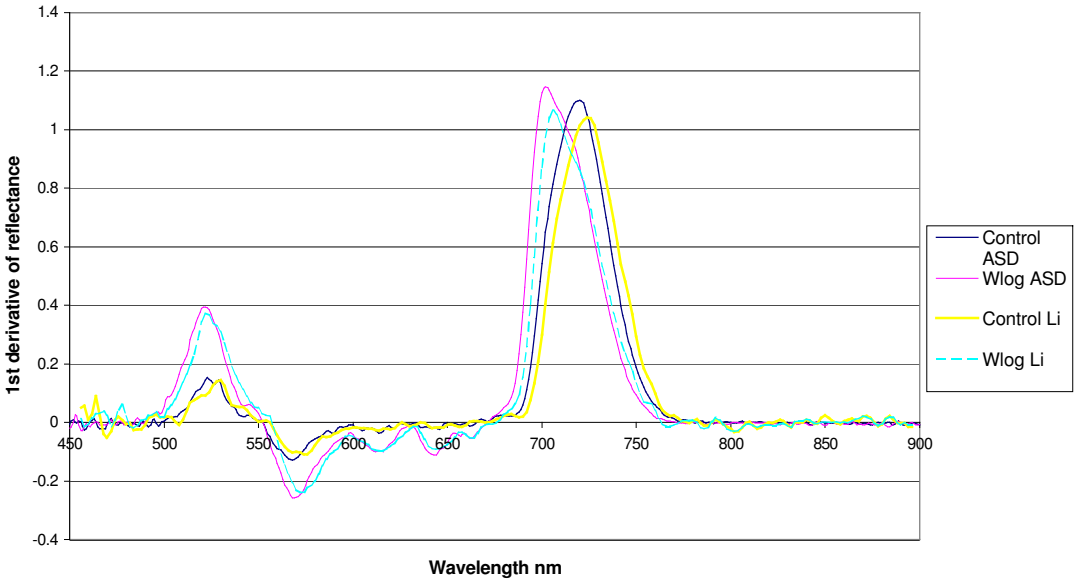

Figure 4.30 Graph comparing the ASD and LI-1800 data for the first derivative of reflectance for waterlogged bean 8/8/00

4.5 Chlorophyll analysis

Total chlorophyll content of the plant leaves was measured at the end of the exposure trials, if sufficient leaves remained to be able to carry out chlorophyll extraction. Chlorophyll analysis of bean was only carried out twice because generally at the end of a trial there were insufficient leaves left to enable analysis to take place.

Table 4.2 Summary of mean chlorophyll content (µg cm^{-2})

Date	Treatment	Species	Total Chl Control µg cm^{-2}	Standard error	Ratio *a:b* control	Total Chl Treatment µg cm^{-2}	Standard error	Ratio *a:b* treatment
06/11/00	Argon	Barley	30.68	3.29	3.14	11.46	0.81	1.79
06/11/00	Wlog	Barley	27.13	1.41	2.85	14.41	2.29	2.83
22/12/00	Argon	Barley	44.73	3.88	3.0	37.51	3.05	2.7
22/12/00	Wlog	Barley	41.51	4.29	2.81	29.01	2.52	2.88
16/02/01	Argon	Barley	39.17	1.41	2.87	36.05	1.89	2.81
25/06/01	Wlog	Barley	34.94	1.86	2.57	24.01	1.87	2.67
25/06/01	Wlog	Bean	35.13	1.89	2.51	17.01	1.74	2.33
9/11/01	Argon	Bean	43.71	2.94	2.9	32.42	2.51	2.7

Combination of three data sets for argon-flooded barley illustrates the change in chlorophyll content between control and treatment plants (Figure 4.31). Figure 4.32 illustrates the effect of waterlogging on the chlorophyll content of barley.

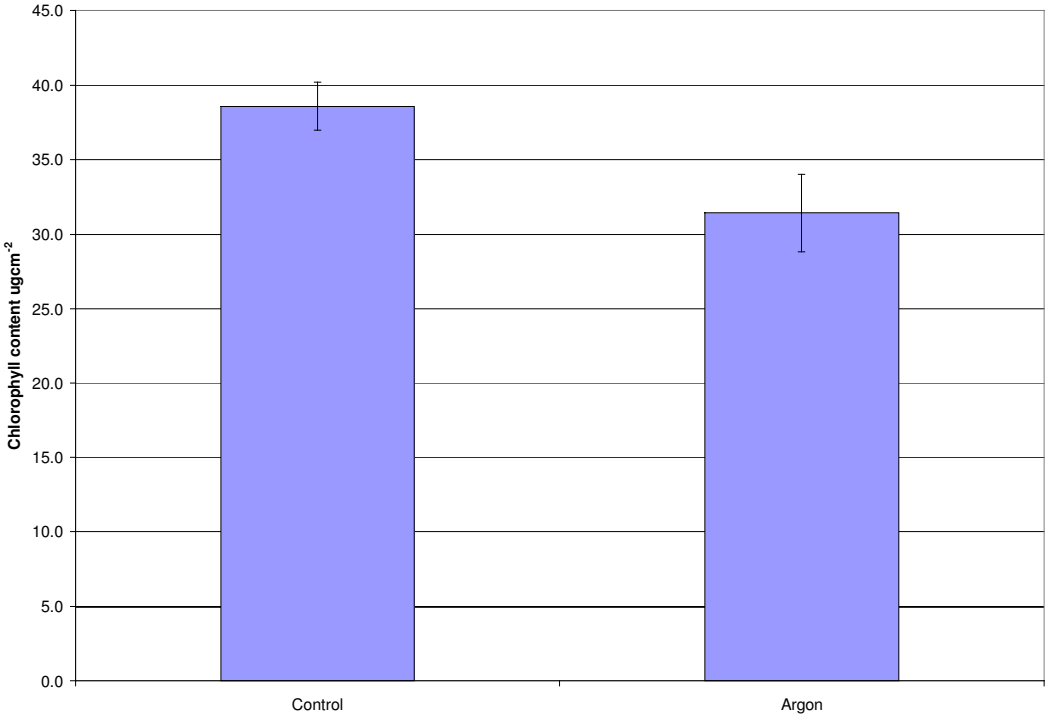

Figure 4.31 Effect of flooding soil with argon on the chlorophyll content of barley

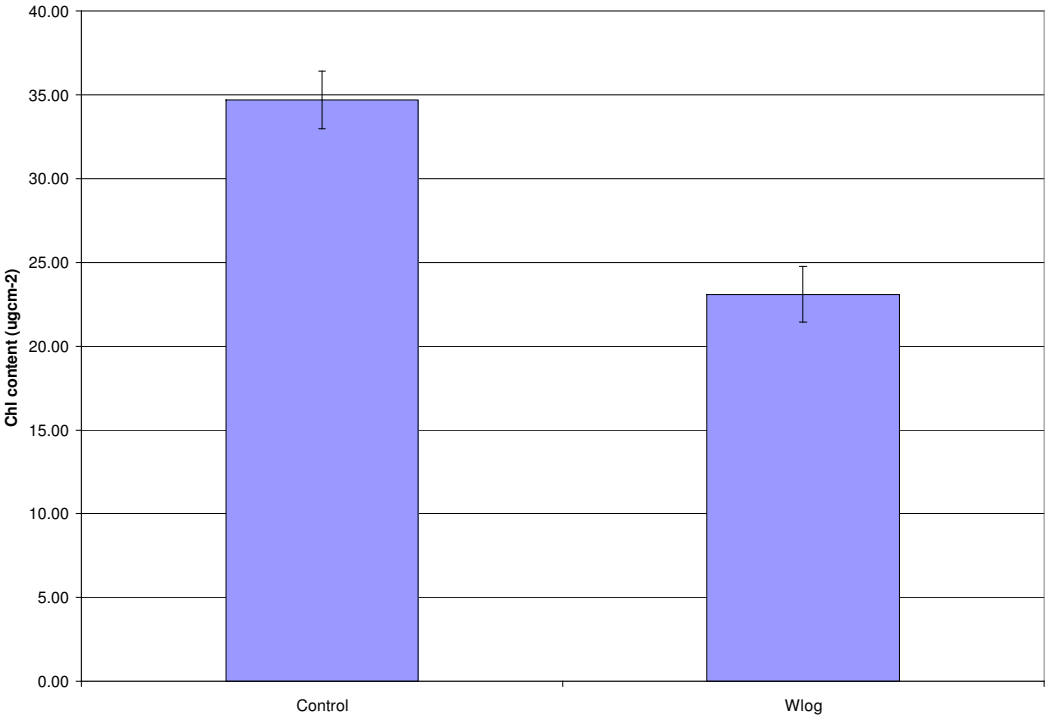

Figure 4.32 Effect of waterlogging on the chlorophyll content of barley

4.6 Dry matter analysis

Dry weights (g cm^{-2}) and equivalent water thickness (cm) were measured at the end of several trials. Generally the dry weight of barley was in the region of 2.4 x 10^{-3} g cm^{-2} (SE = 1.28 x 10^{-4}) and the equivalent water thickness was 0.016 cm (SE = 9.4 x 10^{-4}) and there were no significant differences between the control and treatment plants. Only on two occasions was there a significant change between the control and treatment plants in these factors. In one trial of argon-flooded barley there was a significant change ($p = 0.009$) in the equivalent water thickness from 0.014 cm for control plants to 0.011 cm for argon-flooded plants. In a separate argon-flooded barley trial there was a significant difference ($p=0.0006$) in the dry weight from 0.0022 to 0.0026 g cm^{-2} between the control and the treatment plants.

4.7 Application of the data to the PROSPECT model

PROSPECT is a radiative transfer model based on a "generalised plate model" that represents the optical properties of plant leaves using the leaf hemispherical reflectance and transmittance from 400 to 2500 nm. The scattering of light is described by the refractive index of the leaf materials and a parameter characterising the leaf mesophyll structure (*N*) (Jacquemoud and Baret 1990). In the "plate model" it is assumed that a leaf is composed of a pile of *N* homogenous layers separated by air spaces. Monocotyledons with compact mesophyll have typical values of *N* of between 1 and 1.5, whereas dicotyledons with a spongy parenchyma with air spaces on the abaxial (lower) surface have typical *N* values of 1.5 to 2.5.

PROSPECT version 3.01 was used to model the data obtained during the exposure trials and to compare the PROSPECT predicted reflectance with the values measured with the LI-1800 spectroradiometer. Data input into the model were the total chlorophyll content (μg cm^{-2}), the dry matter per unit area (g cm^{-2}) the equivalent water content (cm) and a value for *N* that relates to the cellular arrangement within the leaf.

The value of N is not directly measurable and must be determined from the spectral data. The model was run using varying values for *N* (2 sig. fig) until the best fit, judged by eye, was obtained between the predicted values and the measured values in the region where absorbance by chlorophyll was at a minimum – in the near infrared region (Jacquemoud and Baret 1990). Figure 4.33 shows the effect of varying *N* in the simulation of spectra for control barley leaves from 22/12/00. The other parameters used in the simulation were the measured values of chlorophyll, dry matter and equivalent water thickness. The value of *N* fitted at the infrared was used as in this area chlorophyll has the least effect on the reflectance. The best value was typically *N*=1.5 for barley leaves and *N*=1.3 for bean leaves.

For barley leaves, the reflectance predicted by the PROSPECT model in the visible was generally underestimated when compared to the reflectance actually measured for the leaves in the integrating sphere. PROSPECT modelled the reflectance from bean leaves more closely (Figure 4.34, Figure 4.35).

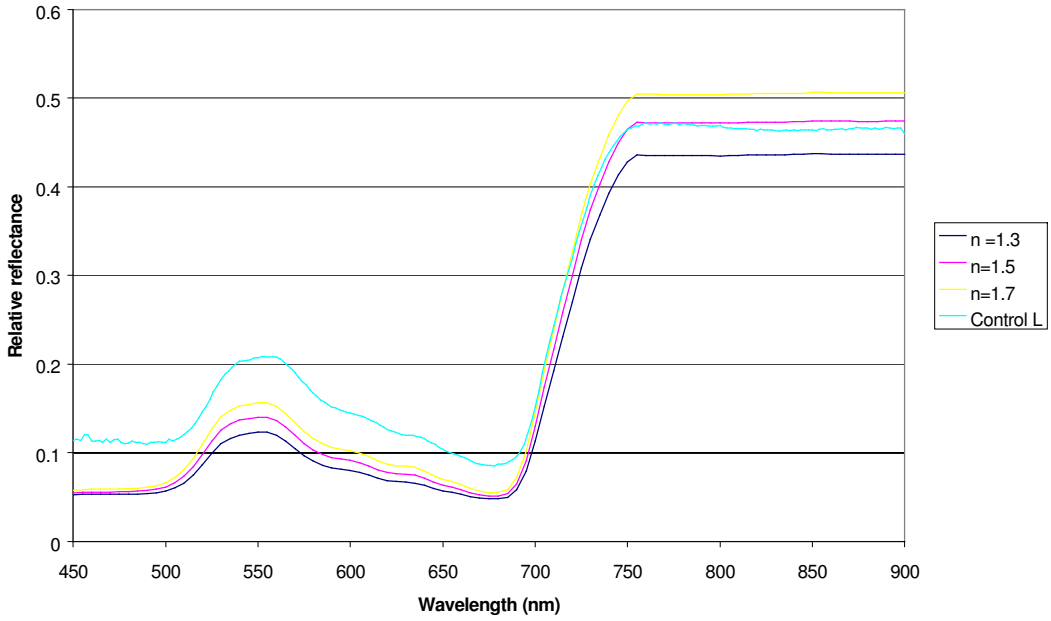

Figure 4.33 Effect of varying the value of *N* in the PROSPECT model for barley leaves (22/12/00) compared with the LI-1800 measurement

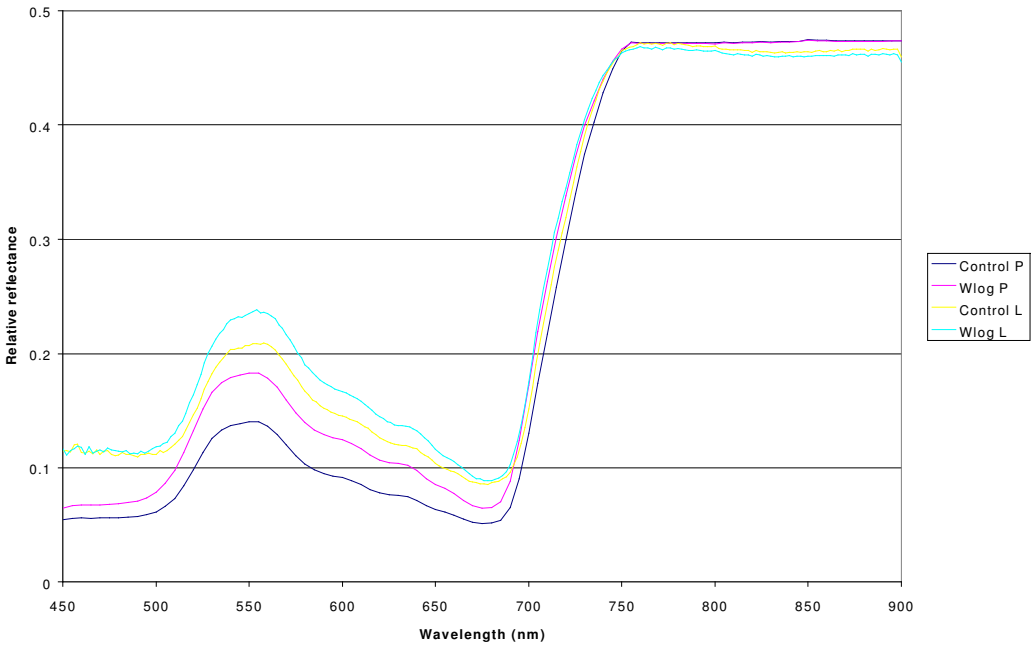

Figure 4.34 Comparison of PROSPECT and measured reflectance for control and waterlogged barley leaves (22/12/00) with *N*=1.5

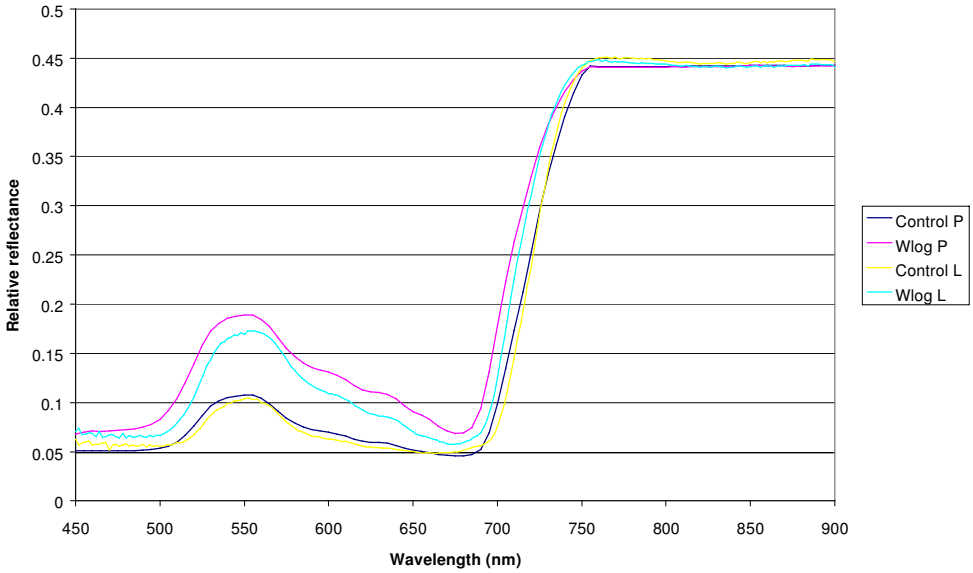

Figure 4.35 Comparison of PROSPECT and measured reflectance for control and waterlogged bean leaves (22/6/01) with *N*=1.3

Comparisons at wavelengths 550, 600, 650 and 680 nm (Table 3.2) were carried out between the predicted and measured reflectance for eight data sets (Table 4.3).

Table 4.3 Plant data used for comparing PROSPECT predicted and LI-1800 measured reflectance

Plant	Treatment	Date of chlorophyll analysis
Barley	Waterlogged	2/11/00
Barley	Waterlogged	22/12/00
Barley	Waterlogged	22/6/01
Barley	Argon	2/11/00
Barley	Argon	22/12/00
Barley	Argon	16/2/01
Bean	Waterlogged	22/6/01

Bean	Argon	9/11/01	

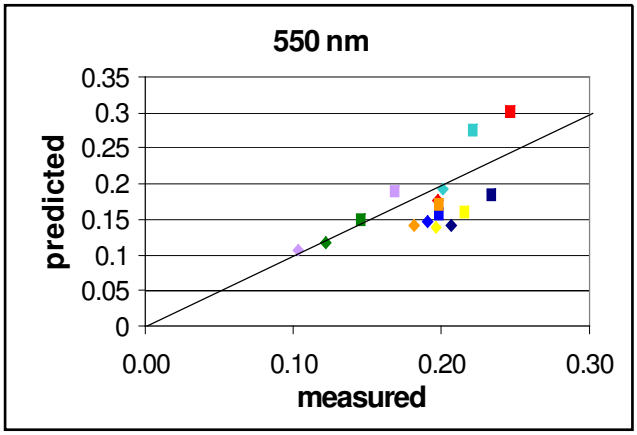
550 nm
predicted
measured
0.35
0.3
0.25
0.2
0.15
0.1
0.05
0
0.00
0.10
0.20
0.30

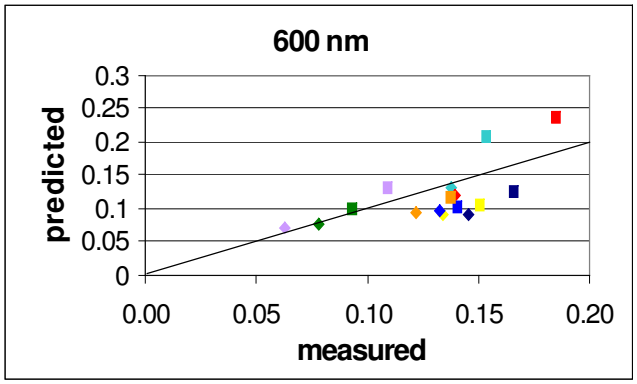
600 nm
predicted
measured
0.3
0.25
0.2
0.15
0.1
0.05
0
0.00
0.05
0.10
0.15
0.20

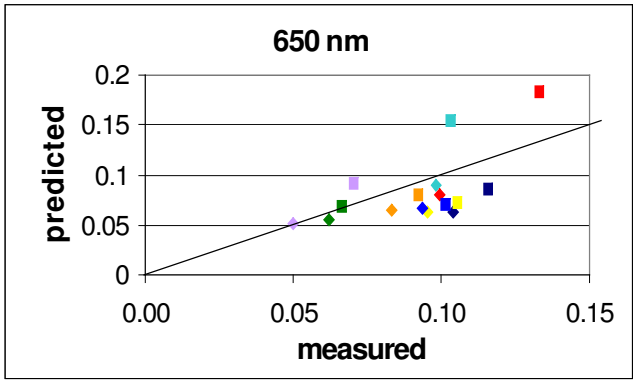
650 nm
predicted
measured
0.2
0.15
0.1
0.05
0
0.00
0.05
0.10
0.15

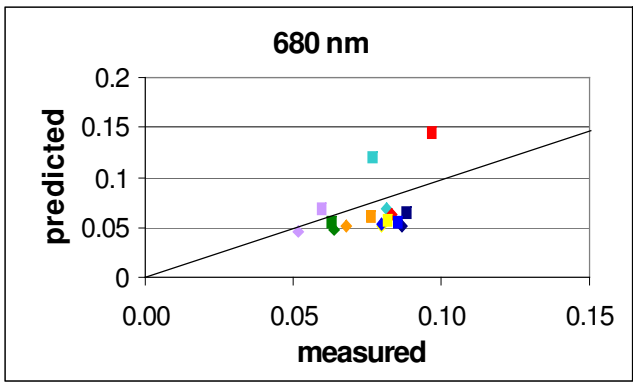
680 nm
predicted
measured
0.2
0.15
0.1
0.05
0
0.00
0.05
0.10
0.15

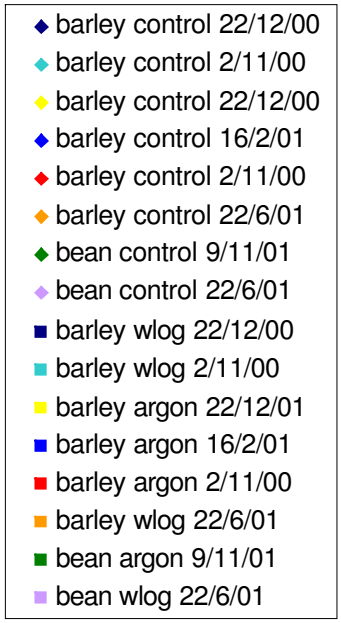
barley control 22/12/00
barley control 2/11/00
barley control 22/12/00
barley control 16/2/01
barley control 2/11/00
barley control 22/6/01
bean control 9/11/01
bean control 22/6/01
barley wlog 22/12/00
barley wlog 2/11/00
barley argon 22/12/01
barley argon 16/2/01
barley argon 2/11/00
barley wlog 22/6/01
bean argon 9/11/01
bean wlog 22/6/01

Figure 4.36 Comparison between reflectance predicted using the PROSPECT model and measured using the LI-1800 spectroradiometer

The measured reflectance was higher than the predicted reflectance in most cases. PROSPECT modelled the reflectance for bean more closely (lilac and green symbols). The control and treatment data for each data set in most cases tend to lie parallel to the line that represents a perfect match between the measured and predicted data, thus suggesting a systematic underestimation of the reflectance by the PROSPECT model.

4.8 Conclusions

Most of the methods used for displacing oxygen from soil led to increases in reflectance of the treated plants at all visible wavelengths when compared to the control plants. Waterlogging of all species gave the greatest increase in reflectance, possibly because this method of oxygen displacement was easiest to maintain.

Displacement of oxygen using natural gas showed the smallest increase in reflectance, which was probably due to the constraints on the study due to safety reasons. Gassing with natural gas could only be maintained during working hours, which enabled the soil air to become re-oxygenated between treatments. It is expected that continual gassing with methane would lead to greater changes in reflectance, similar to those found with the surrogate gases.

Oxygen displacement using argon also led to systematic increases in reflectance in the visible wavelengths, with the effect being greater on barley than on bean.

In the single experiment conducted, nitrogen had no significant effect on either the reflectance or the position of the red-edge. It is thought that this may have been due to nitrogen being a biologically active gas, already being present in concentrations of 78% in air. This trial was only carried out on bean, a species that has the ability to fix

nitrogen for its own use, and thus is unlikely to be stressed by the addition of extra nitrogen to the soil.

All treatments except nitrogen led to a shift in the position of the red-edge maximum towards the blue with the greatest shift being seen in waterlogged bean.

The effect on the reflectance (relative to a barium sulphate reference disc) in the near infrared varied from a decrease in reflectance of over 0.128 to an increase in reflectance of almost 0.029. However, there was a tendency for the infrared reflectance to be either minimally changed or decreased, with only argon-treated barley and nitrogen-treated bean showing significant increases.

The first derivative of the reflectance curves showed that at 524 nm there was generally an increase in magnitude for the treated plant when compared to the control plant. At most other wavelengths the treated plant showed a decrease in magnitude of the first derivative. The exception was for the nitrogen trial that showed no difference between the control and treated plants. Although the position of the red-edge of treated plants was seen to shift to the left, there was no consistent change in the magnitude of the first derivative, which could either increase or decrease relative to the control.

Differences were observed between the monocotyledons and dicotyledons in the shape of the graph of the first derivative of reflectance, particularly in the wavelength range that identifies the red-edge, with monocotyledons showing a double peak with the major peak at 704 nm and a second peak or shoulder at 722 nm which shifted towards the major peak as the plants became stressed. Dicotyledons showed a single peak at

the red-edge positioned between 710 and 722 nm and this peak moved as the plant became stressed.

In summary, displacement of oxygen from the soil by a variety of methods was seen to cause stress symptoms in the plants evidenced by an increase in reflectance.

While it was not possible for safety and economic reasons to fully emulate the effect of leaking natural gas, the alternative methods applied to reduce soil-oxygen show stress responses that are consistent with those found in limited studies with natural gas. The results suggest that the stress responses are generic and that the alternative methods applied here are appropriate surrogates for direct gassing with natural gas.

5 Field work

5.1 Introduction

It was important to measure spectral changes in a field situation in order to confirm that changes observed in the laboratory were also visible in field crops subjected to leaking natural gas. Changes in reflectance spectra due to stress responses would enable leaking gas pipes to be identified by remote sensing via satellite.

The location of a leaking gas pipe that passed beneath an arable field was identified in Louth, Lincolnshire, which allowed spectral measurements to be made in 2001.

5.2 Description of field site

The field site was located on Wrisdale farm, Louth, Lincolnshire (Grid reference TF 333862). Figure 5.1 shows the location of the field site on the outskirts of Louth.

The gas pipe is at a depth of approximately 0.7 m below the field surface and is a Victorian 12 inch cast iron main that is part of the North Lincolnshire Grid. It is used to supply coal gas from Grimsby to Skegness but now transports natural gas. The gas main is jointed every 5 yards and leaks tend to occur at every other joint. Some leaks in the pipe had been repaired by Transco, but the leaks in the field had not been repaired as the crop would need to be disturbed and there are plans to replace the main.

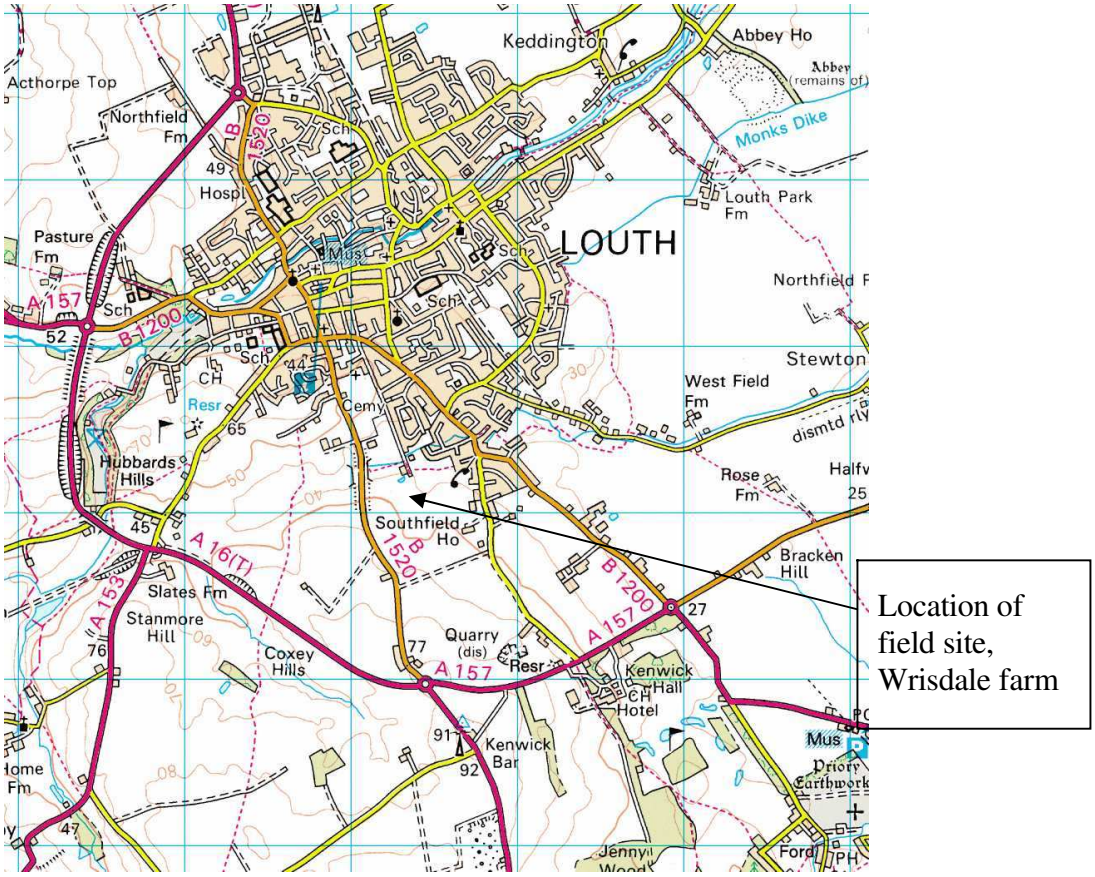

Figure 5.1 Ordnance Survey map showing location of Wrisdale farm.

Figure 5.2 Patches of decreased growth of barley above leaking gas pipelines.

Barley (*Hordeum vulgare* L. cv Vanessa) had been planted in September 2000. A preliminary visit to the field site in January 2001 identified large patches of yellowed and decreased growth of the barley seedlings. The patches were approximately 2 m diameter and were situated at about 10 metre intervals that probably coincide with joints in the pipeline (Figure 5.2).

A second visit to the field site at Wrisdale farm was carried out on 1st May 2001 when the crop was more advanced, and a third visit on 16th June 2001.

5.3 Gas measurements

In order to measure the gas concentration in the soil, a 1.2 cm hole was first punched in the soil to a depth of 40 cm, using a barholer. A gas collection probe was then inserted into the hole and gas extracted for 30 seconds using a GMI Gascoseeker. The Gascoseeker measures natural gas concentration in the range 0–100 % LEL and then from 0-100 % volume. The Gascoseeker is similar in design and operation to the Gasurveyor that was used in the laboratory trials.

Gas concentrations measured during the preliminary visit were variable but showed that at a depth of approximately 40 cm the natural gas concentration was between 79 % LEL (approximately 4% by volume of gas) and 20% by volume gas. The highest gas concentrations were measured in the centre of the bare patches of crop. At a distance of 4 m from the gas pipeline no natural gas was detected.

During the second visit on 1st May 2001, gas concentrations could not be detected at the surface. At a depth of 40 cm, natural gas levels were measured at 195 ppm (0.019%) in the centre of areas of decreased growth. The low concentration of natural

gas may have been due to lower pipeline gas pressures as the higher spring temperatures reduced demand for gas, or to increased bacterial activity due to warmer soil conditions leading to oxidation of the gas before reaching the surface. Atmospheric conditions experienced on the day may also have had an effect on gas detection. The conditions were high atmospheric pressure (1025 hPa), maximum temperature of 13.2º C and a northeasterly wind gusting to 7.6 m s^{-1} (17 mph) (Data supplied by British Atmospheric Data Centre and Ian Trowsdale, Climatological Observer Society, Louth). High atmospheric pressure suppresses movement of gas in the soil (Harris *et al.* 1995) and therefore in high-pressure conditions the natural gas would be less detectable at the surface. Wind will also have an effect on the detection of gas as it reduces local concentrations of gas in the near-surface pores within the soil and will also assist with the removal of gases from the surface (Harris *et al.* 1995).

During the third visit, on 16th June 2001 gas measurements were taken at the surface. Very low concentrations (~ 4 ppm) of natural gas were occasionally detected at the centre of the patches of decreased crop growth. No gas was detected elsewhere.

5.4 Spectral scans of vegetation

On 16th May 2001 the field was visited in order to take spectral scans of the barley. The barley crop had grown to 20 cm height while the patches over the leaks had a few small plants growing on them. Measurements were taken under clear skies between 13:00 and 15:00 BST.

Three transects were laid across the pipeline to enable spectral scans to be taken (Figure 5.3). The first bare patch in the field was not measured due to disturbance of the area at the edge of the field, and the proximity of hedges. 10 m transects were laid

across the pipeline, passing 1 metre from the centres of the second and the third bare patches in the barley. This was done in order to determine if there were any spectral changes in apparently healthy vegetation due to the influence of the leaking gas pipe and also to reduce the spectral effect of the bare ground in the centre of the patches. Pegs were placed along the transect at 2 m intervals so that 5 measurements were taken at each site. At the fourth bare patch a 5 m transect was laid that passed through the centre of the bare patch. At this site the pegs were placed at 1 m intervals. The peg at position 1 at each site was used as a control as this was furthest from the position of the pipeline and was assumed to be unaffected by gas.

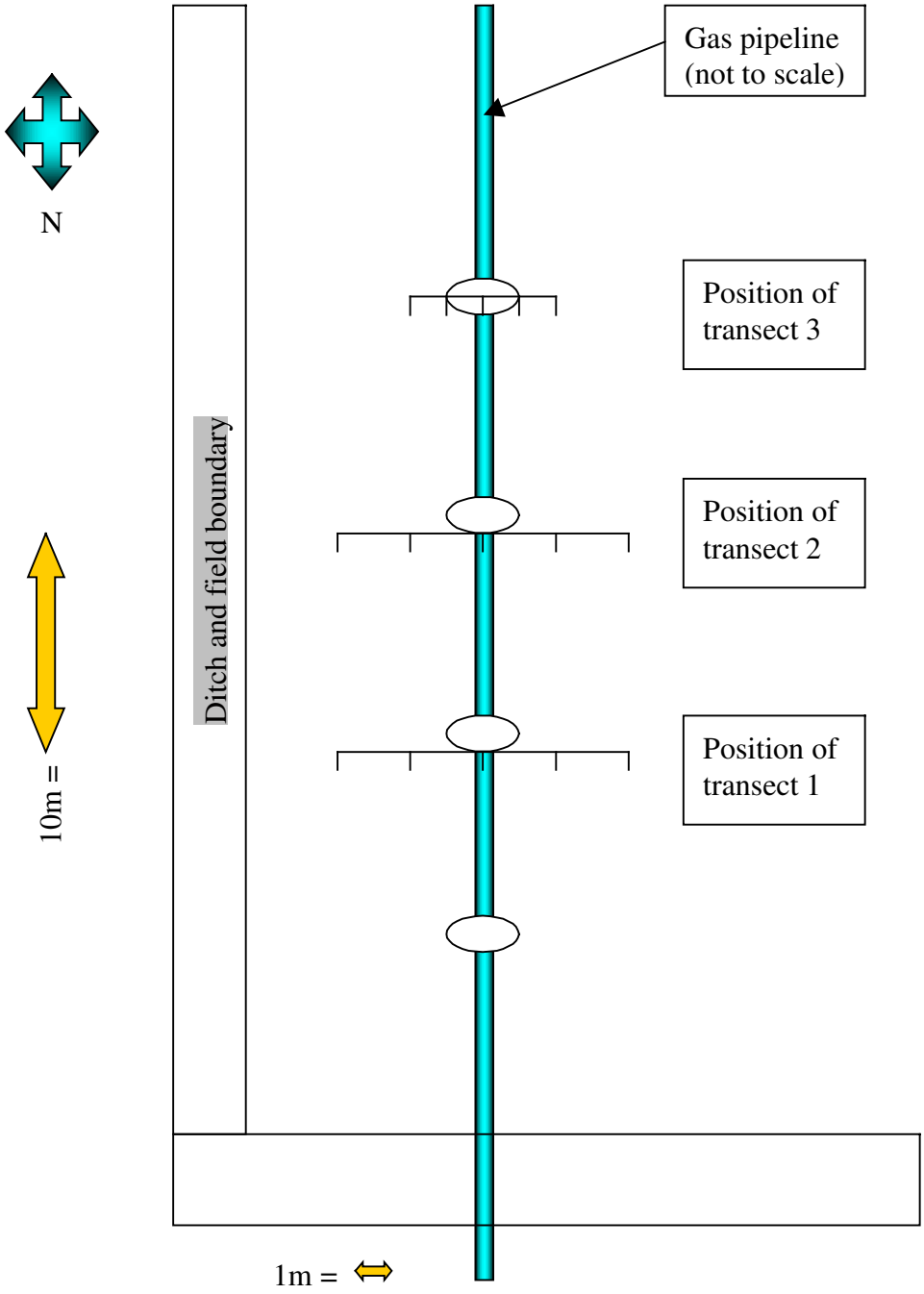

Figure 5.3 Schematic plan of Wrisdale farm, Louth showing the position of the gas pipeline, decreased growth crop patches and the position of transects and data

At each peg along the transect, spectral scans covering the wavelength range 450 to 900 nm at 1 nm wavelength intervals were taken using the LI-1800 spectroradiometer fitted with a fibre optic probe. The probe was taped to a tripod at a height of 1.2 m. Measurements were made at an inclination angle of about 15° facing into the sun to avoid shading the target area. Scans of a Halon reference panel (30 x 30 cm) mounted on a tripod table were made at the beginning and end of each set of five transect measurements (Figure 5.4). Each scan took approximately 1 minute to perform and each transect was completed within 8 minutes to minimise the effect of changing sun angle. On this occasion conditions were bright and sunny with few clouds and thus light conditions were not changing appreciably.

The field of view of the fibre optic probe was approximately 10°, corresponding to an area of about 320 cm^2 at a height of 1.2 m. This ensured that when scanning the reference plate the probe was viewing only the plate and not any of the surrounding vegetation or soil.

On the third visit spectral scans were taken across the pipeline at the second and third bare patch but deteriorating weather conditions meant that further scans could not be taken. Visual observations of the state of the crop were taken, and leaf samples were collected so that laboratory measurements of leaf reflectance and chlorophyll content could be performed.

Figure 5.4 Setting up equipment in field site in May 2001 (Photograph courtesy of Dr. M. Steven).

5.5 Data analysis of field spectra

Spectral data collected in the field were analysed using the same methods as were used for the laboratory measurements. The reflectance obtained from the canopy was referenced against the reflectance measured from the halon panel. The data was adjusted to absolute reflectance by multiplying by the calibrated reflectance factor of the halon panel. In order to reduce any effects of changing solar conditions the calibrated data were smoothed as described in section 3.8.2. The smoothing procedure was applied twice to further remove noise and assist in the identification of the red-edge position by first-derivative calculations.

5.6 Sample collection

5.6.1 Collection of plant samples

After spectral scans had been taken, plant samples were collected from each peg site. Four complete plants were collected from each peg site complete with a clump of soil to help prevent dehydration of the plants during the journey back to Nottingham University. The plants were labelled and placed in polythene bags and transported in a cool box. On arrival at Nottingham the plants were stored in a cold room at 4°C until leaf spectral scans and chlorophyll analysis could be carried out.

5.6.2 Laboratory analysis of spectra

Spectral scans of four leaves from each peg position were taken on the day following collection. Scans were taken using the LI-1800 spectroradiometer fitted with an integrating sphere, as described in section 3.5.2.1. Following spectral scans of the barley leaves, the scanned leaves were placed in polythene bags, labelled and stored at 4°C for later chlorophyll analysis. All the other leaves were bagged and labelled for leaf area analysis to enable equivalent water thickness to be calculated.

5.6.3 Chlorophyll analysis of plant samples

Chlorophyll analysis was carried out within 24 hours of the spectral scans. From each leaf, four 1 cm diameter discs were removed and chlorophyll extracted as described in section 3.6. Chlorophyll analysis of 4 leaves (one from each plant collected) was carried out for each peg site.

5.6.4 Equivalent water and dry matter analysis of plant samples

The equivalent water thickness and dry matter content of the leaves was calculated by determining the leaf area and dry weight for 5 leaves from each peg site as described in section 3.7. Four replicates were carried out for the plants collected from each peg site.

6 Spectral changes in crops exposed to leaking underground gas pipes

6.1 Spectral reflectance of barley canopy.

Wrisdale farm in Louth was first visited on 18th January 2001 to view the effect of a leaking pipeline. The crop was small and spectral measurements were not taken. On 1st May 2001, the site was revisited, the weather conditions were fine and sunny and spectral measurements of the barley canopy were taken along three transects placed across the leaking section of the gas pipe (Chapter 5). Measurements were taken at three areas of decreased crop growth. On 16th June 2001 the farm was visited for a third time when weather conditions turned cloudy and wet.

6.1.1 1st May 2001 - Site 1 and 2

The crop growth was further advanced than it had been during the visit in January. The plants were approximately 20 cm in height; growth was dense with no soil visible between the plants, except in the areas above the gas leaks. Here there was some vegetation but it was retarded in growth and soil was visible between the plants. Figure 6.1 shows a photograph of the area of decreased crop growth at site 1.

Figure 6.1 Photograph of area of decreased crop growth above gas pipeline at Site 1.

6.1.2 Relative reflectance

Relative reflectance of vegetation was measured at pegs positioned at 2 m intervals across the gas pipeline. Figure 6.2 shows the approximate positions of the transects through the patches which were not circular and not always immediately above the pipeline.

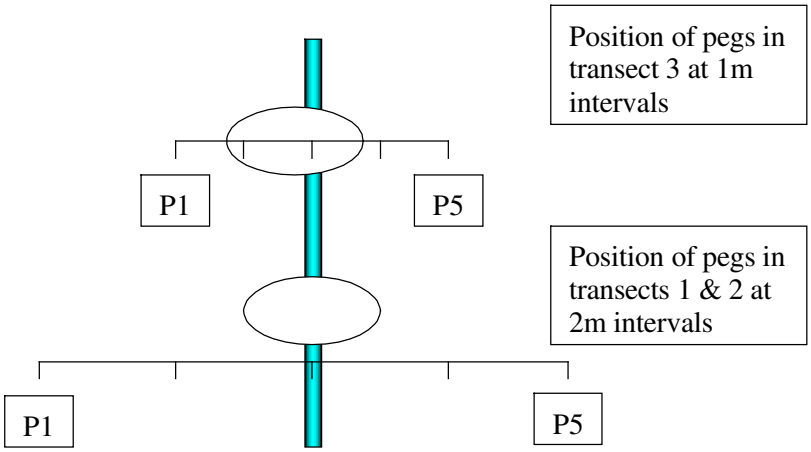

Figure 6.2 Diagram illustrating positions of transects

Spectral scans at Site 1 showed that vegetation at peg 1, furthest from the gas pipeline, had the lowest reflectance in the visible wavelengths and peg 3, which was directly above the gas pipe, had the highest reflectance. Reflectance from vegetation at pegs 2 and 4 were similar and slightly higher than that observed for peg 1. Reflectance of vegetation at peg 5, which was the same distance from the pipeline as peg 1, had higher reflectance than expected. (Figure 6.3). This may be because this peg was close to the farmer's field access track. At Site 2, which was situated approximately 10 m further along the pipeline, similar spectral measurements were obtained. Peg 3 again had the highest reflectance in the visible wavelengths and peg 1 the lowest. Pegs 2, 4 and 5 all had similar reflectance (Figure 6.4).

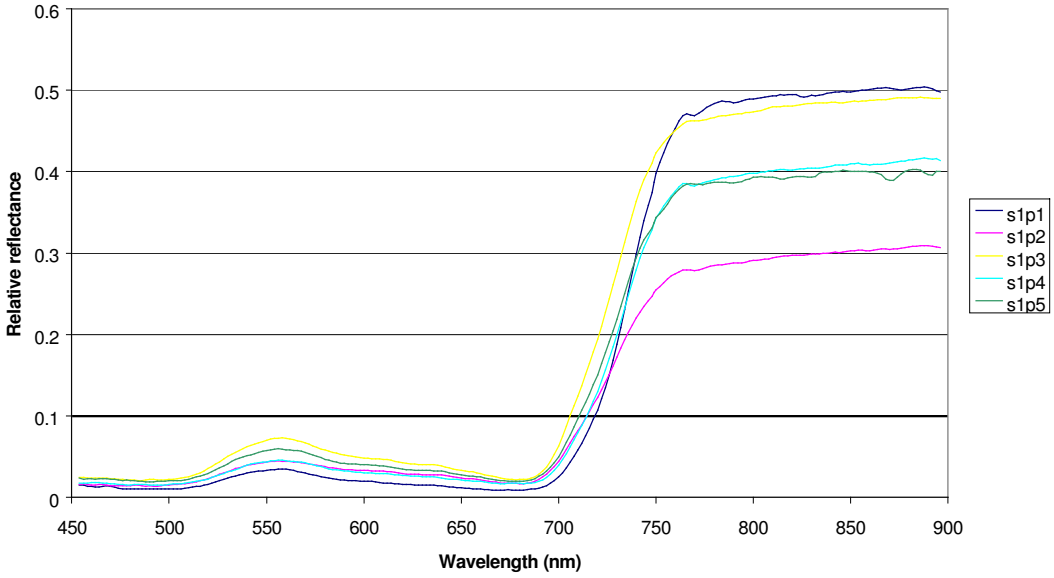

Figure 6.3 Plots of relative reflectance measured at Site 1 at 2m intervals across a gas pipeline on 1 May 2001 at Louth, Lincolnshire (S1p1 refers to site 1 peg 1 etc)

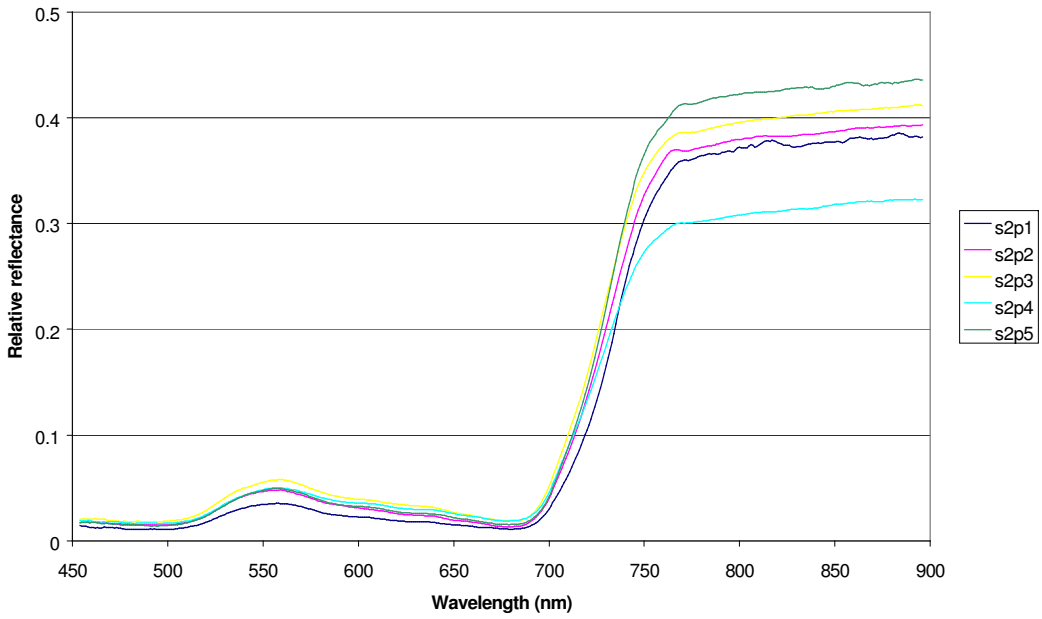

Figure 6.4 Plots of relative reflectance measured at Site 2 at 2m intervals across a gas-pipeline on 1 May 2001 at Louth, Lincolnshire (S2p1 refers to site 2 peg 1 etc.)

At both sites reflectance in the near infra-red varied considerably, but there was no consistent pattern as to which site had the highest infra-red reflectance. At site 1, the order of increasing level of reflectance was peg 2, 5, 4, 3 and 1, whereas at site 2 the order of reflectance was peg 4, 1, 2, 3 and 5.

6.1.2.1 Analysis of red-edge

Analysis of the first derivative of reflectance spectra from Sites 1 and 2 showed that the position of the red-edge changed depending on how close to the pipeline the crops were growing (Figure 6.5 and Figure 6.6).

At site 1, the first derivatives of reflectance for the vegetation show a main peak that identifies the red-edge with the position of the peak moving from 736 to 728 nm as the gas leak is approached. A similar pattern is seen at site 2 where the main peak moves from 737nm (at pegs 1 and 5) to 727 nm in the centre of the transect. Figure 6.7 shows the red-edge position of the crops growing across the pipeline at Sites 1 and 2. The position of the pipeline was 4 m from the edge of the field. Both transects show that the red-edge moved to shorter wavelengths closer to the pipeline. The patches of decreased growth above the pipeline were not circular but varied in shape. The decreased growth at site 1 was pear shaped with the narrow end of the patch towards the edge of the field, which explains the minimum red-edge position observed at the 2-metre position.

The position of the red-edge of the crops growing immediately above the pipeline showed a decrease of 10 nm (from 737 nm to 727 nm) when compared with the crops

growing furthest from the pipeline (Figure 6.7). The magnitude of the peak also tends to decrease as the pipeline is approached but the effect is not so clear cut (Figure 6.8).

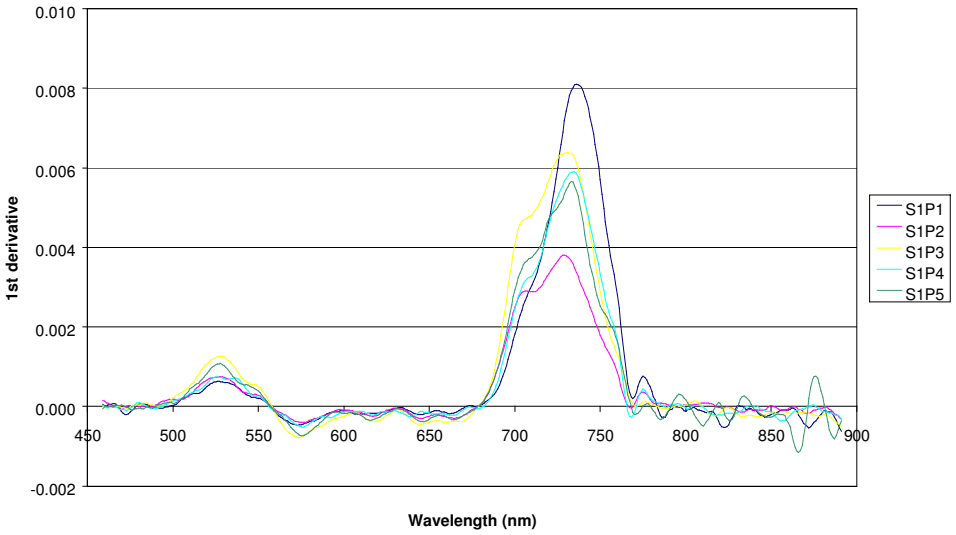

Figure 6.5 First derivative of reflectance of crops growing across a gas pipeline at Site 1, Louth, Lincolnshire.

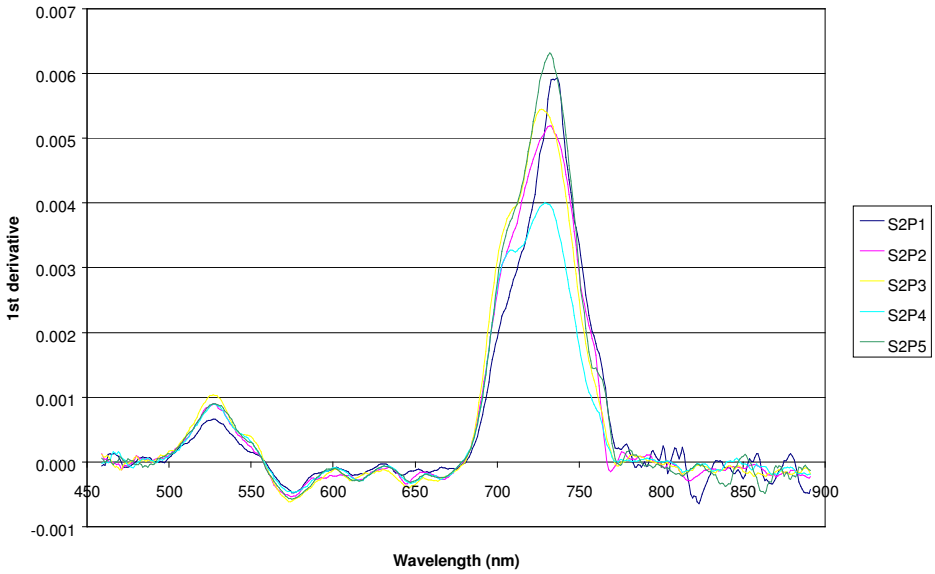

Figure 6.6 First derivative of reflectance of crops growing across a gas pipeline at Site 2, Louth, Lincolnshire.

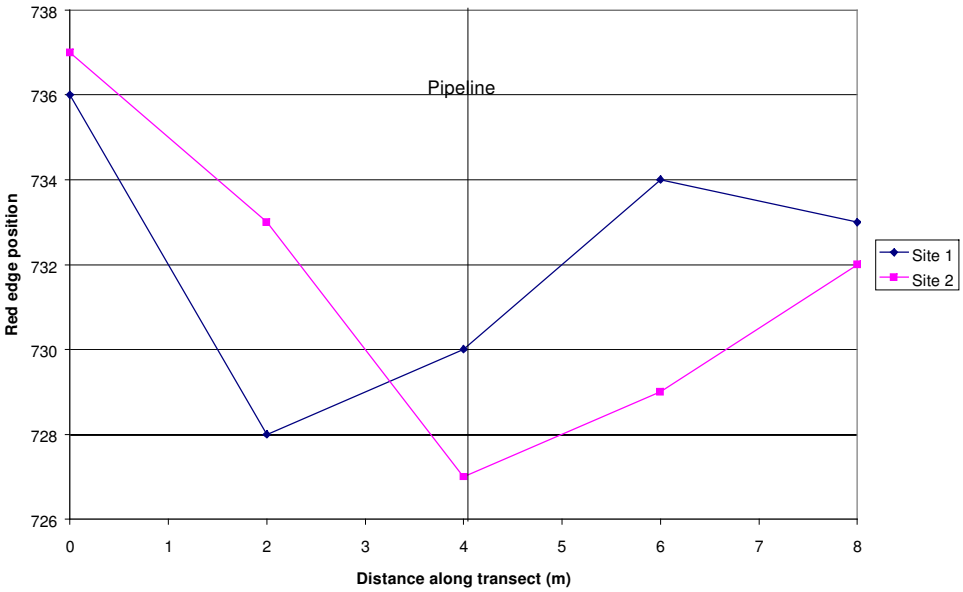

Figure 6.7 Red-edge position of crops growing at Site 1 and Site 2.

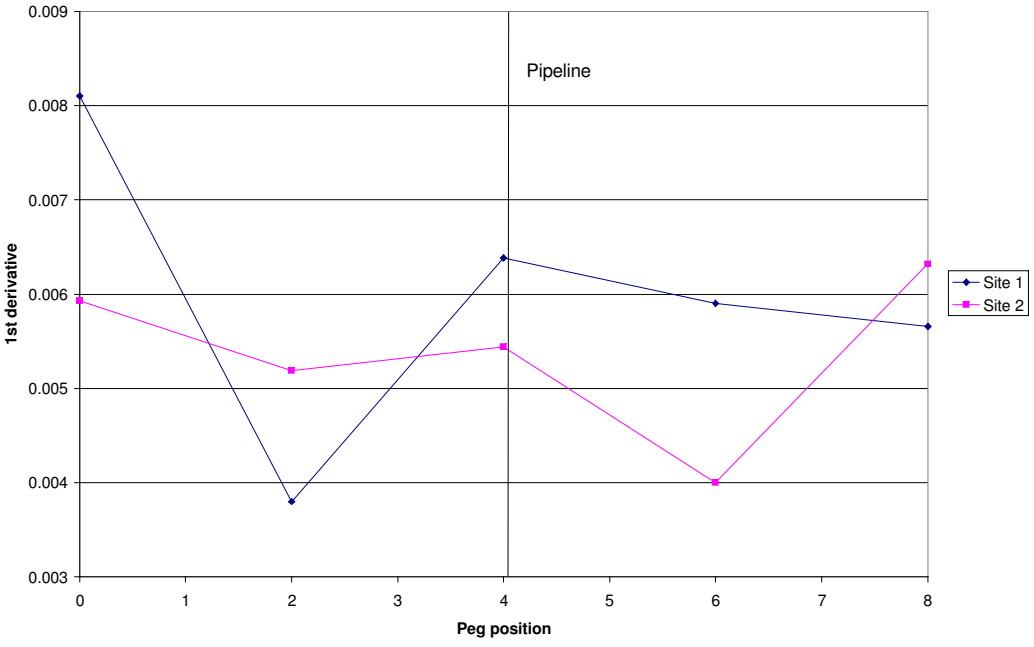

.

Figure 6.8 Amplitude of major peak identifying the red-edge position in crops growing at site 1 and 2

Several features were visible in the peak that identifies the red-edge (Figure 6.5 and Figure 6.6). At site 1, the vegetation at peg 1 showed a single peak with a red-edge position at 736 nm and a small decrease of the peak observed at 758 nm. The peaks obtained from the remaining pegs show the main peak that identifies the red-edge with a shoulder to the left of the main peak. The position of this peak is between 704 and 710 nm. Where present, the amplitude of this shoulder increases as the gas leak is approached (Figure 6.9). At site 2 only pegs 3 and 4 show a shoulder to the left of the major peak. However, there is a broadening of peaks 2 and 5 when compared to peg 1.

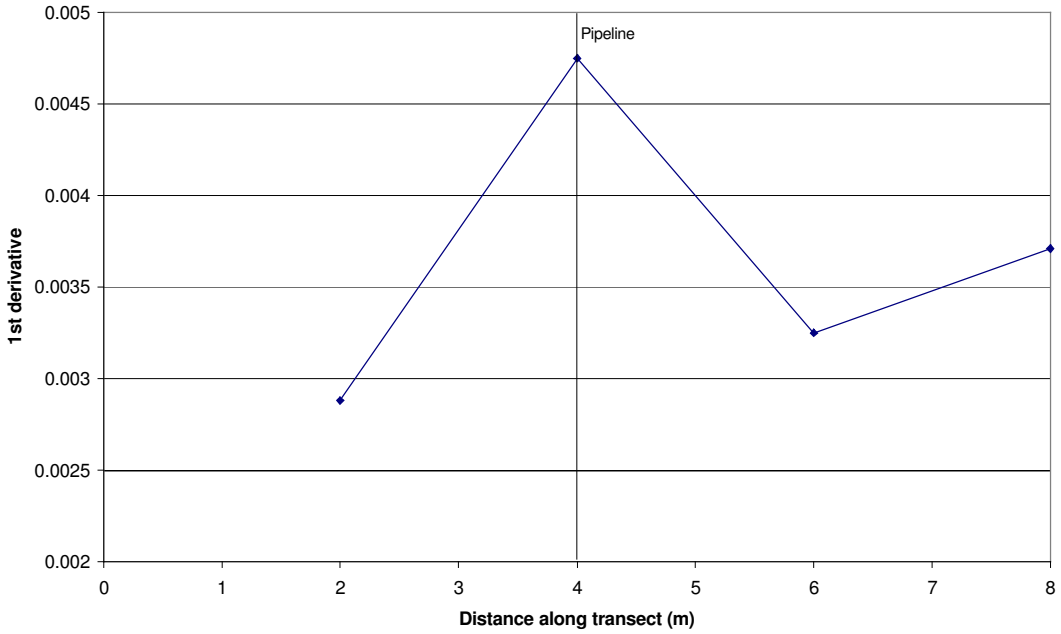

Figure 6.9 Amplitude of first derivative at the minor peak within the red-edge (704 – 710 nm), transect 1

At both sites 1 and 2, a second smaller feature was also visible to the right of the major peak as a small broadening of the peak at 758 nm. The amplitude of this broadening tended to decrease close to the gas leak (Figure 6.10).

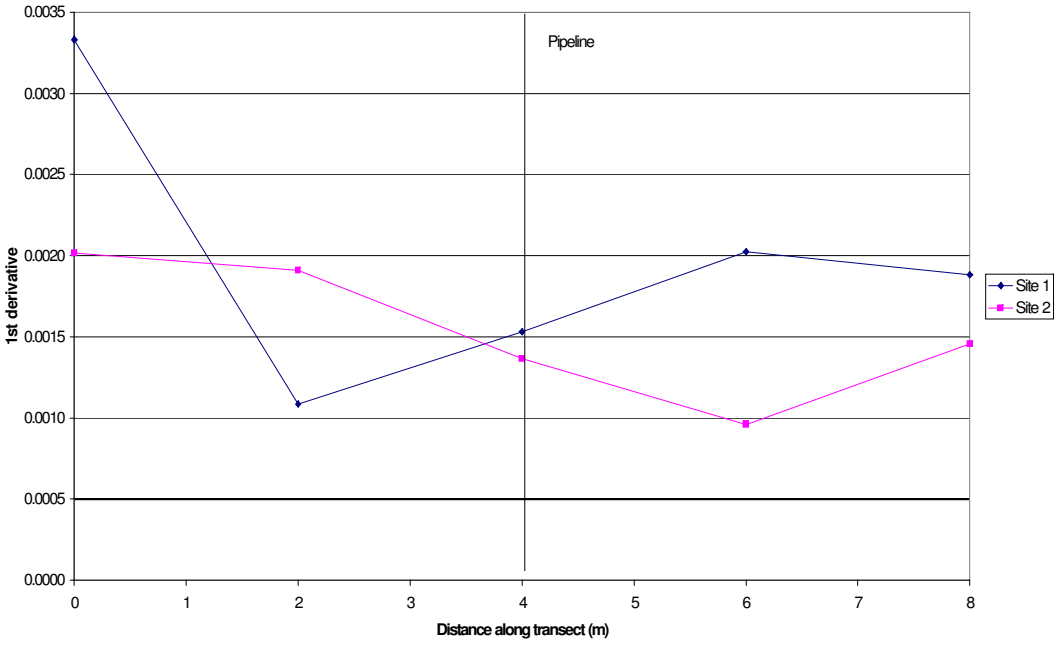

Figure 6.10 Amplitude of first derivative at the minor peak within the red-edge at 758 nm

6.1.2.2 Analysis of other first derivative peaks at sites 1 and 2, 1/5/01.

At sites 1 and 2 the first derivatives at the selected wavelengths (Table 3.3) varied as the gas leak was approached. At 524 nm there was an increase in the magnitude of the first derivative as the gas leak was approached. At 574 and 644 nm, there was a decrease in the first derivative that led to an increase in the depth of the trough, as the gas leak was approached. At 616 nm, which was also a trough there were contrasts between the two sites with site 1 showing an increase in the depth of the trough at the gas leak and site 2 showing an increase. At 600 and 634 nm the magnitude of the peak

decreased. At 600 nm the greatest decrease at site 1 was seen at peg 3 whereas at site 2 the greatest decrease was at peg 2. At 634 nm the greatest decrease was seen at peg 4 for site 1 and peg 3 for site 2 (Figure 6.11).

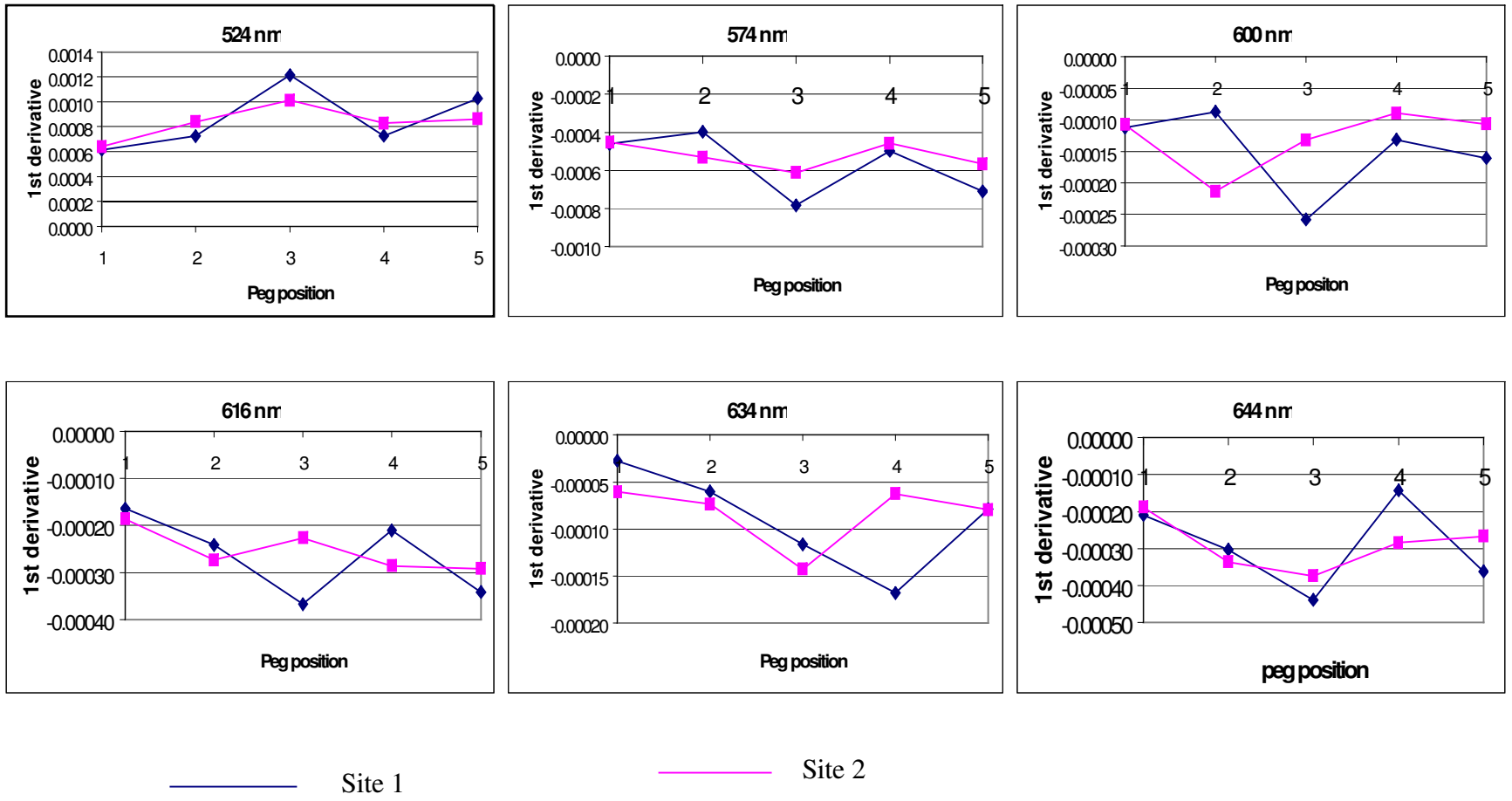

Figure 6.11 First derivative of reflectance at selected wavelengths at site 1 and 2, Louth, 1/5/01

6.1.3 1st May 2001- Site 3

At site 3 the transect was laid through the centre of the area of decreased crop growth and 5 pegs were placed at 1 m intervals (Figure 6.2). Crop growth was very low in this area with large areas of bare soil visible (Figure 6.12).

Figure 6.12 Area of decreased growth at Site 3, peg 3.

6.1.3.1 Relative reflectance

Relative reflectance in the wavelength range 520-580 nm showed that peg 1 had the lowest reflectance. The relative reflectances at the other 4 peg sites were higher, but were all similar. However, between 580 and 700 nm, reflectance at peg 3 was highest, followed in decreasing order of reflectance by peg 4, peg 5, peg 2 and finally peg 1 with the lowest reflectance (Figure 6.13).

6.1.3.2 Red-edge analysis

The first derivative of reflectance (Figure 6.14) shows that for peg 1 the position of the red-edge is furthest into the red at 733 nm and again shows a single peak. Peg 3 also shows a single peak that is positioned furthest towards the blue at 702 nm. Peg 3 was positioned in the centre of the patch of decreased vegetation. Figure 6.15 shows that the position of the red-edge moved from 733 nm at the edge of the transect to 702 nm for peg 3 in the centre of the area of decreased growth. This large shift of the red-edge towards the blue end of the spectrum was probably due to the decreased amount of vegetation and increased proportion of soil visible in this transect. The shape of the peak for the other pegs shows a shoulder appearing to the left of the peak with the shoulder developing into a second peak that becomes more prominent at about 707 nm.

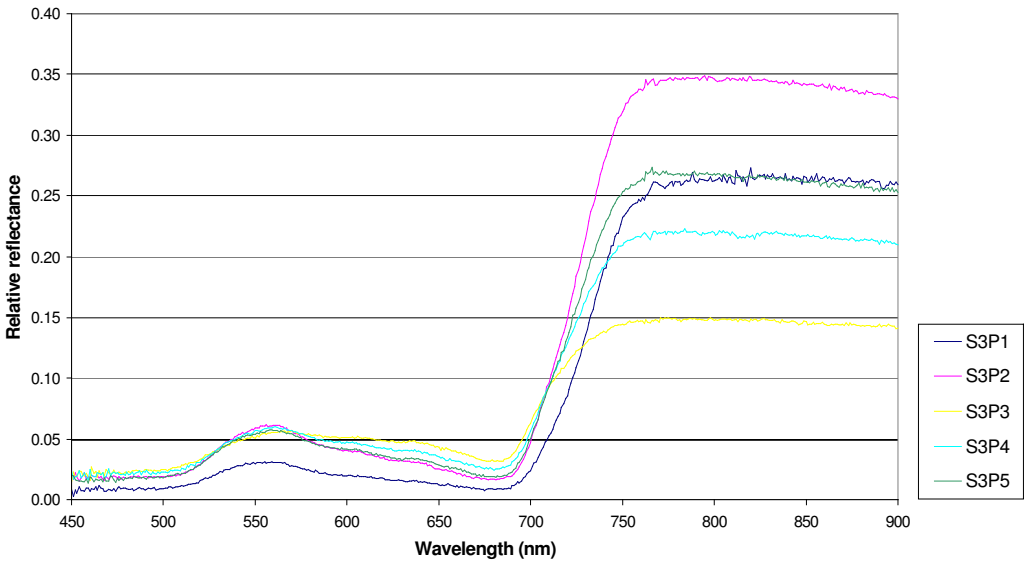

Figure 6.13 Relative reflectance of crops growing across a gas pipeline at Site 3, Louth, 1/5/01.

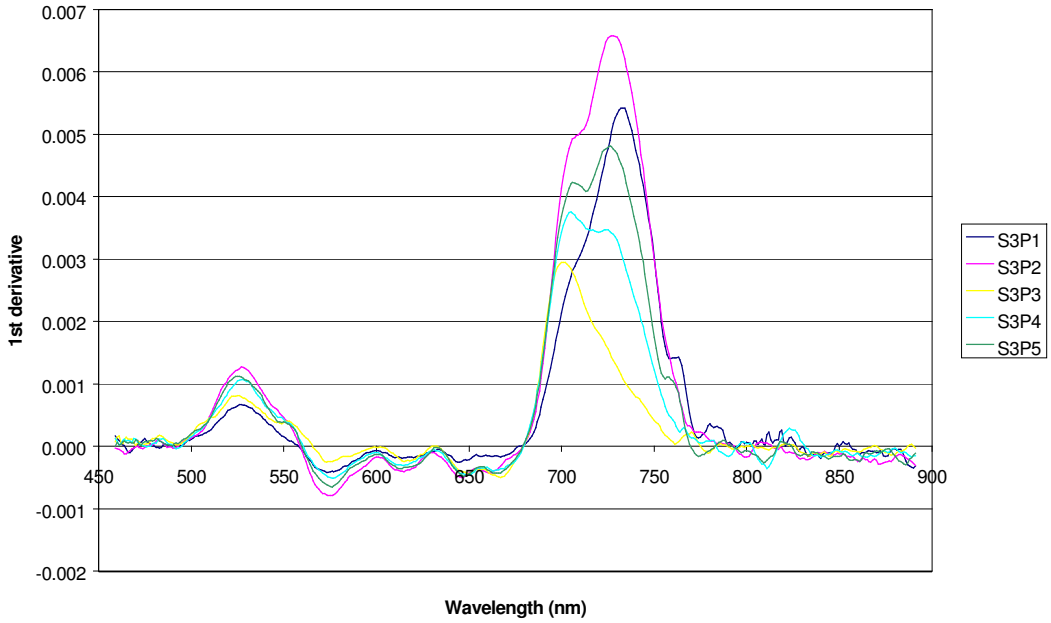

Figure 6.14 First derivative of reflectance of crops growing across a gas pipeline at Site 3, Louth, 1/5/01.

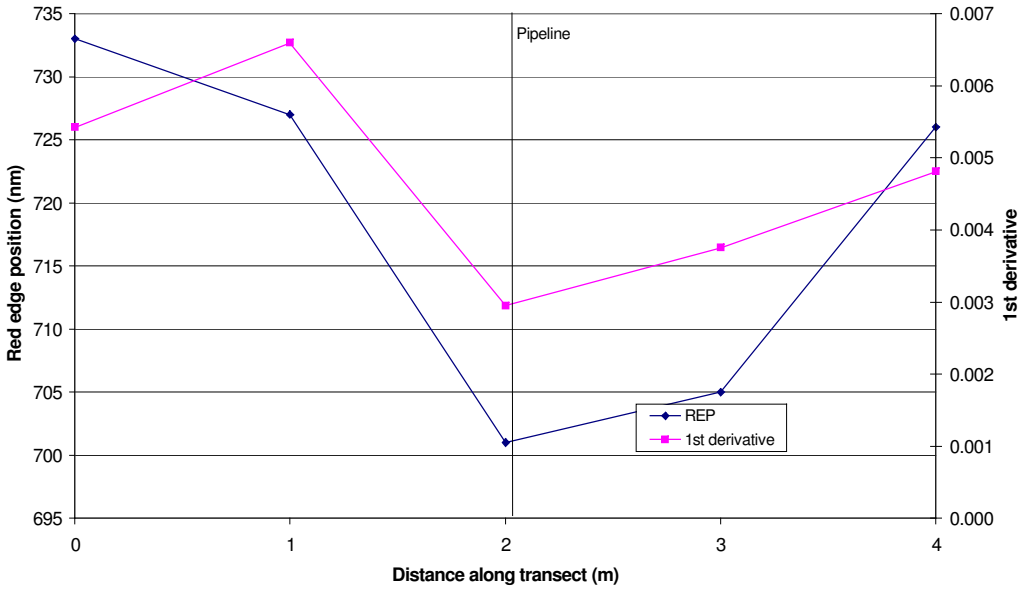

Figure 6.15 Position and magnitude of red-edge of crops growing at Site 3.

6.1.3.3 Analysis of other peaks within the first derivative at site 3, 1/5/01

At site 3 variations were also seen in the first derivative of reflectance at selected wavelengths. At 524 nm there was an increase in the first derivative at peg 2. At 574 nm there was a fluctuation in the first derivative as the gas leak was crossed with an increase in the depth of the trough at peg 2 and an increase at peg 3. At 600 nm again there is a fluctuation in the first derivative with a decrease in the amplitude of the peak at peg 2 and an increase at peg 3 and at 634 nm there is a decrease in the amplitude of the peak at peg 2. At 616 and 644 nm the depth of the trough increases as the gas leak is approached (Figure 6.16).

At site 3 the transect passed through the centre of the bare patch at this site and pegs were positioned at 1 m intervals and more of the transect appeared to be within the influence of the gas leak. Thus changes in the first derivative are less obvious than at sites 1 and 2 where more of the scanned vegetation was outside of the sphere of influence of the gas leak. However, when the first derivatives for pegs 2 to 4 of sites 1 and 2 are compared with the first derivatives obtained from site 3 there are similarities as pegs 2 to 4 are comparable to the shorter transect length of site 3. At 574 nm there is an increase in the first derivative at peg 2 that is similar to the increase at close to peg 3 at sites 1 and 2. At the other selected wavelengths there are decreases at peg 2 which again correspond to the decrease in first derivative close to peg 3 at sites 1 and 2. The maximum change at site 3 occurs at peg 2, whereas the maximum changes at sites 1 and 2 occur at peg 3 suggesting that the bare patch at site 3 is not centred above the gas pipe.

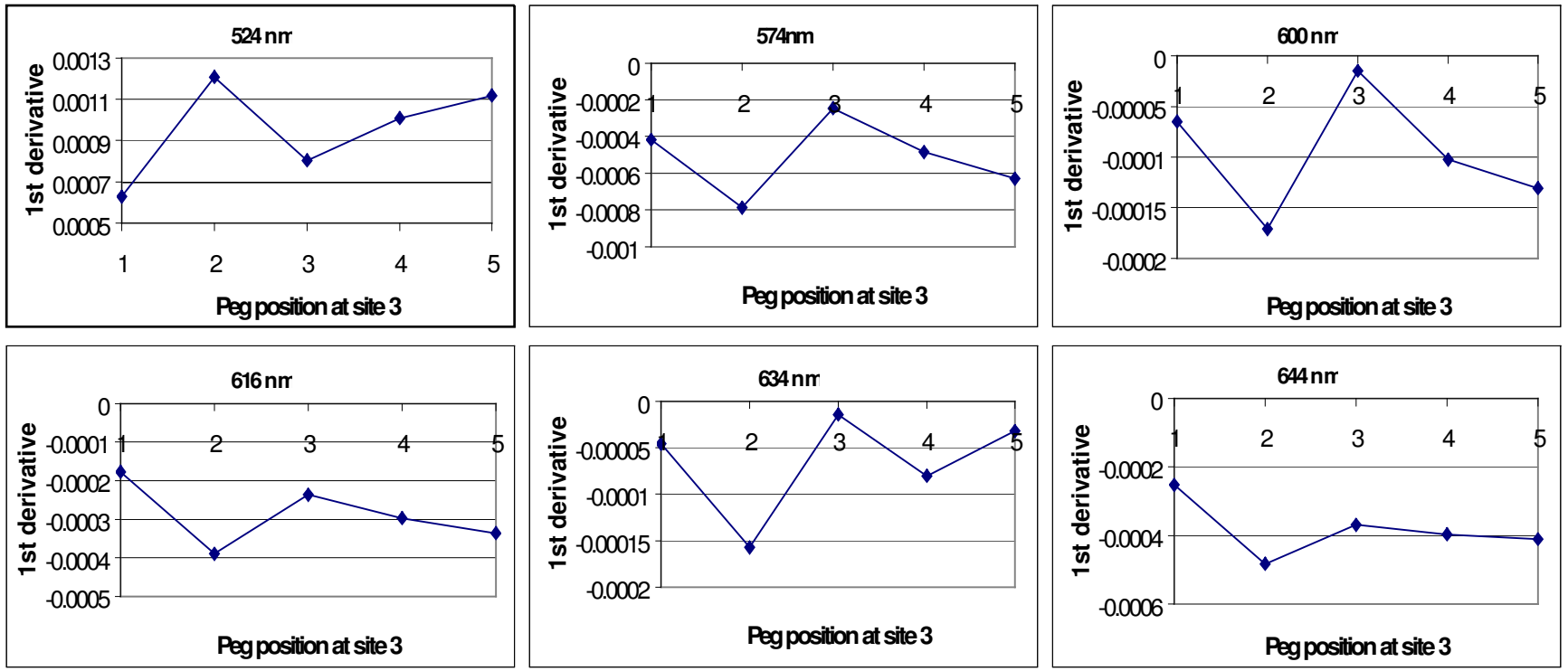

Figure 6.16 First derivative of reflectance at selected wavelengths at site 3, Louth, 1/5/01

6.2 Spectral reflectance of leaves from sites 1 and 2, May 2001

6.2.1 Relative reflectance

Reflectance analysis of leaves collected during the field visit was carried out in the lab within 24 hours of collection. Relative reflectance was measured using the LI-1800 spectroradiometer fitted with an integrating sphere and showed that the ranking of the reflectance was similar to that observed in the field (Figure 6.3) in that highest visible reflectance (Figure 6.17) was observed in leaves collected from pegs 2 and 3 and the lowest reflectance was from peg 1. Visible reflectance from leaves from peg 5 was lower than that obtained in the field. Peg 5 was situated close to a farmer's access track and so the field measurement may have been observing some soil during the scan. Measurement with the integrating sphere would not have been affected in this way and so shows more directly any response of the vegetation to gas-induced stress.

The main difference observed between the laboratory measurement of the leaves and the field measurement of the canopy is in the infrared region. In the leaf samples there is very little difference in the relative reflectance in the infrared.

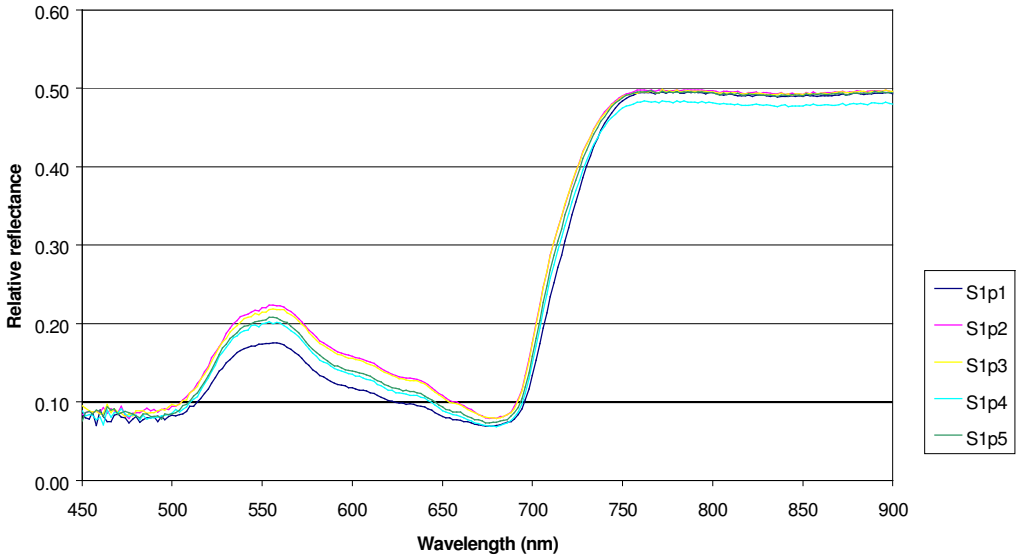

Figure 6.17 Relative reflectance of leaves collected from site 1, Louth, 1/5/01.

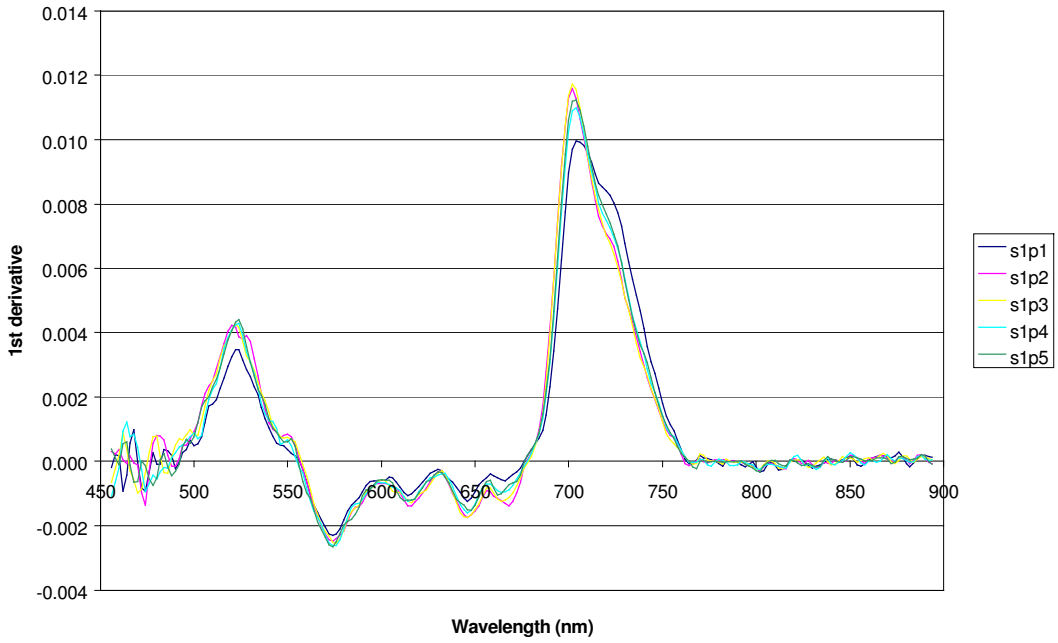

Figure 6.18 First derivative of reflectance from leaves collected from site 1, Louth, 1/5/01

6.2.2 Red-edge analysis

The first derivative of reflectance of leaves from the field site (Figure 6.18) was similar to that obtained from other laboratory measurements of barley leaves (Section 4.3). The leaves from peg 1, which were furthest from the pipeline and therefore expected to be least affected by the leaking gas show a peak at 704 nm followed by a shoulder to the right of the peak at 722 nm. The shape of the shoulder is not as developed as in the laboratory measurements of pot-grown barley, possibly because there was a 24-hour delay in performing the spectral scans of the field leaves and some deterioration of the leaves had taken place. With samples from closer to the pipeline (pegs 2,3 and 4) the shoulder at 722 nm shifts to shorter wavelengths and merges into the main peak.

For the leaf spectra, the position of the point of inflection (the red-edge) varies from 705-702 nm (Figure 6.19), which is in contrast to the changes observed in the field where the red-edge shifts from 737-727 nm. Figure 6.20 shows the change in magnitude of the first derivative of reflectance at 722 nm and illustrates that, particularly for site 1, the magnitude decreases as the pipeline is approached.

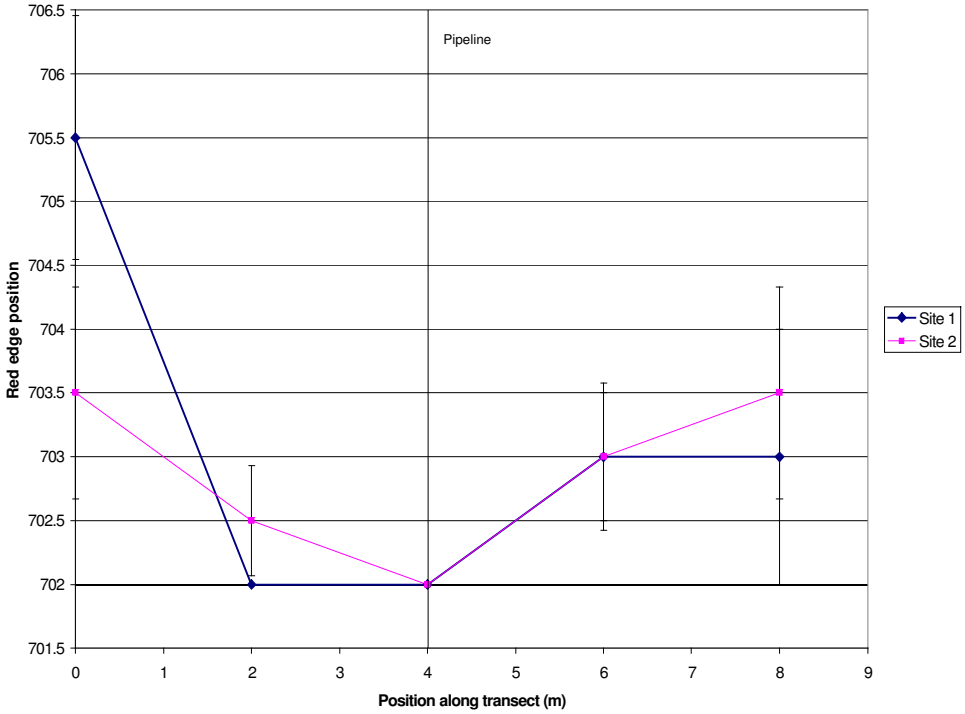

Figure 6.19 Red-edge position of leaves collected from Site 1 and 2, 1/5/01

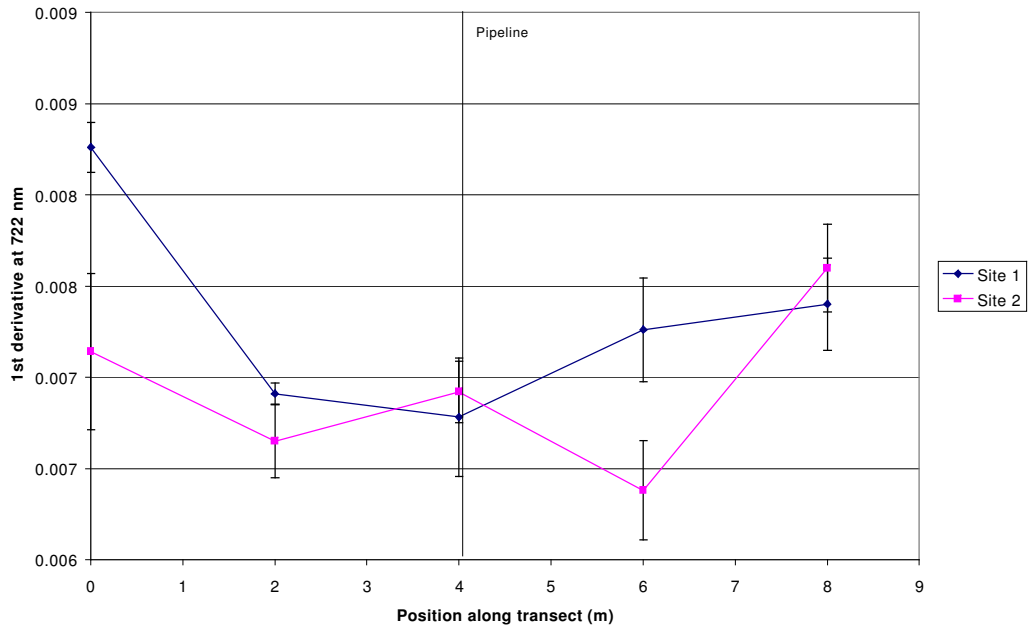

Figure 6.20 Magnitude of first derivative of reflectance at 722 nm for Site 1 and 2, 1/5/01

6.2.3 Analysis of other peaks within the first derivative

Differences between leaves collected from site 1 and 2 were observed in the first derivatives at selected wavelengths. At 524 nm there was an increase in the magnitude of the first derivative across the transect at site 1, but leaves from site 2 showed a decrease at peg 4. At 574 nm, site 1 showed a small increase in the depth of the trough as the transect is crossed but site 2 only showed an increase in the depth of the trough around the gas leak. At 616 and 644 nm both site 1 and 2 showed an increase in the depth of the trough as the gas leak is approached. 600 and 634 nm are both peaks in the first derivative plot and site 2 shows a decrease in the height of the peak at peg 2. Differences are less obvious from site 1 showing a fluctuation as the transect is crossed at 600 nm and only small changes at 634 nm (Figure 6.21).

In most cases the pattern of the first derivative is similar to those obtained from the field measurements although the magnitudes of the first derivatives are greater for the leaves.

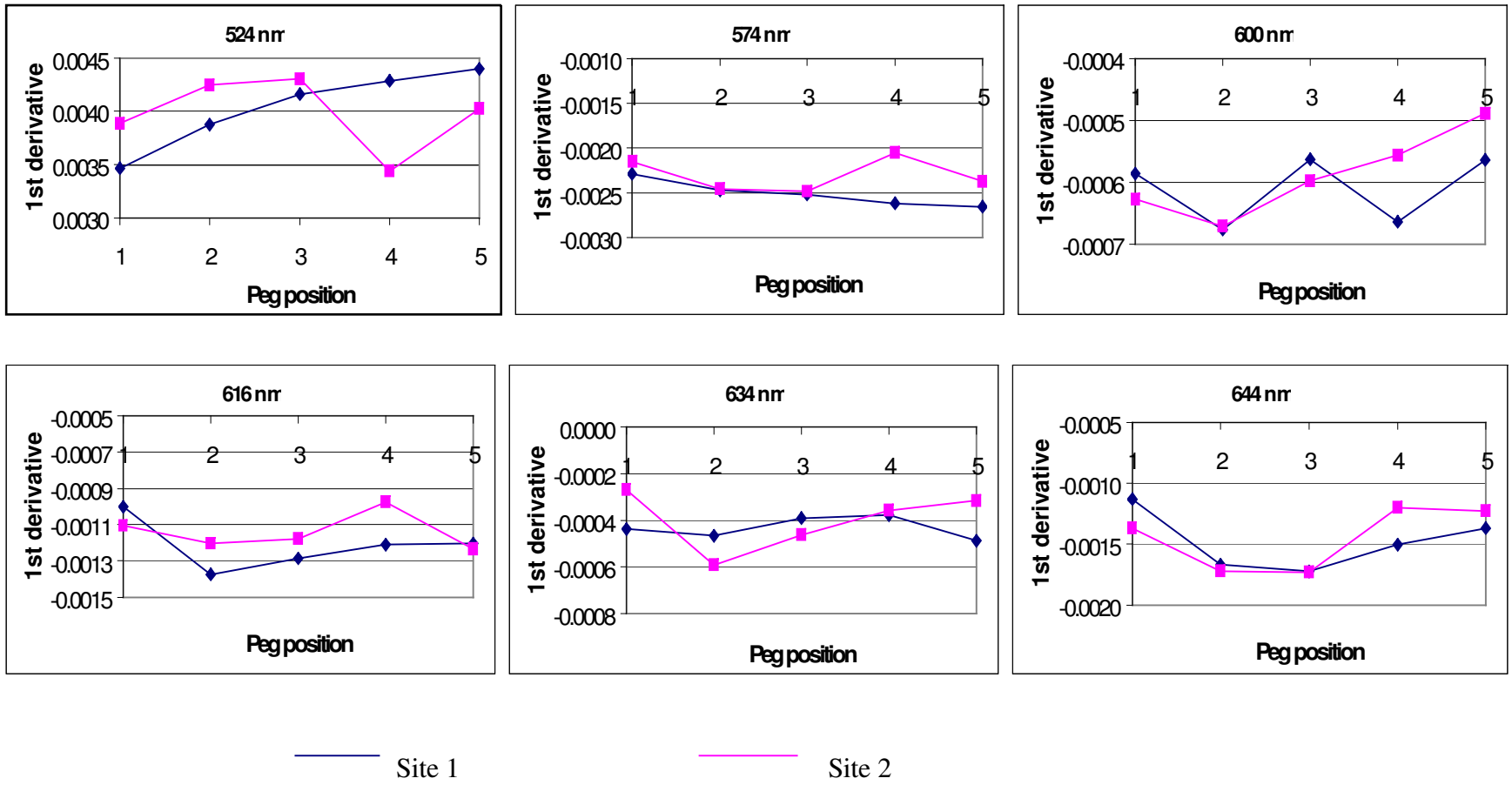

Figure 6.21 First derivative of reflectance at selected wavelengths for leaves collected from site 1 and 2,Louth, 1/5/01

6.3 Leaves collected from Site 3, 1st May 2001

6.3.1 Relative reflectance

Measurements of the leaves from site 3 showed that reflectance at peg 3 was the highest in the visible wavelengths (Figure 6.22) with reflectance of leaves decreasing in order from pegs 5, 1, 2 and 4. This does not mimic the position along the transect or proximity to the pipeline. These leaves were collected along a transect that passed through the centre of the area of decreased growth where the vegetation was very underdeveloped. The transect was shorter than that used for site 1 and 2 and so all the vegetation was possibly under the influence of the pipeline.

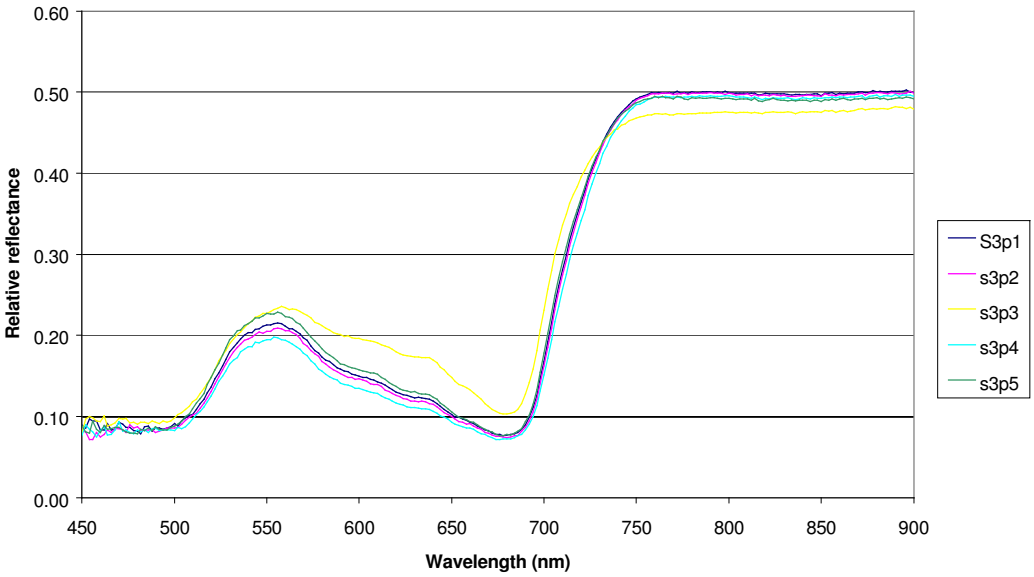

Figure 6.22 Relative reflectance of leaves collected from Site 3, Louth, Lincolnshire.

The relative reflectance is related to the position of the peg above the pipeline, but did not differentiate between pegs either side of the pipeline.

6.3.2 Red-edge analysis

The position of the red-edge and the magnitude of the first derivative of reflectance at 722 nm also showed that there was a decrease in these values above the gas pipeline but that there was little difference between in the pegs either side of the pipeline. The red-edge position of the leaves varied between 702 and 704 nm at pegs 1, 2, 4 and 5 and decreased to 699 nm for peg 3, a pattern that was mimicked in the magnitude of the first derivative at 722 nm (Figure 6.23).

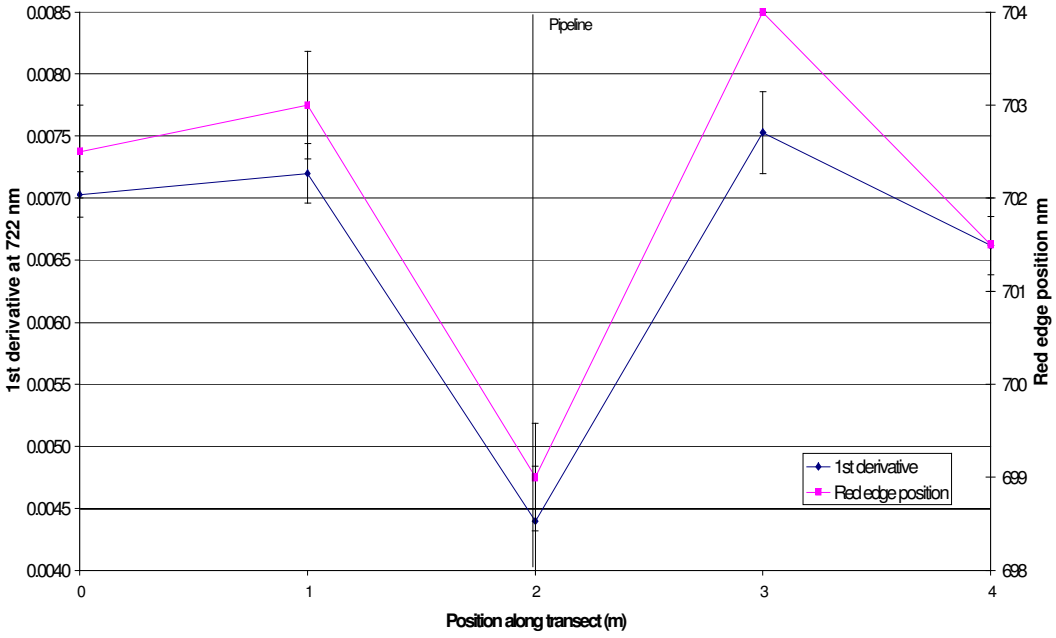

Figure 6.23 Magnitude of first derivative at 722 nm and position of red-edge for leaves collected from site 3, Louth, 1/5/01

6.3.3 Analysis of other peaks within the first derivative plot

First derivatives of selected wavelengths for leaves collected from site 3 showed changes around the position of the gas leak. At 524 nm there was an increase in the magnitude of the peak around the gas leak. The first derivatives at 600 and 634 nm are

both relative peaks and both show an increase in the magnitude of the peaks around pegs 2 and 3. There is a decrease in the depth of the trough around the gas leak at 574 nm whereas the trough at 616 nm shows little change as the transect is crossed. The first derivative of the trough at 644 nm fluctuates as the transect is crossed with an increase in the depth of the trough at pegs 3 and 5.

The pattern of the first derivatives from the leaves collected from site 3 are different to the first derivatives from the field measurements but they do appear similar to the plots for leaves taken between pegs 2 and 4 from site 1 and 2.

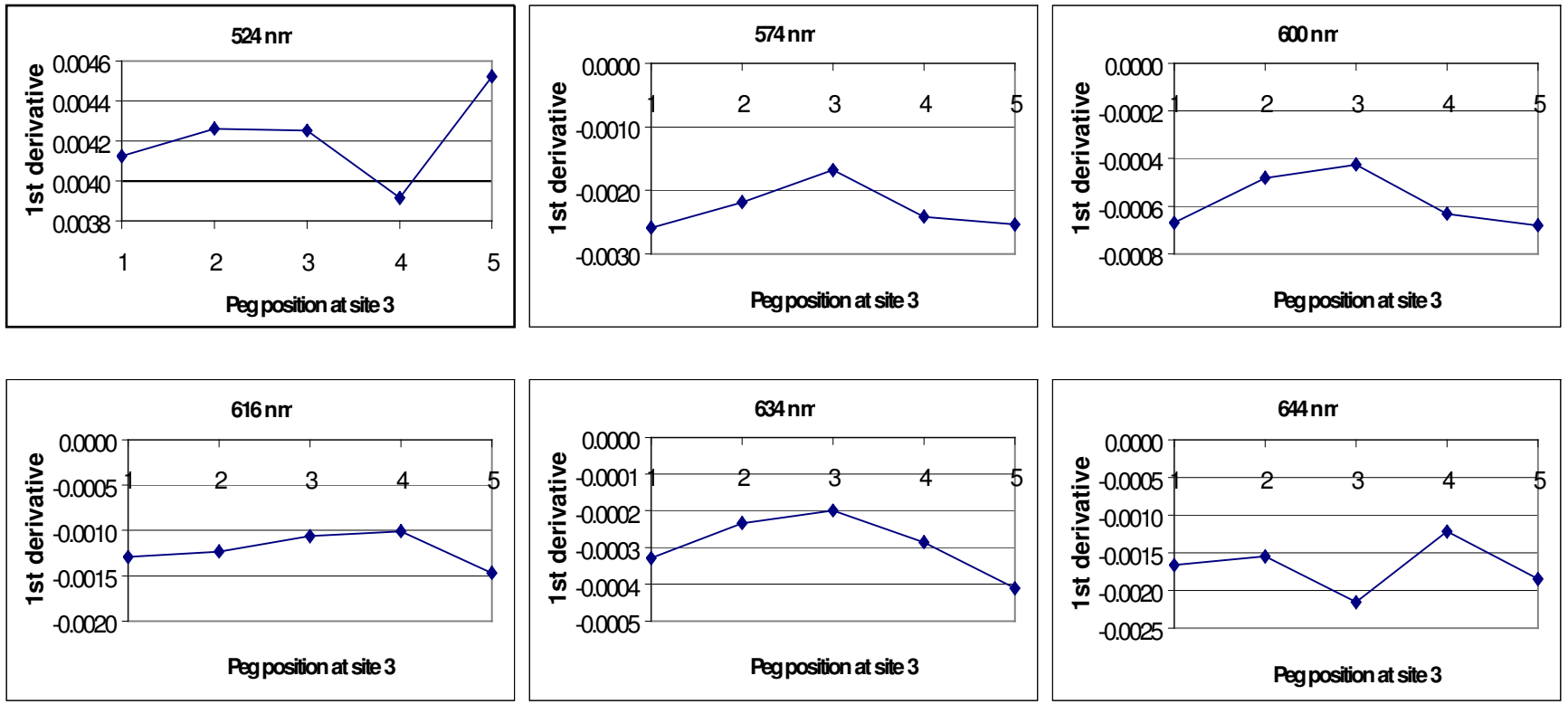

Figure 6.24 First derivative of reflectance at selected wavelengths for leaves collected from site 3, Louth, 1/5/01

6.4 Plant analysis of leaves collected on 1/5/01

6.4.1 Chlorophyll analysis

Total chlorophyll content (μg cm^{-2}) was determined for the leaves collected from each site. Maximum chlorophyll content was measured in the leaves from peg 1 at both sites 1 and 2, but there was little difference in the chlorophyll content of the leaves from pegs 2 to 5 and it did not reflect their position in relation to the pipeline (Figure 6.25). The chlorophyll content of leaves collected from site 3 decreased as the position of the pipeline was approached (Figure 6.26). This reflects the collection of samples from closer to the pipeline at this site and that the transect passed through the centre of the area of decreased growth where the plants were very underdeveloped and stressed.

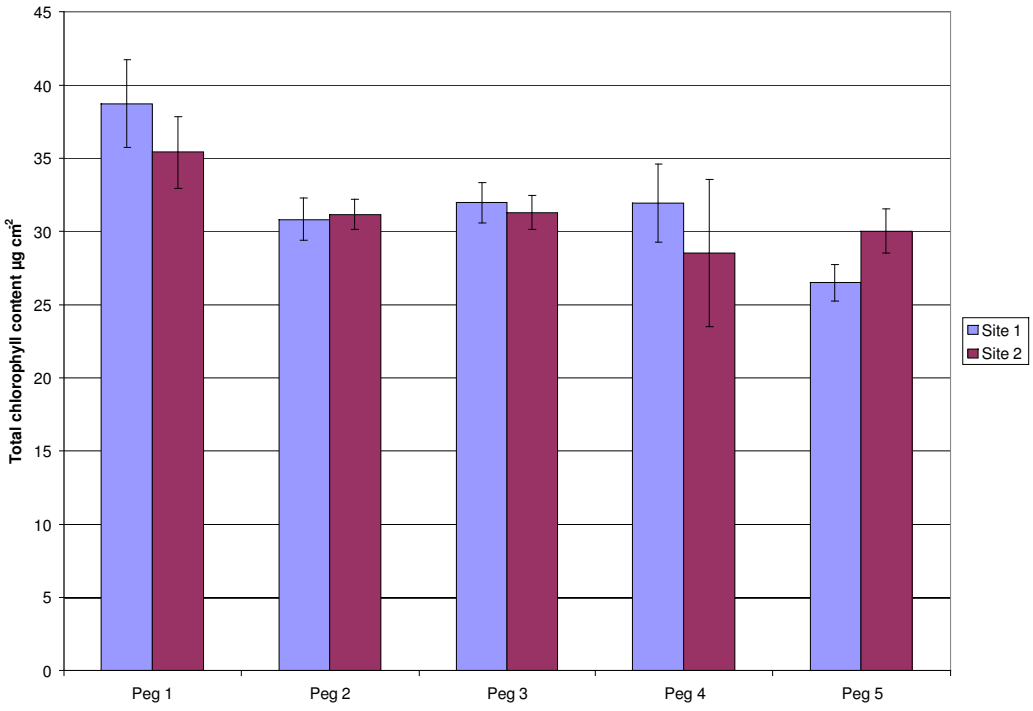

Figure 6.25 Total chlorophyll content for leaves collected from site 1 and 2, 1/5/01

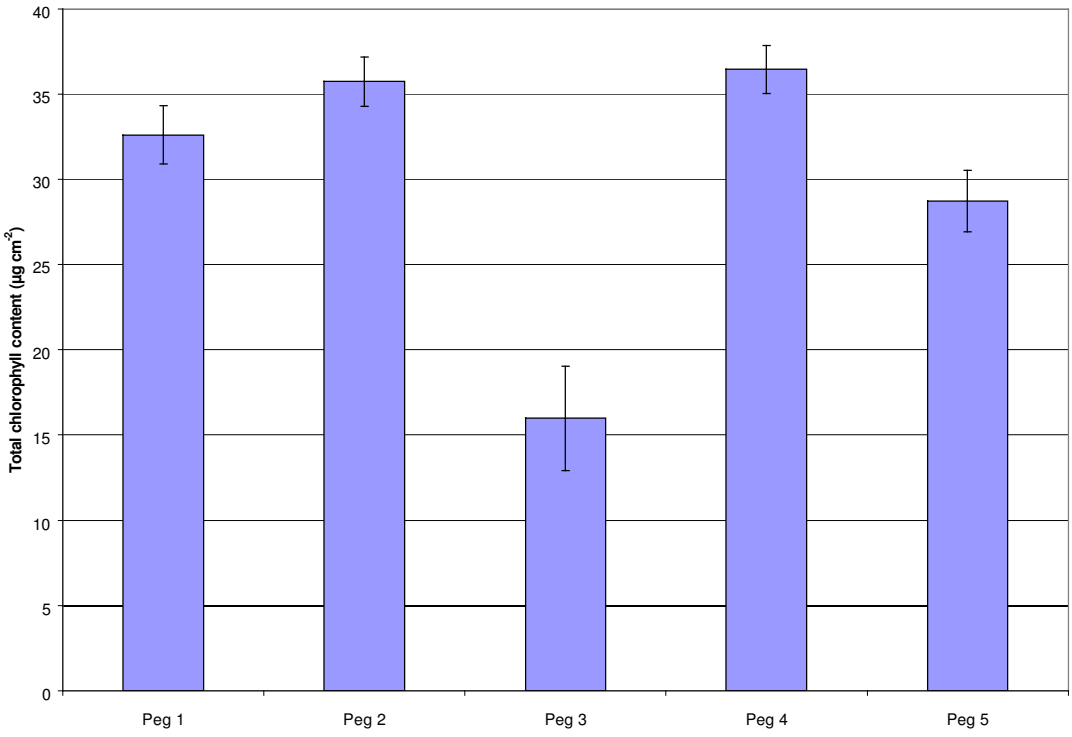

Figure 6.26 Total chlorophyll content for leaves collected from site 3

6.4.2 Dry matter analysis

The amount of dry matter per unit area (g cm^{-2}) and the equivalent water thickness (cm) was determined for the leaves collected at the field site. Figure 6.27, Figure 6.28, Figure 6.29 and Figure 6.30 show that as the position of the gas pipeline was approached there was an increase in the dry matter content and the equivalent water content of the leaves collected. This was observed at all three sites.

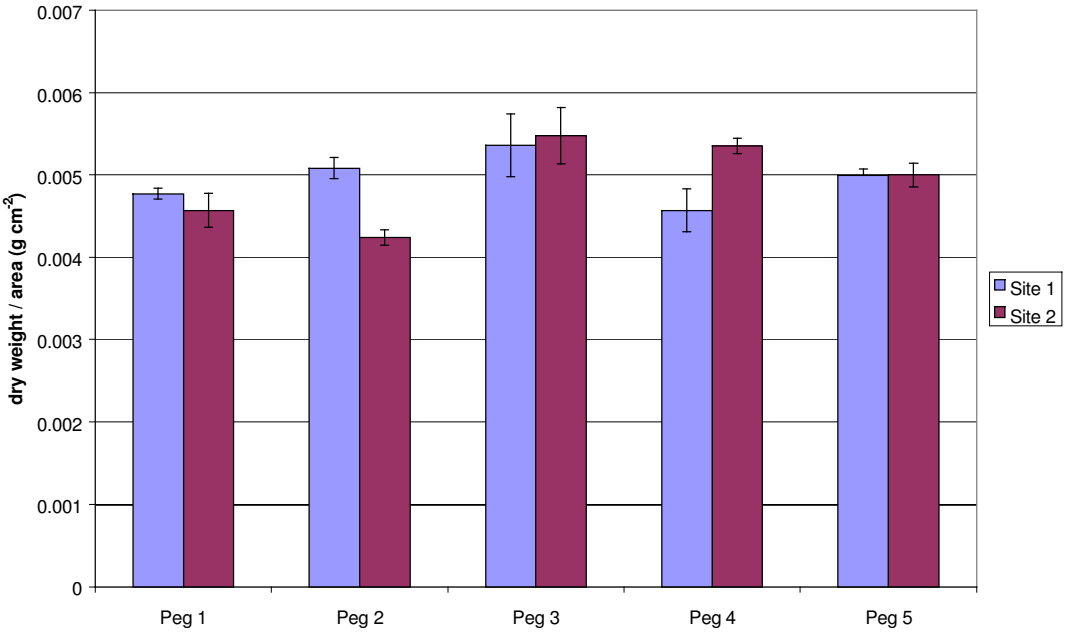

Figure 6.27 Dry matter content of leaves collected from Louth 1/5/01 (site 1 and 2)

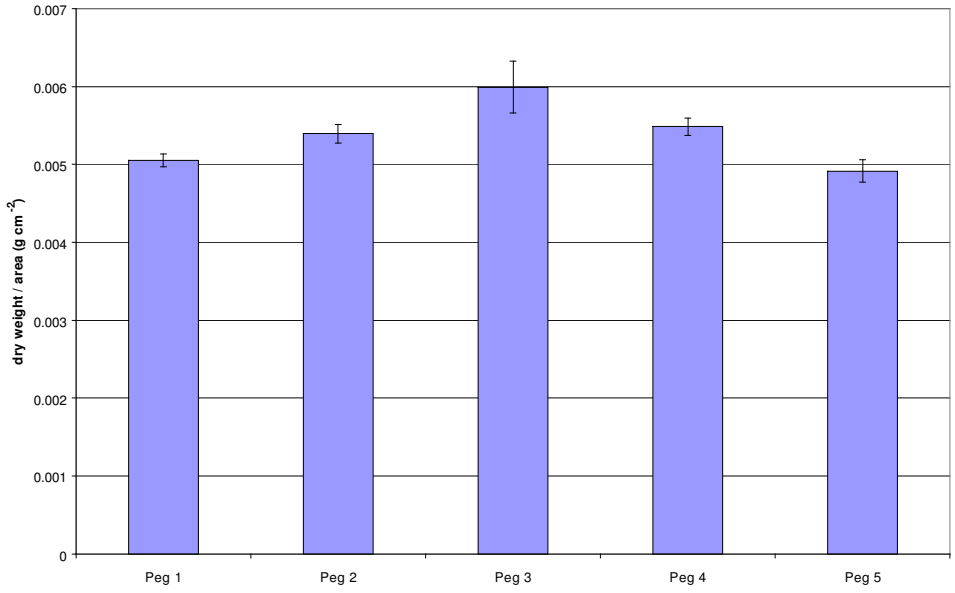

Figure 6.28 Dry matter content of leaves collected from Louth 1/5/01 (site 3)

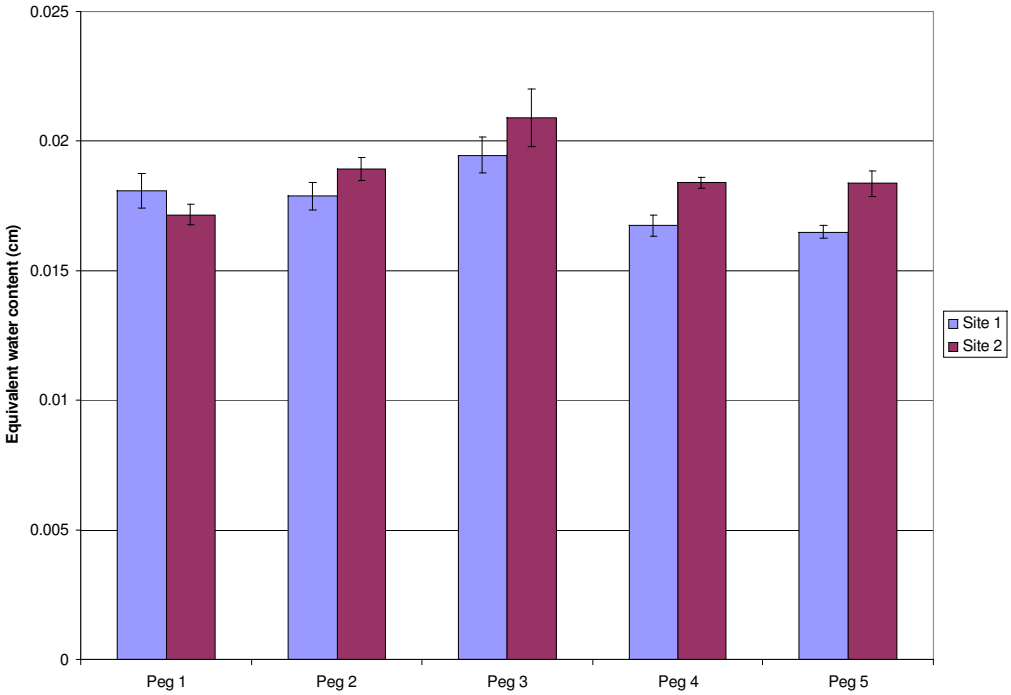

Figure 6.29 Equivalent water thickness of leaves collected from Louth 1/5/01 (site 1 and 2).

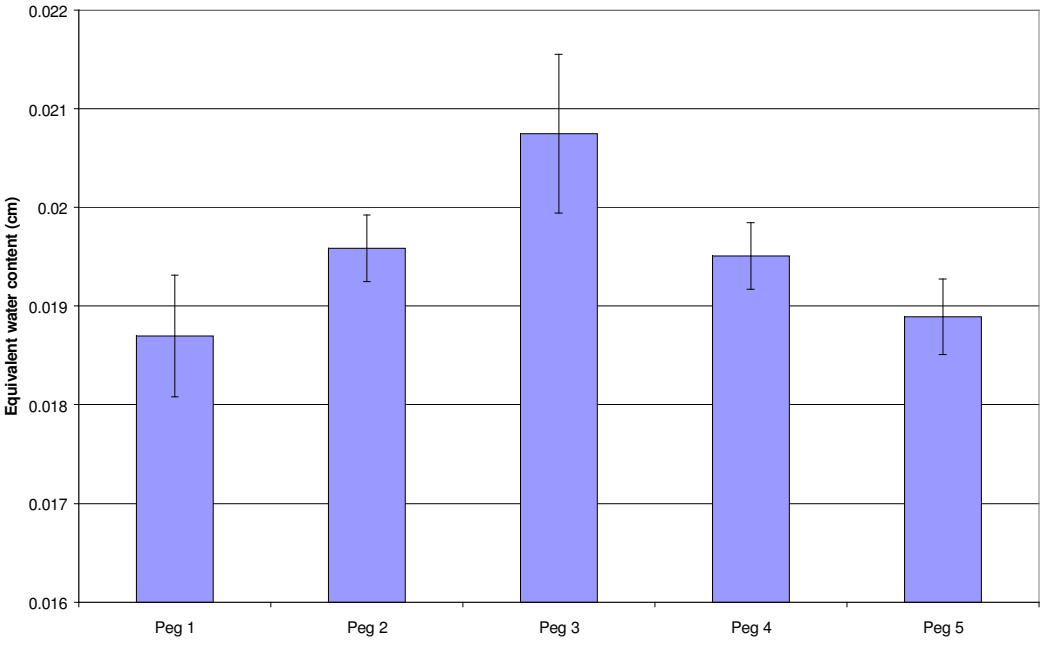

Figure 6.30 Equivalent water thickness of leaves collected from Louth 1/5/01 Site 3

6.5 Visit 3 – 16th June 2001

On this occasion the weather conditions were cloudy and became wet. The crop development was advanced, grain heads had formed and the leaves had begun to senesce and turn yellow. Figure 6.31 illustrates the extent of the crop development on this visit. An area of decreased growth above the gas pipeline can also be seen as a depression in the crop.

It was observed that in some of the areas of decreased growth visited previously, the vegetation had grown and was now greener than in the rest of the field. Figure 6.32 shows one of the depressed areas of growth above the gas pipeline. It can be seen that the crop surrounding the area is advanced with grain heads, whereas the growth that has occurred in the area above the pipeline is underdeveloped with green leaves still present.

Figure 6.31 Extent of barley crop development on 19/6/01. Area of decreased growth above pipeline is visible.

Figure 6.32 Area of decreased growth above the pipeline.

6.5.1 Relative reflectance 19/6/01

Spectral scans were taken on this occasion but the changing light conditions between the start and end of scanning meant that results were variable. Figure 6.33 shows that at site 1 the minimum visible reflectance is now from peg 3, which overlies the gas leak. Maximum reflectance was observed from peg 1, which was furthest from the pipeline and was most advanced in development. The fluctuations observed in the data from peg 1 are due to the changing light conditions throughout the scan and prevented analysis of first derivatives.

At site 2 reflectance of the peg site above the gas leak is still at a maximum with reflectance from peg 1 at a minimum (Figure 6.34). This is similar to the ranking of reflectance observed during the May visit.

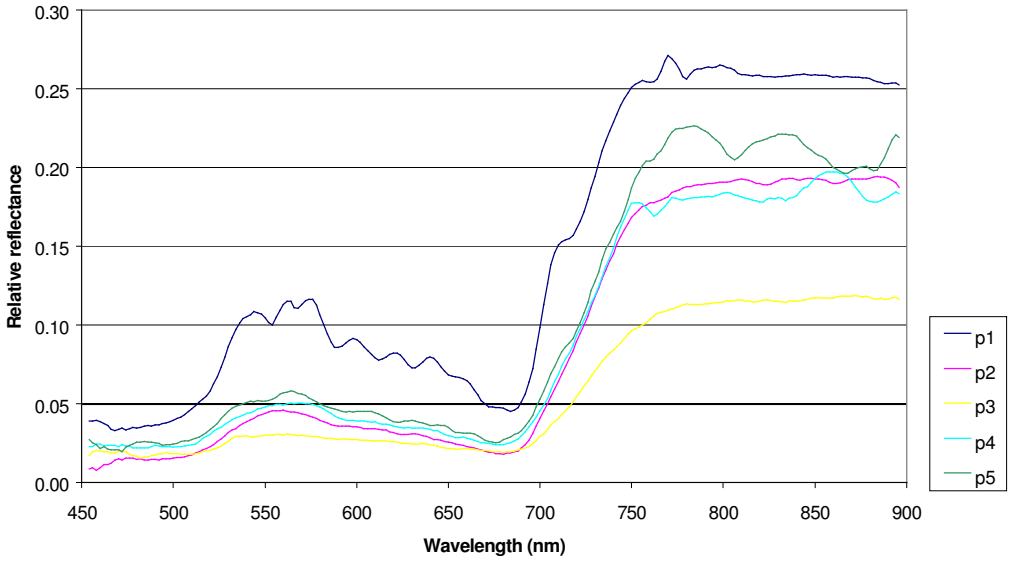

Figure 6.33 Relative reflectance taken from site 1, Louth 19/6/01 (p1 = reflectance from position 1, p2 =reflectance from position 2 etc)

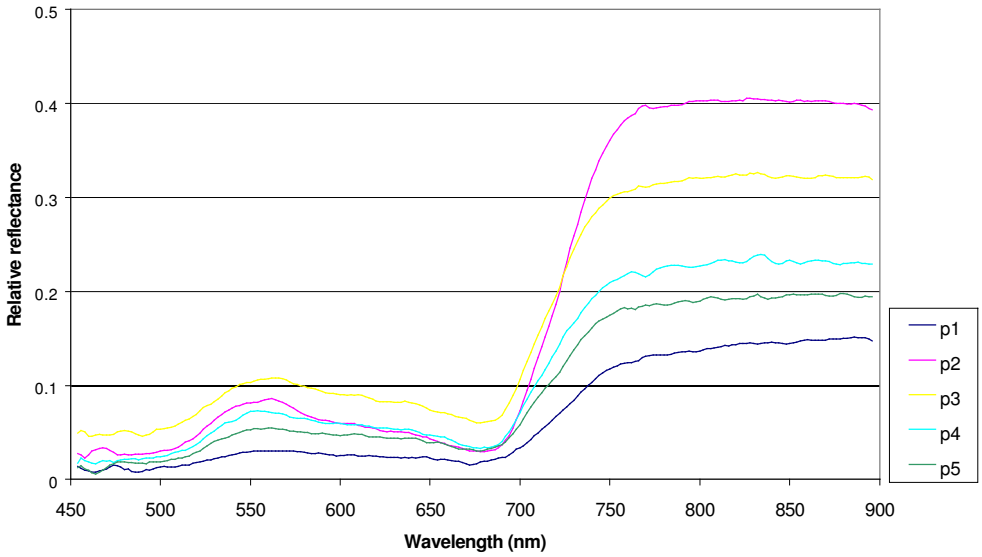

Figure 6.34 Relative reflectance taken from site 2, Louth, 19/6/01

6.6 Reflectance from leaves collected from Louth 19/6/01

6.6.1 Relative reflectance

Leaves collected during the field visit were scanned in the laboratory with the LI-1800 fitted with the integrating sphere and show that the leaves from site 1 with the highest reflectance in the visible are from the vegetation growing above peg 1. Reflectance in the visible from the other pegs is similar, although reflectance from peg 3 is increased in the region 572 to 700 nm. There is some variability in the reflectance in the infrared with that from peg 1 being the lowest and from pegs 2 and 5 the highest (Figure 6.35). At site 2 leaves from the area above the pipeline (peg 3), have higher relative reflectance in the visible region. Reflectance from peg 2 is also raised as it is still

under the influence of the gas leak. There is little difference in the reflectance from the leaves collected from the other positions along the transect (Figure 6.36). Reflectance in the near infra-red is similar for all positions.

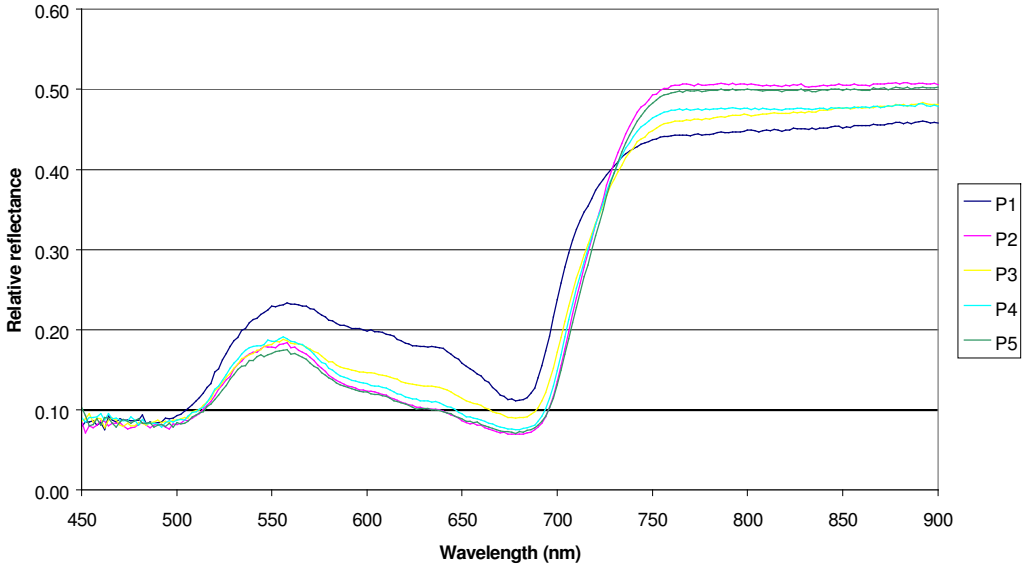

Figure 6.35 Relative reflectance from leaves collected from site 1, Louth, 19/6/01

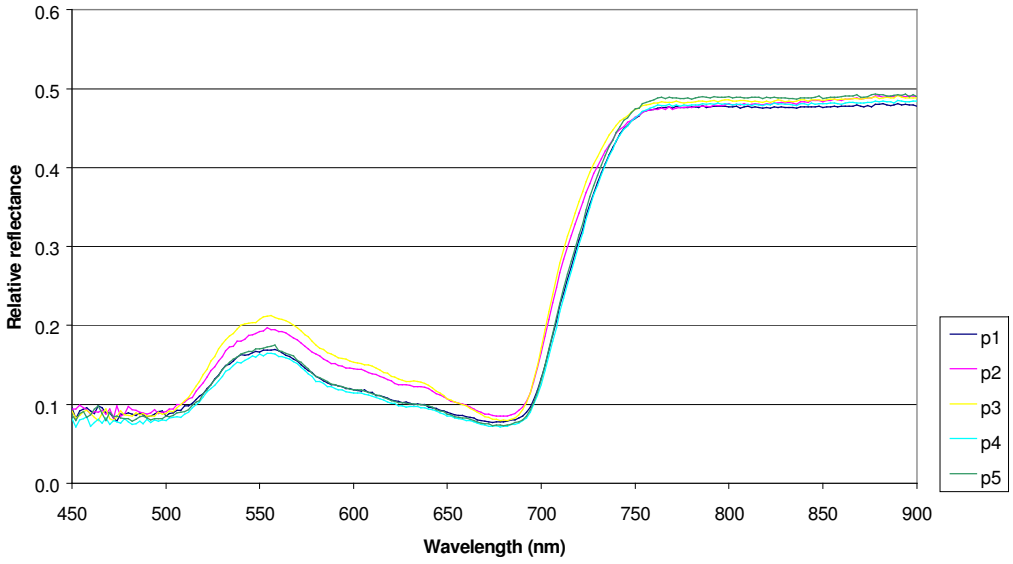

Figure 6.36 Relative reflectance of leaves collected from site 2, Louth, on 19/6/01

6.6.2 Red-edge analysis

The pattern of the first derivative is similar to that observed from the leaves collected on the previous site visit. At sites 1 and 2 the point of maximum inflection showing the position of the red-edge is a single peak at around 704 nm with a shoulder at 722 nm for pegs 2 and 5 for site 1 and for pegs 1, 4 and 5 at site 2. The other plots show a movement of the shoulder towards the blue to form a single peak at the position of maximum inflection (Figure 6.37 and Figure 6.38). The red-edge position varies between 708 and 698 nm for site 1, with the lowest red-edge position being at peg 1, and 706 nm and 702 nm for site 2 with pegs 2 and 3 having the shortest red-edge position. These patterns are also shown when plotting the magnitude of the first derivative of reflectance at 722 nm (Figure 6.39 and Figure 6.40).

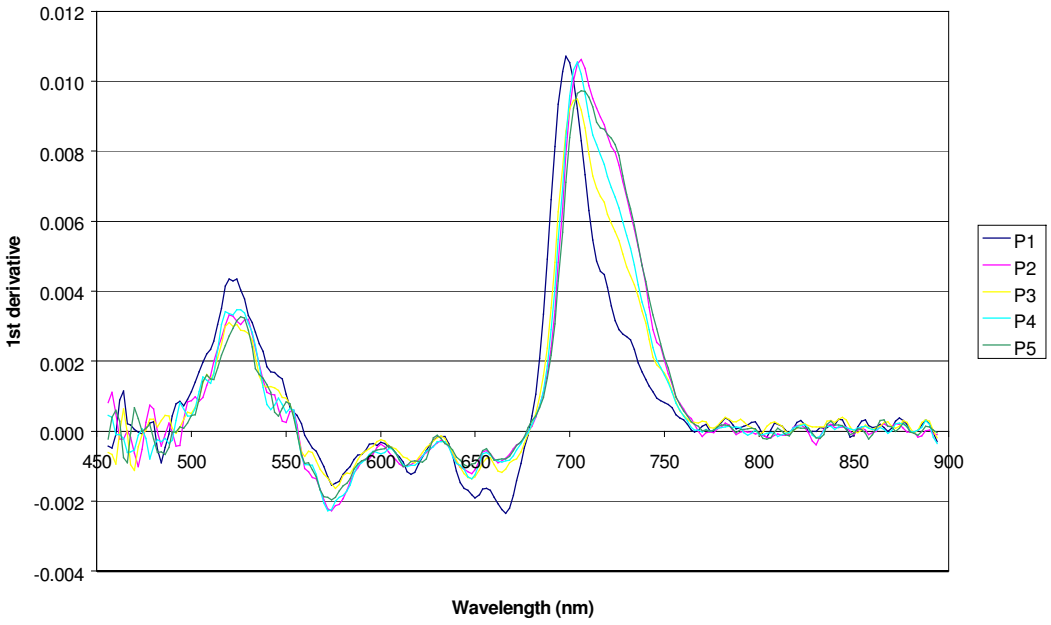

Figure 6.37 First derivative of reflectance for leaves collected from site 1, Louth, 19/6/01

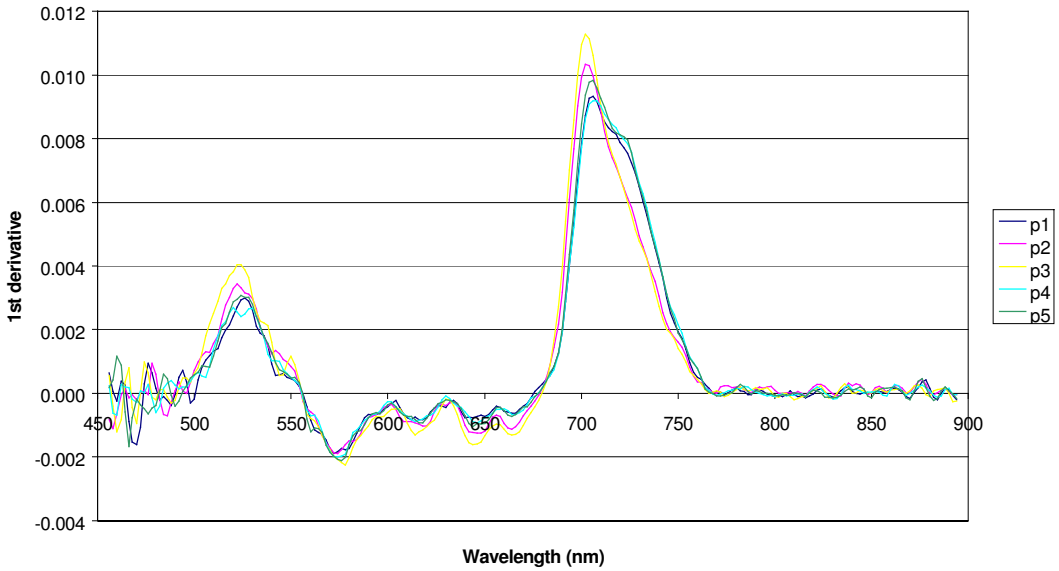

Figure 6.38 First derivative of reflectance for leaves collected from site 2, Louth 19/6/01

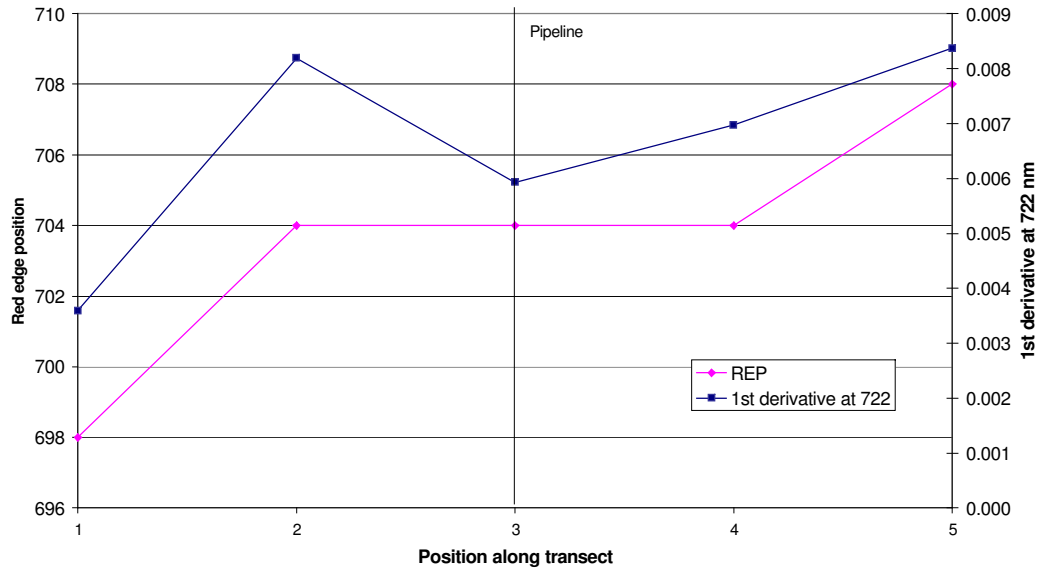

Figure 6.39 Red-edge position and magnitude of first derivative at 722 nm for leaves collected from site 1, Louth,19/6/01

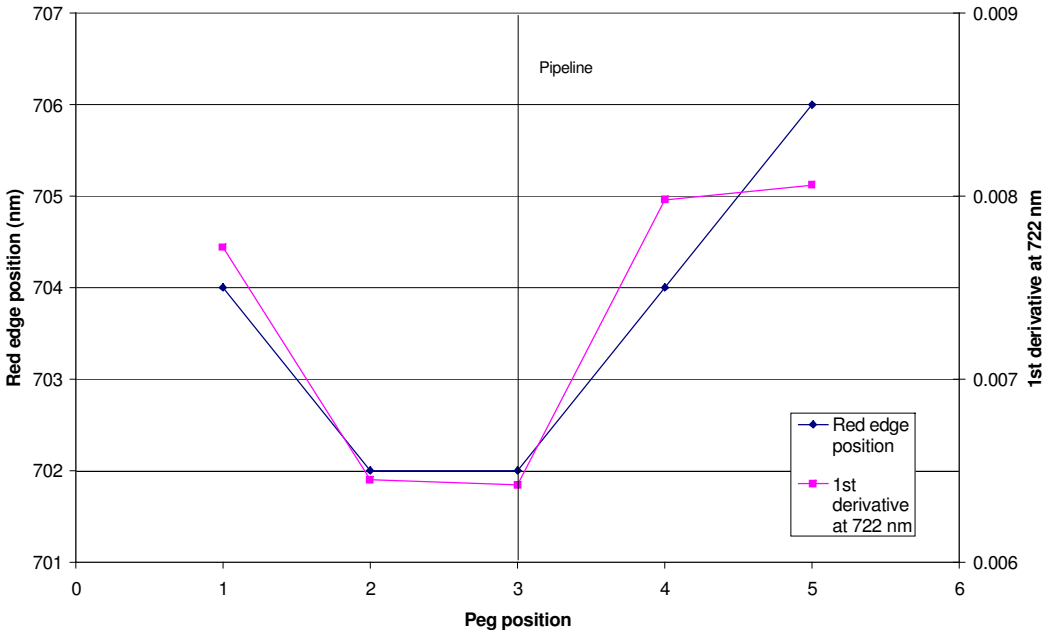

Figure 6.40 Red-edge position and magnitude of first derivative of reflectance at 722 nm of barley leaves collected from site 2, Louth 19-6-01

6.6.3 Analysis of other peaks within the first derivative plot

Differences were observed in the other peaks within the first derivative between site 1 and 2. The results reflect the observed differences in the field where at site 1 the crop above the gas leak appeared greener than the surrounding crop and at site 2 the crop above the leak appeared more stressed than the surrounding crop.

At 524 nm there was a decrease in the magnitude of the first derivative as the gas leak was approached at site 1. At site 2 there was an increase in the magnitude as the leak is approached, whereas on previous visits there had been an increase in the magnitude. At 600 and 634 nm, which are also peaks within the first derivative, site 1 shows an increase in the magnitude of the first derivative whereas site 2 shows a decrease.

At 574 nm site 1 shows a fluctuation in the first derivative as the pipeline is approached with increases in the depth of the trough at pegs 2 and 4. Site 2 shows

little difference in the depth of the trough as the transect is crossed. At 616 nm site 1 shows a decrease in the depth of the trough and site 2 shows an increase and at 644 nm there is an increase in the depth of the trough at peg 3 for both sites 1 and 2.

By performing an average of the data collected from sites 1 and 2 it was possible to compare changes that had occurred between the two visits. Only at 634 and 644 nm do there appear to be changes with time in the first derivative around the gas leak. At 634 nm there was a decrease in the amplitude of the peak around peg 2 (Figure 6.42). The effect at 644 nm was similar but weaker.

At all wavelengths except 524 nm there is an increase in the magnitude of the first derivative on 19/6/01 relative to 1/5/01. At 524 nm there is a slight decrease in the first derivative.

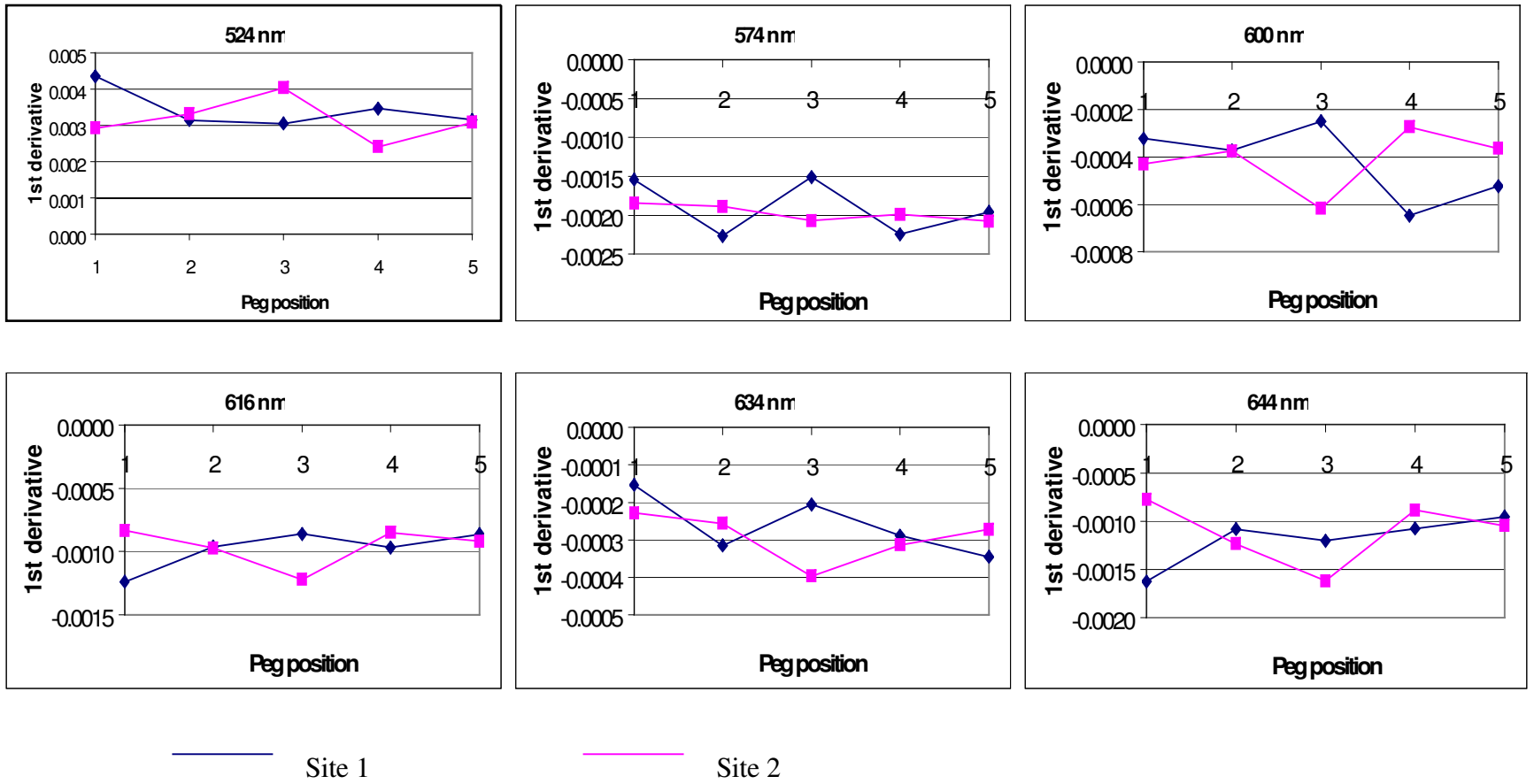

Figure 6.41 First derivative of reflectance at selected wavelengths for leaves collected from site 1 and 2, Louth, 19/6/01

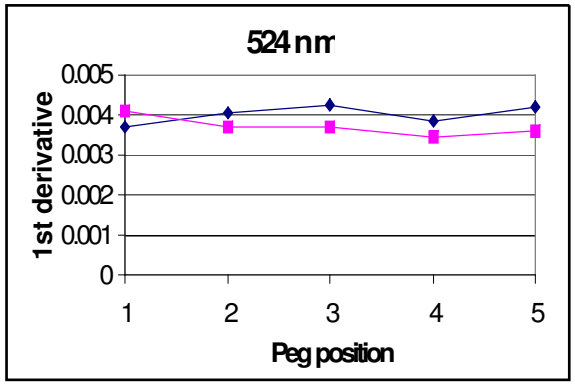
524 nm
1st derivative
0.005
0.004
0.003
0.002
0.001
0
1
2
3
4
5
Peg position

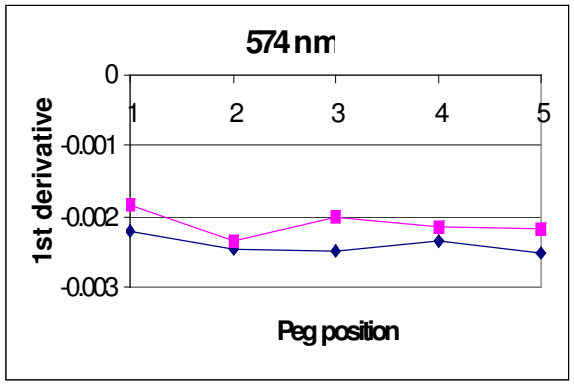
574 nm
1st derivative
0
-0.001
-0.002
-0.003
1
2
3
4
5
Peg position

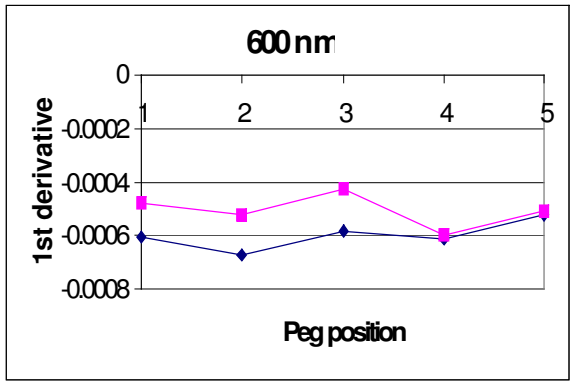
600 nm
1st derivative
0
-0.0002
-0.0004
-0.0006
-0.0008
1
2
3
4
5
Peg position

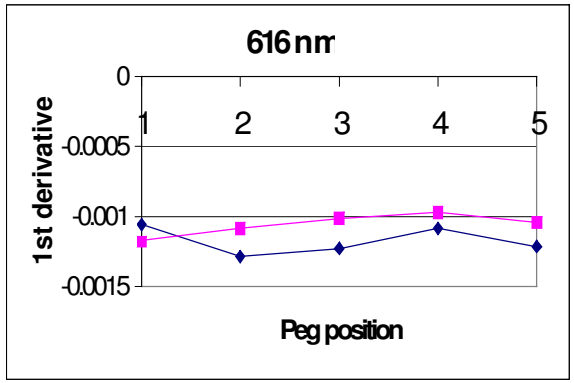
616 nm
1st derivative
0
-0.0005
-0.001
-0.0015
1
2
3
4
5
Peg position

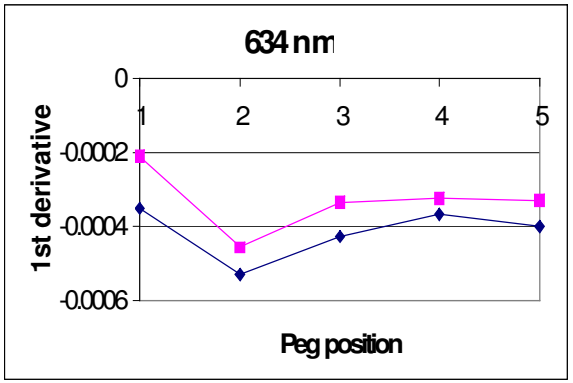
634 nm
1st derivative
0
-0.0002
-0.0004
-0.0006
1
2
3
4
5
Peg position

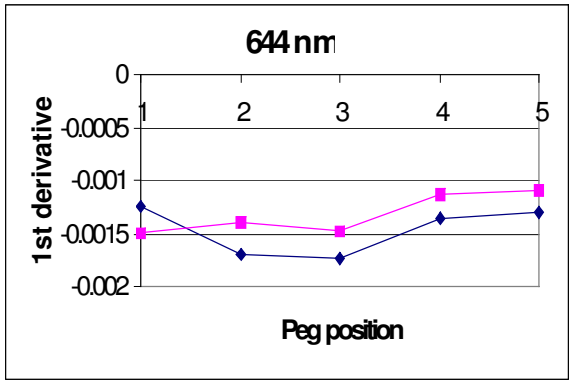
644 nm
1st derivative
0
-0.0005
-0.001
-0.0015
-0.002
1
2
3
4
5
Peg position

1/5/01

19/601

Figure 6.42 Change in 1st derivative of leaves collected from Louth on the 1/5/01 and 19/6/01

6.7 Chlorophyll analysis of leaves collected from Louth 19/6/01

Chlorophyll analysis of the leaves collected was performed. The poor condition of the leaves due to the development of the crop and the wet conditions under which the leaves were collected meant that only two replicates of chlorophyll analysis could be performed and dry matter analysis was not carried out. Chlorophyll analysis from site 1 showed that the chlorophyll content decreased along the transect and close to the pipeline except for peg 1 which had a very low chlorophyll content. Site 2 showed that the leaves collected from peg two had less chlorophyll than the rest of the samples. Peg 2 was not overlying the gas pipeline but did appear to be still within the influence of the gas leak. Maximum chlorophyll content was observed from peg 1 and there was little difference in the chlorophyll content from pegs 3, 4 and 5 (Figure 6.43).

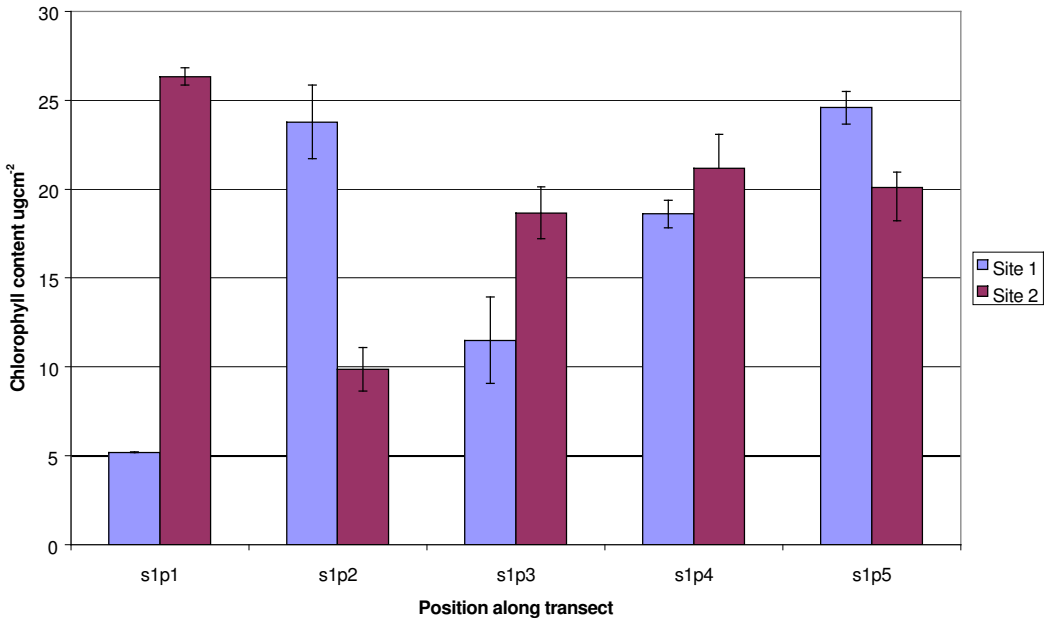

Figure 6.43 Chlorophyll analysis for leaves collected from sites 1 and 2 19/6/01

The chlorophyll content and red edge position was compared for leaves collected from all sites on both dates. A comparison was also made of the chlorophyll content and the amplitude of the first derivative at 722 nm

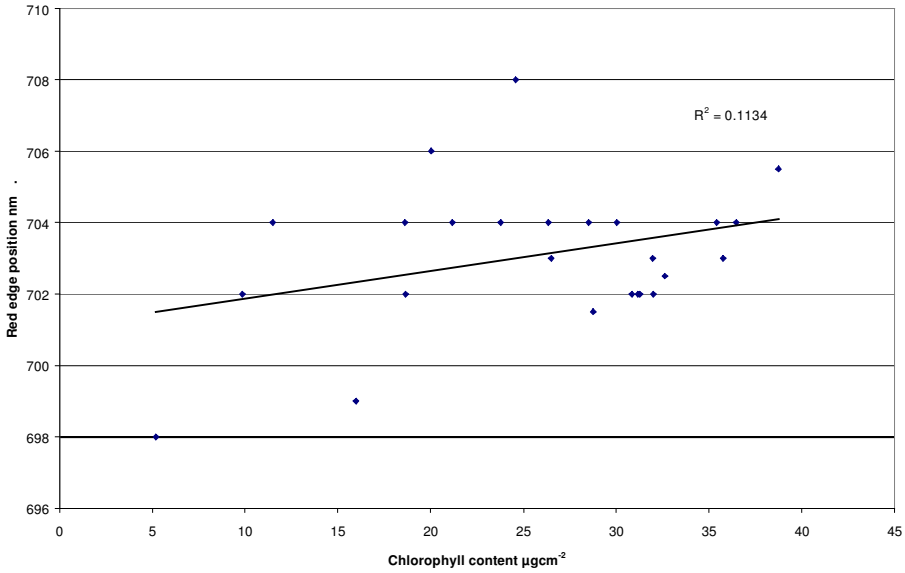

Figure 6.44 Comparison between red edge position and chlorophyll content. Data collected from all sites on 1/5/01 and 19/6/01

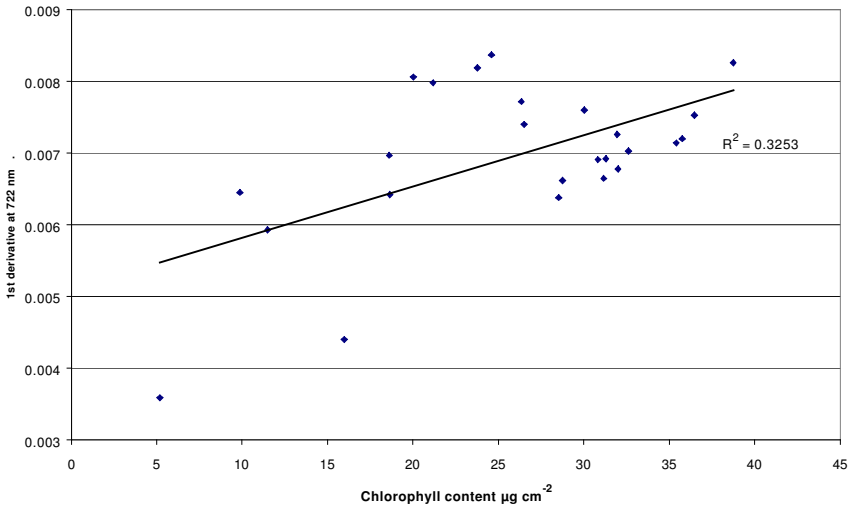

Figure 6.45 Comparison of chlorophyll content and amplitude of 1st derivative at 722 nm. Data collected from all sites on 1/5/01 and 19/6/01

6.8 Application of narrow-band ratios for gas leak detection

As an alternative to derivative analysis to identify gas leaks the ratios of narrow-bands of reflectance data centred at 550, 600, 630, 680 and 800 nm wavelengths were investigated.

The average of five measurements was taken to give a 10 nm bandwidth centred on each of the selected wavelengths. The wavelengths selected for ratio analysis, were based on wavelengths identified in Table 3.2 with the exception that 630 nm was selected as the position of the minor reflectance peak, rather than 650 nm as suggested by Gemmel (1988). These wavebands were selected as they encompassed plateau areas on the reflectance plot as opposed to the wavebands of the derivative plots that showed the positions of maximum slope. A 10 nm waveband rather than a point measurement was selected to minimise noise.

The ratio of each waveband was calculated relative to 800 nm, (which is the maximum reflectance peak and is related to the effect of cell structure and discontinuities within the leaf), and to 680 nm, (which is the absorption maximum and is related to the chlorophyll concentration within the leaf).

Data chosen for analysis was that from site 3, collected on 1/05/01 as this transect passed through the centre of the bare patch and may identify any effects due to the decreased canopy growth in the centre of the bare patch, and data from sites 1 and 2 collected on 19/06/01 to identify any canopy changes that may have occurred with maturity of the crop.

6.8.1 Ratio analysis of canopy and leaf reflectance for site 3 (1st May 2001)

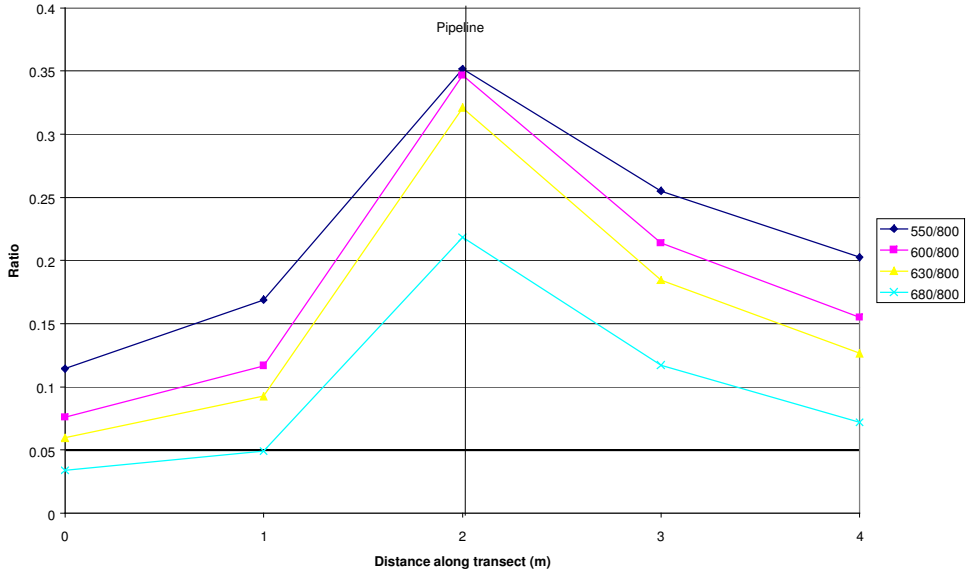

Figure 6.46 Ratio analysis of 10 nm wavebands of canopy reflectance for Site 3, 01/05/01 relative to a 10 nm waveband centred at 800 nm.

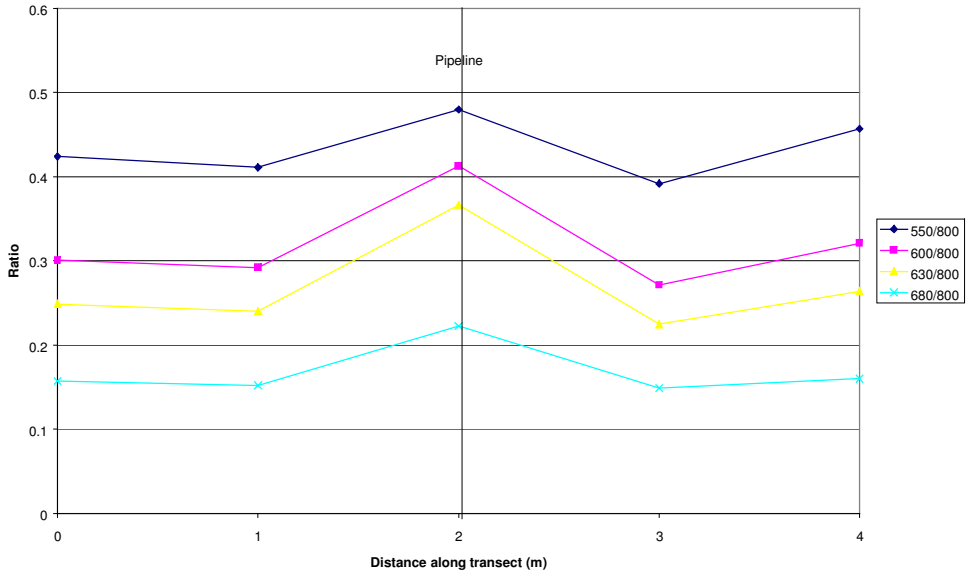

Figure 6.47 Ratio analysis of 10 nm wavebands of leaf reflectance for Site 3, 01/05/01 relative to a 10 nm waveband centred at 800 nm.

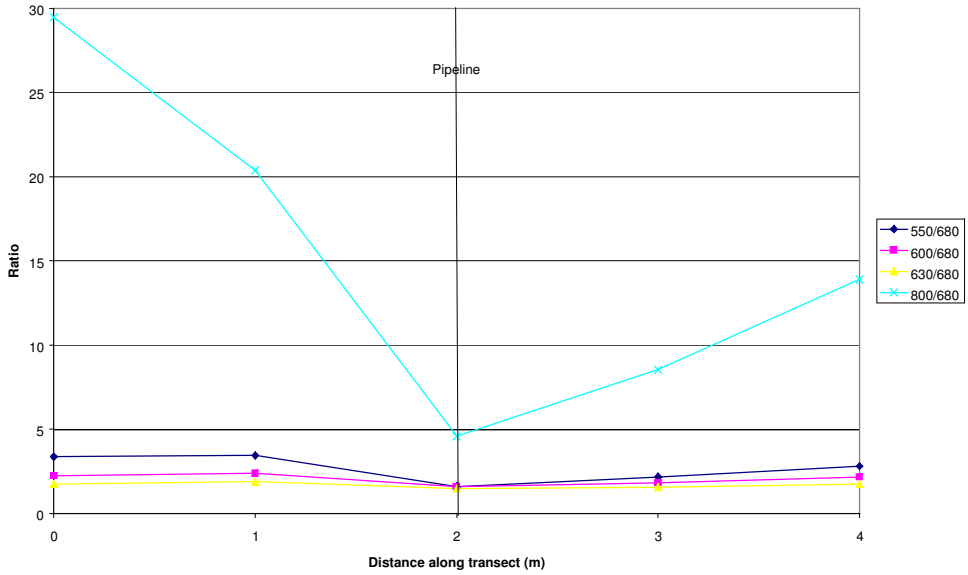

Figure 6.48 Ratio analysis of 10 nm wavebands of canopy reflectance for Site 3, 01/05/01 relative to a 10 nm waveband centred at 680 nm.

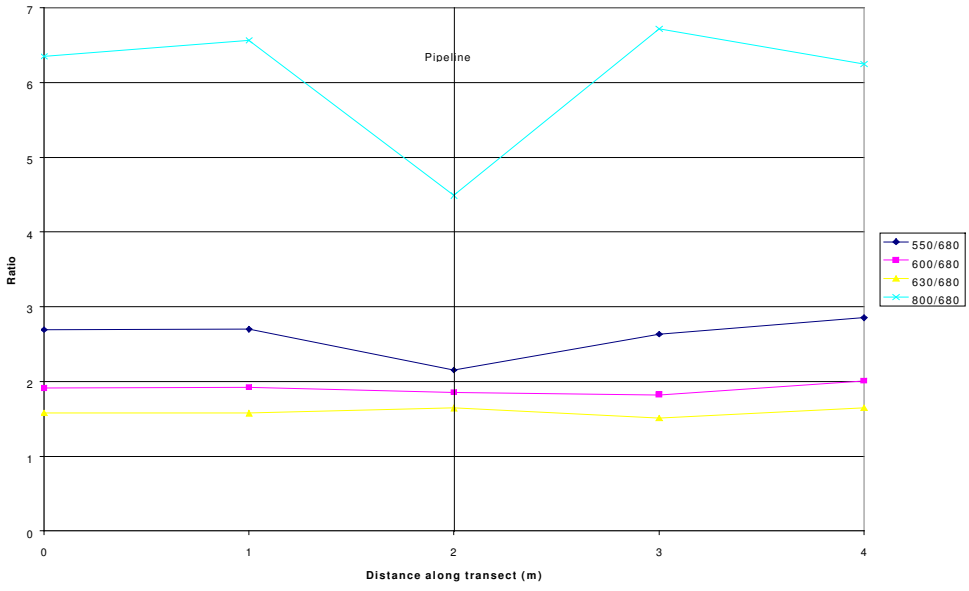

Figure 6.49 Ratio analysis of 10 nm wavebands of leaf reflectance for Site 3, 01/05/01 relative to a 10 nm waveband centred at 680 nm.

6.8.2 Ratio analysis of canopy and leaf reflectance for sites 1 and 2 (19th June 2001)

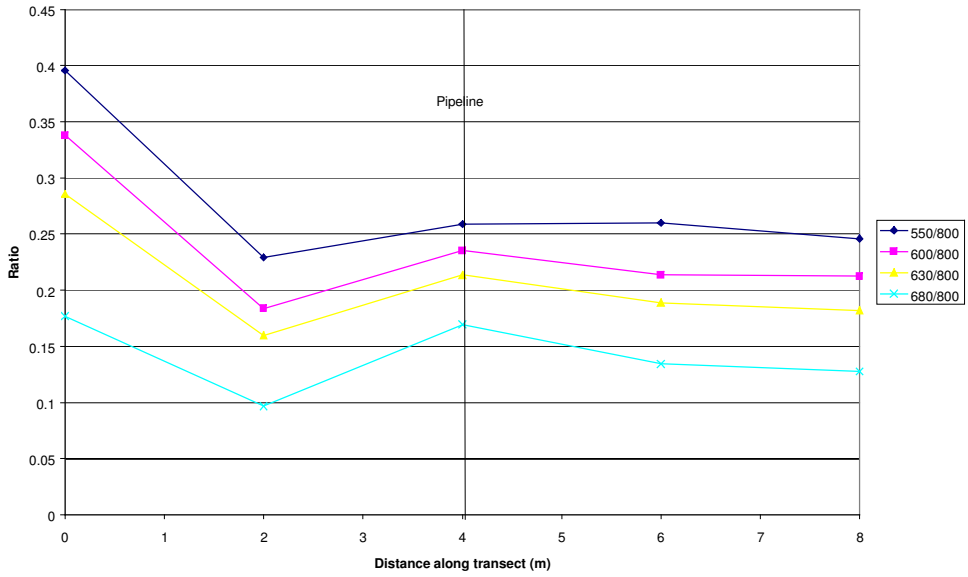

Figure 6.50 Ratio analysis of 10 nm wavebands of canopy reflectance for Site 1, 19/06/01 relative to a 10 nm waveband centred at 800 nm.

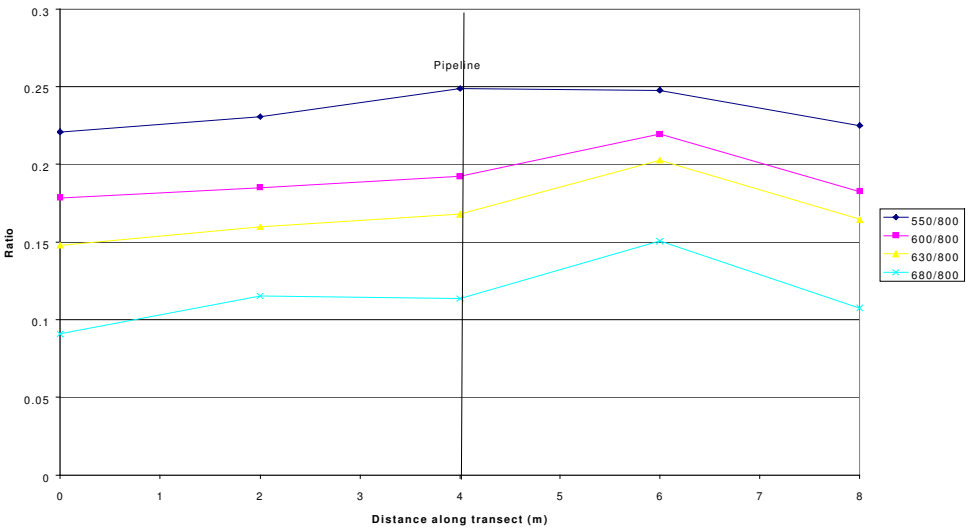

Figure 6.51 Ratio analysis of 10 nm wavebands of canopy reflectance for Site 2, 19/06/01 relative to a 10 nm waveband centred at 800 nm.

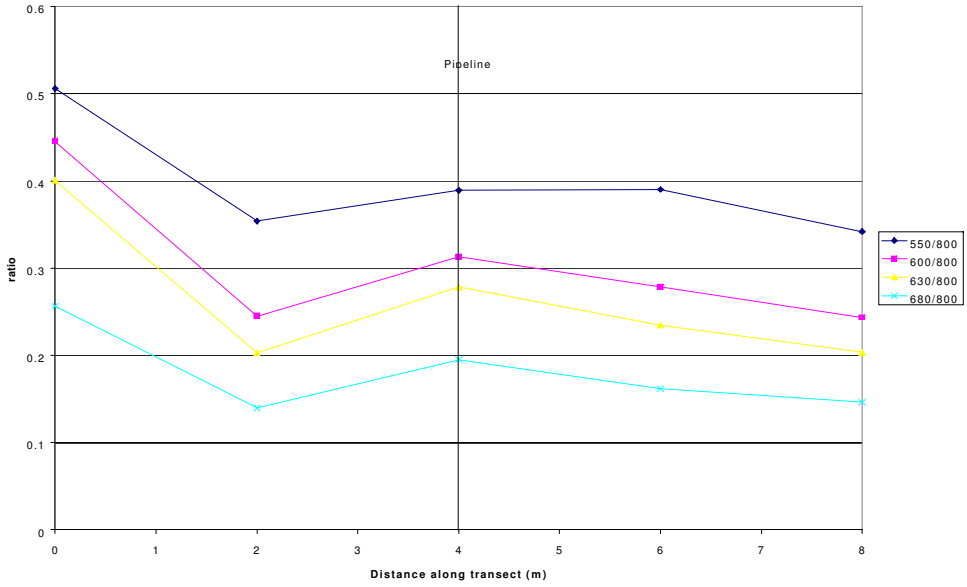

Figure 6.52 Ratio analysis of 10 nm wavebands of leaf reflectance for Site 1, 19/06/01 relative to a 10 nm waveband centred at 800 nm.

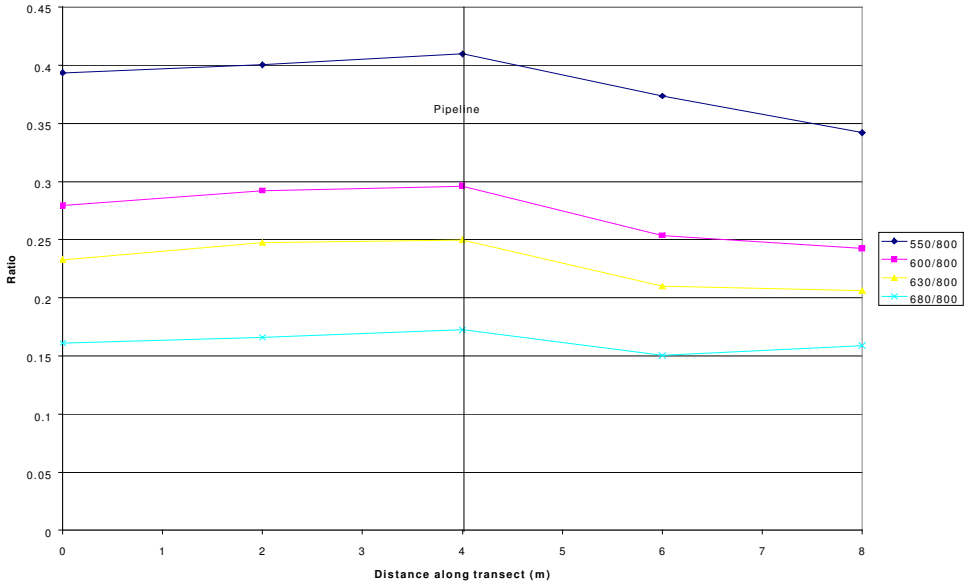

Figure 6.53 Ratio analysis of 10 nm wavebands of leaf reflectance for Site 2, 19/06/01 relative to a 10 nm waveband centred at 800 nm.

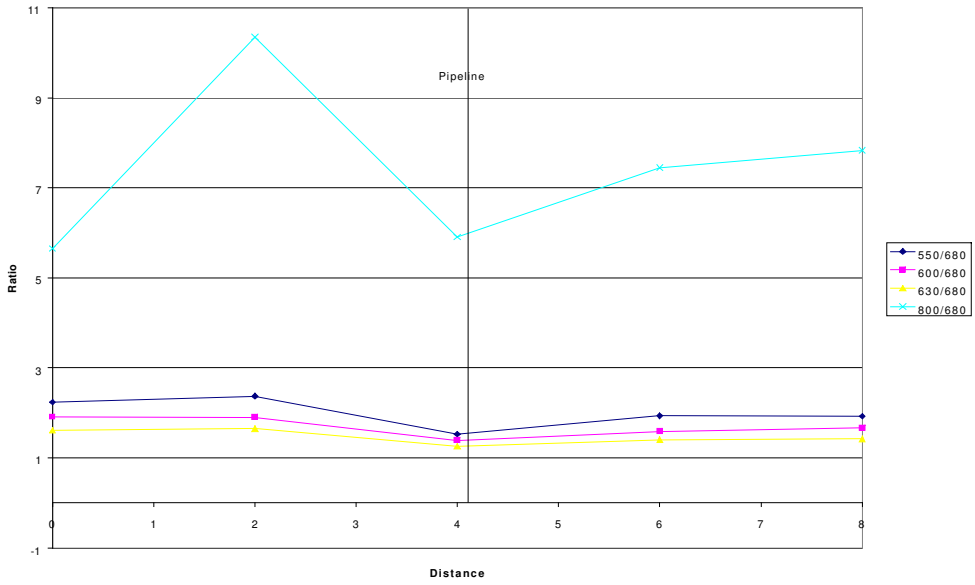

Figure 6.54 Ratio analysis of 10 nm wavebands of canopy reflectance for Site 1, 19/06/01 relative to a 10 nm waveband centred at 680 nm.

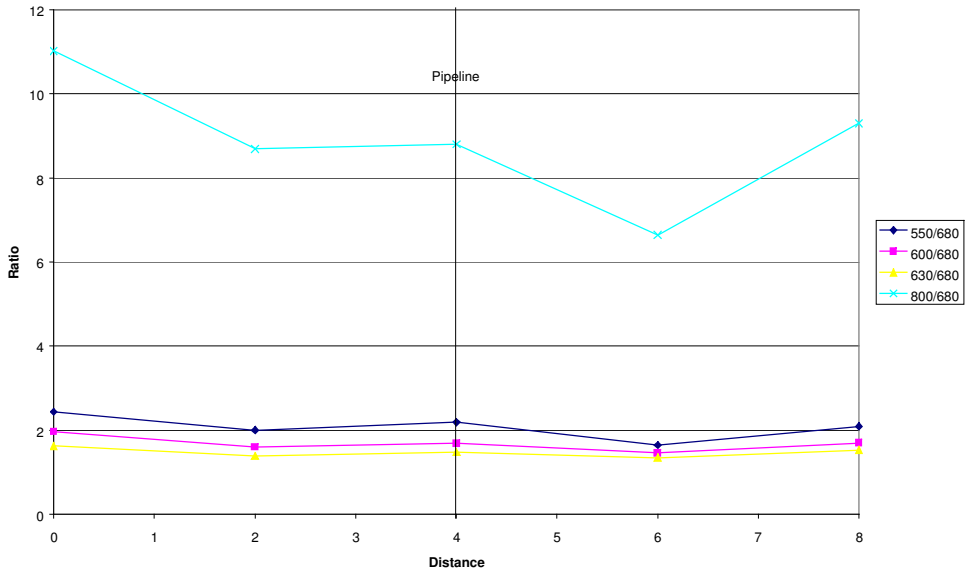

Figure 6.55 Ratio analysis of 10 nm wavebands of canopy reflectance for Site 2, 19/06/01 relative to a 10 nm waveband centred at 680 nm.

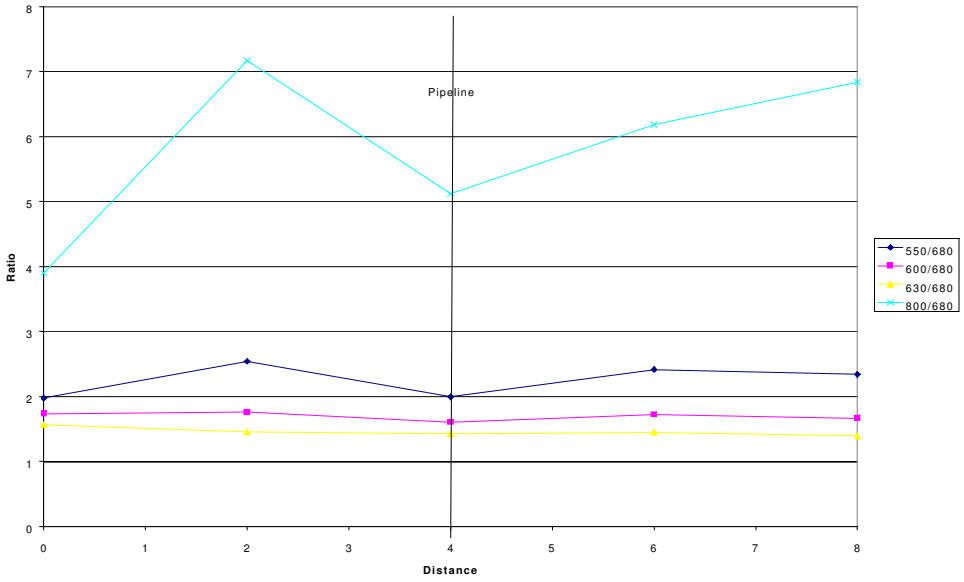

Figure 6.56 Ratio analysis of 10 nm wavebands of leaf reflectance for Site 1, 19/06/01 relative to a 10 nm waveband centred at 680 nm.

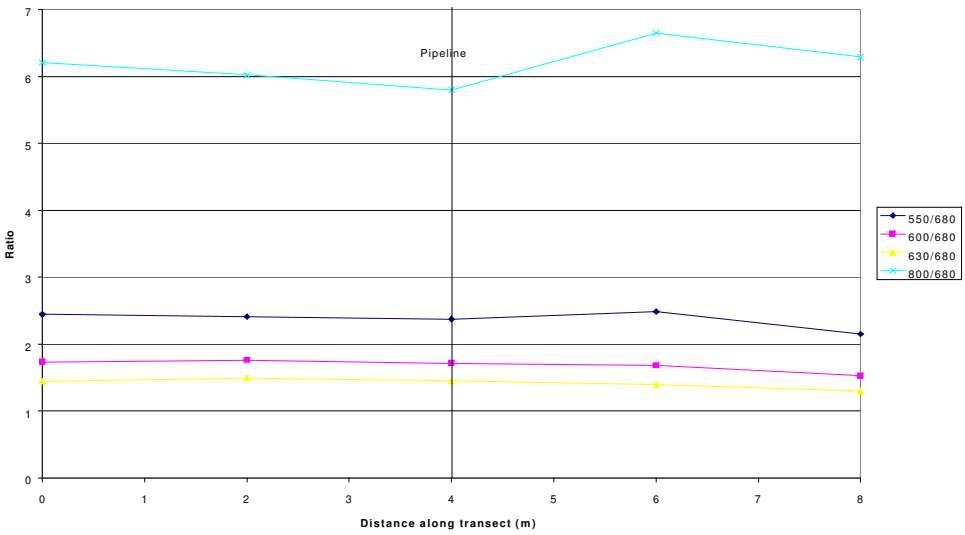

Figure 6.57 Ratio analysis of 10 nm wavebands of leaf reflectance for Site 2, 19/06/01 relative to a 10 nm waveband centred at 680 nm.

6.9 Summary

Decreased growth of the barley crop was observed above the leaking pipeline. Spectral scans showed increased reflectance in the areas of decreased growth and lower reflectance in areas further away from the pipeline. The first derivative of reflectance showed that the red-edge position moved from 737 nm to 727 nm above the pipeline.

During a later visit crops had grown within the area of the leak but were less dense than the rest of the field and development was depressed. The crop in the rest of the field had formed grain heads and the leaves had started to senesce and turn yellow, whereas the plants above the leaking pipeline were smaller, still vegetative and had green leaves.

Similar patterns were observed in laboratory scans of the leaves but the red-edge position varied between 706 and 702 nm.

Plant analysis showed that there was little change in the chlorophyll content of the leaves collected but that there was an increase in dry matter content and equivalent water content from the leaves that were collected above the pipeline.

7 Discussion

This chapter is a summary of the research findings and a discussion of the contribution and limitations of the research.

The overall aims of the research were to investigate whether spectral changes could be identified in vegetation subjected to leaking underground gas and thus assist in the development of a remote sensing system to identify gas leaks.

There were two main objectives. Firstly, to identify spectral changes in plants subjected to alternative methods of oxygen displacement and to compare these spectral changes to those observed with leaking natural gas and thus to determine if the effects were specific to natural gas leakage or if they were generic to the effect of oxygen deficiency in the soil. Secondly, to measure spectral reflectance from a crop growing above a leaking gas pipe to determine if changes were visible on a canopy scale.

7.1 Spectral changes in leaves subjected to various methods of oxygen displacement.

This research showed that leaves exposed to different methods of displacing oxygen from the soil showed increased reflectance in the visible regions and little difference in the infrared irrespective of the oxygen displacement method used. Bean leaves showed greater increases in reflectance than barley with the greatest changes being observed when displacing soil oxygen with water. Displacement of soil oxygen with natural gas showed the smallest changes. This result was probably due to the effect of dis-continuous oxygen displacement. For safety reasons, displacement with natural gas could only be performed for eight hours per day and this led to re-oxygenation of the soil overnight. The greatest changes in reflectance appeared in the third week of

the trial (after day 14), which is consistent with the observations of Pysek and Pysek (1989) who found that the first symptoms were observed in vegetation between 15 to 30 days after exposure to a leaking gas main.

All treatments showed changes in the first derivative of reflectance with movements in the position of the red-edge. In bean it was generally found that the position of the red-edge moved to longer wavelengths for the control plants as they matured, but not for treatment plants. Hence there was the appearance that displacement of oxygen from the soil led to a shift in the red-edge to relatively shorter wavelengths. This effect was also observed by Gates (1965) who showed that the absorption edge of the reflectance curve at 700 nm shifted progressively and systematically towards longer wavelengths with time and by Horler (1983) who showed that red-edge shifts associated with phenological crop development of winter wheat and spring barley were towards longer wavelengths as chlorophyll concentration increased with crop maturity, and then reverted to shorter wavelengths as senescence began. Miller (1991) also showed that reflectance from the leaves of four varieties of trees showed a shift in the red-edge position towards longer wavelengths as the leaves matured (between Julian day 140 and 222) followed by a period when the red-edge shifted towards shorter wavelengths (Julian day 223-290) following the stages of early leaf development through to maturation and senescence. It is therefore surmised that the displacement of oxygen from the soil does not cause a direct shift to shorter wavelengths but that the development of the plant is suppressed, preventing the shift to longer wavelengths normally associated with a developing plant.

Radish plants subjected to waterlogging showed a movement of the red-edge to longer wavelengths in both the control and treated plants but the red-edge of the waterlogged

plants remained at a shorter wavelength than those of the control. The rooting system of radish plants was shallower than that of the bean and barley plants, so they were more likely to be able to obtain oxygen diffusing into the surface. The leaves of radish also tended to turn red as the trial progressed showing the effect of red pigments in the spectra. Curran *et al.* (1991) showed that the effect of the red pigment amaranthin was to increase the absorption of visible radiation and thus move the red-edge to longer wavelengths. This may explain the steep movement of the red-edge in control and waterlogged radish to longer wavelengths as the leaves turned red after four weeks of treatment, in contrast to waterlogged bean where the effect of waterlogging was to prevent movement of the red-edge to longer wavelengths.

In all species studied, changes were observed in the magnitude of the first derivative at other wavelengths, with the main differences occurring at 524 nm where the treatment led to an increase in the magnitude of the peak. The largest changes at other wavelengths were observed at 616 and 644 nm. Changes at these wavelengths may have been due not only to the decreasing amount of total chlorophyll in the exposed plants but also to the change in the ratio of chlorophyll *a* to chlorophyll *b* (Table 4.2). In most cases the ratio of chlorophyll *a* to *b* decreased in the treated plants, which may have led to a shift in the wavelengths at which the chlorophyll was absorbing.

Barley showed similar effects to bean, with both argon and waterlogging treatments generating an increase in reflectance in the visible wavelengths by the third week of the trial. There was a change in the first derivative at other wavelengths but these were not as marked as in bean.

The main difference between the reflectance of bean and barley is in the shape of the peak that identifies the red-edge. In bean the red-edge was identified by a single peak

occurring in the first derivative of reflectance at between 702 and 722 nm. In barley, a double peak was observed in the peak identifying the red-edge. A single peak was observed at 704 nm that did not shift, but the position of the second peak (at 722 nm) shifted to shorter wavelengths such that in stressed plants the peak narrowed to become a single peak at about 704 nm.

Differences in the shape of the peak that defines the red-edge may be related to the different leaf structures of monocotyledons and dicotyledons. Near-infrared reflectance is strongly affected by the size of the cells, the number of cell layers and the thickness of the leaf mesophyll. The internal structure of mono- and dicotyledons differs. In dicotyledons the upper and lower epidermises are separated by the mesophyll which is composed of a layer of columnar palisade parenchyma cells and a layer of spongy mesophyll. There are many air spaces between the spongy mesophyll cells. In monocotyledons the leaf is more compact with fewer air spaces and there are no columnar cells below the upper epidermis (Gausman 1985). Leaves of dicotyledons have higher reflectance than monocotyledons because the spongy mesophyll is more developed (Guyot 1990) and allows more light scattering between the cell walls. As the red-edge peak is determined by the shift from low reflectance in the red to high reflectance in the near infrared, differences in reflectance due to leaf structure may affect the shape of the peak in the first derivative in this region.

The hypothesis of the research was that leaking natural gas displaces oxygen from the soil and that plant roots therefore suffer from oxygen deficiency. Three main methods were chosen to displace oxygen from the soil to determine if the effects were specific to natural gas leakage or were generic to oxygen deficiency. Although all these

methods were used to displace oxygen from the soil, the effects on the soil will have been different in each case.

The first method of oxygen displacement was with natural gas, which is an organic compound utilised by bacteria as an energy source. Thus, where natural gas is leaking there is not only the physical displacement of the oxygen from the soil by the flow of gas but also the effect of bacteria and other soil organisms oxidising the gas. This effect is expected to enhance the oxygen deficiency and increase the concentration of CO_2 in the soil.

The second method of oxygen displacement was with water, which will displace the oxygen in the soil by filling the soil spaces with water. Oxygen diffuses more slowly through water than through air and thus replacement of the oxygen from the surface is slower. Removal of gaseous products produced in the waterlogged soil will also be slower through the water and there may be a build up of toxic chemicals that could have an effect on the plants. Ethylene concentrations are known to increase in waterlogged soils and this has deleterious effects on plant growth causing inhibition of root growth and stimulation of adventitious root formation (Godwin and Mercer 1983).

The third main treatment was displacement of soil oxygen with argon. This treatment was expected to have a similar effect to displacement with natural gas. However, argon is an inert gas and as such will not be oxidised by bacteria, so the enhanced CO_2 levels are unlikely to build up and displacement effects will be slower.

Although the methods of oxygen displacement used were likely to have different effects in the soil, the effects on the reflectance spectra of the plant were all similar,

suggesting that the effects are generic to oxygen displacement from the soil and not a specific effect of leaking natural gas.

7.2 Spectral changes in field crops exposed to leaking natural gas.

The patches of decreased growth in the field of barley were seen to cover an area with diameter of approximately 2 m. This was consistent with observations made by Hoeks (1972a) in which he stated that the radius of the sphere of influence of a gas leak could vary from 1 to 15 m depending on the size of the leak, soil type and moisture content. Also Schollenberger (1930) noted that leaking gas pipes killed all oat seedlings in a 1 to 1.3 m diameter area and stunted the seedlings beyond that until at 4 to 5 m no injury was apparent.

Crops growing above a leaking gas pipe showed an increase in reflectance in the visible in the plants growing closest to the gas leak. Pysek and Pysek (1989) noted a change in the green colour of leaves, a change in the shape of reflectance curves and a decrease in the near-infrared reflectance in plants growing near an artificial gas leak. Changes were also observed in reflectance in the near-infrared but this was not consistent with distance from the gas leak. At points near the leak there was also a shift in the position of the red-edge by 10 nm towards shorter wavelengths. There was an increase in the peak at 524 nm similar to that observed in laboratory measurements of plants subjected to different methods of soil oxygen displacement. Decreases in the magnitude of the first derivative at other selected wavelengths were also observed with the greatest changes occurring at 574 and 644nm.

Reflectance from the leaves that were collected from the crop and measured in the laboratory was similar to the reflectance observed from the crop in that the highest

reflectance was from the area closest to the gas leak. The main difference between the reflectance from the canopy and the leaves was in the position of the red-edge. The canopy red-edge was positioned at between 727 and 737 nm whereas the red-edge of the individual leaves was positioned at around 704 nm, which was comparable to the red-edge position of the laboratory measurements of barley leaves subjected to soil oxygen displacement. The difference between the positions of the red-edge in the field and laboratory data was due to the differences between leaf and canopy reflectance. The laboratory measurements of leaves collected from the field and the leaves subjected to different methods of soil oxygen displacement were measurements of single leaves placed in an integrating sphere. Measurements taken from the field were measurements of canopy reflectance taken with a fibre-optic probe. This signal will include signals from the vegetation canopy composed of many layers of leaves, weeds and soil and will be affected by changes in the natural illumination. However, the red-edge position has been shown to be virtually unaffected by soil or atmosphere (Horler 1983, Clevers 2001) and so the main differences will be due to the fact that the canopy is composed of many layers of leaves as opposed to the single leaf studied in the laboratory. Miller *et al.* (1990) showed that when measuring a stack of leaves the red-edge occurs at longer wavelengths than when measuring a single leaf, due to the increase in the sample biomass and the leaf area index (LAI). Myers and Allen (1968) showed increased reflectance as the number of leaf layers increased because of increased multiple transmission and reflectance from leaves. Similarly, Horler (1983) showed that the effect of leaf stacking was to increase the reflectance in the infrared and thus cause a shift in the red-edge to longer wavelengths.

Differences in the shape of the first derivative were also observed. In the leaf spectra from both the field crop and the laboratory experiments of soil oxygen displacement, it was seen that in barley there was a double peak in the first derivative that identifies the red-edge. The major peak was present at around 704 nm and a second peak was observed at 722 nm. The position of the second peak was seen to move towards the first peak to combine and produce a single peak as the leaf became stressed. The second peak was less pronounced in the leaves collected from the field site but this may be due to the delay in the measurement of the reflectance resulting in deterioration of the chlorophyll and drying of the leaves. However, there was a decrease in the magnitude of the second peak as the gas leak is approached.

The canopy red-edge position was at between 727 and 738 nm but there were also two further features within the red-edge peak. A peak was visible to the left of the main peak at around 704 nm and there was a second shoulder in the peak at around 758 nm. Railyan and Korobov (1993) and Boochs *et al.* (1990) noticed underlying components in the red-edge situated at 700, 715, and 745 nm. Similar effects were seen in the red-edge of a grass canopy by Jago and Curran (1996) and Llewellyn *et al.* (1999). While studying grassland canopies at a site contaminated with oil, Jago and Curran (1996) found double-peaked maxima with positions of approximately 709 nm and 693 nm. The position of the major peak changed depending on the amount of contamination within the plot. Areas of low contamination showed the position of the major peak at the longer wavelength whereas areas of high contamination showed the major peak at shorter wavelengths. Modelling suggested that the position of the peak was dependant on the amount of understory and that at areas of low contamination there was little understory, so the red-edge of the canopy dominated. Llewellyn *et al.* (1999) also

found multiple first derivative features with peaks at 700 and 729 nm. They found that the shorter wavelength feature indicated grassland with high levels of soil contamination whereas the longer wavelength feature indicated those at low levels of contamination; the transition from one red-edge position to another was not a gradual change but instead a switch in dominance of features.

The red-edge position of the barley canopy growing at a distance from the gas leak had the major feature at around 739 nm with a small contribution to the peak at 758 nm. For the crop growing close to the gas leak, the major peak shifted towards shorter wavelengths and decreased in amplitude; the influence of the peaks at 704 – 710 nm increased, whereas that at 758 nm decreased. The red-edge position of leaves measured in the laboratory showed that the major peak was positioned at 704 nm with a minor feature at 722 nm. When the leaves were taken from close to the gas leak the influence of the feature at 722 nm decreased. Similar effects were seen with barley leaves that had been subjected to oxygen displacement from the soil by flooding with water or argon gas. Horler *et al.* (1983) also identified two peaks in derivative spectra, the first at around 700 nm was attributed to the chlorophyll content in the plant leaves and the second one at around 725 nm was attributed to leaf scattering.

In the leaves from the field study, there was no significant difference in the amount of chlorophyll across the pipeline but there were increases in the amount of dry matter and equivalent water content. Thus from plants close to the gas leak we observe the changing influence of leaf scattering. There was no visible difference in the crops along the transect at sites 1 and 2 but the red-edge features suggest that there was less scattering and that the canopy was less dense close to the gas leak. At site 3 the transect passed through the centre of the bare patch. The red-edge was dominated by

those features related to chlorophyll, and the features related to scattering were less obvious. Features related to scattering became more prominent either side of the bare patch.

The reflectances from the field crop and the leaves data differ in the way that the measurements were taken. The reflectance from the leaves was measured using an integrating sphere with directional-hemispherical measurement. This method measured the reflectance purely from the leaf. The canopy reflectance was obtained using a fibre optic probe and measured the reflectance from a canopy of leaves as opposed to a single leaf and may also have included some background reflectance from the surrounding soil.

On the third visit (19/6/01) it was observed that in some areas the crop growing above the gas leak was visibly greener than the rest of the crop. Poor weather conditions meant that the spectral scans obtained were not suitable for first derivative analysis and so it was not possible to determine the position of the red-edge. The greenness of the crop may indicate that the growth of the crop was merely delayed due to the gas leak. This could be compared with the laboratory experiments where the red-edge of control plants was seen to move towards longer wavelengths as the plants matured but that the red-edge of the treated plant did not move.

It is also possible that the crop above the gas leak was receiving some nutrient effect from the breakdown of the gas by bacteria. As the roots slowly grow beyond the area of the gas leak, additional nitrates may be formed by bacteria thus allowing the crop to compensate. This effect was seen by Yang *et al.* (1999) who found that wheat crops growing near a gas leak were greener and had a red-edge at longer wavelengths than the rest of the crop. They suggested that bacterial oxidation of the hydrocarbons was

producing nutrients for the crop. Increased organic matter in the region of a gas leak observed by Hoeks (1972a) may also have increased the nutrients available for the crop. The stage of crop growth may determine which effect is observed, with higher visible reflectance early in the development stages and lower reflectance at the later development stages as the rest of the field ripens and turns yellow but the gassed crop is still developing.

There was little difference in the amount of chlorophyll measured from the leaves collected from the field site but there was a difference in the amount of dry matter and the equivalent water thickness. The dry matter and equivalent water thickness both increased in the crops growing above the gas leak. A possible explanation for this is that oxygen deficiency leads to a slowdown in the growth of the roots and an inability to absorb water and other nutrients. As the chlorophyll concentration did not decline to the same extent in the leaves, photosynthesis and carbohydrate production would have continued but the decreased activity of the roots would have reduced the sink for photosynthetic products thus leading to a decrease in the root to shoot ratio. The products would have remained in the shoot, leading to an increase in dry matter. Decreased water absorption from the roots would also have led to closure of the stomata to conserve water and a consequent increase in the equivalent water thickness.

The chlorophyll content of leaves collected in June showed that the chlorophyll content decreased with proximity to the gas leak. However, the poor weather conditions on this visit meant that few of the collected leaves were suitable for measurement. Hence it was not possible to measure the dry matter or equivalent water thickness of the leaves and comparisons could not be made with leaves collected from the May visit.

Comparisons of the chlorophyll content with the red-edge position and the amplitude of the first derivative at 722 nm showed that there was little correlation between these variables (R^2 = 0.11 and 0.33 respectively). Several authors have studied the correlation between the red-edge position and chlorophyll concentration. Horler *et al.* (1983) found that red edge shifts were related to chlorophyll content and Munden *et al.* (1994) found that canopy studies showed a linear relationship between red edge and chlorophyll concentration. In contrast Demetriades-Shah *et al.* (1990) suggested that the red edge may be a good estimator of chlorophyll levels in individual leaves but not for canopy chlorophyll levels. The lack of correlation between the red-edge and chlorophyll content from the leaves collected from the field may be due to deterioration of the chlorophyll content following collection from the field and the 24-hour delay in measuring reflectance of the leaves and 48 hour delay in performing chlorophyll analysis.

Communications with farmers suggest that the effects on the vegetation growing above the gas leak first become apparent in the late winter months. It is said that the seeds germinate but that as the soil warms and the roots start to grow, shoot growth slows and the decreased growth patterns become visible above the leak. This is consistent with the increased pressure through the pipelines in the winter months causing seepage through the joints. Warming soils also cause increased bacterial growth that may utilise the methane as an energy source. During the summer months gas pressure in the pipelines is decreased, there is less seepage from the joints and the soil can reoxygenate allowing some growth of the crops even though it may be retarded. However, this hypothesis is not consistent with the work of Hoeks (1972) who

suggested that the effects of gas leaks would be greater in the summer months as this was when there would be the greatest bacterial growth.

7.3 Narrow-band ratio analysis

Narrow-band ratio analysis was performed on leaf and canopy data obtained from the field visits on 1/5/01 and 19/6/01.

7.3.1 Summary of narrow-band ratio analysis, Site 3 (01/05/01)

The transect at site 3 (1/05/01) passed through the centre of the bare patch and ratios relative to 800 nm were expected to show the effect of canopy and cellular structure in regions where the leaking gas had led to a decreased canopy and greater area of soil showing. The reflectance ratio for the canopy showed an increased ratio relative to 800 nm around the area of the gas pipe, which may be due to decreased canopy thickness and less developed plants. This effect was also seen in the leaf data although was less pronounced. This may be explained by differences in the cell structure. It was observed that the specific leaf dry matter and the equivalent water thickness was increased in the leaves collected from peg 3 (in the centre of the bare patch), suggesting a greater number of cells and greater thickness of the leaf.

Ratios calculated relative to 680 nm were expected to show the effects of chlorophyll content. Little difference was observed in these ratios in the canopy or leaf data except for the ratio of 800 to 680 nm, which was related to the canopy effects.

7.3.2 Summary of narrow-band ratio analysis, Sites 1 and 2 (19/06/01)

Ratios calculated on the reflectance from site 1 and 2 measured on 19/06/01 showed less distinct changes as the pipeline was crossed. Ratios of canopy reflectance relative to 800 nm were slightly increased above the leaking gas pipe but to a lesser extent than

those from site 3 (1/05/01). This is possibly due to the fact that the crop was more mature and the vegetation under the influence of the leaking gas had been able to recover as the gas pressure had decreased and the roots had developed beyond the sphere of influence of the gas. The bare patches were less visible on this date as the canopy had expanded. The increase in the ratio at site 1 (0m) is possibly due to the effect of the edge of the field. The leaves from this position contained less chlorophyll than the leaves collected from other positions and this may have been due to greater maturity of the crop as it was shaded less by other vegetation. At site 2 there was no edge effect, and the ratio is slightly raised around peg 4, (6m). This is in contrast to changes identified in first derivative analysis that showed the sphere of influence of the gas pipe was around pegs 2 and 3.

The ratios of reflectance relative to 800 nm for the leaf data at site 1 and 2 were very slightly raised around the position of the gas pipe, this may have been due to decreased chlorophyll content; however, the changes were very small.

Small changes were observed in ratios of reflectance relative to 680 nm for both leaf and canopy data. The greatest changes were observed for the ratio of 800 nm relative to 680 nm and again show the canopy effects. Although the canopy had expanded and the vegetation growing above the leaking gas pipe had matured the canopy was still less dense than in the vegetation that was not affected by the leaking gas. Effects in the leaf data were very small.

Ratio analysis may be useful in identifying canopy changes in vegetation affected by leaking gas, particularly in the early growth stages where differences in canopy density due to the retarded development of vegetation under the sphere of influence of leaking gas are observed. Ratios relative to 800 nm best show changes in the canopy density

above the leaking gas pipe. When the gas pressure is reduced the development of the vegetation is able to progress and the canopy becomes denser such that there is little difference between the gassed and non-gassed canopy and the ratio analysis is thus less able to identify the position of the gas leak. Derivative analysis was still able to identify changes in the red-edge position in leaves at this latter growth period and so may be better able to identify damage due to gas leakage when vegetation changes are not obviously visible. However, it was not performed on canopy data because weather conditions had resulted in noisy data, and so it was not possible to determine if changes in the red-edge position would have been able to identify the position of the gas leak in the canopy.

The two techniques may be complementary, with narrow-band ratio analysis perhaps having advantages for implementation of remote sensing of gas leaks from satellites where the scanning of wider bands will result in reduced cost and complexity when compared to the use of hyperspectral measurements required for derivative analysis.

7.4 The Prospect model

The PROSPECT model generally underestimated leaf reflectance. Although Jacquemoud and Baret (1990) showed a strong correlation (R=0.99) between measured and predicted values of reflectance, there was a tendency for the PROSPECT model to underestimate the lowest values of reflectance. In our study we were looking at wavelengths between 450 and 900 nm. At wavelengths between 450 and 680 nm, the relative reflectance is in this low range of 0.05 and 0.2, which is in the low range where the PROSPECT model is known to underestimate reflectance.

Aldakheel and Danson (1997) also found that the PROSPECT model underestimated reflectance in dehydrating leaves by 18% across most of the spectrum studied. They suggested that errors may arise due to the fact that although carotenoids are included within the model other accessory pigments are not. Data input into the model only includes values for the measured total chlorophyll *a* and *b* content. It is possible that structural changes may occur in the chlorophyll molecule during extraction although the solvent used in this research was the same as the solvent used by Jacquemoud and Baret (1990). It is also assumed in the model that the absorbing materials, the pigments and water, are uniformly distributed within the leaf. This is not correct, as chlorophyll pigments are located in the chloroplasts that are mainly positioned in the columnar palisade cells in the upper layers of the leaf.

Other effects may have influenced the comparison of this study with the PROSPECT model: the area of leaf used for chlorophyll and water content analysis was not the exact area that was used for measurement of reflectance with the LI-1800; several different leaves were used for the determination of equivalent water thickness and dry matter analysis; a time delay occurred between the measurement of reflectance and the determination of chlorophyll content. Analysis was normally carried out between 24 – 48 hours following reflectance measurements. Samples were kept dark and refrigerated to prevent deterioration but some chlorophyll breakdown and drying of the leaves may have occurred thus leading to underestimation of the equivalent water content and total chlorophyll content values that were used as input in the model.

The PROSPECT model was able to model reflectance from dicotyledons more accurately than monocotyledons. In order to model the reflectance from bean a value of $N = 1.3$ was used, this value providing the best fit between measured and modelled

data in the near-infrared region. However, Jaquemoud and Baret (1990) had suggested that values of N = 1.5 to 2.5 should be used. N is a value related to the number of cell layers within the leaf separated by air spaces. Due to the delay in determining dry matter and chlorophyll content, deterioration of the leaves may have led to breakdown of the cell structure leading to more air spaces between the cells, thus underestimating the value of N needed for the model. Aldakheel and Danson (1997) suggested that although the model accounted for changes in equivalent water content it did not account for changes in leaf internal structure that accompanied leaf dehydration and that higher values of N were required as dehydration occurred. However, we needed to use lower levels of N for bean than were expected.

The PROSPECT model gives an estimate of the effects of stress on leaves using just three biophysical variables and confirms that the reflectance of the stressed leaf is increased in the visible. However, it tends to underestimate reflectance, particularly in the visible wavebands. Moreover, plant leaves must be destroyed in order to determine the dry matter and chlorophyll contents. Although the model is not a substitute for measured reflectance, in the absence of reflectance measurements (for example during bad weather conditions in the field), biophysical analysis would enable comparative changes to be estimated and the data understood.

A further use of the PROSPECT model would be in extending the data available by using biophysical and biochemical data collected by other researchers who had not measured reflectance.

7.5 Differences in the reflectance measurements obtained with the ASD and the Licor

Both the LI-1800 and ASD Fieldspec Pro spectroradiometers were used in the laboratory measurements of reflectance of leaves from plants that had been treated with soil oxygen displacement by a variety of methods. Differences were observed in the reflectance from leaves measured by each of the instruments.

Both instruments gave increased reflectance in the visible regions of the spectra and shifts in the position of the red-edge towards shorter wavelengths when the plants were stressed. However, in most cases the LI-1800 showed a higher absolute magnitude of reflectance than the ASD, and in all cases the ASD showed the position of the red-edge at between 5 – 10 nm shorter wavelengths than the LI-1800.

There are many possible reasons for the difference in reflectance obtained with the two instruments. The first is that the reflectance from the leaves was measured in a different manner for each instrument. When using the LI-1800 the reflectance from the leaves was measured in an integrating sphere relative to a barium sulphate disc. Relative reflectance obtained from the LI-1800 was adjusted using a standard barium sulphate curve that was provided by EPFS (Personal communication – E. Rollin). The barium sulphate reference curve was not specific to the particular barium sulphate disc and thus any dirt or deterioration of the surface of the reference disc would have led to an increased reflectance being recorded for the target. In contrast, when measuring reflectance using the ASD, a fibre optic probe at 90° to the sample was used to collect radiation and reflectance was relative to a spectralon panel. Reflectance obtained from the ASD was referenced to the spectralon panel that had a unique calibration file to correct the reflectance to 100% (Personal communication EPFS).

When measuring reflectance of leaves with the LI-1800, bean leaves were not detached from the plant whereas with barley and radish, leaves were detached and positioned quickly and easily within the integrating sphere port where illumination was with a 20 W halogen bulb. Scanning took approximately 2 minutes immediately following positioning of the leaf in the integrating sphere and thus dehydration of the leaves was unlikely to have occurred. When measuring reflectance with the ASD, illumination of the leaves was with a 1000 W bulb positioned at a distance of 1 m and at an angle of 45°. All leaves were detached from the plants and placement of the leaves was critical to ensure that the fibre optic probe was viewing only the leaf and not the background cloth. Due to the area viewed by the fibre optic probe it was necessary to select larger leaves that were possibly healthier and more mature than typical leaves used with the LI-1800 and thus reflectance would be lower in the visible than was measured with the LI-1800. Heating of the leaves caused by the 1000 W lamp led to drying of the leaves. Although measurement of reflectance is very fast with the ASD, positioning of the leaves and scanning of the spectralon panel meant that leaves were detached for longer than when measuring with the LI-1800. Measurement of the leaves with the ASD took approximately 5 minutes but under the heat of the lamp the leaves were visibly wilting which would have led to increased reflectance in the near infrared. Aldakheel and Danson (1996) showed that reflectance from spinach leaves dehydrating over a six-hour period increased by 10 % in the near infrared.

In most cases (8/11) the reflectance measurements with the LI-1800 were carried out a few days (2 to 5) after the reflectance had been measured with the ASD and so the plants had been subjected to additional stress. Thus reflectance in the visible could be

expected to be higher. The leaves that were measured in each case were also different as when measuring with the ASD the leaves were detached and destroyed with each measurement.

Another reason for the difference in reflectance between the two instruments is the difference in specifications of the instruments. The LI-1800 was about 20 years old whereas the ASD was less than 5 years old. It was discovered that the LI-1800 was affected by a dark current signal that was dependant on whether the instrument was operated under battery (2 mV) or mains power (6 mV). The effect of the dark current meant that reflectance was increased in the visible. As the dark current was uniform across all wavelengths, the effect of the dark current was greatest where reflectance was low, particularly in the visible. Adjustments for the dark current were made. The ASD has an optimisation procedure that is run at the beginning of scanning and adjusts for dark current automatically. It was not possible to detect if there was any residual dark current that should have been corrected for.

A study of the first derivative spectra showed that the difference in the red-edge position that was observed between the ASD and the LI-1800, whereby the ASD showed the red-edge at shorter wavelengths than the LI-1800 was a systematic offset. All red-edge peaks obtained from the ASD reflectance spectra were at between 4 and 6 nm shorter wavelengths than those obtained from the LI-1800. This offset may have been due to the different methods of measuring reflectance, or possibly to the age of the LI-1800 in that the calibration of the wavelengths may have drifted.

The differences identified in the reflectance measured with the two instruments suggest that although both instruments are capable of detecting stress caused by decreased oxygen content in the soil, consistency of instrument and method should be used to

determine reflectance. Problems arise particularly in using the ASD Fieldspec Pro in measuring reflectance from single leaves due to the size of the area to be viewed and the dehydrating effect from the lamp used to illuminate the subject. Use of the LI-1800 as a field measurement instrument is also a problem due to the time taken to scan a canopy (approximately 1 minute) and the effect of changing light conditions during the scan. This is particularly a problem with UK weather conditions. The ASD Fieldspec scans at a faster rate (milliseconds) and thus is less likely to be affected by changing light conditions. The Fieldspec Pro is thus a better instrument for taking canopy measurements in the field whereas the LI-1800 fitted with an integrating sphere is better suited to measurements of detached leaves in the laboratory.

7.6 Ability of remote sensing to detect stress

This research has shown that changes in reflectance and red-edge position occur in vegetation growing above gas leaks and in vegetation subjected to various methods of soil oxygen depletion. Safety requirements in the use of natural gas meant that it was not possible to evaluate fully the effects of a gas leak on vegetation but the work carried out suggests that the changes are generic effects of soil oxygen depletion and are not specific to changes caused by leaking natural gas.

This generic effect means that remote sensing will not be sufficient in isolation to identify gas leaks, as it will not be able to distinguish between leaking gas, bad drainage (causing waterlogging) or even compaction of the soil or other stresses that may lead to chlorosis of the leaves. Other researchers have also shown that remote sensing is able to identify plant stress but not to distinguish what is actually causing the stress (Carter 1993, Masoni *et al.* 1996) However, if remote sensing were to be used to identify leaking gas pipes it could be applied in conjunction with pipeline maps.

Changes in reflectance detected along the line of the pipeline could signal areas that need further investigation. This could lead to identifying gas leaks, areas of bad drainage which could pose corrosion problems for the pipeline or even areas where a farmer regularly turns his tractor causing compaction of the soil and thus putting additional stress on the pipeline.

If satellites are to be used to monitor pipelines and detect gas leaks it will be necessary for them to have a short return period. Pipelines are monitored on a fortnightly basis at present. It is difficult for satellites to get clear images at this frequency. The IKONOS satellite has a potential repeat period of 3 days that could be sufficient for monitoring pipelines in principle, but it may not be possible to provide images through the cloud cover over the UK, particularly during the winter months.

High spatial resolutions would be required with sensors able to locate features smaller than 1 m. This would enable areas containing narrow pipelines to be viewed and allow comparison of vegetation growing above the pipeline to be compared with vegetation growing either side of or further along a pipeline and thus be able to identify areas of increased reflectance.

7.7 Future research directions

This research has provided a basis for the study of vegetation stress caused by leaking natural gas. It has shown that changes in reflectance are observed when bean, under laboratory conditions and barley, in field conditions are exposed to gas leaks. However, the limitations of the experimental procedures in this research, due to safety requirements have meant that it has not been possible to fully investigate the effects that natural gas has on vegetation. Insufficient plants were treated to enable a study of

the effect of natural gas on plant physiology, for example changes in the leaf area or in growth of roots. A larger scale field investigation under natural conditions would enable studies to be carried out on gas exposed plants from germination through to harvest.

Due to the late discovery of the field site at Louth during this research, it was not possible to fully study the vegetation effects caused by the accidental gas leak. Further study would enable investigation at the site, and the use of remote sensing to identify further the effects of the gas leak will help to determine whether changes in the reflectance spectra are specific to natural gas exposure or generic effects of oxygen deficiency in the soil. The use of the ASD Fieldspec Pro in the field would enable reflectance measurements to be measured over a greater wavelength range and thus possibly identify changes associated with leaf moisture or structure.

A European consortium has been formed to investigate the ability of remote sensing to detect third party incursion, landslips and methane leakage affecting natural gas pipelines. The project, with the acronym PRESENSE (Pipeline Remote Sensing for Safety and Environment) includes studies to be made of vegetation affected by gas leaks as well as addressing issues of pipeline security. The project aims include the development of a satellite remote sensing system that will be able to detect gas leaks by viewing vegetation. The development of this system would mean that pipelines would no longer need to be monitored by helicopter, with resulting improvements in safety, noise pollution and cost effectiveness. Rapid detection of gas leaks through vegetation monitoring would also help to decrease the amount of methane released to the atmosphere, thus reducing both economic losses and greenhouse gas emissions.

8 Appendix A

8.1 Consolidated list of laboratory experiments

Table 8.1 Consolidated list of laboratory experiments performed in this study

Treatment	Crop	Date	No of days	Reflectance difference %						Red-edge shift (nm)
Wavelength (nm)				550	600	650	680	700	800	
Methane	Bean(1)	21/06/00	7	5.2	5.3	3.5	0.4	6.1	0.4	706-706
Methane	Bean(1)	30/06/00	16	18.8	25.8	23.1	9.0	21.9	-6.8	706-704
Methane	Bean(1)	06/07/00	22	12.1	23.1	20.4	9.3	21.1	-1.7	704-702
Methane	Bean(1)	17/07/00	33	7.5	6.1	4.5	3.0	9.8	0.0	708-706
Methane	Bean(2)	10/08/00	11	3.2	7.0	7.4	8.4	4.1	4.7	710-712
Methane	Bean(2)	25/08/00	25	13.1	17.1	10.3	5.4	16.9	0.9	708-704
Methane	Bean(2)	01/09/00	32	5.3	7.3	7.6	4.2	7.6	-0.7	706-706
Methane	Bean(3)	28/09/00	15	1.5	2.4	0.0	-4.1	-0.7	-0.7	704-702
Argon	Bean(1)	01/09/00	2	5.6	6.7	3.4	0.0	6.3	1.2	708-708
Argon	Bean(1)	08/09/00	9	-3.3	1.7	1.1	0.6	-0.6	-2.7	714-710
Argon	Bean(1)	14/09/00	15	21.6	26.3	17.5	9.7	25.5	4.2	718-708
Argon	Bean(1)	18/09/00	19	21.1	29.3	14.9	6.0	25.8	-5.4	720-708
Argon	Bean(1)	25/09/00	26	14.5	13.1	4.9	-0.1	18.4	-4.3	722-710
Argon	Bean(2)	25/05/01	10	1.6	8.6	5.9	0.9	3.7	-28.6	710-710

Argon	Bean(2)	01/06/01	17	19.2	21.5	11.3	3.9	9.3	-5.4	720-710
Argon	Bean(2)	08/06/01	25	24.8	25.8	12.5	4.3	23.5	-3.6	722-708
Argon	Bean(3)	27/07/01	4	-15.2	-13.2	-7.3	-4.1	-13.8	-1.3	708-714
Argon	Bean(3)	03/08/01	11	-2.5	-1.8	-0.2	11.7	-2.2	2.7	716-716
Argon	Bean(3)	10/08/01	18	13.8	11.8	5.8	3.0	12.1	0.5	720-716
Argon	Bean(3)	17/08/01	25	13.6	8.3	1.3	-0.8	11.6	-0.2	720-714
Argon	Bean(4)	12/10/01	3	-5.2	-11.9	-11.4	-8.3	-6.1	-2.2	708-708
Argon	Bean(4)	19/10/01	10	-3.6	-5.6	-7.4	-7.9	-1.9	-3.2	716-708
Argon	Bean(4)	25/10/01	17	5.3	1.9	-4.3	-7.8	7.6	-2.6	718-710
Argon	Bean(4)	02/11/01	24	15.0	12.4	0.9	-4.5	-4.3	0.9	722-708
Argon	Bean(4)	09/11/01	31	19.7	19.8	6.8	-0.5	22.3	-0.7	720-707
Argon	Barley(1)	06/10/00	3	6.7	6.0	-14.2	2.6	5.0	6.4	704-704
Argon	Barley(1)	13/10/00	10	8.3	13.5	15.7	13.1	11.6	-0.7	704-704
Argon	Barley(1)	20/10/00	17	57.3	82.0	85.8	57.9	80.0	-0.7	706-700
Argon	Barley(1)	02/11/00	30	24.7	15.1	37.1	16.4	34.5	-4.0	704-702
Argon	Barley(2)	11/12/00	6	10.5	14.3	19.1	21.6	15.8	0.7	728-726
Argon	Barley(2)	18/12/00	13	7.7	7.1	3.1	-2.6	7.6	-1.7	724-704
Argon	Barley(2)	22/12/00	17	9.6	12.7	11.0	2.7	11.4	-4.4	704-704
Argon	Barley(3)	29/01/01	14	7.0	10.1	11.3	8.7	12.7	0.0	704-704
Argon	Barley(3)	05/02/01	21	-1.1	0.8	1.0	1.0	0.8	-4.3	704-704
Argon	Barley(3)	16/02/01	32	4.2	6.8	8.6	7.8	5.7	-0.9	704-704
Argon	Barley(4)	02/03/01	10	-2.2	-3.2	-2.4	-1.9	-3.8	-0.2	704-706
Argon	Barley(4)	09/03/01	17	6.0	7.1	4.1	0.7	6.8	-0.2	706-706
Argon	Barley(4)	16/03/01	24	14.1	16.4	12.1	4.4	13.7	0.9	706-704
Argon	Barley(4)	30/03/01	38	27.5	31.9	25.5	10.3	32.4	-2.3	706-702
Waterlog	Barley(1)	06/10/00	3	-9.4	-10.3	-8.6	-9.0	-9.7	-11.8	704-704
Waterlog	Barley(1)	13/10/00	10	-18.7	-21.4	-24.8	-23.7	-21.1	-16.5	704-704

Waterlog	Barley(1)	20/10/00	17	16.1	16.7	20.4	7.0	18.1	-1.1	706-704
Waterlog	Barley(1)	02/11/00	30	10.4	11.6	6.1	-6.1	13.8	-6.2	704-702
Waterlog	Barley(2)	11/12/00	6	-3.6	-4.6	-2.5	1.5	-5.1	0.4	704-704
Waterlog	Barley(2)	18/12/00	13	2.8	1.7	2.2	0.1	2.3	-1.5	704-704
Waterlog	Barley(2)	22/12/00	17	13.5	14.5	11.5	2.0	15.1	-0.6	704-702
Waterlog	Barley(3)	02/03/01	8	5.9	6.1	7.2	4.9	6.4	0.9	704-704
Waterlog	Barley(3)	09/03/01	15	5.6	4.8	2.0	-0.9	5.3	-0.7	706-704
Waterlog	Barley(3)	16/03/01	22	6.3	6.7	7.4	3.9	7.9	-2.0	704-704
Waterlog	Barley(3)	23/03/01	29	20.3	22.2	18.5	8.3	20.2	0.7	704-704
Waterlog	Barley(3)	30/03/01	36	23.4	32.1	31.3	19.5	30.2	-2.6	704-702
Waterlog	Barley(4)	01/06/01	11	21.0	30.4	32.6	21.5	27.9	-2.8	704-702
Waterlog	Barley(4)	08/06/01	18	-1.1	0.9	2.4	2.1	0.8	-4.6	704-704
Waterlog	Barley(4)	15/06/01	25	16.1	18.8	16.4	8.2	18.3	-1.1	704-702
Waterlog	Barley(4)	22/06/01	32	9.4	13.1	14.3	10.2	11.4	-0.9	704-704
Waterlog	Bean(1)	09/05/00	28	112.9	107.2	52.9	11.8	-78.1	-6.8	724-702
Waterlog	Bean(2)	22/05/00	12	66.9	85.4	54.5	21.3	76.5	0.9	716-702
Waterlog	Bean(3)	20/06/00	8	55.3	71.6	48.9	15.4	67.9	-0.9	710-702
Waterlog	Bean(4)	17/07/00	10	26.2	20.3	5.3	-1.9	19.9	-0.9	720-710
Waterlog	Bean(4)	01/08/00	24	68.9	51.0	14.8	-1.5	60.2	2.2	722-708
Waterlog	Bean(4)	10/08/00	33	73.0	57.2	17.6	1.5	61.8	-1.7	722-704
Waterlog	Bean(5)	11/05/01	9	-2.1	-2.0	-1.5	2.3	-1.9	-1.1	706-708
Waterlog	Bean(5)	18/05/01	16	10.6	10.9	8.7	5.4	6.0	3.1	714-714
Waterlog	Bean(5)	25/05/01	23	17.9	18.8	5.8	1.4	16.4	-2.2	720-708
Waterlog	Bean(5)	01/06/01	30	28.4	24.6	9.4	1.2	24.3	-5.4	720-708
Waterlog	Bean(5)	08/06/01	37	38.3	37.3	22.0	8.1	37.5	-0.2	722-708
Waterlog	Bean(5)	15/06/01	44	53.8	55.1	31.2	12.1	56.0	-2.8	722-706
Waterlog	Bean(5)	22/06/01	51	64.1	74.4	40.7	15.7	65.8	-0.7	722-704
Waterlog	Bean(6)	13/07/01	5	6.9	6.2	3.4	-0.5	3.2	-2.0	710-708

Waterlog	Bean(6)	27/07/01	19	56.1	60.9	35.5	15.1	63.5	2.4	720-704
Waterlog	Bean(6)	03/08/01	26	44.8	94.7	19.6	6.4	43.6	2.5	718-706
Waterlog	Bean(6)	10/08/01	33	36.2	31.8	14.2	3.5	36.7	-1.7	722-704
Waterlog	Radish(1)	15/05/00 pre wlog		16.7	16.7	11.2	4.2	17.4	6.0	710-706
Waterlog	Radish(1)	22/05/00	10	5.8	8.3	9.5	7.8	7.2	0.0	708-706
Waterlog	Radish(2)	21/06/00	8	14.5	26.1	26.9	19.9	25.6	-1.7	708-704
Waterlog	Radish(2)	30/06/00	17	34.9	51.6	53.3	39.4	54.2	1.9	710-704
Waterlog	Radish(2)	06/07/00	23	47.8	57.4	49.4	30.0	64.0	3.3	720-704
Waterlog	Radish(3)	18/07/00		26.3	48.6	48.9	27.8	48.3	-3.4	712-706
Waterlog	Radish(3)	02/08/00		14.1	13.0	13.1	8.5	16.3	2.3	720-712
Waterlog	Radish(3)	10/08/00		22.2	16.6	5.7	-0.2	20.6	-0.2	722-712
Nitrogen	Bean	17/07/00	14	-4.6	-3.8	-4.4	-6.1	-3.3	-0.9	720-720
Nitrogen	Bean	01/08/00	29	21.0	13.0	9.7	5.1	15.0	1.1	722-724
Nitrogen	Bean	10/08/00	38	-1.5	1.4	1.4	2.8	-2.9	4.7	724-724

9 Appendix B

9.1 Program to transfer and display an LI-1800 text file into Microsoft excel in a form suitable for data processing.

This transect contains a full listing of the macro written in Visual Basic for Applications which was used to extract data from a single linear text file and rearranging it into a single array suitable for processing within Microsoft Excel.

```
Sub Licor()
'
' Licor Macro
' Macro recorded 15/09/00 by John and Karon Smith
'
Dim SRow As Integer
Dim TRow As Integer
Dim TCol As Integer
Dim Data
Dim Name

SRow = 1
TRow = 1
TCol = -1
Data = ""
Name = ""

Sheets.Add after:=Worksheets(1)
Worksheets(1).Activate
Data = Worksheets(1).Cells(SRow, 1)
While Data <> Empty
```

```
    Worksheets(1).Activate
    Select Case Data
      Case "FILE:"
        If Name <> Worksheets(1).Cells(SRow, 2) Then
          TCol = TCol + 2
          TRow = 1
          Name = Worksheets(1).Cells(SRow, 2)
          Cells(SRow, 2).Select
          Selection.Copy
          Worksheets(2).Activate
          Cells(TRow, TCol + 1).Select
          ActiveSheet.Paste
          Application.CutCopyMode = False
          TRow = 2
          SRow = SRow + 2
        Else
          SRow = SRow + 2
        End If
      Case "450"
        Range(Cells(SRow, 1), Cells(SRow + 225, 2)).Select
        Selection.Copy
        Worksheets(2).Activate
        Cells(TRow, TCol).Select
        ActiveSheet.Paste
        Application.CutCopyMode = False
        SRow = SRow + 226
      Case Else
        SRow = SRow + 1
    End Select
    Data = Worksheets(1).Cells(SRow, 1)
Wend
End Sub
```

10 Appendix C

10.1 Program to open multiple linear files created with the ASD Fieldspec Pro and transfer them into Microsoft excel in a form suitable for data processing.

This transect contains a full listing of the macro written in Visual Basic for Applications which was used to open multiple linear text files and rearranging them into single arrays on separate worksheets suitable for processing within Microsoft Excel.

```
Option Explicit

Sub ASD()
'
' ASD Macro
' Macro recorded 16/07/00 by John and Karon Smith

Dim NumOfFirstFile1 As Integer
Dim NumOfLastFile1 As Integer
Dim FileIdent1 As String * 1
Dim NumOfFirstFile2 As Integer
Dim NumOfLastFile2 As Integer
Dim FileIdent2 As String * 1
Dim DirDate As String * 8
Dim n As Integer

NumOfFirstFile1 = InputBox("Please enter number of first control file: ")
NumOfLastFile1 = InputBox("Please enter number of last control file: ")
```

```
FileIdent1 = InputBox("Please enter the file identification letter for control: ")
NumOfFirstFile2 = InputBox("Please enter number of first treatment file: ")
NumOfLastFile2 = InputBox("Please enter number of last treatment file: ")
FileIdent2 = InputBox("Please enter the file identification letter for treatment: ")
DirDate = InputBox("Please enter the date of the directory as dd-mm-yy: ")

'open a new workbook for the results
Workbooks.Add
'rename workbook¬
ActiveWorkbook.SaveAs FileName:= _
    "C:\WINDOWS\Profiles\Karon\My Documents\FieldSpec\portspec\" & DirDate & "\results.xls" _
    , FileFormat:=xlNormal, Password:="", WriteResPassword:="", _
    ReadOnlyRecommended:=False, CreateBackup:=False

For n = NumOfFirstFile1 To NumOfLastFile1

  Workbooks.OpenText FileName:= _
    "C:\WINDOWS\Profiles\Karon\My Documents\FieldSpec\portspec\" & DirDate & "\" & FileIdent1 & Format(n, "000") & ".REF", _
    Origin:=xlWindows, StartRow:=1, DataType:=xlDelimited, TextQualifier:= _
    xlDoubleQuote, ConsecutiveDelimiter:=False, Tab:=True, Semicolon:=False, _
    Comma:=False, Space:=False, Other:=False, FieldInfo:=Array(1, 1)
Next

'first 2 columns of data

Windows(FileIdent1 & Format(NumOfFirstFile1, "000") & ".REF").Activate
```

```
Range("a27:b2177").Select
'Selection.End(xlDown).Select
Selection.Copy
Windows("results.xls").Activate
Worksheets("sheet1").Activate
Range("a2").Select
ActiveSheet.Paste
Range("B1").Select
Application.CutCopyMode = False
ActiveCell.FormulaR1C1 = FileIdent1 & Format(NumOfFirstFile1, "000")

For n = NumOfFirstFile1 + 1 To NumOfLastFile1
   Windows(FileIdent1 & Format(n, "000") & ".REF").Activate
   Range("b27:b2177").Select
   'Selection.End(xlDown).Select
   Selection.Copy
   Windows("results.xls").Activate
   Worksheets("sheet1").Activate
   Cells(2, n + 1).Select
   ActiveSheet.Paste
   Cells(1, n + 1).Select
   Application.CutCopyMode = False
   ActiveCell.FormulaR1C1 = FileIdent1 & Format(n, "000")
Next

For n = NumOfFirstFile2 To NumOfLastFile2

   Workbooks.OpenText FileName:= _
      "C:\WINDOWS\Profiles\Karon\My Documents\FieldSpec\portspec\" & DirDate & "\" & FileIdent2 & Format(n, "000") & ".REF", _
      Origin:=xlWindows, StartRow:=1, DataType:=xlDelimited, TextQualifier:= _
      xlDoubleQuote, ConsecutiveDelimiter:=False, Tab:=True, Semicolon:=False, _
```

```
        Comma:=False, Space:=False, Other:=False,
FieldInfo:=Array(1, 1)
Next

'first 2 columns of data

Windows(FileIdent2 & Format(NumOfFirstFile2, "000") &
".REF").Activate
Range("a27:b2177").Select
'Selection.End(xlDown).Select
Selection.Copy
Windows("results.xls").Activate
Worksheets("sheet2").Activate
Range("a2").Select
ActiveSheet.Paste
Range("B1").Select
Application.CutCopyMode = False
ActiveCell.FormulaR1C1 = FileIdent2 &
Format(NumOfFirstFile2, "000")

For n = NumOfFirstFile2 + 1 To NumOfLastFile2
   Windows(FileIdent2 & Format(n, "000") & ".REF").Activate
   Range("b27:b2177").Select
   'Selection.End(xlDown).Select
   Selection.Copy
   Windows("results.xls").Activate
   Worksheets("sheet2").Activate
   Cells(2, n + 1).Select
   ActiveSheet.Paste
   Cells(1, n + 1).Select
   Application.CutCopyMode = False
   ActiveCell.FormulaR1C1 = FileIdent2 & Format(n, "000")
Next

End Sub
```

11 References.

Adams R.S. & Ellis R. (1960). Some physical and chemical changes in the soil brought about by saturation with natural gas. *Soil Science Society of America-Proceedings* **24**, 41-44.

Adamse A.D., Hoeks J, DeBont J.A.M, & van Kessel J.F (1972). Microbial activity in soil near Natural Gas Leaks. *Archive fűr Mikrobiologie* **83**, 32-51.

Alberto M.C.R, Neue H.U, Lantin R.S & Aduna J.B. (1996). Determination of soil-entrapped methane. *Communications in Soil Plant Analysis*. **27, (5-8)**, 1561-1570

Anderson J.E. & Perry J.E. (1991). Characterisation of wetland plant stress using leaf spectral reflectance: Implications for wetland remote sensing. *Wetlands*, **16,** (4), 477-487.

Andersen K (2000). An introduction to the facilities of the NERC Equipment Pool for Field Spectroscopy (NERC EPFS). In: Tadina F. Ed. *Proceedings of the annual conference of the NERC Airbourne Remote Sensing facility*. Keyworth, Nottingham. 12-13 December 2000.

Arif M.A.S & Verstraete W. (1995). Methane dosage to soil and its effect on plant growth. *World Journal of Microbiology and Biotechnology*. **11,** (5), 529-535.

Arthur J. J, Leone I. A. & Flower F.B. (1985). The response of tomato plants to simulated landfill gas mixtures. *Journal of Environmental Science and Health*, **A20,** (8), 913-925.

ASD (1999). *Technical Guide* 3rd edition. Analytical Spectral Devices, Inc. Colorado, USA

BG plc (1997) *New Land from Old*, Property Division, Hampshire.

Bammel B.H & Birnie R.W. (1994). Spectral reflectance response of Big sagebrush to hydrocarbon-induced stress in the Bighorn

basin, Wyoming. *Photogrammetric Engineering & Remote Sensing*. **60**, (1), 87-96

Barrett E.C & Curtis L.F. (1976.) *Introduction to Environmental Remote Sensing*. 2nd edition. Fletcher & Son Ltd. Norwich.

Bender M & Conrad R. (1995). Effect of CH_4 concentrations and soil conditions on the induction of CH_4 oxidation activity. *Soil Biology & Biochemistry*, **27, 2**, 1517-1527.

Berrenger M (2000) *Digital Processing of Signals, Theory and Practice*. 3rd edition. John Wiley & Sons New York.

Black C.A. (1957). *Soil - Plant relationships*. John Wiley and Sons, New York.

Blackburn G.A. (1998). Spectral indices for estimating photosynthetic pigment concentrations: a test using senescent tree leaves. *International Journal of Remote Sensing*, **19,** (4), 657-675.

Bogner J, Meadows M & Czepiel P. (1997). Fluxes of methane between landfills and the atmosphere: natural and engineered controls. *Soil Use and Management*, **13, (4)**, 268-277.

Boochs F, Kupfer G, Dockter K & Kuhbauch W (1990). Shape of the red-edge as a vitality indicator for plants. *International Journal of Remote Sensing*, **11 (10**) 1741-1753.

Bruinsma J (1963). The quantitative analysis of chlorophylls *a* and *b* in plant extracts. *Photochemistry and Photobiology*, **2**, 241-249

Cambell J.B (1996). *Introduction to Remote Sensing*. 2nd edition. Taylor & Francis Ltd. London.

Carter G.A. (1991). Primary and secondary effects of water content on the spectral reflectance of leaves. *American Journal of Botany*, **78, (7)**, 916-924.

Carter G.A (1993). Responses of leaf spectral reflectance to plant stress. *American Journal of Botany*, **80,(3)**, 239-243.

Carter G.A. (1994). Ratio of leaf reflectances in narrow wavebands as indicators of plant stress. *International Journal of Remote Sensing*, **15, (3)**, 697-703.

Carter G. (1998). Reflectance wavebands and indices for remote estimation of photosynthesis and stomatal conductance in pine canopies. *Remote Sensing of Environment,* **63**, 61-72.

Carter G.A. & Miller R.L. (1994). Early detection of plant stress by digital imaging within narrow stress-sensitive wavebands. *Remote Sensing of Environment*, **50**, 295-302.

Carter G.A. Cibula W.G. & Miller R.L. (1996). Narrow band reflectance imagery compared with thermal imagery for early detection of plant stress. *Journal of Plant Physiology*, **148**, 515-522.

Chappelle E.W, Kim M.S, & McMurtrey J.E. (1992). Ratio analysis of reflectance spectra (RARS): An algorithm for the remote estimation of the concentrations of chlorophyll *a*, chlorophyll *b* and carotenoids in soybean leaves. *Remote Sensing of Environment*, **39**, 239-247.

Clevers, J.G.P.W, DeJong G.F, Epema E.A & Addink E.A. (2001) MERIS and the red-edge index. *International Journal of Applied Earth Observation and Geoinformation*, (in press)

Clymo R.S & Pearce D.M.E. (1995). Methane and carbon dioxide production in, transport through, and efflux from a peatland. *Philosophical Transactions of the Royal Society London A*. **350**, 249-259.

Crowhurst D. & Manchester S.J. (1993). The measurement of methane and other gases from the ground. Construction Industry Research and Information Association. Report 131.

Coty V.F. (1967). Atmospheric Nitrogen fixation by hydrocarbon-oxidising bacteria. *Biotechnology and*

Bioengineering **IX**:25. In Hoeks J.(1972) Effect of leaking natural gas on soil and vegetation in urban areas. *Agricultural Research Reports* **778**, Wageningen

Curran P.J. & Milton E.J. (1983). The relationship between the chlorophyll concentration, LAI and reflectance of a simple vegetation canopy. *International Journal of Remote Sensing*, **4, (2)**, 247-255.

Curran P.J, Dungan J.L, Macler B.A & Plummer S.E. (1991). The effect of red leaf pigment on the relationship between red-edge and chlorophyll concentration. *Remote Sensing of Environment.* **35**, 69-76.

Czepiel P.M, Crill P.M & Harris R.C. (1995). Environmental factors influencing the variability of methane oxidation in temperate zone soils. *Journal of Geophysical research* **100**, 9359-9364.

Datt B. (1998). Remote sensing of chlorophyll *a*, chlorophyll *b*, chlorophyll *a+b* and total carotenoid content in eucalyptus leaves. *Remote Sensing of Environment,* **66**, 111-121.

Davis J.B, Coty V.F, & Stanley J.P. (1964). Atmospheric Nitrogen fixation by methane-oxidising bacteria. *Journal Bacteriology*, **88**, 468-472. In Hoeks J.(1972) Effect of leaking natural gas on soil and vegetation in urban areas. *Agricultural Research Reports* **778**, Wageningen.

Demetriades-Shah T.H, Steven M.D & Clark J.A (1990). High resolution derivative spectra in remote sensing. *Remote Sensing of Environment*, **33**, 55-64

De Oliviera W.J & Crosta A.P (1976). Detection of hydrocarbon seepage in the Sao Francisco basin, Brazil, through Landsat TM, soil geochemistry and airborne / field spectrometry data integration. *Eleventh Thematic Conference and Workshop on applied Geologic Remote Sensing.* Las Vagas, February 1996.

De Oliveira W.J, Crosta A.P & Goncalves J.L.M. (1997). Spectral characteristics of soils and vegetation affected by hydrocarbon gas: A greenhouse simulation of the Remansa Do Fogo seepage. *Twelfth International Conference and Workshops on applied Geologic Remote Sensing*. Denver, Colorado, 17-19 November 1997.

De Wit (1978). Morphology and function of root and shoot growth of crop plants under oxygen deficiency. In: *Plant Life in Anaerobic Environments*. Ed. D.D. Hook & R.M.H Crawford. Ann Arbor Science.

Denmead O.T. (1979). Chamber systems for measuring nitrous oxide emission from soils in the field. *SSSA*, **43** (1), p89 In Erno B & Schmitz R (1996) Measurements of soil-gas migration around oil and gas wells in the Lloydminster area. *Journal of Canadian Petroleum Technology*, **35, (7)**, 37-46.

Downing H.G, Carter G.A, Holladay K.W and Cibula W.G (1993) The radiative equivalent water thickness of leaves. *Remote Sensing of Environment*, **46**, (1), 103-107

Drew M.C (1983). Plant injury and adaptation to oxygen deficiency in the root environment: A review. *Plant and Soil,* **75**, 179-199.

Drew M.C & Lynch J.M (1980). Soil anaerobiosis, microorganisms, and root function. *Annual Review of Phytopathology*, **18**, 37-66

Drew M.C & Sisworo E.J (1979). The development of waterlogging damage in young barley plants in relation to plant nutrient status and changes in soil properties. *New Phytologist*, **82**, 301-314

Erno B. & Schmitz R. (1996). Measurements of soil-gas migration around oil and gas wells in the Lloydminster area. *Journal of Canadian Petroleum Technology*, **35, (7)**, 37-46.

Filella I. & Penuelas J. (1994). The red-edge position and shape as indicators of plant chlorophyll content, biomass and hydric status. *International Journal of Remote Sensing*, **15, (7)**, 1459-1470.

Gates D.M, Keegan H.J, Schelter J.C & Weidner V.R (1965). Spectral properties of plants. *Applied Optics* **4**, (1), 11-20.

Gausman H.W (1985). Plant leaf optical parameters in visible and near-infrared light. *Graduate Studies No. 29*. Lubbock, Texas. Texas Tech Press.

Gemmel F. (1988). Effects of SO_2 on the spectral properties of leaves. PhD thesis, University of Nottingham.

Gitelson A.A, Merzlyak M.N. (1997). Remote estimation of chlorophyll content in higher plant leaves. *International Journal of Remote Sensing*, **18, (12)**, 2691-2697.

Glinski J & Stepniewski W (1985). *Soil Aeration and its Role for Plants*. CRC Press.

Godwin R, Abouguendia Z. and Thorpe J. (1990). Response of soils and plants to natural gas migration from two wells in the Lloydminster area. Saskatchewan Research Council Publication no. E-2510-3-E-90.

Godwin T.W & Mercer E.I (1983) Introduction to Plant Biochemistry. Pergamon Press, Oxford.

Greenwood D.J (1968). Effect of oxygen distribution in the soil on plant growth, In: *Root Growth, Proceedings of the Easter School in Agricultural Science*, University of Nottingham 1968, Ed. W.J. Whittington, Butterworths

Gustafson F. G. (1944). Is natural gas injurious to flowering plants? *Plant Physiology,* **19**, 551-558.

Harper H.J. (1939). The effect of natural gas on the growth of micro-organisms and the accumulation of nitrogen and organic matter in the soil. *Soil Science*: **48**, 461-468.

Harries C. R, Witherington P.J. & McEntee (1995). Interpreting Measurements of Gas in the Ground. Construction Industry Research and Information Association Report 151.

Hillel D. (1998). *Environmental Soil Physics.* Academic press.

Hoeks J. (1972)a. Changes in composition of soil air near leaks in natural gas mains. *Soil Science* **113**, 46-54.

Hoeks J. (1972)b. Effect of leaking natural gas on soil and vegetation in urban areas. *Agricultural Research Reports* **778**, Wageningen.

Hoque E. & Hutzler J.S. (1992). Spectral blue-shift of red-edge monitors damage class of Beech trees. *Remote Sensing of Environment*, **39**, 81-84.

Horler D.N.H, Dockray M. & Barber J. (1983). The red-edge of plant leaf reflectance. *International Journal of Remote Sensing*, **4,(2)**, 273-288.

IPCC (1992). Climate change: The IPCC 1990 and 1992 Assessments. World Meteorological organisation / Intergovernmental panel on climate change.

Jacquemoud S & Baret F (1990) PROSPECT: A model of leaf optical properties spectra. *Remote Sensing of Environment*, **34**, 75-91.

Jago R.A (1998) Remote sensing for chemical monitoring. PhD thesis, University of Southampton.

Jago R.A, Cutler M.E.J & Curran P.J (1999). Estimating canopy chlorophyll concentration from field and airborne spectra. *Remote Sensing of Environment*, **68**, 217-224

Lamb B, Westberg H, Kashinkunti R, Czepiel P, Crill P, Harriss R, Kolb C & McManus M (1996). Oxidation of methane in soils from underground natural gas pipeline leaks. Final Report GRI-94-0257.35 Gas Research Institute. Chicago, USA

Larcher W (1987). Streß bei pflanzen. Naturwissenschaften 74, 158-167, Quoted in Lichtethaler H K (1996). Vegetation stress: an introduction to the stress concept. *Journal of Plant Physiology* **148**, 4-14.

Liang G-C, Lui H-H, Kung AH, Mohacsi A, Miklos A & Hess P (2000). Photoacoustic trace detection of methane using compact solid-state lasers. *Journal Physical Chemistry A*, **104**, (45), 10179-10183.

LI-COR (1983) *LI-1800 Portable Spectroradiometer – Instruction Manual*.

Llewellyn G.M, Kooistra L & Curran P.J. (1999). The effect of soil contamination on grassland spectra. In Proceedings of the 25th annual conference of the Remote sensing society, University of nottingham.

Mariotti M, Ercoli L & Masoni A (1996). Spectral properties of iron-deficient corn and sunflower leaves. *Remote Sensing of Environment* **58**, 282-288

Marschner H (1995) *Mineral Nutrition of Higher Plants*. Second edition. Academic Press. London.

Masoni A, Ercoli L & Mariotti M. (1996). Spectral properties of leaves deficient in Iron, Sulphur, Magnesium and Manganese. *Agronomy Journal*, **88**, 937-943.

Miller J.R, Wu J, Boyer M.G, Belanger M & Hare E.W. (1991). Seasonal patterns in leaf reflectance red-edge characteristics. *International Journal of Remote Sensing*, **12**, (7) 1509-1523.

Milton N.M, Ager C.M, Eisworth B.A & Power M.S. (1989) Arsenic- and selenium –induced changes in spectral reflectance and morphology of soybean plants. *Remote Sensing of Environment*, **30**, 263-269

Milton N. M, Eisworth B. A. & Ager C. M. (1991). Effect of phosphorus deficiency on spectral reflectance and morphology of soybean plants. *Remote Sensing of Environment*, **36**, 121-127.

Munden R, Curran P.J & Catt J.A. (1994). The relationship between red edge and chlorophyll concentration in the Broadbalk winter wheat experiment at Rothampstead. *International Journal of Remote Sensing*, **15**, (3), 705-709.

Myers V.I, & Allen W.A. (1968). Electrooptical remote sensing methods as non-destructive testing and measuring techniques in agriculture. *Applied Optics.* **7**, 1818-1838

Pickerill J.M & Malthus T.J (1998). Leak detection from rural aqueducts using airborne remote sensing techniques. *International Journal of Remote Sensing*. **19**, 12, 2427-2433

Ponnamperuma F.N (1972). The chemistry of submerged soils. *Advances in Agronomy*. **24**, 29-96

PRESENSE (2001) Project proposal ENK6-CT2001-00553

Pysek P & Pysek A. (1989). Changes in vegetation caused by experimental leakage of natural gas. *Weed Research*, **29,** (3), 193-204.

Railyan V. Ya, & Korobov R.M (1993). Red edge of canopy reflectance spectra of *Triticale*. *Remote sensing of Environment*, **46**, 173-182

Rock B.N, Hoshizaki T & Miller J.R. (1988). Comparison of in situ and airbourne spectral measurements of the blue shift associated with forest decline. *Remote Sensing of Environment*, **24**, 109-127

Rollin E.M, Emery D.R & Kerr C.H (1996) *Analytical Spectral Devices (ASD) Fieldspec FR Spectroradiometer –User Handbook Version 1*. Equipment Pool for Field Spectroscopy, University of Southampton.

Savitzky A & Golay M.J.E. (1964). Smoothing and differentiation of data by simplified least squares procedures. *Analytical Chemistry* **36**, 1627-1639

Schollenberger C.J. (1930). Effect of leaking gas upon the soil. *Soil Science* **29**, 260-266.

Sojka R.E, Stolzy L.H & Kaufmann M.R (1975). Wheat growth related to rhizosphere temperature and oxygen levels. *Agronomy Journal*, **67**, (5), 591-596

Steven M.D, Malthus T.J, Demetriades-Shah T.H, Danson F.M &Clark J.A. (1990) Spectral indices for crop stress. In: *Applications of Remote Sensing in Agriculture*. Edited by Steven M.D & Clark J.A. Butterworths, London 1990

Steven M.D, Werker R & Milnes M. (1997). Assimilation of satellite data in crop monitoring and yield prediction. In: *Physical Measurements and Signatures in Remote Sensing*. Edited by Guyot G & Phulpin T, A.A.Balkema, Rotterdam 1997.

Trought M.C.T & Drew M.C (1980). The development of waterlogging damage in wheat seedlings (Tritium Aestivum L.) I. Shoot and root growth in relation to changes in the concentrations of dissolved gases and solutes in the soil solution. *Plant and Soil* **54**, 77-94

Trought M.C.T & Drew M.C (1980). The development of waterlogging damage in wheat seedlings (Tritium Aestivum L.) II. Accumulation and redistrbution of nutrients by the shoot. *Plant and Soil* **56**, 187-199

Tsai F & Philpot W (1998). Derivative analysis of hyperspectral data. *Remote Sensing of Environment* **66**, 41-51

Van Noordwijk M, Martikenen P, Bottner P, Cuevas E, Rouland C & Dhillon S.S (1998). Global change and root function. *Global Change Biology*, **4**, 759-772.

Watt Committee Report no. 28 (1994). Methane Emissions. Report of a working group appointed by the Watt Committee on Energy. Ed. Professor Alan Williams.

Whalen S.C, Reeburgh W.S & Sandbeck K.A (1990). Rapid methane oxidation in a landfill cover soil. *Applied Environmental Microbiology* **56**, 3405-3411

Williams G.M & Hitchman S.P. (1989). The generation and migration of gases in the sub-surface. *Methane-Facing the problems*, Symposium Nottingham.

Wooley J.T. (1971). Reflectance and transmittance of light by leaves. *Plant Physiology*, **47**, 656-662.

Yang H, Zhang J, Van der Meer F & Kroonenberg S.B (1999). Spectral characteristics of wheat associated with hydrocarbon microseepages. *International Journal of Remote Sensing.* **20**, (4), 807-813

Zwiggelaar R (1998) A review of the spectral properties of plants and their potential use for crop/weed discrimination in row-crops. *Crop Protection*, **17**, (3), 189-206

12 List of Web Sites

(1). The Origins and Progress of the Gas Industry over 200 Years. Http://www.igaseng.com/gashist.htm Accessed on 1/10/2001

(2). Delivering Gas Http://www.transco.uk.com . Accessed on 1/10/2001

(3) Lattice group annual report 2000 http://annuals.lattice-group.com/ Accessed on 16/10/01

(4) National atmospheric emissions inventory (UK methane emissions) http://www.aeat.co.uk/netcen/airqual/emissions/report94.html Accessed on 16/10/01

(5) Data for thermal conductivities of gases http://www.physicsofmatter.com/Book/Chapters/Chapter5/5.html Accessed on 18/10/01

(6) NERC Earth observation data centre http://www.neodc.rl.ac.uk Accessed on 8/1/02

(7) Remote sensing instruments database http://www.es.ucsc.edu Accessed on 14/1/02

(8) Earth observing 1 http://eo1.gsfc.nasa.gov/Technology/Hyperion.html Accessed on 30/5/02

(9) Digital globe[1] http://www.digitalglobe.com/?goto=products/qb_standard Accessed on 30/5/02

(10). History of John Innes compost Http://rareplants.co.uk/johninne.htm Accessed on 1/10/2001